Practical Point-of-Care Medical Ultrasound

James M. Daniels
Richard A. Hoppmann
Editors

Springer

Practical Point-of-Care Medical Ultrasound

James M. Daniels • Richard A. Hoppmann
Editors

Practical Point-of-Care Medical Ultrasound

Springer

Editors
James M. Daniels, MD, MPH, RMSK
Department of Family and Community Medicine and Orthopedic Surgery
SIU Primary Care Sports Medicine Fellowship
Southern Illinois University School of Medicine
Springfield, IL, USA

Richard A. Hoppmann, MD
Ultrasound Institute
University of South Carolina School of Medicine
Columbia, SC, USA

ISBN 978-3-319-22637-8 ISBN 978-3-319-22638-5 (eBook)
DOI 10.1007/978-3-319-22638-5

Library of Congress Control Number: 2015951721

Springer Cham Heidelberg New York Dordrecht London

Printed on acid-free paper

Springer International Publishing AG Switzerland is part of Springer Science+Business Media (www.springer.com)

Dedication from Richard A. Hoppmann, MD
"In dedication to my wife, Anne."

Dedication from James M. Daniels, MD
*"We all teach, more by example than words.
Thanks, Mom!"*

Contents

Contributors

Keith Reeves Barron Jr., MD Ultrasound Institute, University of South Carolina School of Medicine, Columbia, SC, USA

Paul Bornemann, MD Department of Family and Preventative Medicine, University of South Carolina School of Medicine, Columbia, SC, USA

Satyakant Chitturi, MD, MBBS SIU Primary Care Sports Medicine Fellowship, Southern Illinois University School of Medicine, Quincy, IL, USA

Daniel M. Couri, MS, MD Department of Internal Medicine and Radiology, Southern Illinois University School of Medicine, Springfield, IL, USA

Brad Cowley, DO Division of Emergency Medicine, Southern Illinois University School of Medicine, Springfield, IL, USA

Jonathan dela Cruz, MD, RDMS Division of Emergency Medicine, Southern Illinois University School of Medicine, Springfield, IL, USA

James M. Daniels, MD, MPH, RMSK Department of Family and Community Medicine and Orthopedic Surgery, SIU Primary Care Sports Medicine Fellowship, Southern Illinois University School of Medicine, Springfield, IL, USA

Alexei O. DeCastro, MD Department of Family Medicine, Medical University of South Carolina, Charleston, SC, USA

Richard A. Hoppmann, MD, FACP Department of Internal Medicine, University of South Carolina School of Medicine, Columbia, SC, USA

Dae Hyoun Jeong, MD SIU Primary Care Sports Medicine Fellowship, Southern Illinois University School of Medicine, Quincy, IL, USA

Chinmay Patel, DO Division of Emergency Medicine, Southern Illinois University School of Medicine, Springfield, IL, USA

Victor V. Rao, MBBS, DMRD, RDMS Ultrasound Institute, University of South Carolina School of Medicine, Columbia, SC, USA

Antonio Riero, MD Department of Pediatric Emergency Medicine, Yale-New Haven Children's Hospital, New Haven, CT, USA

John Rocco MacMillan Rodney, MD, RDNS Department of Family Medicine Obstetrics, Christian Brothers University, Memphis, TN, USA

Linda Savage SIU Primary Care Sports Medicine Fellowship, Southern Illinois University School of Medicine, Quincy, IL, USA

Michael S. Wagner, MD Ultrasound Institute, University of South Carolina School of Medicine, Columbia, SC, USA

Ximena Wortsman, MD Department of Radiology, Faculty of Medicine, Institute for Diagnostic Imaging and Research of the Skin and Soft Tissues, Clinica Servet, University of Chile, Las Condes, Chile

Sevan Yeghiazarian, MD Division of Emergency Medicine, Southern Illinois University School of Medicine, Springfield, IL, USA

Chapter 1
Introduction

Richard A. Hoppmann and James M. Daniels

This book is a primer for both students and teachers of point-of-care ultrasound (POCUS). This is a term that began to be used in medical curriculum only a decade ago, but it has now become the standard of care in some areas of clinical medicine.

POCUS is not designed to replace the traditional, detailed ultrasound exam. It is designed to be used by the health-care provider at the bedside in real time to answer a specific question such as *Does this patient with right upper quadrant abdominal pain have a gallstone*. Traditionally, the clinician would utilize the patient history, physical examination and possibly laboratory tests to make a diagnosis. If an ultrasound test were desired, the study would be scheduled and the patient would be sent to another location to have it performed. A highly trained technician (sonographer) or radiologist would perform the examination and the radiologist would interpret the study. A detailed report would be generated and relayed to the clinician at a later time.

POCUS relies on the integration of the patient history, physical examination and the ultrasound performed and interpreted by the clinician at the point of care. Thus, the clinician has the information needed at the time and place it is needed to make an accurate diagnosis and clinical management decisions. Table 1.1 demonstrates the main differences between POCUS and traditional ultrasound.

Physicians, other than radiologists, such as cardiologists and gynecolgists have already incorporated ultrasound into their clinical practices. Other medical

---

R.A. Hoppmann, M.D., F.A.C.P.
Department of Internal Medicine, University of South Carolina School of Medicine, Columbia, SC, USA
e-mail: Richard.Hoppmann@uscmed.sc.edu

J.M. Daniels, M.D., M.P.H., R.M.S.K. (✉)
Department of Family and Community Medicine and Orthopedic Surgery, SIU Primary Care Sports Medicine Fellowship, Southern Illinois University School of Medicine, Springfield, IL, USA
e-mail: jdaniels@siumed.edu

J.M. Daniels, R.A. Hoppmann (eds.), *Practical Point-of-Care Medical Ultrasound*, DOI 10.1007/978-3-319-22638-5_1

specialties have started to use ultrasound in a variety of ways. For example, the American College of Rheumatology has integrated POCUS into their training with a focus on musculoskeletal ultrasound. There would be much to gain if subspecialists using ultrasound were to expand their applications to include additional diagnoses that could directly benefit their patients.

POCUS, as we know it today, was first introduced into medical student education in a comprehensive, integrated way at the University of South Carolina School of Medicine in 2006. The seeds of this book were planted over a decade ago in the Family Medicine Department of Southern Illinois University School of Medicine when it received a grant to study how medical students and resident physicians learned. Many of the learning issues at that time are relevant today with learning point-of-care ultrasound. These two projects are intertwined throughout this book. The following two figures show much of what was learned.

All practitioners have a competency skill set that they use on a regular basis. Traditionally, primary care providers have a broad base of knowledge, i.e., immunization schedule for a pediatric patient, longitudinal treatment of chronic disease states such as hypertension and diabetes, psychosocial issues affecting the patient and their family. Subspecialty providers have a narrower focus of knowledge but it is at a deeper level, i.e., endoscopic evaluation and treatment of the GI system, catheterization and stent placements in the cardiovascular system.

As can be seen in Fig. 1.1, the total amount of medical knowledge may be the same for the subspecialist and the primary care clinician but with a difference in depth and breadth of knowledge. One can think of this as comparing a high resolution picture of a patient at one point in time to a long "grainy" video clip of the patient over time. Each view of the patient is useful in different ways.

The focus of this project is to take an organic approach to the practice of medicine. This approach focuses on the areas of overlap between disciplines and to build upon them. We believe that this process is how students learn a new subject. See Medical Students area in Fig. 1.1. The student most closely aligns with a primary care orientation at the beginning of their training then changes to more of a subspecialty orientation in residency depending on the chosen field of study.

Table 1.1 Differences between POCUS and traditional ultrasound

POCUS	Traditional ultrasound
Performed and interpreted by the clinician	Performed and interpreted by a radiologist or performed by a sonographer and interpreted by a radiologist
Performed in real time and integrated with the history and physical examination	Primarily interpreted without the benefit of a detailed history and physical examination
Oftentimes used to answer just one specific question	A protocol examination with detailed information provided
Used as a bedside clinical tool with low to no cost	More comprehensive examination and associated cost

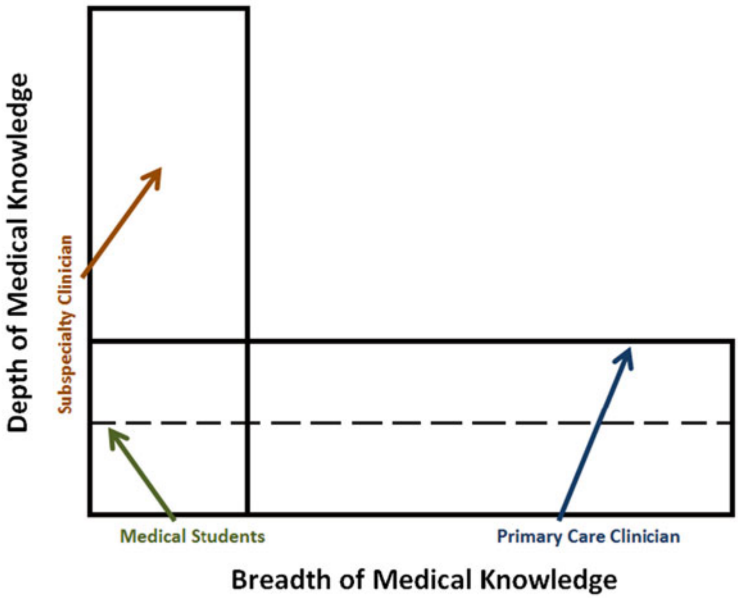

Fig. 1.1 Depth and breadth

As health care changes, providers will need to be more efficient and accurate in their diagnosis and management of patients. This will require a new skill set. POCUS has the potential to improve patient care and the health-care delivery system while adding personal satisfaction and career fulfillment to the practice of medicine. The history and physical examination have long been the basis of our professional practice along with the relationship that we form with our patients. POCUS takes place at the bedside with the patient and offers many opportunities for patient contact, discussion, and education all of which embody the essence of the patient–provider relationship. There is a great deal of literature that has been written on this subject but none makes it clearer than in a famous painting by Sir Luke Fildes (1891) shown in Fig. 1.2.

This scene shows a physician with relatively little technology trying to help a pediatric patient as her family looks on. The doctor is in the patient's home. There may not be much he has to offer, yet his very presence brings comfort to the family. Now picture the child and family in a sterile hospital ICU with state-of-the-art technology and a myriad of health-care providers … all whom they have just met. Neither scene is complete. Technology has replaced intimacy.

Now imagine the primary care provider appropriately trained and competent in POCUS who can bring both the humanistic and state-of-the art technology sides of medicine to the point of care. Thus, we have a more complete picture and one that is better for patient, family, and practitioner. This more comprehensive patient-centered care is what many of the accrediting bodies such as the Liaison Committee

Fig. 1.2 The Doctor by Sir Luke Fildes (1891)

on Medical Education and the Accreditation Council for Graduate Medical Education are recommending for the training of future medical practitioners.

This project also utilized journal articles published about the accuracy of the history and physical examination. The Journal of the American Medical Association has a 2-decade-old meta-analysis series that contains 54 articles and updates on the usefulness of physical examination in the clinical setting. Whenever possible, the chapter authors included this information with their expertise in POCUS. We organized the chapters and presented them using information from various experts in the field of medical education. This included the Stanford 25, a group of clinical exam skills that are recommended for mastery by all health-care providers. Figure 1.3 demonstrates the book concept. Each chapter is laid out with a similar format that allows easy integration of the subject matter.

1. Approach to the Patient: General information about how to approach various patients with a particular problem, i.e., abdominal pain, musculoskeletal injury, etc.
2. Probe Selection: the type of probe selected can make the difference between a useful exam and one that provides limited information.
3. Scanning: Short description of patient and probe position.
4. Anatomy: Correlation of surface anatomy to POCUS anatomy.
5. POCUS and Physical Examination: Do these two entities corroborate? Is one superior to the other?
6. Common Findings and Pathology.

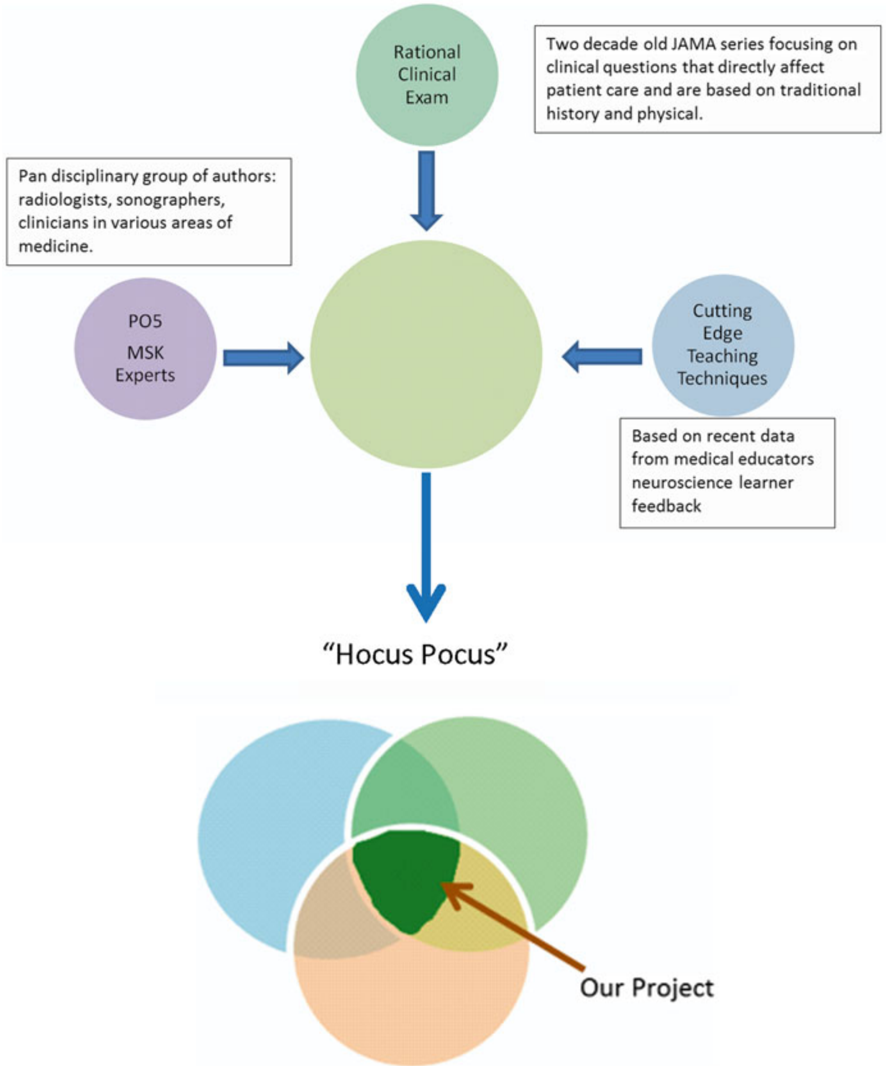

Fig. 1.3 The main concept

The literature has shown that with appropriate training and practice, all levels of health-care providers can learn important components of POCUS. Ultrasound is a skill learned over time and it is the intent of this book to serve as a starting point and reference source that with practice and supervision will allow practitioners to provide better care to their patients. Whether you are a medical student just starting out or an experienced clinician looking to expand your skills outside of your area of expertise, we hope you find this resource useful.

Chapter 2
Abdomen

Paul Bornemann, Michael S. Wagner, and Keith Reeves Barron Jr.

Introduction

The abdominal physical examination often does not help determine the etiology of clinical diseases, especially for those that are life-threatening. Prior to the availability of modern diagnostic imaging, Sir William Osler famously quipped, "there is no disease more conducive to clinical humility than aneurysm of the aorta." Dynamic, point-of-care abdominal ultrasonography can help bridge this historical knowledge gap, providing valuable clinical information at the bedside and offering diagnostic clues for a wide range of pathology.

Approach to the Patient

For most abdominal ultrasonography applications, place the patient in a supine position. Prepare the patient with particular care to respect patient modesty and comfort. If wearing a gown, place a sheet to cover the lower abdomen and pelvis unless this area is to be examined. If the patient is fully clothed, tuck a towel beneath the pants to prevent coupling gel from soiling the clothes.

Ideally, patients should fast several hours prior to abdominal imaging, as bowel gas may obscure abdominal structures. However, this is not always possible as

P. Bornemann, M.D. (✉)
Department of Family and Preventative Medicine, University of South Carolina School of Medicine, Columbia, SC, USA
e-mail: bornfp@gmail.com

M.S. Wagner, M.D. • K.R. Barron Jr., M.D.
Ultrasound Institute, University of South Carolina School of Medicine, Columbia, SC, USA
e-mail: Michael.Wagner@uscmed.sc.edu; Keith.Barron@uscmed.sc.edu

J.M. Daniels, R.A. Hoppmann (eds.), *Practical Point-of-Care Medical Ultrasound*, DOI 10.1007/978-3-319-22638-5_2

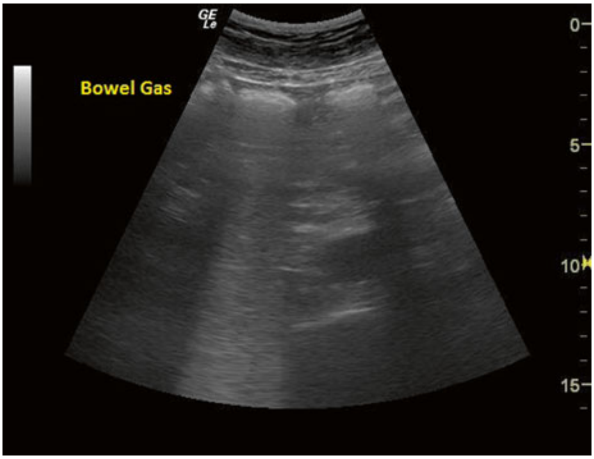

Fig. 2.1 Bowel gas is demonstrated as a bright *white line* at the top of the screen with a *gray* shadow below obscuring the abdominal organs

point-of-care studies are often performed without prior planning. Bowel gas appears as hyperechoic lines with gray to white shadowing below. An example of bowel gas can be seen here in Fig. 2.1. In cases where bowel gas does obstruct visualization of adjacent structures, attempt scanning from a more lateral or posterior location. Also, try to gently apply firm, consistent pressure with the probe to displace air-filled bowel. Try to use a "window" free of gas to visualize adjacent structures by fanning or angulating the probe. When possible, attempt to use the liver and spleen as acoustic windows by directing the ultrasound beam through them. This will allow for good visualization of structures posterior to them.

If the pelvis is to be imaged, instruct the patient to drink water to facilitate bladder filling, as fluid conducts sound well allowing posterior structures to be adequately imaged. Consuming water immediately before the examination may also aid visualization of the pancreas or epigastric structures that lie posterior to the stomach. Hydronephrosis may also become more apparent when the patient is fully hydrated.

Selecting a Probe

Abdominal structures are best imaged with a low-frequency curvilinear probe. Occasionally a phased-array probe may be used. Some handheld units may only have a single low-frequency probe such as a phased array probe that is not interchangeable. Common probes are depicted in Fig. 2.2. Many machines have presets specific to certain abdominal structures and selecting these will help minimize the amount of setting adjustments needed for optimal imaging. Adjusting the frequency even lower than the standard setting may help visualize deeper structures, or may be necessary when imaging obese individuals.

Fig. 2.2 A phased-array (*left*) and curvilinear probe (*right*). Both are low-frequency, allowing for evaluation of deeper structures

Scanning

Kidneys

The kidneys are retroperitoneal structures that are well-situated for ultrasonography. The right kidney is normally easier to image than the left given that the liver provides a large acoustic window. A longitudinal view of the right kidney is obtained in the right upper quadrant. The probe may be placed either anteriorly or in the mid-axillary line, depending on the patient's body habitus and liver size. After fanning through the entire structure, rotate the probe ninety degrees at the mid-kidney level to obtain a cross-sectional view. Length, width and anterior–posterior diameter should be recorded as shown in Fig. 2.3. Repeat this technique at the left flank to visualize the left kidney, using the spleen as an acoustic window. If difficulty is encountered, moving the probe more superiorly and posteriorly may allow better imaging of the left kidney. A seated position that brings the left kidney below the costal margin may also facilitate imaging.

Bladder

The bladder lies anteriorly in the pelvis and is best visualized when filled with urine. Obtain a transverse view by placing the probe anteriorly just above the pubic symphysis in the midline, and angle inferiorly. Measure the depth (anterior–posterior diameter) as well as width (left to right diameter). Rotate along the midline axis ninety degrees to obtain a longitudinal image in the sagittal plane. In this view, record the length (craniocaudal diameter) Fig. 2.4. Some machines will automatically calculate bladder volume, but a formula, which approximates the volume

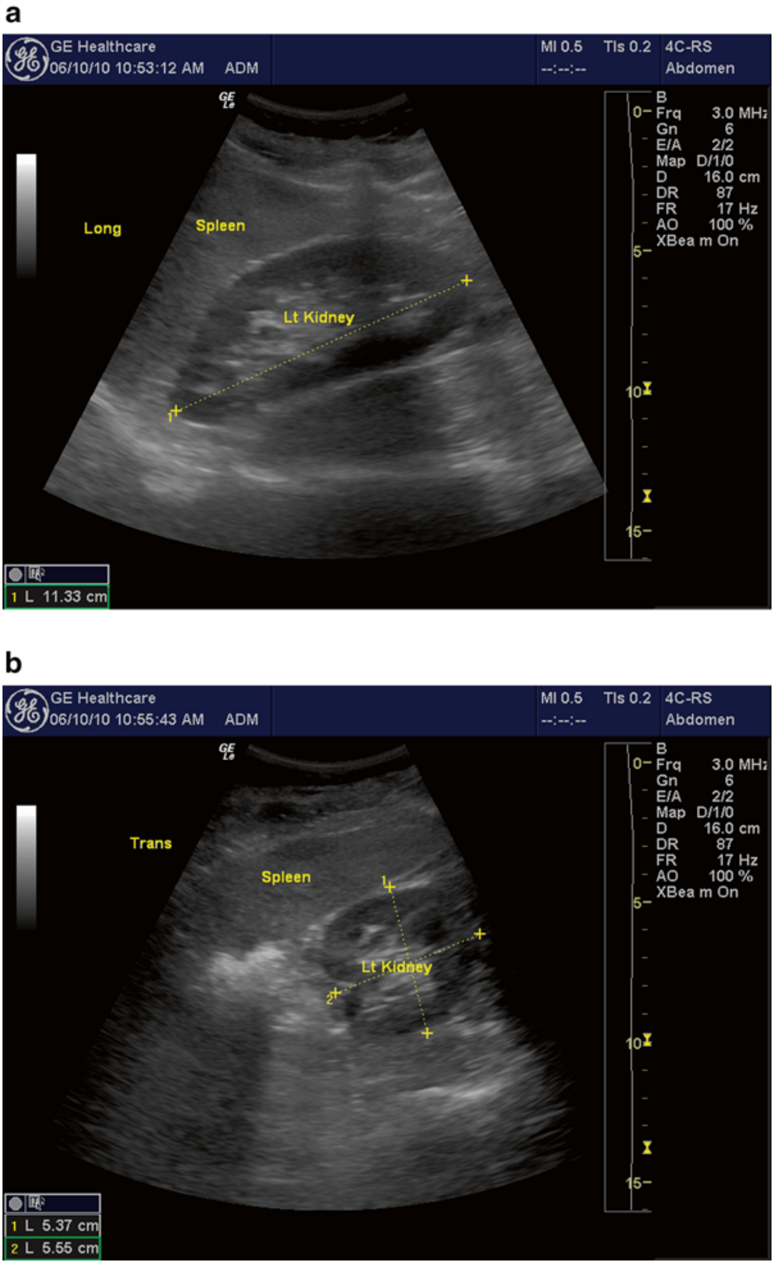

Fig. 2.3 (**a**–**b**) A normal left kidney which lies adjacent to the spleen. Calipers mark the length in a mid-sagittal plane (**a**) as well as anterior–posterior diameter and width in the transverse plane (**b**). (Image courtesy of Victor Rao)

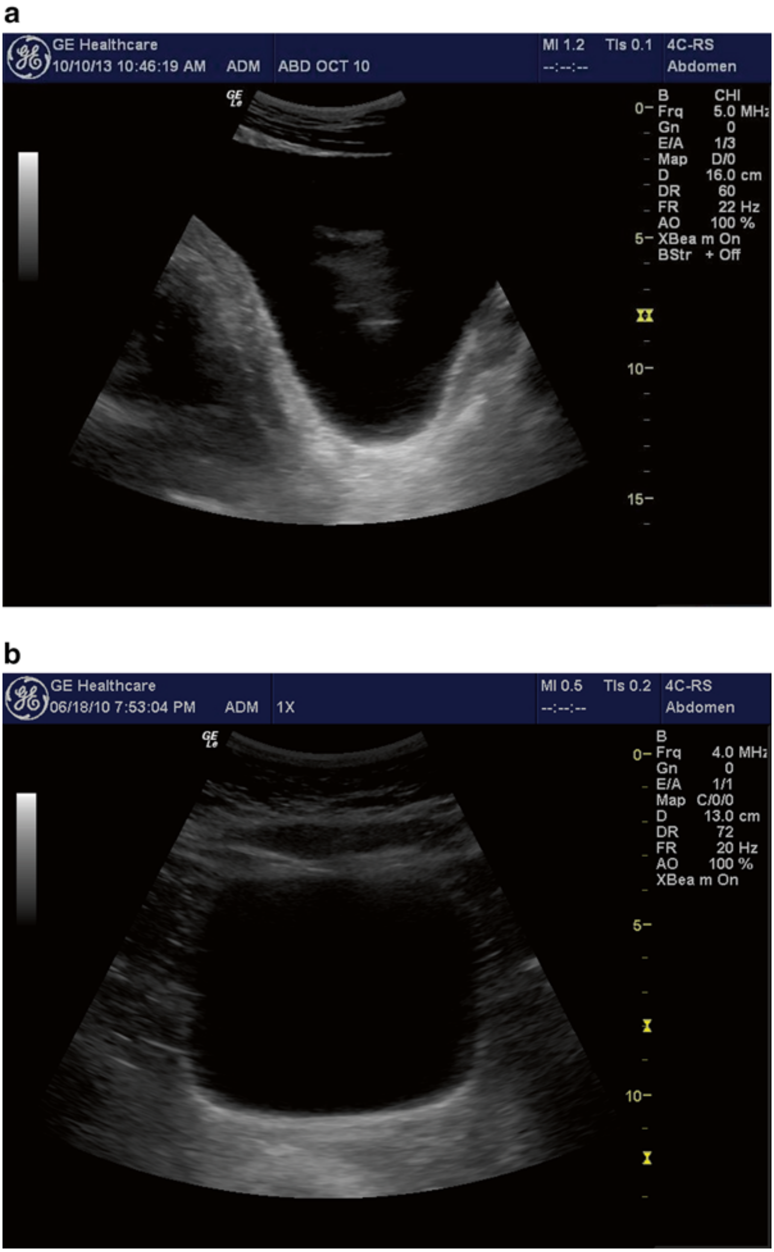

Fig. 2.4 A normal bladder as viewed in the mid-sagittal (**a**) and transverse (**b**) planes. (Image courtesy of Victor Rao)

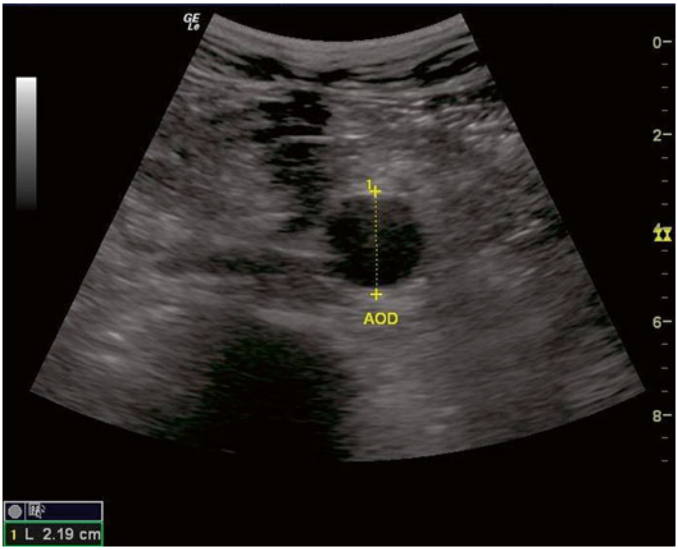

Fig. 2.5 A transverse view of the distal abdominal aorta (AOD) with caliper measurements from outer wall to outer wall

based on assumptions of the normal bladder shape, may be used when all three dimensions are recorded:

$$\text{Volume (ml)} = \text{Depth} \times \text{Width} \times \text{Length} \times 0.52$$

Performing this measurement immediately following voiding will give the post-void residual volume.

Abdominal Aorta

A transverse view is first obtained by placing the probe in the sub-xiphoid position with the probe marker pointing towards the patient's right side. The abdominal aorta is then traced from its proximal origin below the diaphragm to the bifurcation of the iliac arteries. This can then be repeated with the probe marker pointed towards the patient's head for a long axis view of the aorta. In general the probe should be as perpendicular to the aorta as possible in order to avoid oblique cuts that can make the diameter appear larger than it actually is. At least one caliper measurement should be obtained at the widest portion of the aorta seen on the scan. Measurements should be obtained in a transverse view of the aorta as shown in Fig. 2.5. Calipers are placed at the widest segment of the aorta and measurements are taken from the outer wall to outer wall, including thrombus if present.

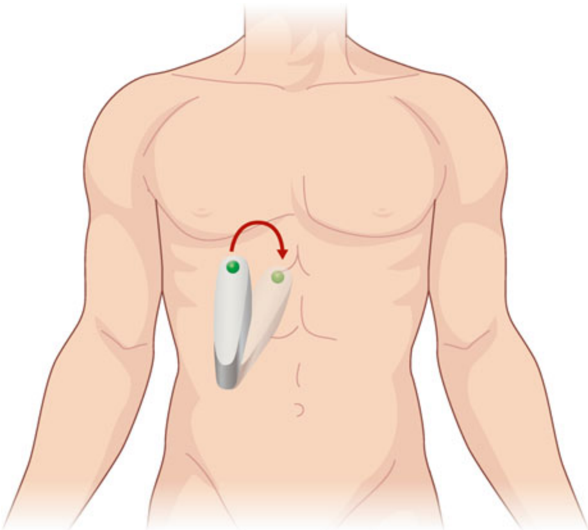

Fig. 2.6 Rotate the probe slightly from the sagittal plan to obtain a long axis view of the gallbladder

Gall Bladder

A long axis view is obtained first by placing the probe with the marker pointing cephalad directly to the right of the midline in the sub-xiphoid position. The probe should be tilted slightly cephalad. A subcostal sweep can be performed by sliding the probe laterally until the gall bladder is visualized. The probe should then be adjusted until the gallbladder is visualized in its long axis. This maneuver is depicted in Fig. 2.6. The probe is then used to completely sweep from one side of the gall bladder to the other. The probe is then rotated 90° to a short axis view and a sweep is repeated from one side to the other. If there is difficulty finding the gallbladder, the patient can hold a deep breath to bring the liver edge below the rib cage. Additionally, if the patient rolls into the left lateral decubitus position the gall bladder may move closer to the abdominal wall and may be easier to visualize.

Focused Assessment Sonography for Trauma (FAST) Exam

The purpose of the FAST exam is to evaluate the pericardial and peritoneal cavity for free fluid. The standard FAST exam is composed of views in four separate locations on the abdomen: the right upper quadrant (RUQ), left upper quadrant (LUQ), suprapubic (SP) or pelvic, and subxiphoid (SX). Starting with the RUQ coronal view, place the probe at the right flank at the level of the costophrenic angle with probe marker towards the patient's head. As the liver usually spans most of the RUQ, the probe can be placed in the anterior, mid, or posterior axillary line. Using the liver as an acoustic window, visualize the liver, kidney, diaphragm, and vertebral bodies. In this view, the region of interest is a potential space between the liver and kidney, known as Morrison's pouch. If intraperitoneal fluid is present, an anechoic space will appear to separate the liver and kidney. This is an abnormal finding and may indicate blood in the abdominal cavity in the setting of trauma. Fan the tail of the transducer up and down to sweep the transducer beam completely through Morrison's Pouch. Slide the probe caudally or angle slightly inferiorly to ensure the inferior tip of the right lobe of the liver is visualized. This is important because free fluid is sometimes seen at the liver tip before tracking into Morrison's Pouch.

Next, place the probe at the left costophrenic angle in the coronal plane with the probe marker towards the patient's head. Using the spleen as an acoustic window, visualize the spleen, kidney, diaphragm, and vertebral bodies. Here it is important to place the probe along the posterior axillary line. Rotating the probe slightly clockwise, so the indicator is towards the patient's axilla, often helps to reduce rib shadows and improve visualization of the diaphragm. If free fluid is present it can generally be seen between the spleen and the diaphragm, while large amounts of free fluid often surround the spleen superiorly and laterally.

Next, place the probe just cephalad to the pubis symphysis with the probe marker towards the patient's head. Using the full bladder as an acoustic window, look for free fluid cephalad and posterior to the bladder in males, and posterior to the uterus in the pouch of Douglas in females. Free fluid will tend to fill in spaces in the pelvis giving it an irregular shape with the appearance of sharp edges. When a large amount of fluid is present, the outline of the bowels is easily seen cephalad to bladder. Fan the tail of the transducer to ensure the entire region is seen. Next, obtain a transverse view by rotating the transducer 90° so the probe marker is pointed towards the patient's right. Fan the tail of the probe up and down to visualize the entire region, looking for anechoic fluid posterior to the uterus in females or posterior and superior to the bladder in males.

Finally, place the probe in epigastrum and slide cephalad into the subxiphoid position, angling towards the patient's head with the probe marker towards the patient's right. Use an overhand grip and position the probe at a relatively shallow angle. Using the left lobe of the liver as an acoustic window, obtain a 4-chamber view of the heart (described in the cardiac chapter) and visualize the interface between the right ventricle and the liver. The presence of pericardial effusion will appear as an anechoic region between the ventricular myocardium and the liver parenchyma. Fan the tail of the probe up and down to visualize the entire pericardium to include the posterior region.

The key components of the FAST exam are depicted in Fig. 2.7.

Small Bowl Obstruction

In a normal abdomen small bowel is usually not visualized. However, in small bowel obstruction (SBO) dilated, fluid filled loops of bowel with abnormal peristalsis can be seen. In the supine patient scan in the more dependent regions along the right and left paracolic gutters, which are away from bowel gas.

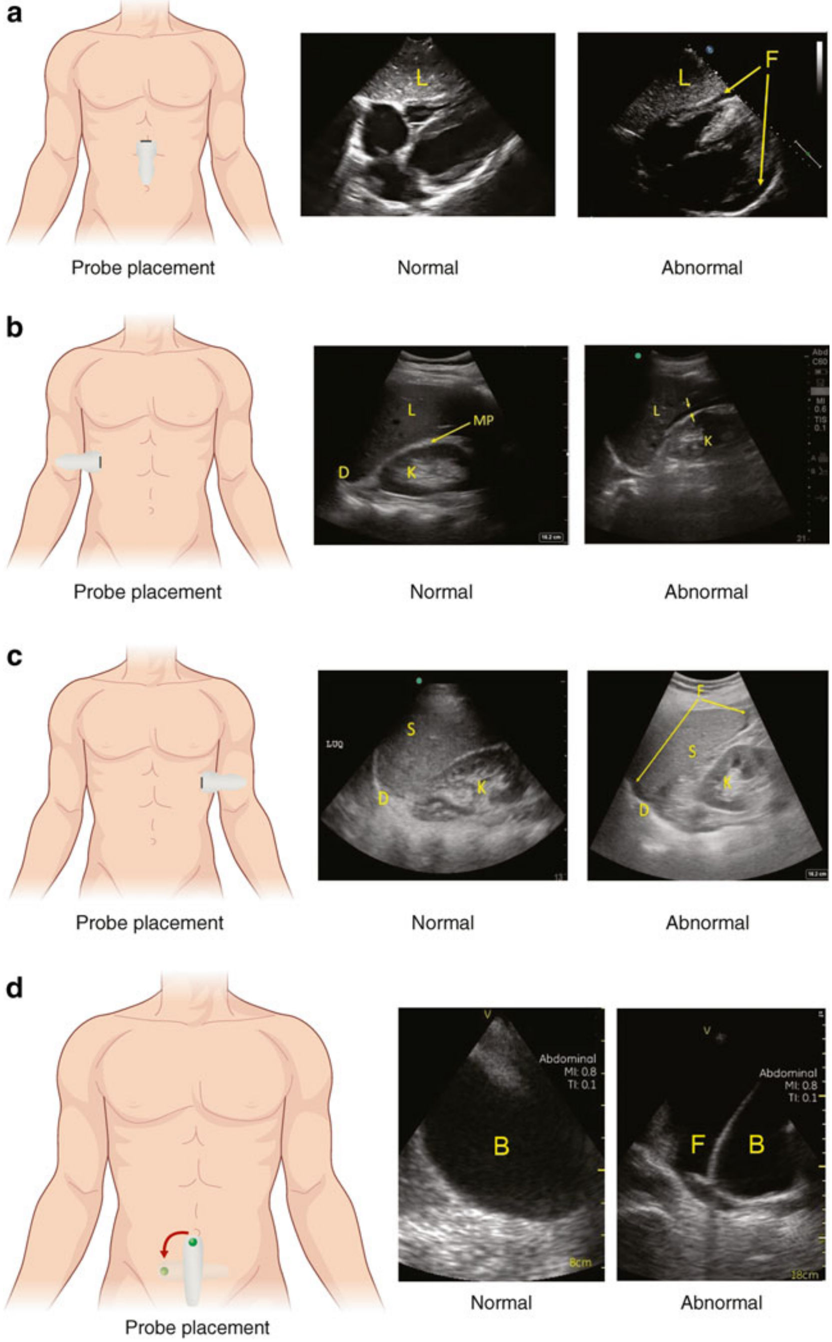

Fig. 2.7 (**a**) Probe points cephalad through liver (L), showing absence or presence of pericardial fluid (F). (**b**) Probe points toward midline in coronal plane, showing absence or presence of free fluid in the Morrison's Pouch (MP) between liver (L) and kidney (K). (**c**) Probe points toward midline in coronal plane, showing absence or presence of fluid (F) surrounding the spleen (S). D = diaphragm. K = kidney. (**d**) Pelvic view in long axis showing normal filled bladder (B) approximated by air-filled bowel. On far right, free fluid (F) cephalad and posterior to bladder

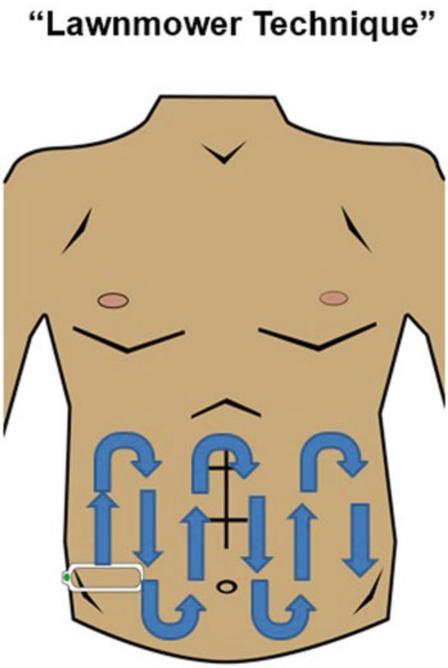

Fig. 2.8 Diagram of "lawn mower" technique for scanning for dilated loops of bowel in small bowel obstruction

Start with the probe in the right lower quadrant with the marker pointed towards the right shoulder and the beam angled across the abdomen in the coronal plane. Fan the tail anteriorly and posteriorly through the abdomen searching for dilated, fluid-filled loops of small bowel. Slide the probe cephalad along the right paracolic gutter while fanning. Repeat the process on the left side. Alternatively, a "lawn mower" technique can be utilized over the entire abdomen as depicted in Fig. 2.8.

When dilated loops of bowel are encountered, rotate the transducer to view loops of bowel in both short and long axis. Atypical probe positions are sometimes needed to visualize dilated loops of bowel along the short and long axis. Measurements should be taken perpendicular to the bowel walls, from outer wall to outer wall. Observe peristaltic activity and movement of contents within the lumen.

Normal Anatomy

Kidneys

The right and left kidneys are surrounded by a brightly echogenic renal capsule, found deep to the liver and spleen, respectively. The renal cortex is normally more echogenic than the pyramids and the kidneys overall are normally less echogenic

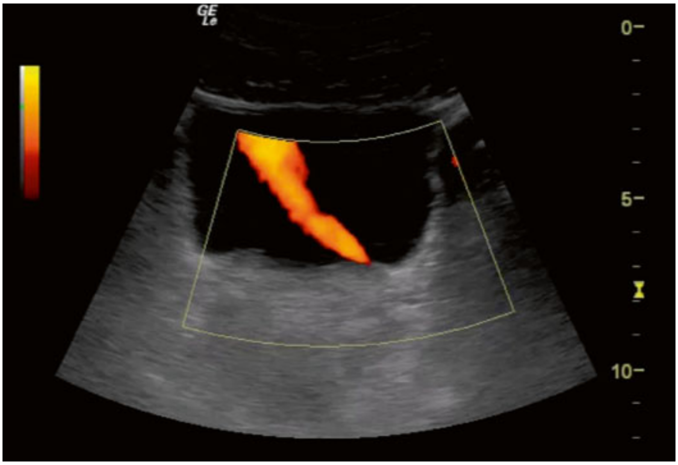

Fig. 2.9 As urine enters the bladder, power Doppler visualizes a ureteral jet in this transverse view

than the liver and spleen; concomitant liver disease may change liver echotexture. Increased renal cortical echogenicity may occur with acute and chronic kidney disease, progressing along with the severity of the disease. The renal medullae contain the renal pyramids which are more hypoechoic. Deep to these lie the echogenic renal sinuses which contain fat and blood vessels. Normal kidney length is 9–12 cm, and 4–6 cm wide.

Bladder

The bladder is normally a smooth, thick-walled, anterior pelvic structure that lies posterior to the pubic symphysis that easily distends when filled with anechoic urine. The sex-specific organs lie posteriorly and may appear more echogenic than surrounding structures due to posterior acoustic enhancement from a fluid-filled bladder. The use of Color Doppler on a full bladder may demonstrate the normal, intermittent flow from the ureters into the bladder, termed "ureteral jets" as shown in Fig. 2.9.

Abdominal Aorta

The first landmark visualized is the spine in the transverse sub-xiphoid window. The spine appears as a curved hyperechoic surface with acoustic shadows obscuring the posterior portion. The abdominal aorta appears as an anechoic circular structure directly superficial and to the left of the spine. The inferior vena cava sits superficial and to the right of the spine. The celiac trunk is the most proximal vessel visualized

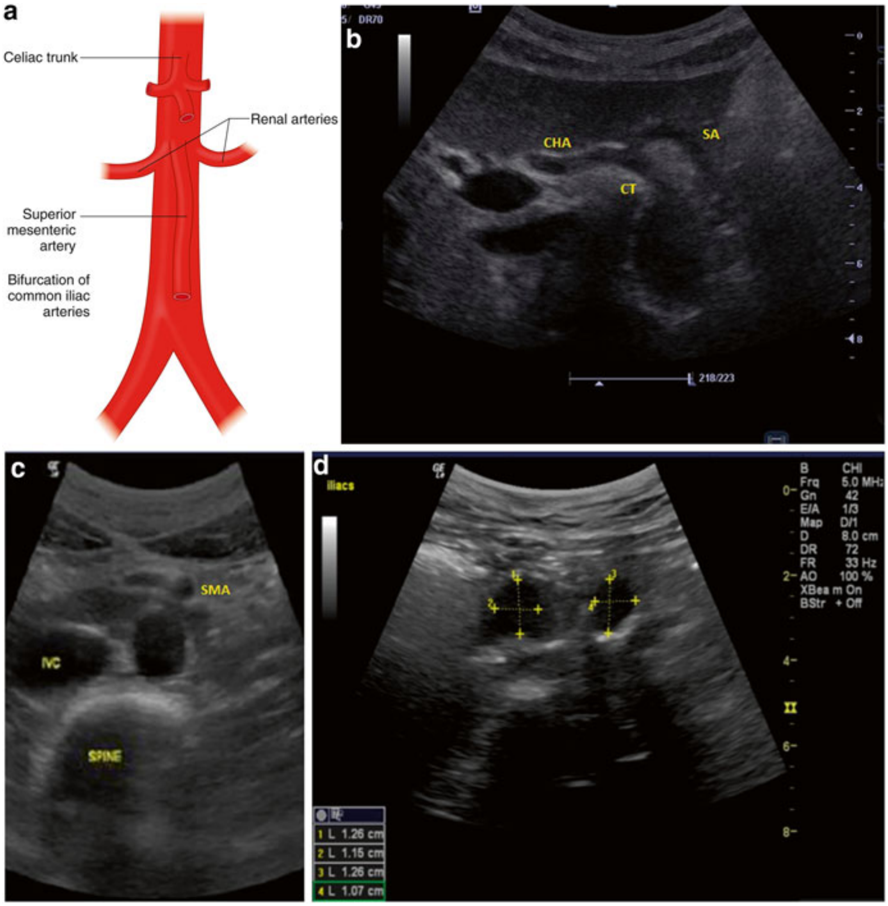

Fig. 2.10 (**a**–**d**) A diagram of the major branching vessels of the abdominal aorta (**a**) along with transverse ultrasound views of the celiac trunk (**b**), superior mesenteric artery (**c**), and the bifurcation of the common iliac arteries (**d**). *SMA* superior mesenteric artery, *CT* celiac truck, *CHA* common hepatic artery, *SA* splenic artery

branching anteriorly from the aorta. The celiac trunk divides into the splenic artery to the left and the common hepatic artery to the right and sometimes resembles a seagull with spread wings. Immediately distal to the celiac trunk the superior mesenteric artery branches anteriorly and then runs parallel to the abdominal aorta before deviating to the right. The left renal vein can be seen branching from the inferior vena cava and running to the left between the aorta and the superior mesenteric artery. Immediately distal to the superior mesenteric artery, the left and right renal arteries can be seen branching from the lateral sides of the aorta. In some patients the renal arteries will be difficult to visualize. The inferior mesenteric artery is usually too small to be easily identified ultrasonographically. The aorta bifurcates into the left and right common iliac arteries at the level of the umbilicus. Normal anatomy of the aorta is depicted in Fig. 2.10.

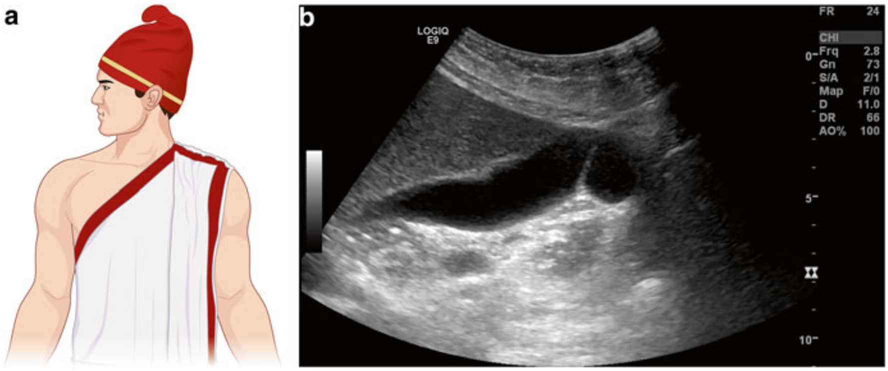

Fig. 2.11 (**a**, **b**) The Phrygian cap is a normal variant found on gallbladder ultrasonography. Here a picture of a person wearing a Phrygian cap (**a**) is compared to the ultrasonographic finding (**b**)

Gall Bladder

The gallbladder is a cystic structure filled with anechoic bile and demonstrating posterior acoustic enhancement. It is surrounded by a hyperechoic, muscular wall. The gallbladder wall can have several folds and the fundus may even fold back on itself in an anatomic variant known as the "phrygian cap" as seen in Fig. 2.11. The portal triad, made up of the portal vein, hepatic artery and common bile duct, is visualized just inferior to the gallbladder in the long axis as shown in Fig. 2.12.

FAST Exam

Right Upper Quadrant (RUQ) View

In the supine patient, Morrison's pouch represents the most dependent portion of the RUQ and is where intraperitoneal fluid is most easily seen. In the absence of free intraperitoneal fluid the superior pole of the kidney should appear to touch the liver. In some patients, perinephric fat may separate liver parenchyma from the kidney and may also have a hypoechoic appearance. However, fat will have small hyper-echoic striations in it and will not track to the liver tip.

Left Upper Quadrant (LUQ) View

The spleen is smaller in size than the liver, so the "window" to direct the ultrasound beam through is smaller and is located more posterior than in the RUQ. The stomach often sits just medial and anterior to the spleen, so gastric air will interfere with visualization of the anatomy if the probe is placed too far anterior.

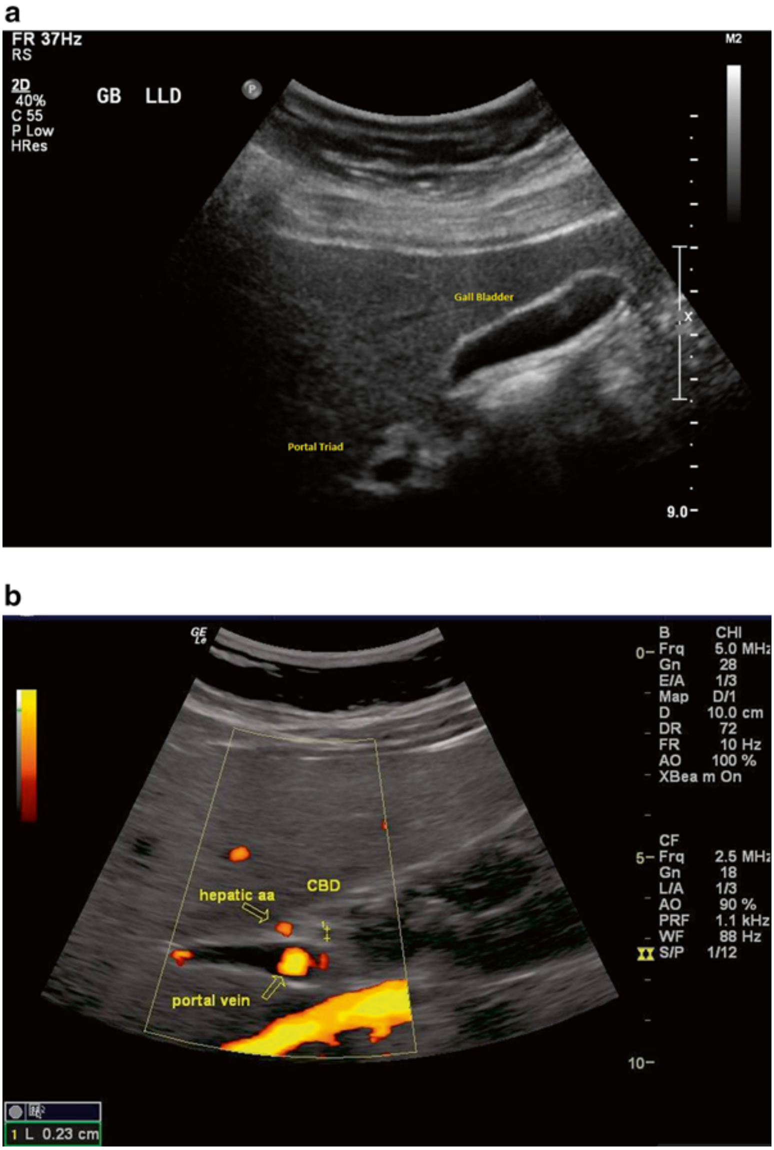

Fig. 2.12 (**a**, **b**) The portal triad visualized with B Mode (**a**) inferior to the gall bladder and zoomed in with power Doppler mode (**b**). Hepatic aa = hepatic artery. *CBD* common bile duct

Suprapubic (SP) View

It is important to remember the bladder is a pelvic and not an abdominal structure, when positioning the probe and angling the ultrasound beam. In males, the most dependent portion of the pelvis is the rectovesicular pouch, posterior to the bladder wall. Here, the seminal vesicles can be seen just cephalad from the prostate as a hypoechoic region. Although when viewed in the transverse plane they may be confused for a small amount of free fluid, fanning demonstrates they are well circumscribed with smooth edges and not well seen in the long axis. In females, the uterus is posterior to the bladder, and the most dependent portion of the pelvis is the rectouterine pouch, or pouch of Douglas. The sex specific organs are depicted in Fig. 2.13a, b.

Subxiphoid (SX) View

Air in the stomach and first portion of the duodenum often sits caudal to the heart just to the left of midline, which may interfere with imaging if the probe is angled too far left. Detailed description of the anatomy of the SX 4 chamber view can be found in the cardiac chapter.

Small Bowel Obstruction (SBO) View

Air within the small bowel will rise to the least dependent portion of the abdomen which is often in the periumbilical region or epigastrum. In very proximal obstructions, finding fluid-filled loops of small bowel may prove difficult. Plicae circulares (or valves of Kerckring) may become prominent ("keyboard sign") and can help differentiate small bowel from large bowel as shown in Fig. 2.14.

How to Use POCUS

Kidneys

Nephrolithiasis is increasingly common, with a prevalence of up to 10–15 % of the US population [1]. Computed tomography has become the most frequent test of choice, but due to concerns of cost and ionizing radiation, ultrasound is now advocated by some as the first-line test of choice in the diagnosis of renal colic.

Renal stones may be directly visualized as echogenic structures within the renal pelvis, ureteropelvic junction, ureters, or even in the ureterovesical junction, often with a posterior shadowing artifact that increases with stone size as shown in Fig. 2.15. The presence of a renal stone may also be indicated indirectly by dilatation of the renal pelvis and calices, indicative of obstructive uropathy as depicted in Fig. 2.16. The size of stone may be correlated with the degree of hydronephrosis. A finding of moderate to severe hydronephrosis should prompt further investigations or surgical referral [2, 3].

Left sided stones may be easily missed given that the left kidney is generally harder to image given its anatomical location as compared with the right kidney. The ureters, distal to the ureteropelvic junction or proximal to the ureterovesical junction, are difficult to image.

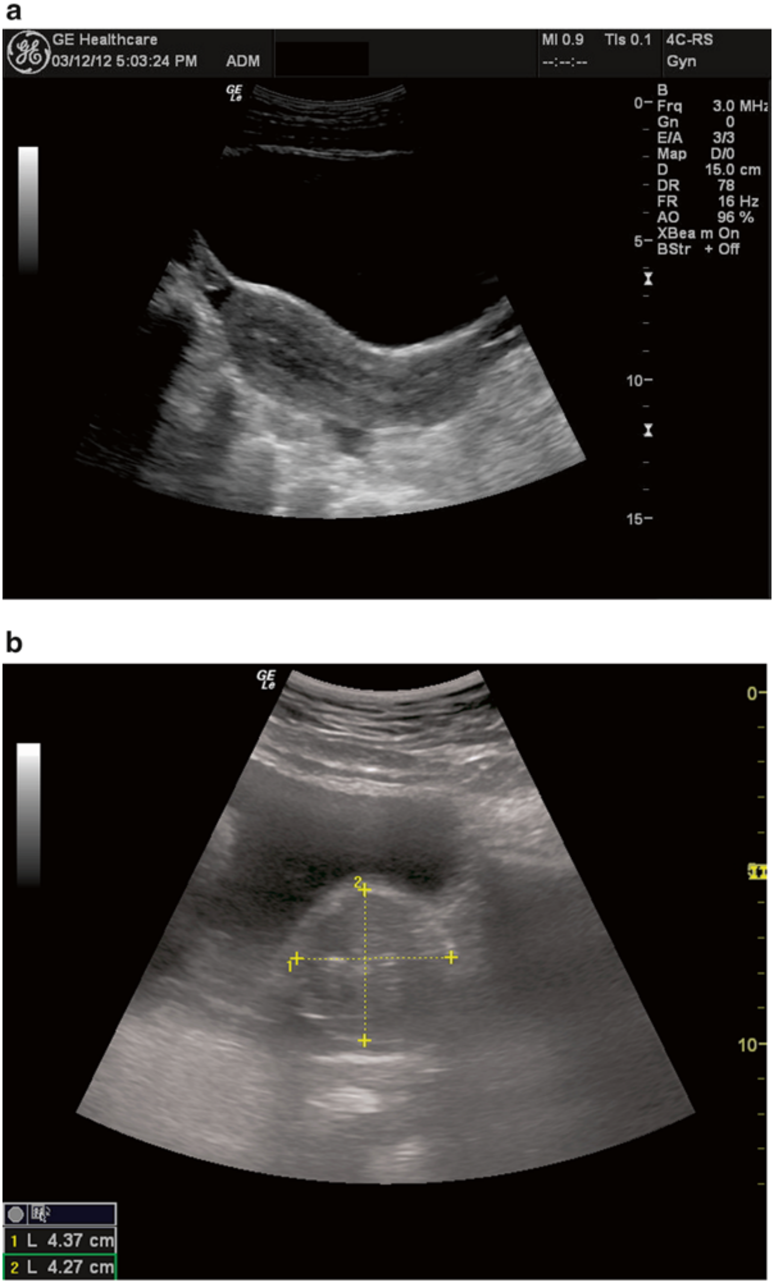

Fig. 2.13 (**a**, **b**) Sex-specific organs lie posteriorly to the bladder. A normal uterus in mid-sagittal plane (**a**). An enlarged prostate compresses the wall of the bladder in transverse plane (**b**). (Image 12a courtesy of Victor Rao)

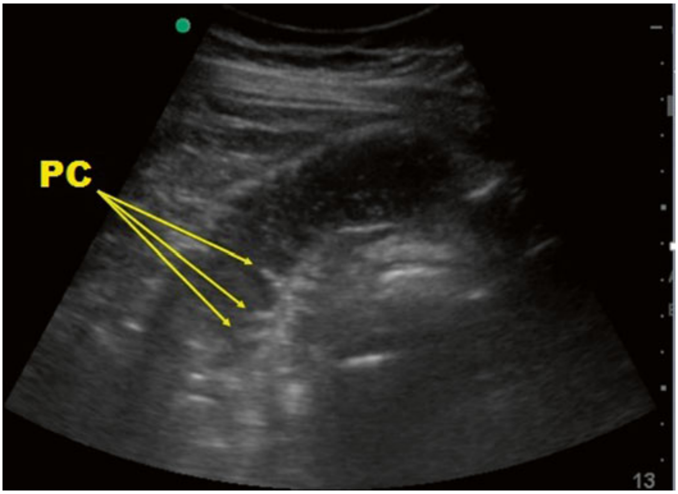

Fig. 2.14 Dilated fluid-filled loop of bowel with plicae circulares visible (PC) this is also known as the "keyboard sign"

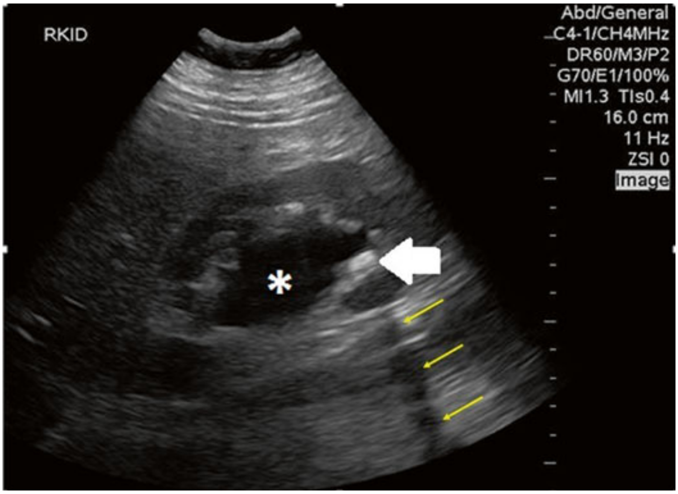

Fig. 2.15 Right kidney with hydronephrosis (*star*). A renal stone is seen as an echogenic object (*thick arrow*) with posterior shadowing (*thin arrows*)

Bladder

Evaluation of incontinence is a common problem in older adults, particularly in women, with prevalence of up to 55 % in women over 65 [4]. Ultrasound can accurately determine the post-void residual volume (PVR), and consequently may be performed when urinary retention is suspected, potentially avoiding the need for

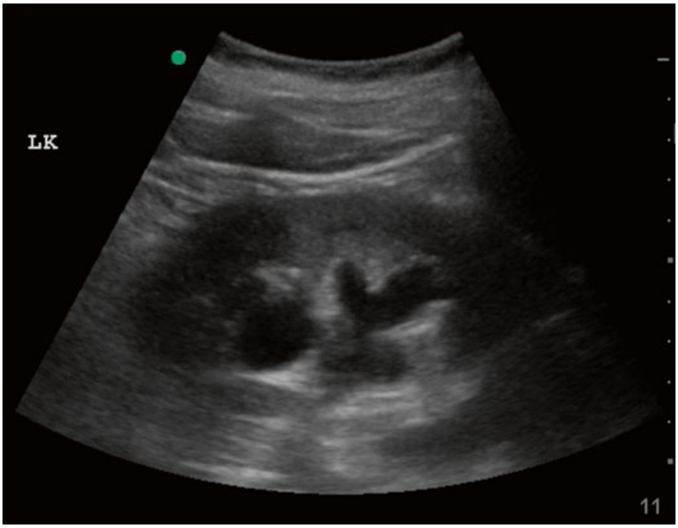

Fig. 2.16 Left kidney with hydronephrosis. The hypoechoic area within the kidney is caused by dilatation of the renal pelvis and calices, which is indicative of obstructive uropathy

bladder catheterization. The PVR is normally less than 50 ml and, in the evaluation of incontinence, a normal PVR argues against the presence of overflow incontinence or neurogenic bladder. This may have implications for clinical practice. While anticholinergic medications may improve overactive bladder or urge incontinence, their use should be avoided if the PVR is elevated.

FAST Exam

The FAST exam has been extensively studied in trauma patients and is by far the most accurate single bedside test in patients with suspected intra-abdominal injury [5]. Accounting for significant study heterogeneity, pooled sensitivity and specificity in adult patients with blunt abdominal trauma are 82 and 99 %, respectively [5]. Compared to the abdominal tenderness on palpation, which has a +LR of 1.4 and –LR of 0.61, a positive FAST exam has a +LR of 32–69 and warrants emergent evaluation. Although the test has a –LR of 0.26 and is not sensitive, a negative FAST exam may reduce the posttest probability of significant intra-abdominal bleeding in cases with a low pretest probability (such as patients presenting in an outpatient clinic) so that no further testing is required [6]. No studies of accuracy by primary care providers currently exist; the FAST exam has been utilized outside the hospital by non-physicians in remote and austere conditions [7, 8]. Though not formally studied for the detection of free fluid in non-trauma patients, the FAST exam greatly augments the standard physical exam to assess for suspected ascites and can clue the clinician into the presence of undiagnosed liver, kidney, or cardiac disease. Currently, clinicians should avoid attempting to diagnose solid organ injury based on their appearance on a FAST exam, though this may change with future research [9]. An extended version of the standard FAST examination (E-FAST) has been established and includes assessment for hemothorax and pneumothorax (see pulmonary chapter for discussion of pleural effusion and pneumothorax).

SBO

In a patient with nausea, vomiting, and abdominal pain, whether acute or recurrent, the question of small bowel obstruction may come up, particularly if the patient has a history of abdominal surgery. It is important to realize no components of the history reliably and accurately predict SBO [10, 11]. The use of examination to rule out abdominal distention has a +LR of 5.64–16.8 though with a –LR of only 0.27. Abdominal X-ray, considered the first-line test for SBO, has been shown to have a pooled sensitivity of around 75 % and a specificity of 66 % [10]. In contrast, abdominal ultrasound has been shown to have a pooled sensitivity of 90 % and a specificity of 96 % [10]. There is limited data that physicians with focused bedside ultrasound training can achieve comparable results to formal studies (sensitivity 94–98 % and specificity of 81–95 %) [11, 12]. These preliminary findings suggest that for low-to-moderate risk patients, ultrasound should be considered a viable alternative to abdominal X-ray and is likely a better test to rapidly exclude SBO. While bedside ultrasound should not replace CT for definitive SBO diagnosis in patients at high risk, it may help expedite treatment or possibly avoid repeat CT scans in patients with recurrent SBO.

Abdominal Aorta

Abdominal aortic aneurysms (AAA) are present in 1.4 % of men aged 50–79 and a history of smoking is the strongest risk factor [13]. Aneurysms are frequently asymptomatic prior to, and highly fatal after, rupture. Ultrasound screening programs have been shown to decrease mortality and to be cost effective [14, 15]. Ultrasound has excellent test characteristics for detecting AAAs with sensitivity of 98.9 % and specificity of 99.9 % [16]. The United States Preventative Services Task Force (USPSTF) recommends that all men aged 65–75 who have a history of smoking receive a one-time ultrasound screening for AAA, whereas evidence was inconclusive for women aged 65–75 with a history of smoking. [17]. The risk that a AAA will rupture increases with the diameter of the aneurysm. Guidelines recommend follow-up intervals for repeat ultrasounds based on the diameter of the aneurysm as

Table 2.1 AAA follow-up

Maximum aorta diameter	Follow-up interval
3.0–3.4 cm	× 3 years
3.5–4.4 cm	× 12 months
4.5–5.4 cm	× 6 months
5.5 cm o more	Refer to specialist

Chaikof EL et al. *J Vasc Surg*. 2009;50(4):S2-S49

illustrated in Table 2.1. Aneurysms larger than 5.5 cm or that are increasing at a rate greater than 1 cm in 12 months should be referred to a vascular surgeon for possible intervention. When aneurysms become symptomatic they are at significantly increased risk of rupture. Symptoms are nonspecific and include abdominal, back, or flank pain. All symptomatic AAAs should be referred for intervention immediately [18].

Gall Bladder

Cholelithiasis is common in the USA. In the age range of 20–74 years, approximately 8.6 % of men and 16.6 % of women have gall stones [19]. Risk factors include increasing age, female gender, obesity, hemolytic anemia, and oral contraceptive use. Gall stones can be asymptomatic or cause symptoms such as biliary colic or cholecystitis. Classic biliary colic presents as right upper quadrant pain with postprandial onset (especially with fatty foods) and lasts several hours. Acute cholecystitis presents with constant, severe right upper quadrant pain and signs of infection such as fevers and elevated white blood cell count. In acute cholecystitis there will usually be a positive Murphy's sign on exam. The Murphy's sign can also be elicited ultrasonographically by placing the probe directly over the gall bladder then having the patient inhale. Either sign is positive if there is pain and inspiratory arrest. Other ultrasonographic findings consistent with acute cholecystitis are gall stones or sludge, gall bladder wall thickening and pericholecystic edema. In expert hands, ultrasound has a sensitivity of 88 % and a specificity of 80 % [20]. If a diagnosis of cholecystitis is not clear then cholescintigraphy should be considered.

Asymptomatic cholelithiasis does not need to be treated. Any patient with symptoms consistent with gall bladder disease and objective findings of cholelithiasis on ultrasonography should be referred for surgical consultation as there is a very high rate of recurrence. This can be done on an elective, outpatient basis. Anyone with suspected acute cholecystitis should be admitted for intravenous antibiotic therapy and referred for definite surgical management to be completed within 1 week of initial diagnosis [21].

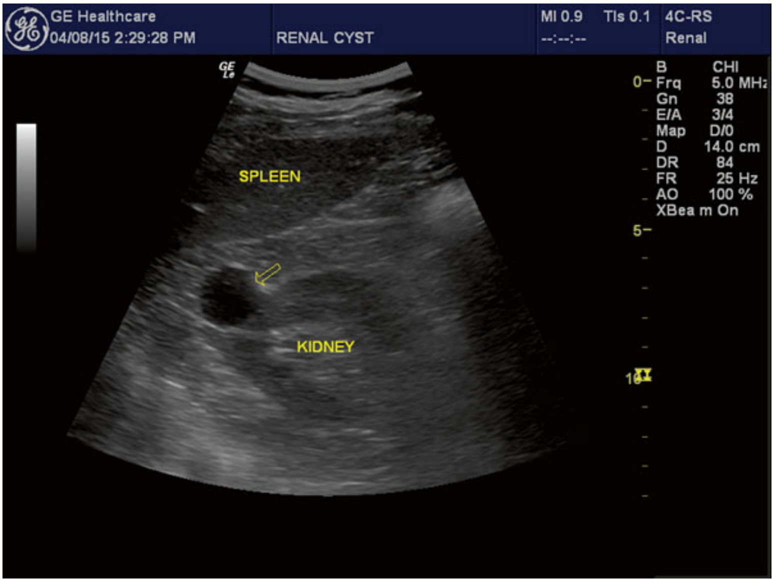

Fig. 2.17 Left kidney with a peripheral renal cyst (*arrow*) which is thin-walled and anechoic. (Image courtesy of Victor Rao)

Common Findings

Kidneys

Renal cysts are commonly encountered as patients age and may range from a single cyst to multiple, which may indicate hereditary disease. They appear as peripherally located oval or circular, hypoechoic structures within the renal parenchyma itself as shown in Fig. 2.17. Thin septations are occasionally seen, but normal cysts have smooth walls without nodularity. Cysts must be differentiated from hydronephrosis which has more centrally located dilatation of the renal pelvis and calices.

Chronic kidney disease has a characteristic appearance on ultrasound. Scans demonstrate decrease renal length correlating with disease progression. The finding of bilaterally small kidneys with echogenic cortices likely indicates the presence of chronic renal pathology.

Fig. 2.18 Fluid-filled loops of bowel in short (*left*) and long (*right*) axis

FAST Exam

In the trauma patient, free fluid visualized in any of the 3 abdominal views should be considered intraperitoneal hemorrhage until proven otherwise. In patients with large amounts of free abdominal fluid, but are hemodynamically stable, other non-traumatic causes such as ascites should be considered.

SBO

Dilated loops of bowel suggestive of small bowel obstruction are defined as greater than 2.5 cm. This is depicted in Fig. 2.18. Although it can be difficult to distinguish ileus from SBO, loops of small bowel should be <2.5 cm in ileus and decreased or absent peristalsis will be present. In obstruction, unless very late in presentation, peristalsis is often present. Luminal content will lose the unidirectional movement and may take on a “to and fro” pattern, like sea fans or debris close to the shoreline. Thickening of the bowel wall and small amounts of fluid between loops of bowel are late and ominous findings. Large amount of ascites should prompt consideration of other medical conditions separate from the SBO.

Abdominal Aorta

An aneurysm is defined as a transverse abdominal aorta measurement of ≥3 cm. A small AAA is shown in Fig. 2.19. Nearly all, AAAs will involve the infra-renal aorta. Some aneurysms will contain an isoechoic mural thrombus and the non-thrombosed portion of the aneurysm can be mistaken as a true lumen as shown in Fig. 2.20. If care is taken to measure from the outer wall to the outer wall of the aorta, this mistake can be prevented.

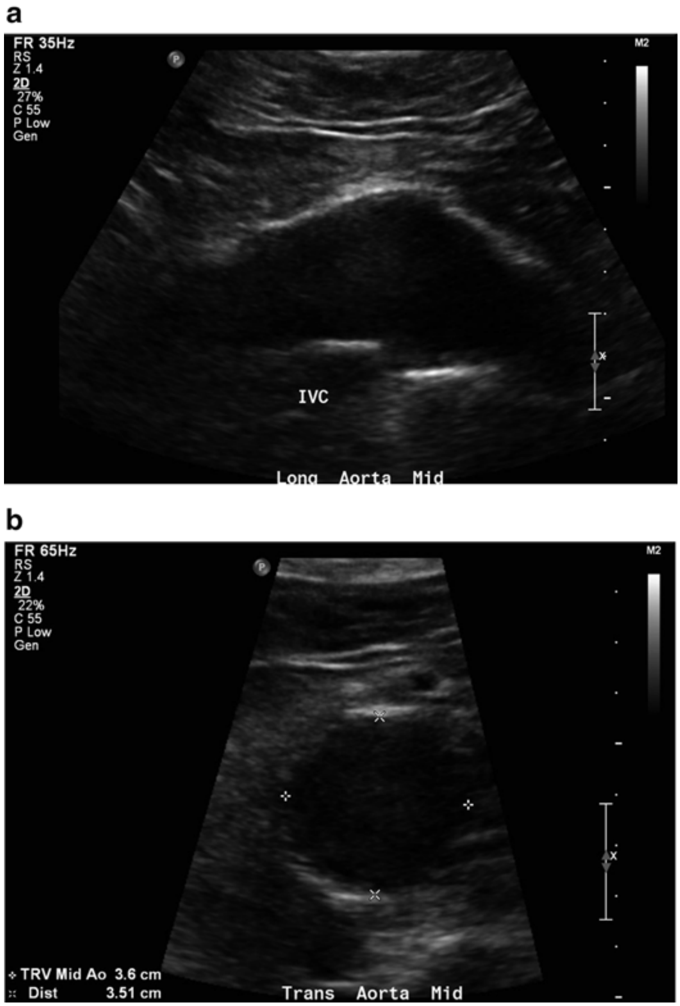

Fig. 2.19 (**a**, **b**) An abdominal aortic aneurysm with images taken in the short (**a**) and long (**b**) axis

Gall Bladder

Gall stones appear as hyperechoic structures with posterior shadowing which are located inside of the gallbladder. They will also move with gravity to the most dependent portion of the gallbladder. Gallbladder polyps can appear similar to stones but will not shadow and will not move with gravity. Gallbladder wall thickness should be measured anteriorly. It is normally less than 4 mm. A thickened gall

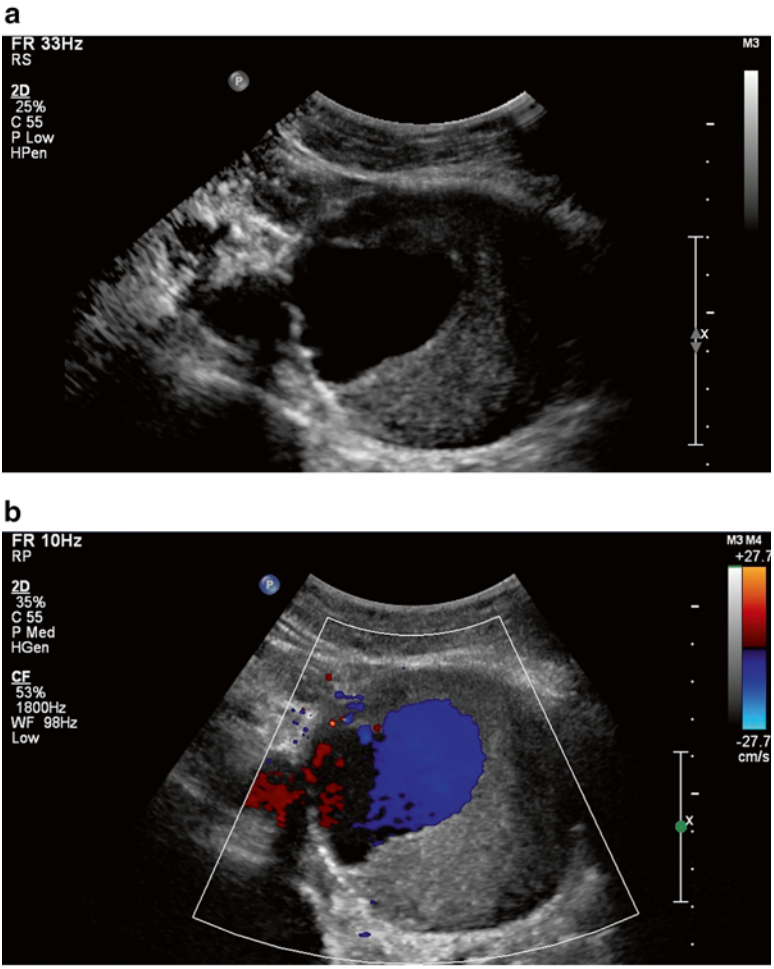

Fig. 2.20 An abdominal aortic aneurysm with a mural thrombus, images here taken in B Mode (**a**) and with color Doppler (**b**)

bladder wall can be a sign of acute cholecystitis or hepatitis. It can also be seen in a contracted gall bladder if a patient has recently eaten. Another sign of acute cholecystitis is pericholecystic fluid, which appears as areas of hypoechoic fluid just outside of the hyperechoic gallbladder wall. If the common bile duct is evaluated, color Doppler should be used to confirm that it is not the hepatic artery. Although the common bile duct will be on the right in 80 % of patients it is a common variant to

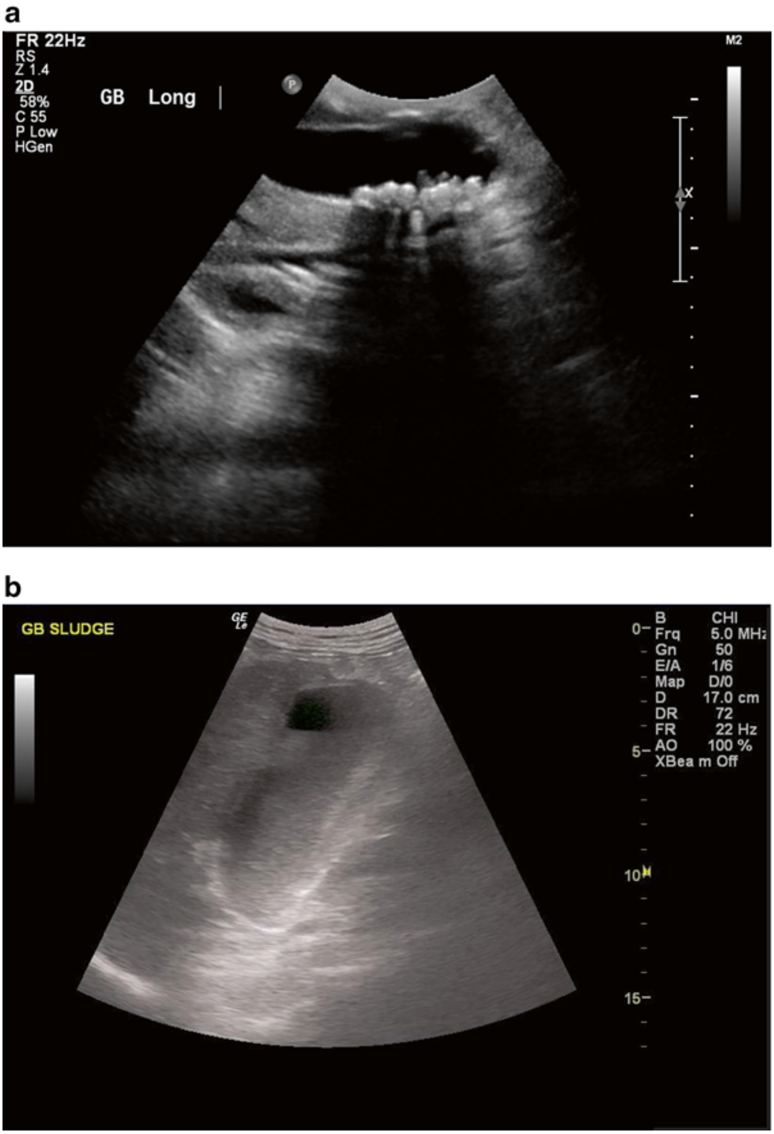

Fig. 2.21 Images of gall bladder pathology. (**a**) A long axis view of the gall bladder with multiple hyperechoic and shadowing stones seen inside. (**b**) Sludge can be seen layering in the gallbladder. (**c**) Thickening of the gall bladder wall is demonstrated—normal wall measurement is 4 mm or less. (**d**) Pericholecystic fluid demonstrated by hypoechoic areas surrounding a thickened gall bladder wall.

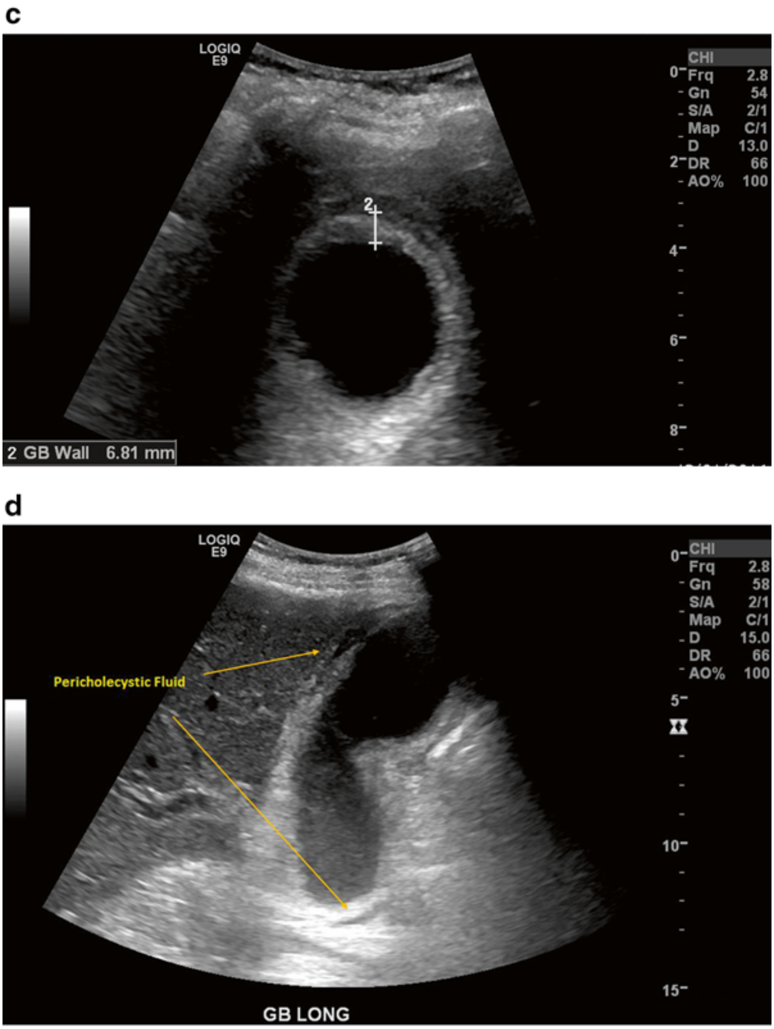

Fig. 2.21 (continued)

have it on the opposite side. The common bile duct normally measures <7 mm in diameter, or 1 mm for every decade of life for patients over 70 years of age. Common causes of enlarged common bile ducts are choledocholithiasis or patients who have had a cholecystectomy. Some of these pathologic findings are shown here in Fig. 2.21. Table 2.2 is a summary of normal measurements.

Table 2.2 Table of normal measurements

Structure	Normal measurements
Kidneys	
Length	9–12 cm
Width	4–6 cm
Bladder	
Post-void residual	<50 cc
Aorta	
Diameter	<3.0 cm
Small bowel	
Diameter	<2.5 cm
Gall bladder	
Anterior wall thickness	≤4 mm
Common bile duct	≤7 mm (or 1 mm for every decade of life)

References

1. Pearle M, Lotan Y. Urinary Lithiasis. In: Wein A, Kavoussi L, Campbell M, editors. Campbell-Walsh urology. 10th ed. Philadelphia, PA: Elsevier/Saunders; 2012.
2. Smith-Bindman R, Aubin C, Bailitz J, Bengiamin RN, Camargo CA, Corbo J, et al. Ultrasonography versus computed tomography for suspected nephrolithiasis. N Engl J Med. 2014;371:1100–10.
3. Dalziel PJ, Noble VE. Bedside ultrasound and the assessment of renal colic: a review. Emerg Med J. 2013;30(1):3–8.
4. Gorina Y, Schappert S, Bercovitz A, Elgaddal N, Kramarow E. Prevalence of incontinence among older Americans. Vital Health Stat. 2014;3(36):1–33.
5. Nishijima DK, Simel DL, Wisner DH, Holmes JF. Does this adult patient have a blunt intra-abdominal injury? JAMA. 2012;307(14):1517–27.
6. Emery M, Flannigan M. How useful are clinical findings in patients with blunt abdominal trauma? Ann Emerg Med. 2014;63(4):463–4.
7. Brooks AJ, Price V, Simms M. FAST on operational military deployment. Emerg Med J. 2005;22:263–5.
8. Wagner MS, Garcia K, Martin DS. Point-of-care ultrasound in aerospace medicine: known and potential applications. Aviat Space Environ Med. 2014;85(7):730–9.
9. Cagini L, Gravante S, Malaspina CM, Cesarano E, Giganti M, Rebonato A, et al. Contrast enhanced ultrasound (CEUS) in blunt abdominal trauma. Crit Ultrasound J. 2013;5 Suppl 1:S9.
10. Taylor MR, Lalani N. Adult small bowel obstruction. Acad Emerg Med. 2013;20(6):528–44.
11. Jang TB, Schindler D, Kaji AH. Bedside ultrasonography for the detection of small bowel obstruction in the emergency department. Emerg Med J. 2011;28(8):676–8.
12. Unluer EE, Bayata S, Postaci N, Yesil M, Yavasi O, Kara PH, et al. Limited bedside echocardiography by emergency physicians for diagnosis of diastolic heart failure. Emerg Med J. 2012;29(4):280–3.
13. Lederle FA, Johnson GR, Wilson SE, Chute EP, Littooy FN, Bandyk D, et al. Prevalence and associations of abdominal aortic aneurysm detected through screening. Aneurysm Detection and Management (ADAM) Veterans Affairs Cooperative Study Group. Ann Intern Med. 1997;126(6):441–9.

14. Cosford PA, Leng GC. Screening for abdominal aortic aneurysm. Cochrane Database Syst Rev. 2007;2:CD002945.
15. Glover MJ, Kim LG, Sweeting MJ, Thompson SG, Buxton MJ. Cost-effectiveness of the National Health Service abdominal aortic aneurysm screening programme in England. Br J Surg. 2014;101:976–82.
16. Lindholt JS, Vammen S, Juul S, Henneberg EW, Fasting H. The validity of ultrasonographic scanning as screening method for abdominal aortic aneurysm. Eur J Vasc Endovasc Surg. 1999;17:472–5.
17. LeFevre ML. Screening for abdominal aortic aneurysm: U.S. Preventive Services Task Force recommendation statement. Ann Intern Med. 2014;161(4):281–90.
18. Chaikof EL, Brewster DC, Dalman RL, Makaroun MS, Illig KA, Sicard GA et al. The care of patients with an abdominal aortic aneurysm: The Society for Vascular Surgery practice guidelines. J Vasc Surg. Elsevier Inc.; 2009;50(4):S2–49.
19. Everhart JE, Khare M, Hill M, Maurer KR. Prevalence and ethnic differences in gallbladder disease in the United States. Gastroenterology. 1999;117(3):632–9.
20. Shea JA, Berlin JA, Escarce JJ, Clarke JR, Kinosian BP, Cabana MD, et al. Revised estimates of diagnostic test sensitivity and specificity in suspected biliary tract disease. Arch Intern Med. 1994;154(22):2573–81.
21. Warttig S, Ward S, Rogers G. Diagnosis and management of gallstone disease: summary of NICE guidance. BMJ. 2014;349:g6241.

Chapter 3
Cardiology

Daniel M. Couri

Approach to the Patient

The standard transthoracic echocardiographic examination traditionally involves four transducer positions or acoustic windows: parasternal, apical, subcostal (subxiphoid), and the suprasternal notch. For the purposes of a "Point of Care" examination in the primary care setting, the parasternal, apical, and subcostal windows are the positions of interest; utilization of the acoustic window located at the suprasternal notch will not be discussed.

When imaging from the parasternal and apical positions, the patient should be placed in the left-lateral decubitus position with the left arm elevated above the head. This not only brings the heart closer to the chest wall, but also accentuates the intercostal space and facilitates probe placement/acoustic window location. Subcostal images are obtained with the patient in the supine position. Image acquisition can occur from either side of the patient and generally reflects the handedness/dexterity (i.e., right vs. left) of the scanning physician.

Selecting a Probe

The transducer for adult echocardiographic imaging is typically a 2.0–2.5 MHz probe. In thinner patients, however, a 5.0 MHz probe can be utilized. Given the necessity for intercostal precordial imaging, cardiac ultrasound probes typically have a small, rectangular footprint.

D.M. Couri, M.S., M.D. (✉)
Department of Internal Medicine and Radiology, Southern Illinois University
School of Medicine, Springfield, IL, USA
e-mail: dcouri@siumed.edu

J.M. Daniels, R.A. Hoppmann (eds.), *Practical Point-of-Care Medical Ultrasound*, DOI 10.1007/978-3-319-22638-5_3

Image Display

"Point of Care" cardiac ultrasonography, not unlike comprehensive transthoracic echocardiography, requires continuous/real-time image optimization to ensure diagnostic accuracy. The imaging depth, sector width, and time gain compensation (TGC) are choreographed according to the clinical objectives of the physician. In general, the entire imaging screen should be utilized to demonstrate the intended cardiovascular image, while simultaneously optimizing both temporal and spatial resolution.

Once 2D imaging is optimized, color flow imaging can be added to visualize intra-cardiac blood flow. Although the detailed nuances of color flow imaging in cardiac ultrasound are beyond the scope of this chapter, color Doppler interrogation of the cardiac valves can provide rapid confirmation of bedside auscultatory findings as well as identification of abnormalities not appreciated on either 2D echocardiography or auscultation. In this regard, i.e., evaluation of the mitral, tricuspid, and/or aortic valves, the color map scale should be set as high as possible.

Parasternal Imaging

Long-Axis: The probe is placed in the left parasternal region, at the level of the 3rd or 4th intercostal space. Long-axis views, i.e., sagittal or coronal sectioning of the heart from the atrioventricular valve plane to the apex (Fig. 3.1), are obtained with

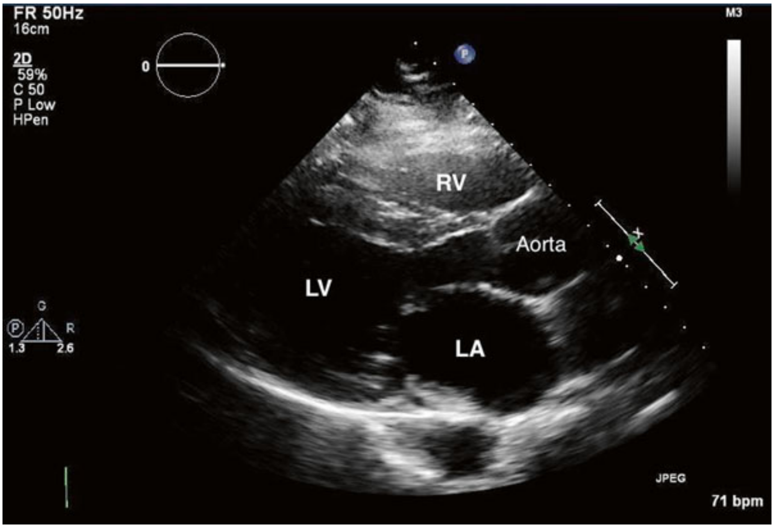

Fig. 3.1 Parasternal long-axis view. Visualization of the right ventricle (RV) superiorly, the left ventricle inferiorly, with the left atrium (LA) and the base or root of the aorta (aorta) on the left of the viewing screen. Also visualized are the left sided heart valves, i.e., the mitral and aortic valves

the transducer groove/notch facing toward the patient's right flank and the ultrasound beam parallel to an imaginary line joining the patient's right shoulder to left flank. As depicted in Fig. 3.1, the long-axis view represents a sagittal section of the heart as viewed from the left side of a supine patient.

The parasternal long-axis (PLAX) view is the most comprehensive single view in the transthoracic echocardiography examination. With this one acoustic window, a qualitative, 2D functional assessment of both ventricles, the left-sided heart valves, and the aortic root can be obtained. The application of color Doppler further augments the interrogation of the mitral and aortic valves.

Short-Axis: Rotating the probe clockwise, (i.e., the plane of the ultrasound beam perpendicular to the plane of previously imaged long-axis view) allows visualizing of the short axis views of the heart. The transducer groove/notch should point superiorly, facing the right supraclavicular fossa, with the imaging beam parallel to an imaginary line joining the left shoulder and right flank.

In a "sweeping" fashion, the transducer is rotated in an anterior/caudal direction from a posterior/cranial angulation. In this manner, a cross section of the right ventricle and left ventricle, extending from the AV valves, through the middle of the ventricles, and out to apex, is obtained. Images are generated as if looking from the apex of the heart up toward the atria, i.e., LV is posterior and on the right, the RV is anterior and on the left (Fig. 3.2).

The parasternal short-axis imaging is classically divided into three regions: (1) Base of the heart—the level of the mitral valve leaflets, (2) Mid-ventricle—the level of the anterolateral and posteromedial papillary muscles, and (3) Apex—distal to the papillary muscle head insertion. In a "Point of Care" environment, parasternal short axis imaging is instrumental in the rapid assessment for ventricular morphology and function.

Apical Imaging

Apical imaging is also obtained with the patient in the left lateral decubitus position. The transducer, however, is placed at or in the immediate vicinity of the point of maximal impulse (typically lateral and inferior to the left nipple). Three primary views are obtained from this position, all complimentary to the three short axis slices obtained from the parasternal windows, i.e., four-chamber view, apical long-axis view, and the two-chamber view. When combined, the apical long-axis and the parasternal short-axis images provide visualization of each segment of the left ventricle and therefore a complete view of left ventricular function.

Apical imaging display is arbitrary and determined via the physician acquiring the images, i.e., with the notch/groove of the transducer pointing upward, the left ventricle is on the right side, and with the notch/groove of the transducer pointing downward, the left ventricle is on the left side.

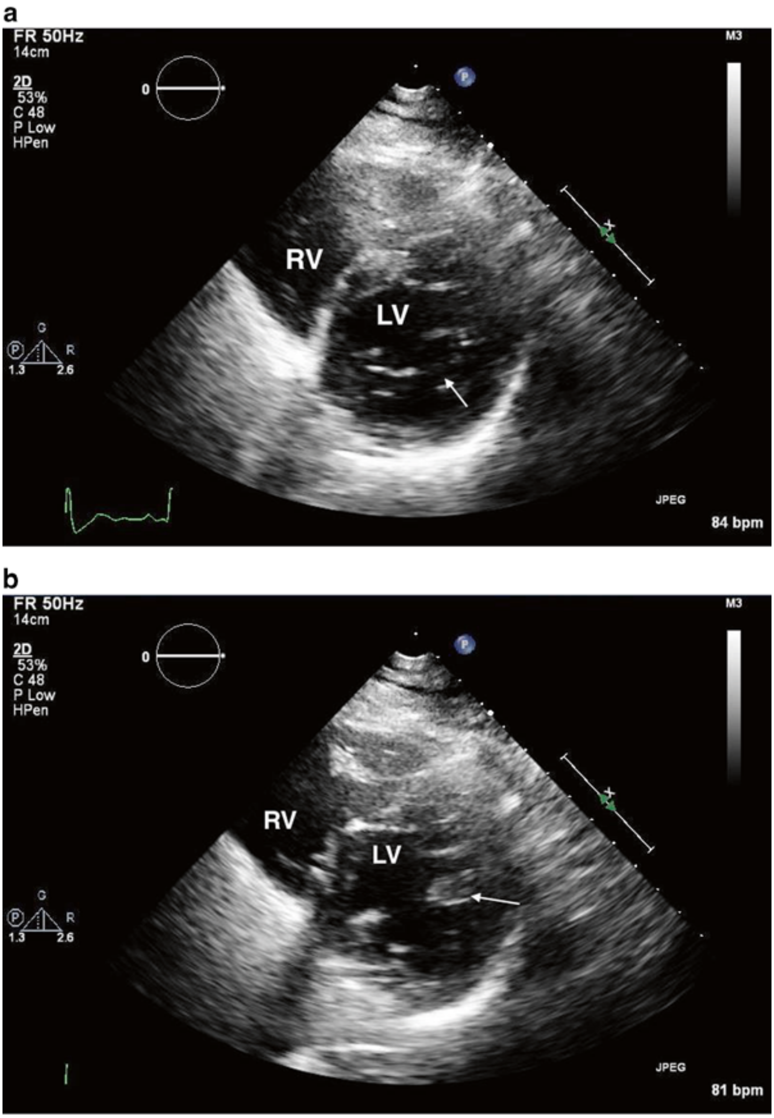

Fig. 3.2 Parasternal short axis views. Multiple short axis images through the right and left ventricles are obtained from the base of the heart (atrioventricular (AV) valve level) to the apex. (**a**) Base of the ventricles: The anterior and posterior mitral valve leaflets are seen in cross section (*arrow*). The right ventricle (RV) is anterior and on the right, the left ventricle (LV) is posterior and on the left. (**b**) Mid-ventricular level: The bodies of the anterolateral and posteromedial papillary muscles are visualized in cross section (*arrow*). (**c**) Apex: The apex of the right (RV) and left (LV) ventricles are displayed in cross section. The heads of the papillary muscle heads are not included in this view

c

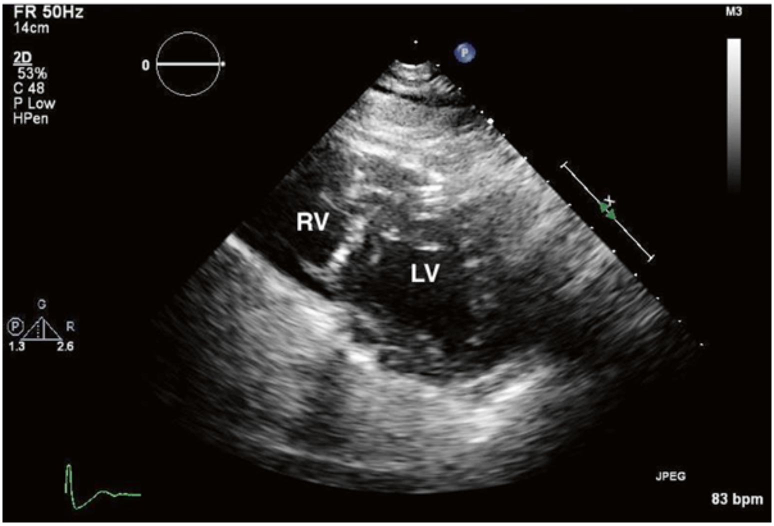

Fig. 3.2 (continued)

Four-Chamber View

With the ultrasound beam directed superiorly and medially (towards the patient's right scapula), the ventricles, atria, interatrial and interventricular septa, and the AV valves are visualized in a single image. The apex of the left ventricular is positioned at the top of the image and the atria at the bottom. The goal of this image, via delicate manipulation the ultrasound beam anteriorly and posteriorly, is to visualize the atrial and ventricular septa in their entirety (Fig. 3.3). With regards to anatomic landmarks, the right-sided chambers are demarcated via the inferior insertion, by 5–10 mm, of the septal leaflet of the tricuspid valve relative to the anterior leaflet of the mitral valve on the left.

Apical Long-Axis View

From the four-chamber view, rotating the ultrasound transducer in a clockwise fashion, the aortic valve and aortic root appear where the crux of the heart was previously seen in the four-chamber window (Fig. 3.4). This view is analogous to the parasternal long-axis view and is the primary window by which qualitative and quantitative assessment of aortic valve pathology and overall myocardial function are obtained, i.e., stroke volume and cardiac output.

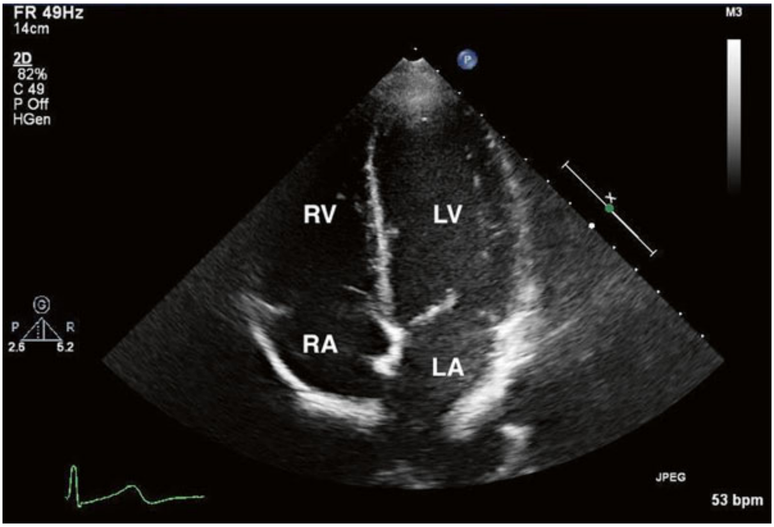

Fig. 3.3 Apical four-chamber view. As per standard echocardiographic convention, the left sided chambers of the heart are displayed on the left side of the imaging screen. The right (RV) and left (LV) ventricles, and the right (RA) and left (LA) atria are partitioned by the interventricular and interatrial septa, which join at the fibrous trigone of the atrioventricular (AV) valves to form the crux of the heart. The atrioventricular valves (mitral and tricuspid) are visualized as well; note the apical displacement, relative to the anterior mitral valve leaflet, of the septal leaflet of the tricuspid valve

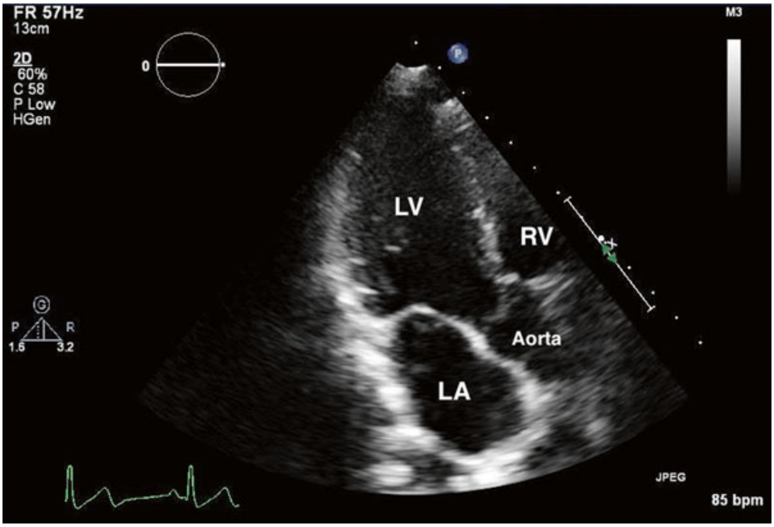

Fig. 3.4 Apical long-axis view. Clockwise rotation from the apical four-chamber position results in a long-axis image displaying the left ventricular outflow tract, the aortic valve, and the base or root of the aorta (Aorta). This view is comparable to the parasternal long-axis view, rotated visually clockwise 90°

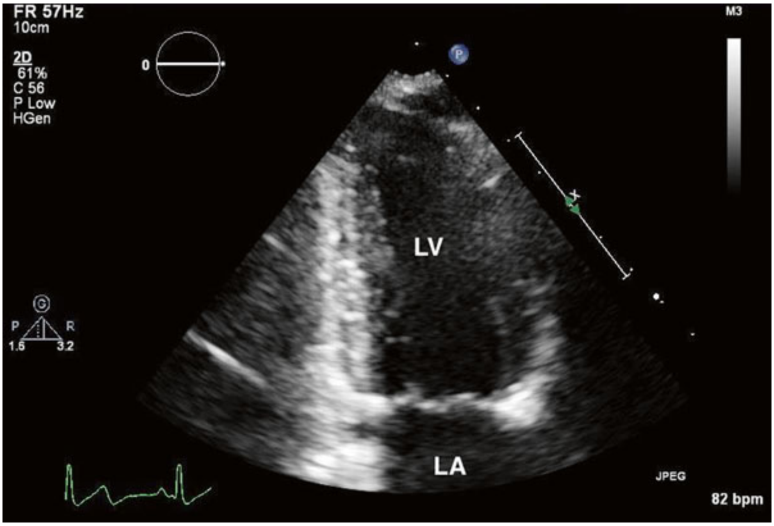

Fig. 3.5 Apical two-chamber view. Clockwise rotation from the apical long-axis view results in a two-chamber image. The entire anterior and inferior walls of the heart are visualized, along with the mitral valve. Left ventricle (LV). Right ventricle (RV)

Two-Chamber View

From the apical long-axis view, further clockwise rotation of the transducer head results in a sagittal view of the left-heart or the two-chamber view (Fig. 3.5). The left atrial appendage is superior (at the atrial level), with the anterior and inferior walls of the visualized in their entirety. Right-sided structures are not visualized in this view.

Subcostal Imaging

Subcostal imaging windows generally provide supplemental/alternative views for visualization of cardiac structure and function in patients with otherwise suboptimal precordial acoustic windows, i.e., chronic obstructive lung disease, etc. Additionally, this location is specifically designed for the noninvasive assessment of right atrial filling pressures and the integrity of the interatrial septum. From a "Point of Care" viewpoint, discussion of subcostal imaging will be limited to the noninvasive assessment of central filling pressures, i.e., long-axis visualization of the inferior vena cava.

Unlike parasternal and apical imaging, subcostal imaging is performed with the patient in the supine position. The ultrasound transducer is placed midline or slightly off-set to the patient's right, with the transducer groove/notch pointed

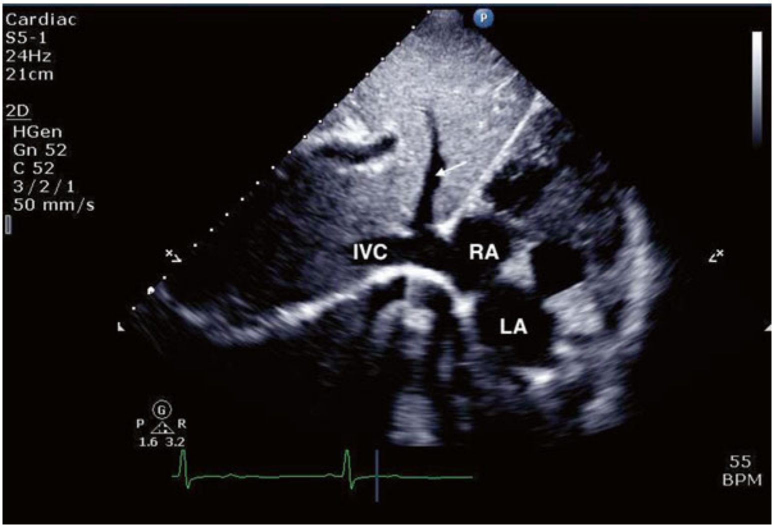

Fig. 3.6 Subcostal view. With the patient supine, the long axis of the inferior vena cava (IVC) is visualized, allowing approximation of right atrial (RA) pressures. Visualization of the hepatic veins (*arrow*), i.e., size and location, can also aid in the assessment of the central volume status. Left atrium (LA)

toward the patient's right flank. Tilting the ultrasound head inferiorly and rightward, the long axis of the inferior vena cava is brought into view. The vessel width and respiratory variation combine to approximate the central venous filling pressure (Fig. 3.6).

Clinical Utility

The clinician's comprehension of the clinical dilemma in question is paramount to the strategic use of bedside echocardiography in a "Point of Care" model. Given the numerous echocardiographic views, judicious selection of imaging planes is essential for the efficient and practical use of this modality; the physical examination is the foundation of this selection process.

The following clinical vignettes highlight the "Point of Care" use of bedside echocardiography.

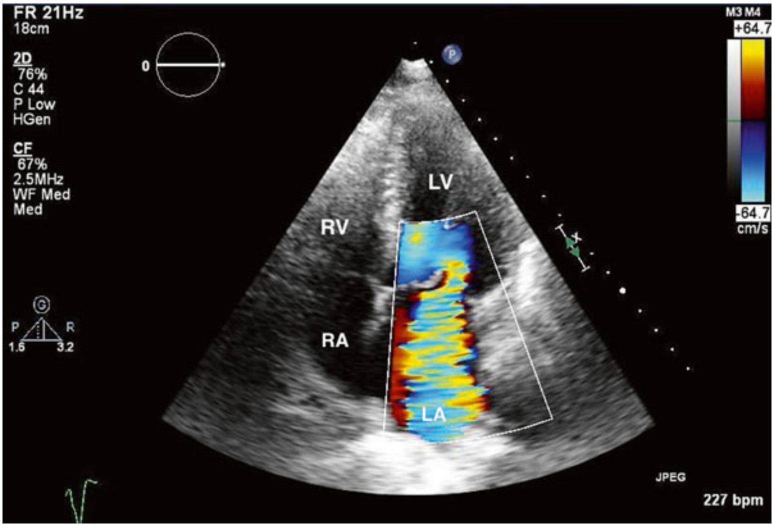

Fig. 3.7 Apical four-chamber view with color Doppler over the mitral valve. Severe, posteriorly directed, mitral valve regurgitation. The left atrium (LA) is severely dilated. Left ventricle (LV). Right ventricle (RV). Right atrium (RA)

1. Incidental murmur: a 75-year-old female with a 6-month history of generalized fatigue, and a 3/6 holosystolic murmur auscultated at the apex. See Fig. 3.7.
2. Palpitations/arrhythmias: a 56-year-old male recently convalescing from a viral upper respiratory infection with intermittent palpitations and associated dizziness; S3 and S4 auscultated at the apex. See Fig. 3.8.
3. Chest pain: an 81-year-old male with 3-month history of exertional chest pain and recent episode of pre-syncope while grocery shopping; 2–3/6 crescendo–decrescendo murmur auscultated at the base. See Fig. 3.9.
4. Shortness of breath: a 63-year-old female with a 12-month history of progressive exertion dyspnea; 1–2/6 diastolic inflow murmur auscultated at the apex. See Fig. 3.10.
5. Hypotension: a 77-year-old male with persistent hypotension, lightheadedness, and fatigue 8 weeks after aortic valve surgery. See Fig. 3.11.

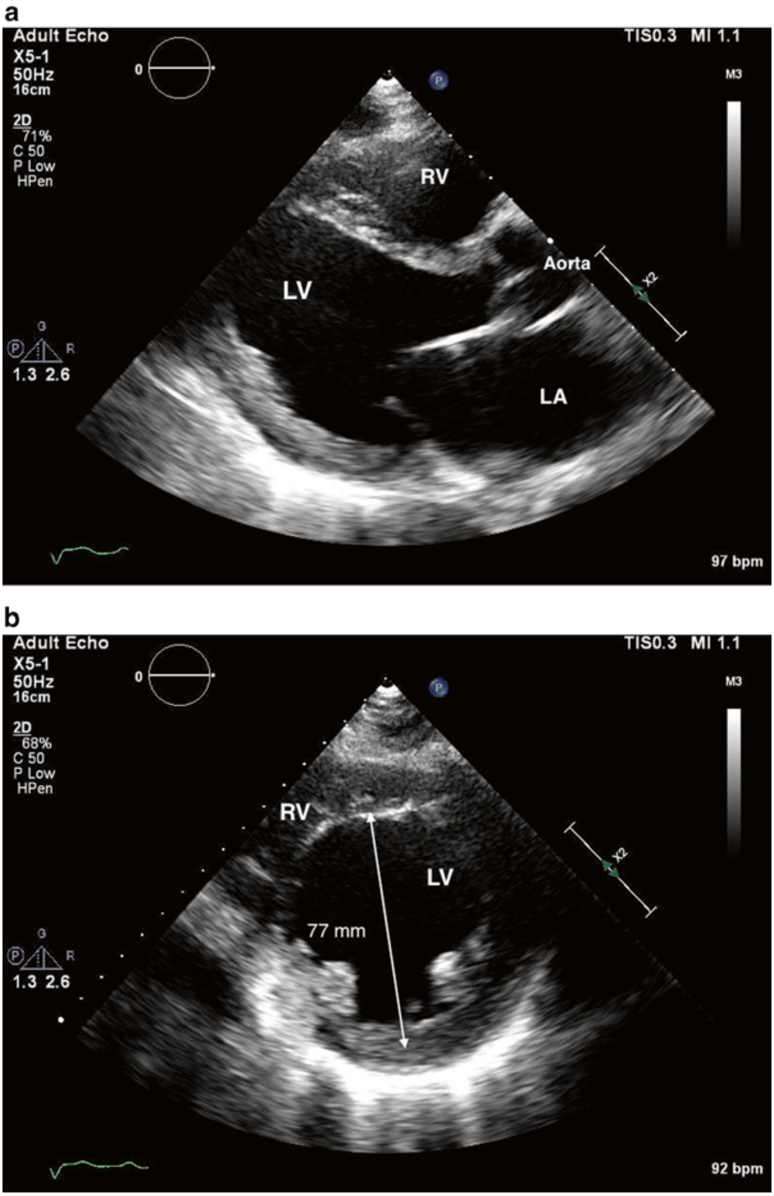

Fig. 3.8 Parasternal long axis (**a**) and corresponding parasternal short axis (**b**) views. Severe left ventricular (LV) enlargement, with an end-diastolic dimension of 77 mm (upper limit of normal 57 mm). The right ventricle (RV), as seen in (**a**), is also enlarged

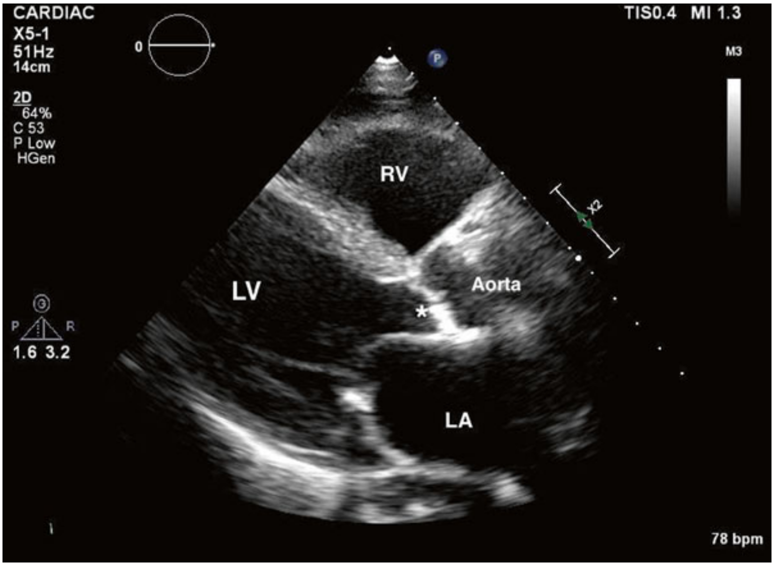

Fig. 3.9 Parasternal long-axis view. The aortic valve (asterisk), as seen in cross section, is severely calcified. On cine imaging, minimal systolic leaflet excursion was noted. Left ventricle (LV). Right ventricle (RV). Left atrium (LA). Base of the aorta/aortic root (Aorta)

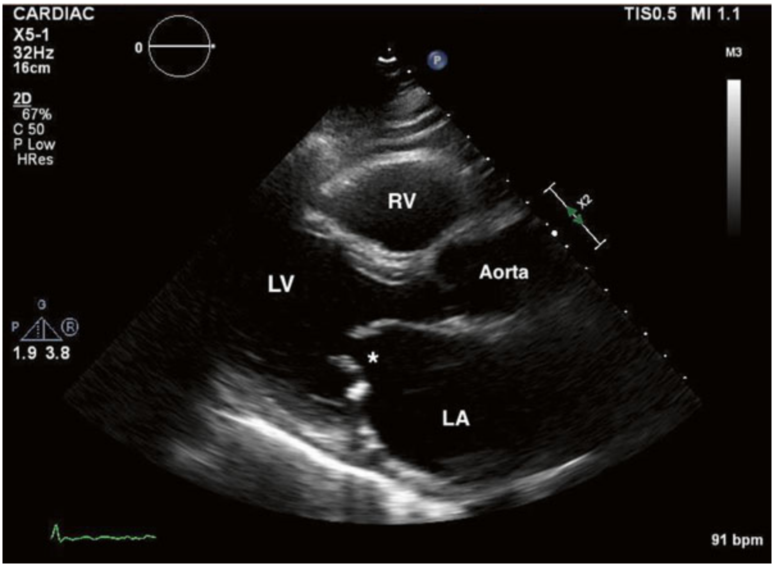

Fig. 3.10 Parasternal long-axis view. Mitral annular calcification with thickened mitral valve leaflets (*asterisk*) and restricted end-diastolic leaflet excursion. Morphology characteristics suggestive of Rheumatic mitral valve disease. Left ventricle (LV). Right ventricle (RV). Left atrium (LA). Base of the aorta/aortic root (Aorta)

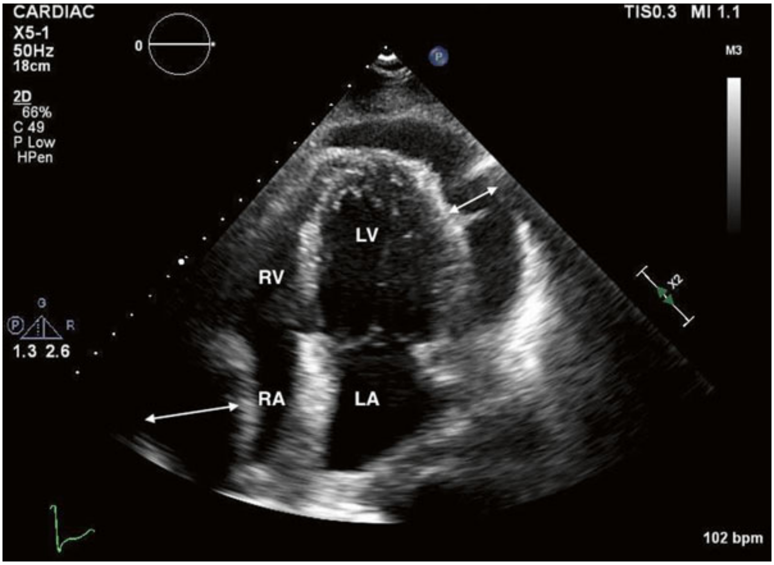

Fig. 3.11 Apical four-chamber view. Near circumferential pericardial effusion (*arrows*), with mass effect on the right atrium (RA) and impaired right atrial filling, i.e., tamponade physiology. Note leftward deviation of the interatrial septum. Thickening of the epicardial surface of the left ventricle, with adherent debris within the pericardial fluid, suggestive of an inflammatory/reactive process. Left ventricle (LV). Right ventricle (RV). Left atrium (LA)

Suggested Readings

1. The Echo Manual, 3rd edition; OH JK, Seward JB, and Tajik AJ. Lippincott Willaims & Wilkins. 2006
2. Solomon SD, Saldana F. Point-of-care ultrasound in medical education – stop listening and look. New England Journal of Medicine March 20, 2014 (370;12), 1083–1085.
3. Roelandt JRTC. The decline of our physical examination skills: is echocardiography to blame? European Heart Journal – Cardiovascular Imaging (2014) 15, 249–252.
4. Llebo MJ, et al. Is pocket mobile echocardiography the next-generation stethoscope? A cross-sectional comparison of rapidly acquired images with standard transthoracic echocardiography. Annals of Internal Medicine 2011;155:33–38.

Chapter 4
Dermatologic Ultrasound

Ximena Wortsman

Introduction

The usage of ultrasound in dermatology has been rapidly growing in recent years, and currently this application has been proven useful for studying common dermatologic entities such as benign and malignant tumors, inflammatory diseases, nail and scalp conditions as well as cosmetic complications [1, 2]. The usage of ultrasound in dermatology started with high and fixed frequency probes that function in small devices.

Currently, common dermatologic conditions are studied with high and variable frequency probes that can reach up to 22 MHz. These probes can vary for example from 7 to 15 MHz, 7 to 18 MHz or 7 to 22 MHz according to the manufacturer. These machines have sensitive color and power Doppler capabilities and high definition for superficial and deep structures. Moreover, with the same probe it is possible to observe the echostructure of the skin layers, tendons, muscles, and even the bony margin in some corporal locations. If more penetration is needed it is possible to change the probe for a lower frequency device [3].

X. Wortsman, M.D. (✉)
Department of Radiology, Faculty of Medicine, Institute for Diagnostic Imaging and Research of the Skin and Soft Tissues,
Clinica Servet, University of Chile, Las Condes, Chile
e-mail: xworts@yahoo.com

J.M. Daniels, R.A. Hoppmann (eds.), *Practical Point-of-Care Medical Ultrasound*, DOI 10.1007/978-3-319-22638-5_4

Main Advantages of Dermatologic Ultrasound

The main advantages are the real time observation of the skin layers and deeper structures in high definition including their patterns of vascularity. Ultrasound is a very good discriminator between lesional and non-lesional tissue, dermatologic and non-dermatologic origin, and endogenous and exogenous structures [1–3].

Main Limitations of Dermatologic Ultrasound

The main limitations of ultrasound in dermatology are the lack of observation of epidermal-only lesions measuring ≤0.1 mm, and the detection of pigments such as melanin [4]. Another limitation is the difficulty of detecting structures obscured by air or bone. This technique also requires a trained operator in dermatologic conditions and a suitable high frequency device [1–3].

Technical Requirements

The requirements for performing this type of ultrasound examination are:

- Multichanneled equipment with a ≥15 MHz compact linear or linear high frequency probe(s).
- An operator trained in dermatologic pathologies and the ultrasound technique.
- The lighting in the room should be managed when dealing with multiple lesions to properly locate the probe [1–3, 5].

Normal Ultrasound Anatomy

Skin

The skin presents a different appearance according to the regions of the body:

Non-glabrous Skin (i.e., Not That of the Palms and Soles)

Epidermis: monolaminar bright hyperechoic epidermis whose echogenicity is mainly provided by the keratin content in the stratum corneum.

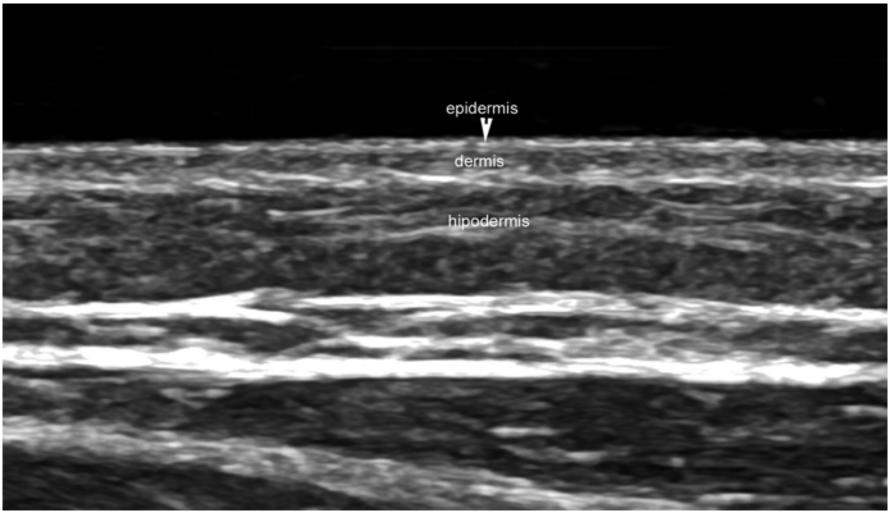

Fig. 4.1 Normal sonographic anatomy of the skin

Dermis: hyperechoic band, less bright than the epidermis. The dermal echogenicity is mainly provided by collagen. A subepidermal hypoechoic band appears in the upper dermis of sun-exposed regions (SLEB: subepidermal low echogenicity band); this corresponds to the deposition of glycosaminoglycans in the skin which is a sonographic sign of photoaging.

Hypodermis (synonym: subcutaneous tissue): a hypoechoic layer with hyperechoic septa. This echogenicity is provided by fatty lobules surrounded by fibrous septa [1–3, 5, 6] Fig. 4.1.

Glabrous Skin (i.e., Palms and Soles)

Epidermis: bilaminar and thick bright hyperechoic layer due to more prominent keratin content.

Dermis and *Hypodermis* present similar appearance to non-glabrous skin [1–3, 5, 6].

Pathology

Epidermal Cyst

Causes: implantation of epidermal elements in the dermis and/or hypodermis.

Ultrasound: The appearance may vary. If the cyst is intact, patients present with a well-defined, round or oval shaped, anechoic structure located in the dermis and/or

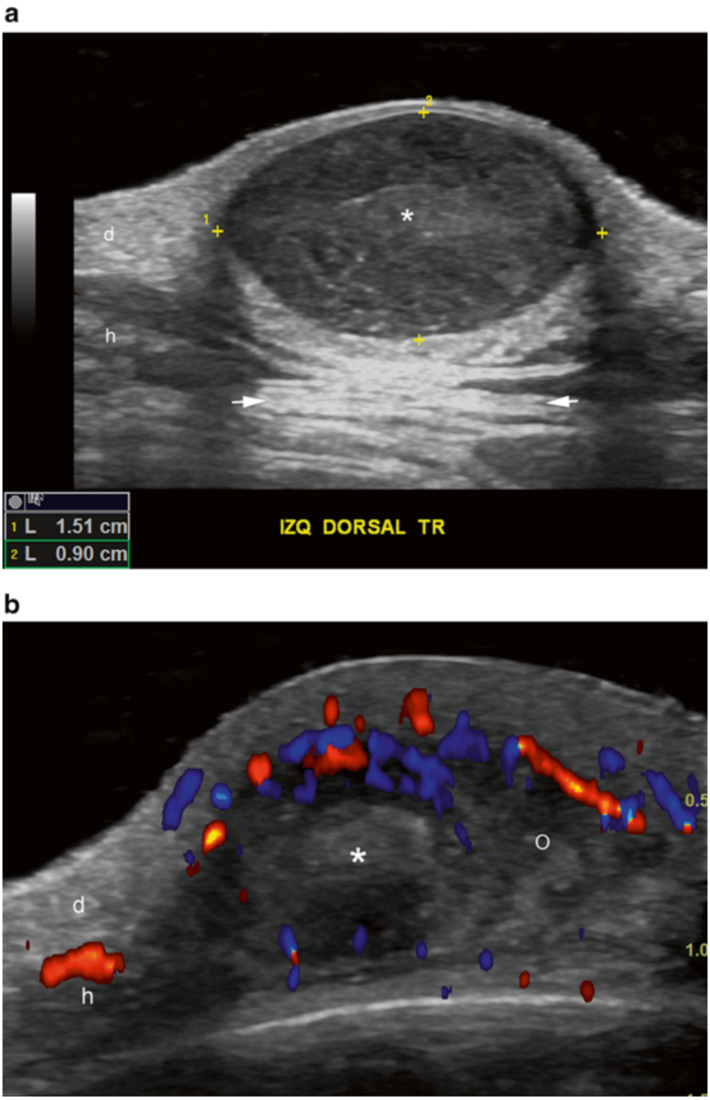

Fig. 4.2 (**a**) (*Top*). Epidermal cyst, intact. Hypoechoic oval shaped structure (*) in the dermis and hypodermis with posterior acoustic enhancement artifact (*arrows*). (**b**) (*Bottom*). Ruptured. On color Doppler the cyst (*) presents inflammation and there is spreading of the keratinous material (o) in the right aspect of the image. (d = dermis; h = hypodermis)

hypodermis with posterior acoustic enhancement artifact (Fig. 4.2a). An anechoic connecting tract to the subepidermal region called "punctum" may also be detected. Giant epidermal cysts can show as hypoechoic with anechoic filiform bands due to compacted keratin deposits and an increased presence of cholesterol crystals; this appearance has been called "pseudotestes appearance" due to their resemblance to

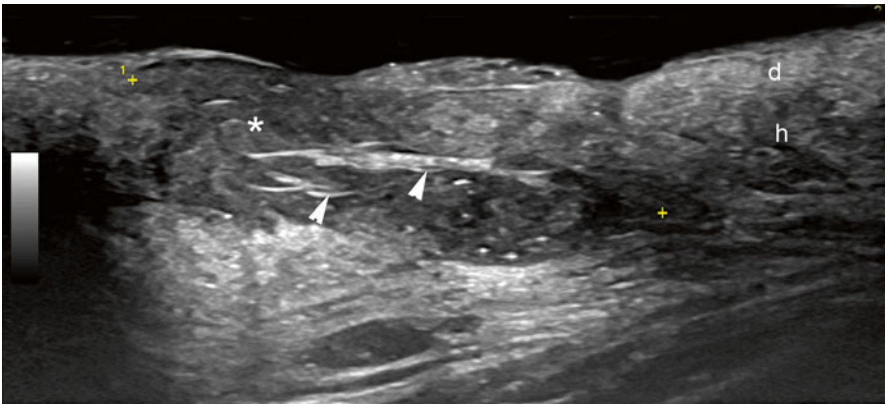

Fig. 4.3 Pilonidal cyst. Notice the hypoechoic structure (*) with fragments of hair tracts (*arrowheads*) involving dermis and hypodermis. (d = dermis; h = hypodermis)

the sonographic pattern of the testes. Inflamed cysts may show hyperechoic material. They are larger in size and have increased peripheral vascularity. When the cyst is ruptured, the cyst becomes irregular and the hypoechoic keratinous material can be seen in the periphery, usually generating a "foreign body-like" reaction [4, 7–9] Fig. 4.2b.

Key Sonographic Sign: The posterior acoustic enhancement artifact.

Pilonidal Cyst

Causes **:** Hairy individuals exposed to chronic friction in the intergluteal region.

Ultrasound **:** A nest of hyperechoic linear tracts that correspond to fragments of hair tracts trapped in the dermis and hypodermis, surrounded by hypoechoic inflammatory tissue (Fig. 4.3). Commonly, these cysts are connected to the base of widened regional dermal hair follicles. On color Doppler they often show hypervascularity in the periphery due to inflammation and/or infection, in the latter case this is a pilonidal abscess. The aim of the ultrasound study is to show the nature, actual axis and extent of the cyst, which may support the surgical planning [1, 2, 10, 11].

Key Sonographic Sign: Hyperechoic linear tracts corresponding to the hair tract fragments.

Pilomatrixoma

Synonyms: Calcifying epithelioma of Malherbe or pilomatricoma.

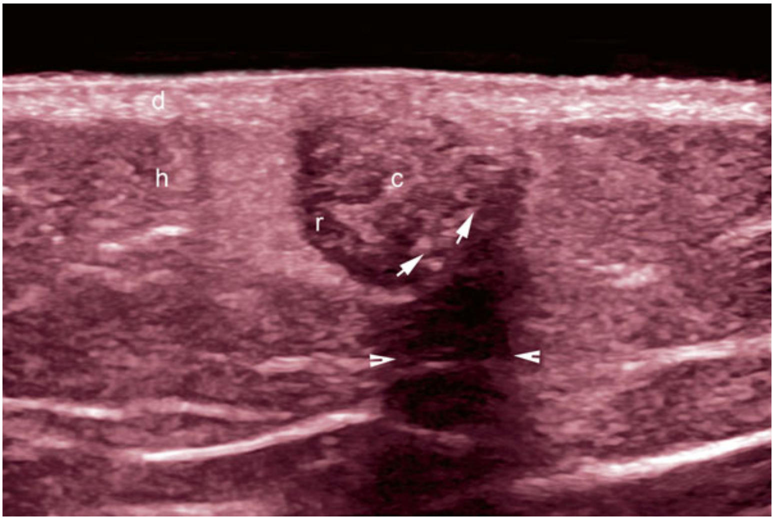

Fig. 4.4 Pilomatrixoma. Target type of nodule with hypoechoic rim (r) and hyperechoic center (c) that shows hyperechoic spots that correspond to calcium deposits (*arrows*). Notice the posterior acoustic shadowing due to the calcium deposits (*arrowheads*). (d = dermis; h = hypodermis)

Causes: This is a hair matrix derived tumor most frequently seen in children and young adults and located in the face and extremities. The rate of clinical diagnostic error reported is up to 56 %, therefore ultrasound has an important role in their diagnosis.

Ultrasound: The "target type" of appearance is the most frequent form of presentation and shows as a dermal and hypodermal nodule with a hypoechoic rim and an hyperechoic center with multiple hyperechoic dots corresponding to the calcium deposits. The degree of calcification of these tumors may vary and in cases with large deposits of calcium, a posterior acoustic shadowing may be detected (Fig. 4.4). The presence of blood flow may be variable, going from hypo to hypervascularity with slow flow arterial and venous vessels in the center and periphery. Rarely, pilomatrixomas can show hypervascularity and clinically mimic a vascular tumor. Another form of presentation is the cystic Pilomatrixoma due to internal bleeding, which appears as an anechoic cystic structure with an eccentric hypoechoic solid nodule with hyperechoic spots [10, 12–15].

Key Sonographic Sign: Hyperechoic spots due to calcifications.

Dermatofibroma

Synonyms: Fibrous histiocytoma and histiocytoma cutis.

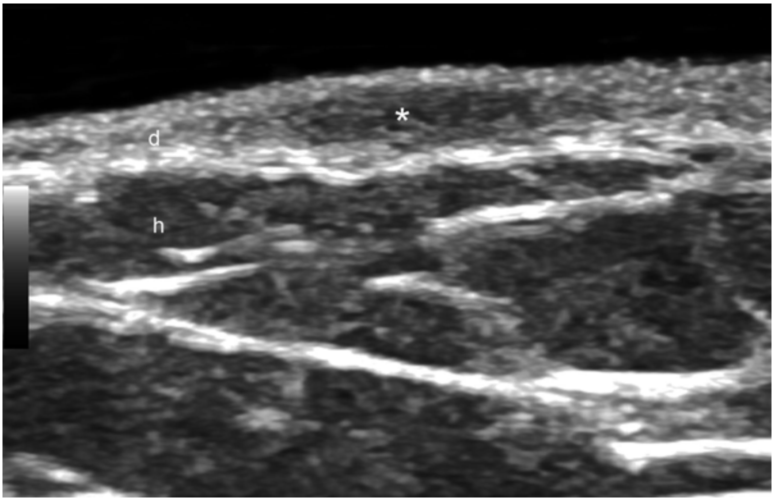

Fig. 4.5 Dermatofibroma. Ill-defined hypoechoic lesion (*) that distorts the regional hair follicles. (d = dermis; h = hypodermis)

Causes: This is a fibromatous tumor most commonly seen in the trunk and extremities of females. It has been postulated to be a reactive reaction to trauma such as an insect bite and also a benign neoplastic disorder.

Ultrasound: An ill-defined hypoechoic and heterogeneous solid dermal structure usually with distortion and enlargement of the regional hair follicles (Fig. 4.5). Vascularity may be variable, commonly with thin, slow flow arterial and venous vessels [10].

Key Sonographic Sign: Distortion of the lesional hair follicles.

Lipoma

Causes: A benign proliferation of mature adipose cells. According to the tissue that accompanies these fatty cells the lipoma may be called fibrolipoma (fibrous tissue) or angiolipoma (capillary vessels). Lipomas are the most common soft tissue tumor and they are usually single, however they can be multiple.

Ultrasound: They show as round or oval shaped hypodermal structures that tend to follow the axis of the skin layers and present hyperechoic septa. Their echogenicity also changes according to the type of tissue that is attached to the adipose cells. Thus, fibrolipomas tend to show hypoechogenicity and angiolipomas present hyperechogenicity. The sonographer should be aware of risky locations of lipomas such as the neck or temple regions where thick vessels or nerves can be located in the vicinity. Occasionally, lipomas can be located underneath the epicranius muscle in the frontal region, an entity called subgaleal lipoma, which may clinically simulate an epidermal cyst or an exostosis. Frequently, lipomas are hypovascular, and the presence of heterogenicity and hypervascularity within the tumor support the suspicion of a malignant transformation [10, 16–18].

Key Sonographic Sign: Structure that follows the axis of the skin layers. Caution; lipomas are usually located in the more superficial areas of the skin. If a lesion is scanned deeper next to the muscle, the patient should be referred for further workups as malignancies can present this way.

Malignant Tumors

Non-melanoma Skin Cancer (NMSC)

GeneralConcepts: NMSC is the most frequent cancer in human beings and frequently affects highly sun-exposed areas of the body such as the face. NMSC is conformed by basal cell (BCC) and squamous cell carcinoma (SCC), BCC being the most common type. Although NMSC is rarely lethal, it is highly disfiguring nevertheless. The ultrasound–histology correlation of the depth of BCC has been reported as excellent.

Ultrasound: They present as hypoechoic and/or heterogeneous oval shaped lesions with irregular or lobulated borders, commonly located in the dermis. BCC typically shows hyperechoic spots within the tumor and the extent of the presence of these spots seems to be correlated with the high or low risk of recurrence of histologic subtypes (Fig. 4.6). BCCs with a higher number of hyperechoic spots (≥7) have

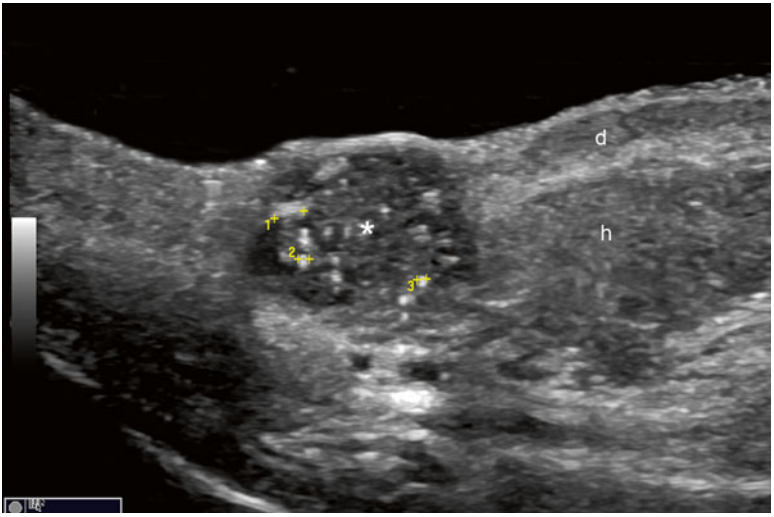

Fig. 4.6 Basal cell carcinoma. Hypoechoic oval shaped structure (*) with hyperechoic spots (between markers) that involves dermis and hypodermis. (d = dermis; h = hypodermis)

been reported to correlate well with more aggressive histologic subtypes such as micronodular, morpheiform, sclerosing, infiltrating, and metatypical subtypes [19–24]. SCCs do not present hyperechoic spots and tend to be more infiltrating than BCCs, more easily extending into the underlying muscle or cartilage. On color Doppler, NMSC presents slow flow vascularity within the lesions with arterial and venous vessels; SCC is usually more hypervascular than BCC [22].

Objective of the Examination: To support the detection of the NMSC lesion, define its extent, including depth, support the prediction of type (BCC or SCC) and also the subtype (high or low risk of recurrence BCC) as well as demonstrate the involvement of deeper layers.

Key Sonographic Sign: Hyperechoic spots for BCC.

Melanoma

*General Concepts:*Melanoma is the most lethal form of skin cancer and is usually a hyperpigmented lesion. However, there are amelanotic melanomas where the pigment is hidden in the tumor. Melanomas tend to rapidly spread into nodal or extranodal metastases.

Primary Tumor

General Considerations: In spite of the fact that melanoma is not the most frequent type of skin cancer, it is the most aggressive type. The recurrence of melanoma has been reported to be up to 46.1 % in lesions of the head and neck region. Importantly, the prognosis of the patient is provided by the depth of the tumor invasion through the Breslow index. This is a histologic measurement of how deep the tumor is. However, ultrasound can also measure the extent of the tumor by providing a sonographic Breslow index. Ultrasound can help to differentiate melanomas that measure < or >1 mm; this can support relevant clinical decisions such as the noninvasive assessment of the free margins for surgery, the size of the excision and the performance of a sentinel node procedure (indicated in melanomas measuring >1 mm).

Ultrasound: They tend to show as well-defined, hypoechoic and or heterogeneous oval shaped and usually fusiform structures located in the dermis and/or hypodermis. Frequently, they show hypervascularity due to their angiogenic power and also may extend to deeper layers (Fig. 4.7a, b). Using color Doppler and contrast enhanced ultrasound studies, it has been reported that the degree of malignancy usually correlates well with the degree of vascularity [25–32].

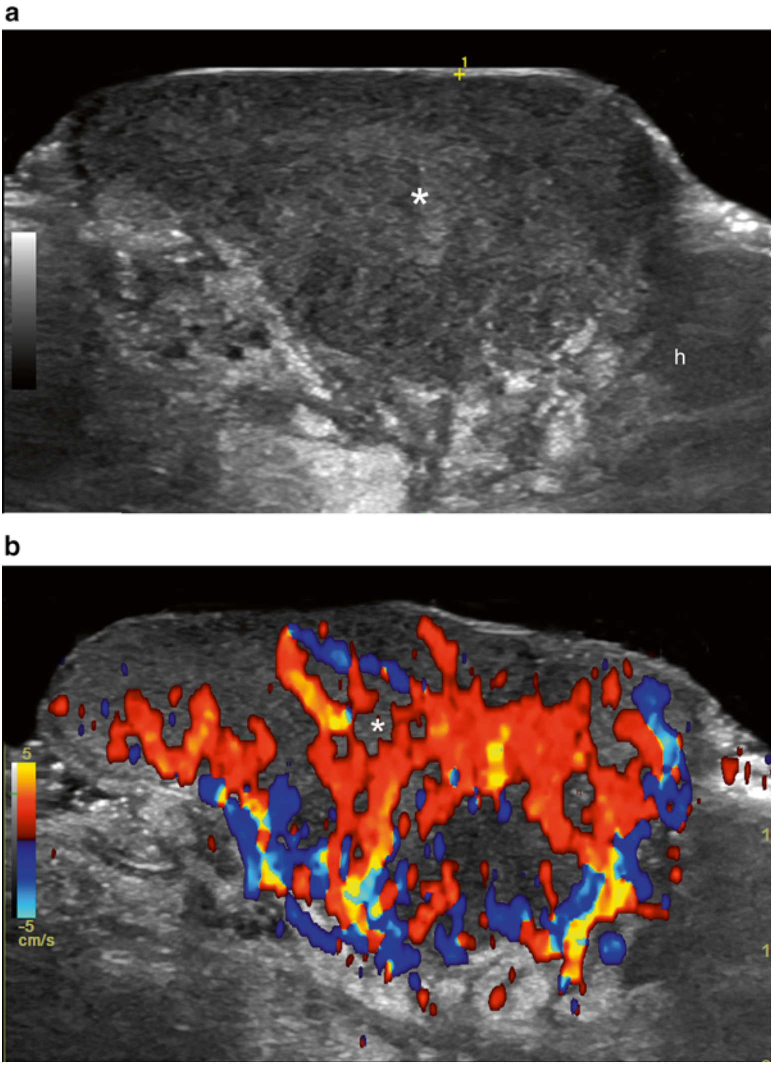

Fig. 4.7 (**a**) (*Top*). Melanoma . Grey scale shows hypoechoic oval shaped mass (*) involving dermis and hypodermis (h). (**b**) (*Bottom*). On color Doppler prominent vascularity is detected within the mass (*)

Locoregional Staging

General Concepts: Ultrasound is more sensitive than clinical palpation for the diagnosis of metastasis. Ultrasound has been proven useful for diagnosing extranodal and nodal metastasis [25].

Extranodal Metastases

These can be separated into satellites (<2 cm from the primary tumor) and in-transit (≥2 cm from the primary tumor). Satellite or in-transit metastases often appear as hypoechoic nodules with irregular borders and increased echogenicity of the surrounding hypodermis due to perilesional edema. Metastases can show anechoic areas, most probably due to increased transmission of the sound in hypercellular regions. Hypervascularity through irregular, thick and tortuous vessels may also be seen [33–40].

Nodal Metastases

Lymph node criteria for benignancy and malignancy are shown in Table 4.1. This staging follows the lymphatic drainage according to the anatomical location of the tumor. Additionally, ultrasound can support a percutaneous fine-needle aspiration (FNA) cytology (FNAC) or biopsy (FNAB) of the lymph nodes [41–44].

Key Sonographic Sign: Fusiform hypoechoic and hypervascular structure in correlation with a hyperpigmented lesion.

Vascular Anomalies

General Concepts: These usually affect the pediatric population and are common lesions for referral. The most common vascular anomalies that are sent for ultrasound examination are hemangiomas and vascular malformations. These have different origins, evolution, treatment and prognosis. Thus, sonographic support in the differentiation of these two entities can be critical for proper management.

Table 4.1 Color Doppler ultrasound of benign and malignant lymph nodes

Ultrasound morphology	Benign	Malignant
Shape	Oval	Round
Center	Hyperechoic	Hypoechoic/anechoic
Cortex thickening	Diffuse	Nodular, eccentric
Ratio longitudinal/transverse	>2	<2
Vascularity	Regular, central	Irregular, peripheral
Cortex vessels	Absent/few	Present/prominent

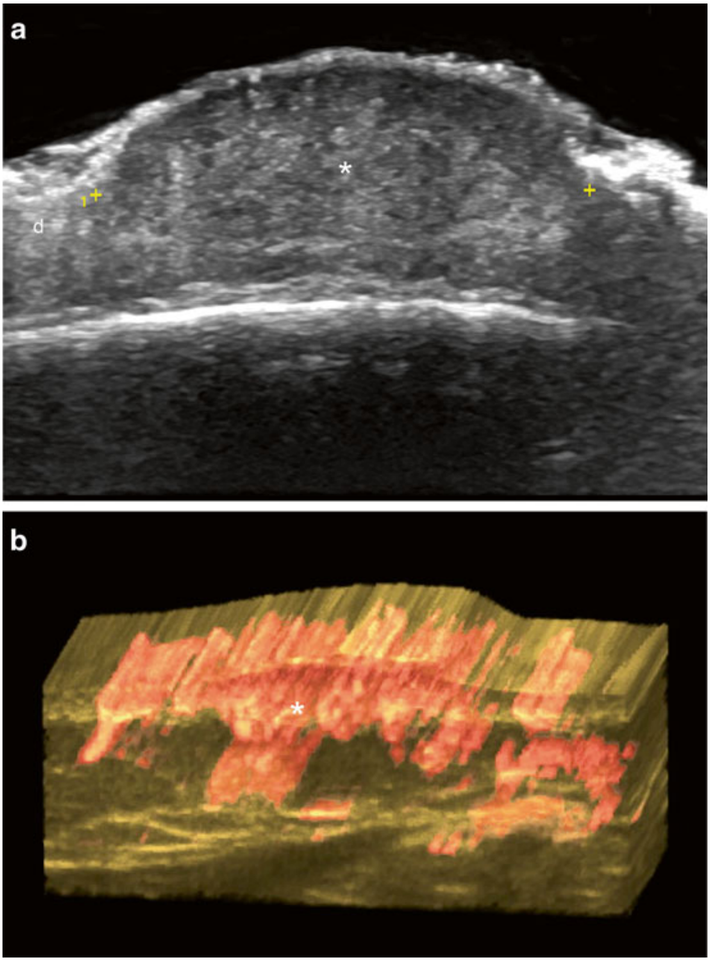

Fig. 4.8 (**a**) (*Top*). Hemangioma partial regression phase. Ill-defined heterogeneous structure (*) that involves dermis and hypodermis. (**b**) (*Bottom*). 3D power angio reconstruction demonstrates areas with prominent vascularity (*) within the lesion and areas without detectable flow

Hemangiomas

General Concepts: These are the most common soft tissue lesions in infancy and present rapid growth during the first year and then they start a slow regression period.

Ultrasound: The sonographic appearance of hemangioma varies according to the phase. In the proliferative phase, they show as an ill-defined hypoechoic mass with hypervascularity that includes arterial and venous vessels and some arteriovenous shunts. In the partial regression phase, the echogenicity becomes mixed and the lesion presents hypoechoic and hyperechoic regions (Fig. 4.8a, b). The blood flow also decreases in this phase. In the total regression phase, the hemangioma turns to hyperechoic and hypovascular. Ultrasound may support the follow-up of the treatment and provide anatomic information on the current extent, phase, and involvement of deeper layers or structures such as muscle, cartilage, glands, or the ocular globe. Also ultrasound can be used for monitoring treatment such as propranolol [45–48].

Key Sonographic Sign: Ill-defined hypoechoic or heterogeneous hypervascular structure that changes in its echogenicity and degree of vascularity over time.

Vascular Malformations

General Concepts: These are errors of morphogenesis and do not comprise an actual tumor. They can be separated according to the type of vessel (arterial, venous, capillary, or lymphatic) and to the high (arterial or arteriovenous) or low flow (venous, capillary, or lymphatic).

Ultrasound: A sonographic sign is the presence of a nest of anechoic tubular structures or lacunar spaces. Thus, on color Doppler ultrasound with spectral curve analysis, they can demonstrate their arterial (with systolic and diastolic component), venous (monophasic), or arteriovenous (to and fro flow) features (Fig. 4.9a, b). Capillary vascular malformations can show epidermal thickening, decreased echogenicity of the upper dermis or increased echogenicity of the hypodermis and lack of blood flow due to their being very slow velocity vessels. Ultrasound can also guide a percutaneous sclerosing procedure [45–47].

Key Sonographic Sign: anechoic tubular and tortuous nest of vessels.

Inflammatory Diseases

Psoriasis

General Concepts: A chronic autoimmune inflammatory disorder that involves the skin, nail, tendons, joints, and bone.

Ultrasound

Skin: psoriatic cutaneous plaques show as thickening of the epidermis and decreased echogenicity of the upper dermis. Occasionally, undulation of the epidermis may also be seen. On color Doppler examination, dermal hypervascularity with slow flow arterial and venous vessels may be detected in the subepidermal region (Fig. 4.10a).

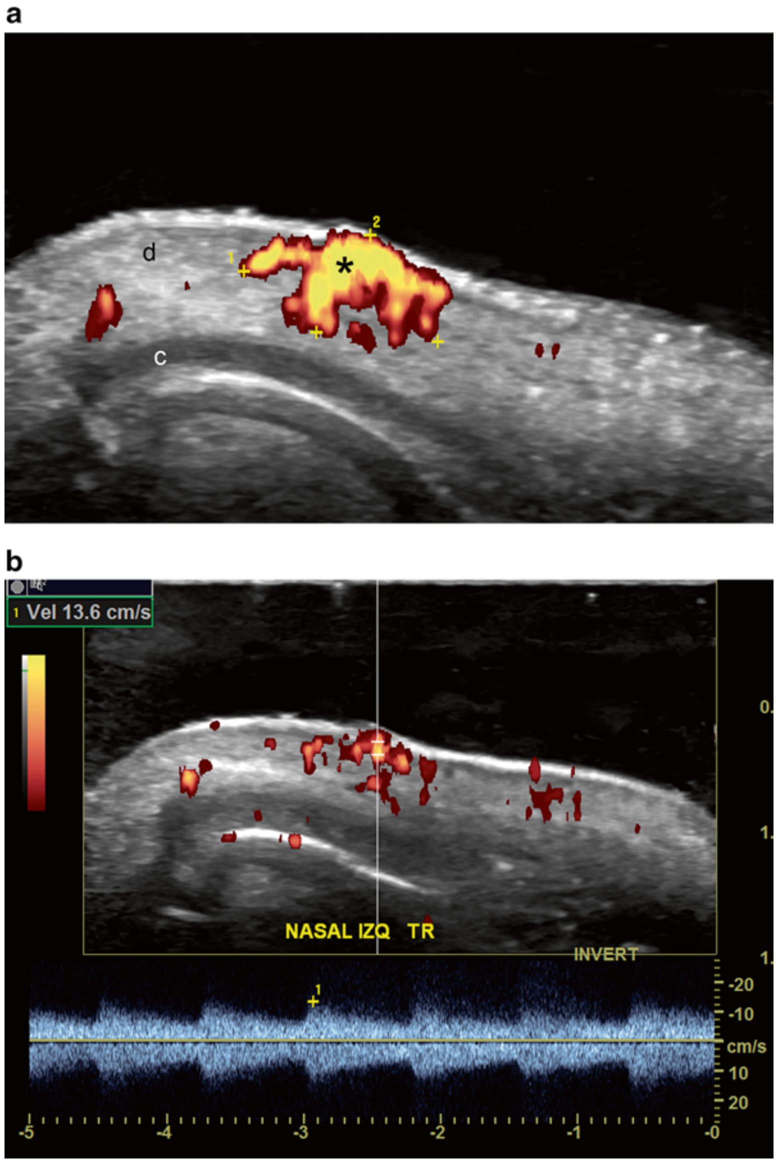

Fig. 4.9 (**a**) (*Top*). High flow arterial vascular malformation. Notice the hypervascular spots in the dermis of the nasal tip. (**b**) (*Bottom*). Spectral curve analysis demonstrates arterial flow. (d = dermis; c = nasal cartilage)

Nail: Progressing from early to late changes there is thickening and decreased echogenicity of the nail bed, focal hyperechoic deposits in the ventral plate, loss of definition of the ventral plate, thickening of the dorsal and ventral plate, wavy plates

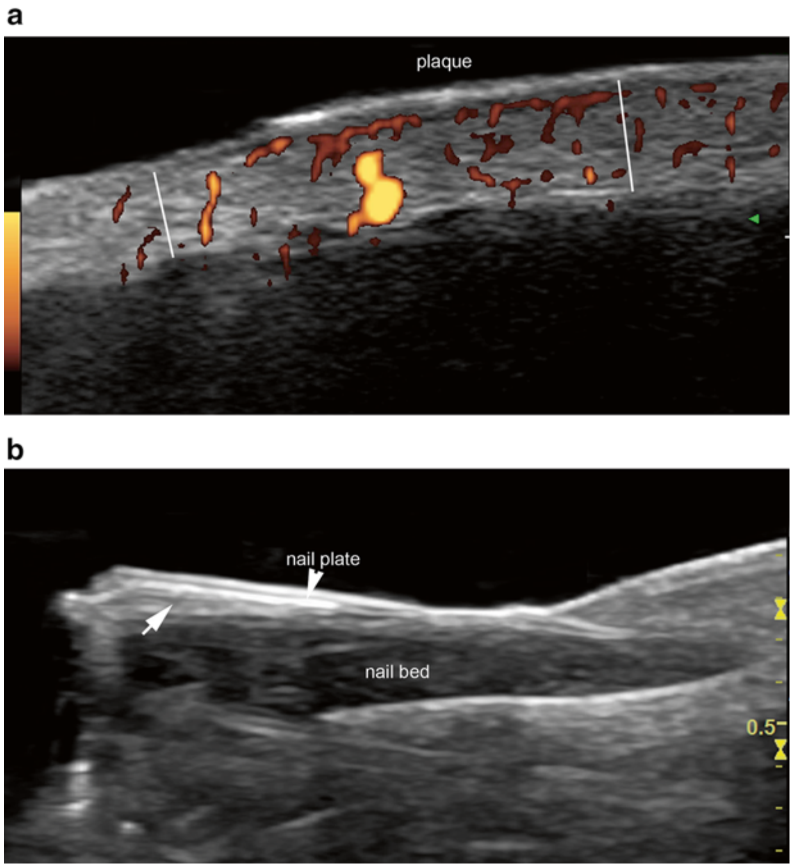

Fig. 4.10 (**a**) (*Top*) Psoriasis. Cutaneous plaque shows epidermal and dermal thickening and increased regional blood flow on power Doppler. The *vertical white lines* are pointing out the normal (*left* aspect) and abnormal regions (*right* aspect). (**b**) (*Bottom*). Nail involvement demonstrates thickening of the ventral plate (*arrow*) and the nail bed

(Fig. 4.10b). Increased blood flow may be detected in the nail bed, most commonly in the proximal region affecting the matrix region.

Tendons: Thickening, hypoechogenicity, or heterogeneous echogenicity of the insertion sites of the tendons (enthesis).

Joints: Increased anechoic fluid due to synovitis.

Bone: Erosions of the hyperechoic bony margin, frequently in the interphalangeal joints of the fingers and toes.

The usage of sonography is usually focused on the assessment of the activity and severity of the disease [49–58].

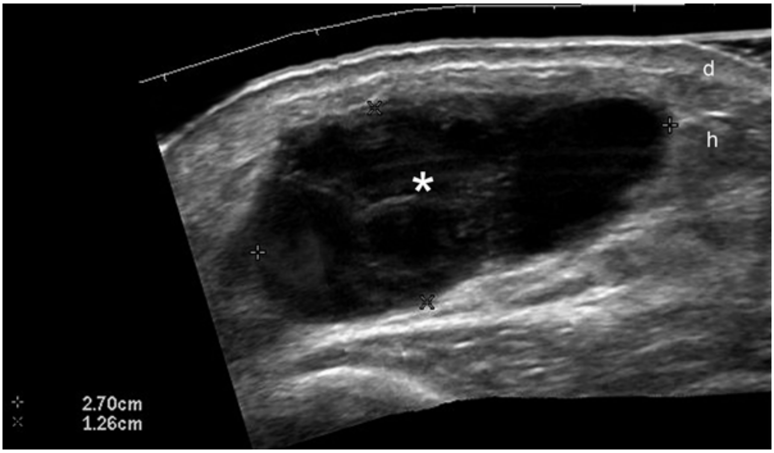

Fig. 4.11 Hematoma. 2.70 cm × 1.26 cm hypoechoic fluid collection (*) in the hypodermis with some echoes

Hematomas–Seromas–Abscesses

Key Sonographic Findings on Ultrasound

Seromas and Hematomas usually show as anechoic or hypoechoic fluid collections that may show hypoechoic echoes due to debris or retained bloody material (Fig. 4.11). Seromas tend to show compressibility with the probe. Hyperechoic septa and prominent peripheral vascularity may appear when the collection becomes an *Abscess*.

Ultrasound supports the diagnosis, provides the extent of these collections, may guide a percutaneous drainage, and also can perform noninvasive monitoring over time [50, 59].

Plantar Warts

General Concepts: An infectious lesion produced by the human papilloma virus. They can be very painful and may be clinically confused with a foreign body or a Morton's neuroma.

Ultrasound: Hypoechoic fusiform structure located in the epidermis and dermis. Frequently hypervascularity is detected in the lesion or sublesional site and the

Table 4.2 Ultrasound appearance of common cosmetic fillers

Filler	Shape	Echogenicity	Artifact	Observations
Pure hyaluronic acid	Round or oval	Anechoic	Posterior acoustic enhancement	Decrease in size in 3–6 months
High density pure hyaluronic acid	Round or oval	Anechoic or hypoechoic	Posterior acoustic enhancement	No significant change in 18 months
Pure silicone	Oval	Anechoic	Posterior acoustic enhancement	No change over time
Silicone oil	Diffuse	Hyperechoic	Reverberance, “snow storm”	No significant change over time
Polymethylmethacrylate	Diffuse	Hyperechoic	Mini-comet tail	No change over time
Calcium hydroxyapatite	Band-like	Hyperechoic	Posterior acoustic shadowing	No change over time
Polyacrylamide	Round or oval	Anechoic	Posterior acoustic enhancement	No significant change in 18 months

Extracted from Refs. [65] and [66]

degree of vascularity is commonly related to the degree of pain of the patient. Regional plantar bursitis can also be found underlying the wart site [50, 60, 61].

Key Sonographic Sign: Epidermal and dermal fusiform hypoechoic lesion in the plantar region.

Cosmetic Applications

Cosmetic Fillers

General Concepts: Nanoparticles used in cosmetics for treating wrinkled and sagging skin. They can be biodegradable (for example pure hyaluronic acid) and non-biodegradable (for example: silicone, polymethylmetacrylate, calcium hydroxyapatite, and polyacrylamide). There are also some mixed formulations of fillers where a synthetic component is added to a biodegradable filler to achieve more long-lasting results (e.g., high density hyaluronic acid).

Ultrasound: The sonographic appearance of cosmetic fillers varies according to the nature of the filler. Biodegradable fillers modify their size over time. The ultrasound appearance of the most common cosmetic fillers is shown in Table 4.2 and Figs. 4.12, 4.13, 4.14, and 4.15 [62–67].

Key Sonographic Signs: Exogenous anechoic or hyperechoic deposits in the dermis and/or hypodermis.

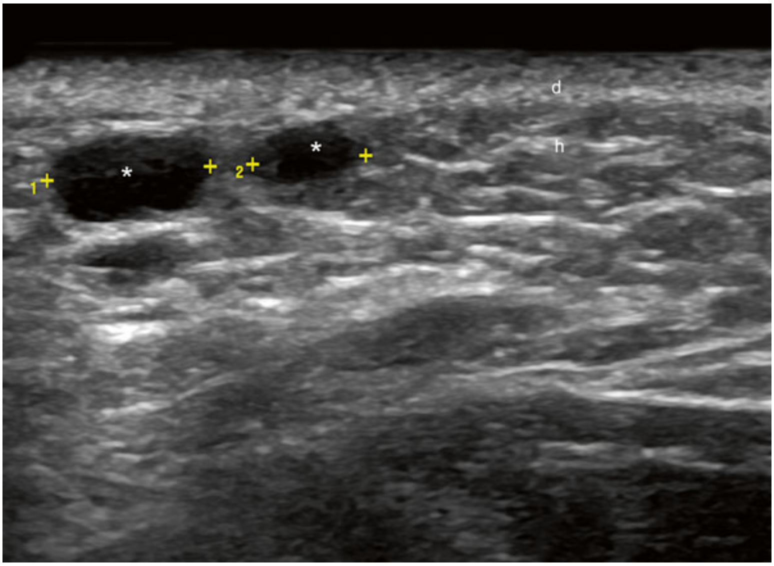

Fig. 4.12 Hyaluronic acid. Anechoic oval shaped deposits in the hypodermis. (d = dermis; h = hypodermis)

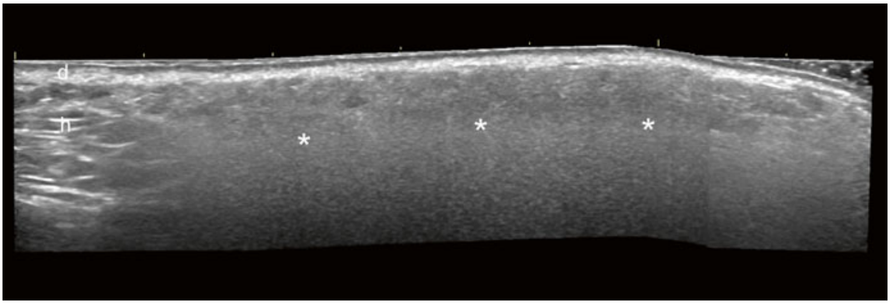

Fig. 4.13 Silicone oil. Hyperechoic deposit (*) in the hypodermis with posterior reverberance artifact and snow storm appearance. (d = dermis; h = hypodermis)

Conclusion

Ultrasound can provide a wide range of anatomical information in common dermatologic conditions that cannot be deduced from clinical examination alone.

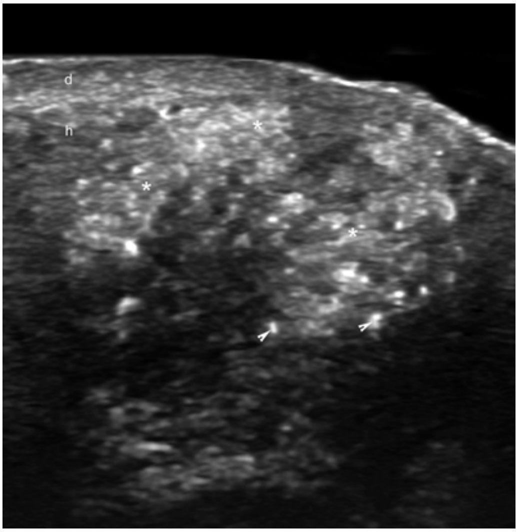

Fig. 4.14 Polymethylmethacrylate (PMMA). Hypodermal hyperechoic deposits with mini-comet tail posterior artifact (*arrowheads*). (d = dermis; h = hypodermis)

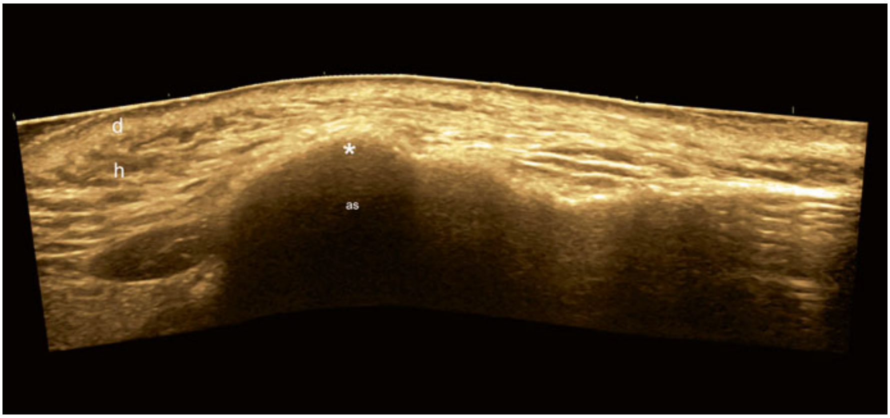

Fig. 4.15 Calcium hydroxyapatite. Hypodermal hyperechoic band (*) with posterior acoustic shadowing artifact (as). (d = dermis; h = hypodermis)

Summary

The dermatologic application of ultrasound has been rapidly growing in recent years due to the development of high frequency and definition probes and machines that have allowed observing the skin and deeper structures. In the present chapter we will review the normal anatomy, the technical requirements and common dermatologic conditions using a practical approach.

References

1. Wortsman X. Common applications of dermatologic sonography. J Ultrasound Med. 2012;31:97–111.
2. Wortsman X. Ultrasound in dermatology: why, how, and when? Semin Ultrasound CT MR. 2013;34:177–95.
3. Wortsman X, Wortsman J. Clinical usefulness of variable-frequency ultrasound in localized lesions of the skin. J Am Acad Dermatol. 2010;62:247–56.
4. Wortsman X. Sonography of cutaneous and ungual lumps and bumps. Ultrasound Clin. 2012. doi:10.1016/j.cult.2012.08.006.
5. Wortsman X. How to start on skin, nail and hair ultrasound: guidance and protocols. In: Wortsman X, Jemec GBE, editors. Dermatologic ultrasound with clinical and histologic correlations. 1st ed. New York: Springer; 2013. p. 597–607.
6. Wortsman X, Wortsman J, Carreño L, Morales C, Sazunic I, Jemec GBE. Sonographic anatomy of the skin, appendages and adjacent structures. In: Wortsman X, Jemec GBE, editors. Dermatologic ultrasound with clinical and histologic correlations. 1st ed. New York: Springer; 2013. p. 15–35.
7. Yuan WH, Hsu HC, Lai YC, Chou YH, Li AF. Differences in sonographic features of ruptured and unruptured epidermal cysts. J Ultrasound Med. 2012;31(2):265–72.
8. Huang CC, Ko SF, Huang HY, Ng SH, Lee TY, Lee YW, Chen MC. Epidermal cysts in the superficial soft tissue: sonographic features with an emphasis on the pseudotestis pattern. J Ultrasound Med. 2011;30(1):11–7.
9. Kim HK, Kim SM, Lee SH, Racadio JM, Shin MJ. Subcutaneous epidermal inclusion cysts: ultrasound (US) and MR imaging findings. Skeletal Radiol. 2011;40(11):1415–9.
10. Wortsman X, Bouer M. Common benign non-vascular skin tumors. In: Wortsman X, Jemec GBE, editors. Dermatologic ultrasound with clinical and histologic correlations. 1st ed. New York: Springer; 2013. p. 119–75.
11. Mentes O, Oysul A, Harlak A, Zeybek N, Kozak O, Tufan T. Ultrasonography accurately evaluates the dimension and shape of the pilonidal sinus. Clinics (Sao Paulo). 2009;64:189–92.
12. Choo HJ, Lee SJ, Lee YH, Lee JH, Oh M, Kim MH, Lee EJ, Song JW, Kim SJ, Kim DW. Pilomatricomas: the diagnostic value of ultrasound. Skeletal Radiol. 2010;39(3):243–50.
13. Solivetti FM, Elia F, Drusco A, Panetta C, Amantea A, Di Carlo A. Epithelioma of Malherbe: new ultrasound patterns. J Exp Clin Cancer Res. 2010;29:42.
14. Roche NA, Monstrey SJ, Matton GE. Pilomatricoma in children: common but often misdiagnosed. Acta Chir Belg. 2010;110(2):250–4.
15. Wortsman X, Wortsman J, Arellano J, Oroz J, Giugliano C, Benavides MI, Bordon C. Pilomatrixomas presenting as vascular tumors on color Doppler ultrasound. J Pediatr Surg. 2010;45(10):2094–8.
16. Fornage BD, Tassin GB. Sonographic appearances of superficial soft tissue lipomas. J Clin Ultrasound. 1991;19(4):215–20.
17. Wagner JM, Lee KS, Rosas H, Kliewer MA. Accuracy of sonographic diagnosis of superficial masses. J Ultrasound Med. 2013;32(8):1443–50.
18. Hung EH, Griffith JF, Ng AW, Lee RK, Lau DT, Leung JC. Ultrasound of musculoskeletal soft-tissue tumors superficial to the investing fascia. Am J Roentgenol. 2014;202(6):W532–40.
19. Bobadilla F, Wortsman X, Muñoz C, Segovia L, Espinoza M, Jemec GBE. Pre-surgical high resolution ultrasound of facial basal cell carcinoma: correlation with histology. Cancer Imaging. 2008;22:163–72.
20. Barcaui Ede O, Carvalho AC, Valiante PM, Barcaui CB. High-frequency ultrasound associated with dermoscopy in pre-operative evaluation of basal cell carcinoma. An Bras Dermatol. 2014;89(5):828–31.

21. Hernández-Ibáñez C, Aguilar-Bernier M, Fúnez-Liébana R, Del Boz J, Blázquez N, de Troya M. The usefulness of high-resolution ultrasound in detecting invasive disease in recurrent basal cell carcinoma after nonsurgical treatment. Actas Dermosifiliogr. 2014;105(10):935–9.
22. Wortsman X, Carreño L, Morales C. Skin cancer: the primary tumors. In: Wortsman X, Jemec GBE, editors. Dermatologic ultrasound with clinical and histologic correlations. 1st ed. New York: Springer; 2013. p. 249–82.
23. Wortsman X. Sonography of facial cutaneous basal cell carcinoma: a first-line imaging technique. J Ultrasound Med. 2013;32:567–72.
24. Wortsman X, Vergara P, Castro A, Saavedra D, Bobadilla F, Sazunic I, Zemelman V, Wortsman J. Ultrasound as predictor of histologic subtypes linked to recurrence in basal cell carcinoma of the skin. Eur Acad Dermatol Venereol. 2014. doi:10.1111/jdv.12660.
25. Nazarian LN, Alexander AA, Rawool NM, Kurtz AB, Maguire HC, Mastrangelo MJ. Malignant melanoma: impact of superficial US on management. Radiology. 1996;199(1):273–7.
26. Wortsman X. Sonography of the primary cutaneous melanoma: a review. Radiol Res Pract. 2012;2012:814396. doi:10.1155/2012/814396.
27. Music MM, Hertl K, Kadivec M, Pavlović MD, Hocevar M. Pre-operative ultrasound with a 12-15 MHz linear probe reliably differentiates between melanoma thicker and thinner than 1 mm. J Eur Acad Dermatol Venereol. 2010;24(9):1105–8.
28. Crisan M, Crisan D, Sannino G, Lupsor M, Badea R, Amzica F. Ultrasonographic staging of cutaneous malignant tumors: an ultrasonographic depth index. Arch Dermatol Res. 2013; 305(4):305–13.
29. Lassau N, Koscielny S, Avril MF, Margulis A, Duvillard P, De Baere T, Roche A, Leclère J. Prognostic value of angiogenesis evaluated with high-frequency and color Doppler sonography for preoperative assessment of melanomas. Am J Roentgenol. 2002;178(6):1547–51.
30. Lassau N, Lamuraglia M, Koscielny S, Spatz A, Roche A, Leclere J, Avril MF. Prognostic value of angiogenesis evaluated with high-frequency and colour Doppler sonography for preoperative assessment of primary cutaneous melanomas: correlation with recurrence after a 5 year follow-up period. Cancer Imaging. 2006;6:24–9.
31. Srivastava A, Woodcock JP, Mansel RE, Webster DJ, Laidler P, Hughes LE, Dwivedi A. Doppler ultrasound flowmetry predicts 15 year outcome in patients with skin melanoma. Indian J Surg. 2012;74(4):278–83.
32. Kato M, Mabuchi T, Yamaoka H, Ikoma N, Tamiya S, Ozawa A, Taguchi M, Kuramochi A, Tsuchida T. Diagnostic usefulness of findings in Doppler sonography for amelanotic melanoma. J Dermatol. 2013;40(9):700–5.
33. Krüger U, Kretschmer L, Thoms KM, Padeken M, Peter Bertsch H, Schön MP, Zutt M. Lymph node ultrasound during melanoma follow-up significantly improves metastasis detection compared with clinical examination alone: a study on 433 patients. Melanoma Res. 2011; 21(5):457–63.
34. Catalano O, Voit C. Locoregional staging of melanoma. In: Wortsman X, Jemec GBE, editors. Dermatologic ultrasound with clinical and histologic correlations. 1st ed. New York: Springer; 2013. p. 293–343.
35. Catalano O, Siani A. Cutaneous melanoma: role of ultrasound in the assessment of locoregional spread. Curr Probl Diagn Radiol. 2010;39(1):30–6.
36. Kunte C, Schuh T, Eberle JY, Baumert J, Konz B, Volkenandt M, Ruzicka T, Schmid-Wendtner MH. The use of high-resolution ultrasonography for preoperative detection of metastases in sentinel lymph nodes of patients with cutaneous melanoma. Dermatol Surg. 2009;35(11): 1757–65.
37. Catalano O, Setola SV, Vallone P, Raso MM, D'Errico AG. Sonography for locoregional staging and follow-up of cutaneous melanoma: how we do it. J Ultrasound Med. 2010;29(5): 791–802.
38. Nazarian LN, Alexander AA, Kurtz AB, Capuzzi Jr DM, Rawool NM, Gilbert KR, Mastrangelo MJ. Superficial melanoma metastases: appearances on gray-scale and color Doppler sonography. Am J Roentgenol. 1998;170(2):459–63.

39. Alexander AA, Nazarian LN, Capuzzi Jr DM, Rawool NM, Kurtz AB, Mastrangelo MJ. Color Doppler sonographic detection of tumor flow in superficial melanoma metastases: histologic correlation. J Ultrasound Med. 1998;17(2):123–6.
40. Catalano O, Voit C, Sandomenico F, Mandato Y, Petrillo M, Franco R, Botti G, Caracò C, Mozzillo N, D'Errico AG. Previously reported sonographic appearances of regional melanoma metastases are not likely due to necrosis. J Ultrasound Med. 2011;30(8):1041–9.
41. Ulrich J, van Akkooi AJ, Eggermont AM, Voit C. New developments in melanoma: utility of ultrasound imaging (initial staging, follow-up and pre-SLNB). Expert Rev Anticancer Ther. 2011;11(11):1693–701. doi:10.1586/era.
42. Voit C, Van Akkooi AC, Schäfer-Hesterberg G, Schoengen A, Kowalczyk K, Roewert JC, Sterry W, Eggermont AM. Ultrasound morphology criteria predict metastatic disease of the sentinel nodes in patients with melanoma. J Clin Oncol. 2010;28(5):847–52.
43. Voit CA, Gooskens SL, Siegel P, Schaefer G, Schoengen A, Röwert J, van Akkooi AC, Eggermont AM. Ultrasound-guided fine needle aspiration cytology as an addendum to sentinel lymph node biopsy can perfect the staging strategy in melanoma patients. Eur J Cancer. 2014;50(13):2280–8.
44. Voit CA, van Akkooi AC, Eggermont AM, Schäfer-Hesterberg G, Kron M, Ulrich J, Sterry W, Schoengen A, Rademaker J. Fine needle aspiration cytology of palpable and nonpalpable lymph nodes to detect metastatic melanoma. J Natl Cancer Inst. 2011;103(23):1771–7.
45. Peer S, Wortsman X. Hemangiomas and vascular malformations. In: Wortsman X, Jemec GBE, editors. Dermatologic ultrasound with clinical and histologic correlations. 1st ed. New York: Springer; 2013. p. 183–248.
46. Paltiel HJ, Burrows PE, Kozakewich HP, Zurakowski D, Mulliken JB. Soft-tissue vascular anomalies: utility of US for diagnosis. Radiology. 2000;214(3):747–54.
47. Dubois J, Patriquin HB, Garel L, Powell J, Filiatrault D, David M, Grignon A. Soft-tissue hemangiomas in infants and children: diagnosis using Doppler sonography. Am J Roentgenol. 1998;171(1):247–52.
48. Kuntz AM, Aranibar L, Lobos N, Wortsman X. Color Doppler ultrasound follow-up of infantile hemangiomas and peripheral vascularity in patients treated with propranolol. Pediatr Dermatol. 2015;32(4):468–75.
49. Wortsman X, Gutierrez M, Saavedra T, Honeyman J. The role of ultrasound in rheumatic skin and nail lesions: a multi-specialist approach. Clin Rheumatol. 2011;30:739–48.
50. Wortsman X, Carreño L, Morales C. Inflammatory diseases of the skin. In: Wortsman X, Jemec GBE, editors. Dermatologic ultrasound with clinical and histologic correlations. 1st ed. New York: Springer; 2013. p. 73–117.
51. Grassi W, Gutierrez M. Psoriatic arthritis: need for ultrasound in everyday clinical practice. J Rheumatol Suppl. 2012;89:39–43.
52. Gutierrez M, Filippucci E, De Angelis R, Salaffi F, Filosa G, Ruta S, Bertolazzi C, Grassi W. Subclinical entheseal involvement in patients with psoriasis: an ultrasound study. Semin Arthritis Rheum. 2011;40(5):407–12.
53. Gutierrez M, De Angelis R, Bertolazzi C, Filippucci E, Grassi W, Filosa G. Clinical images: multi-modality imaging monitoring of anti-tumor necrosis factor α treatment at the joint and skin level in psoriatic arthritis. Arthritis Rheum. 2010;62(12):3829.
54. Gutierrez M, De Angelis R, Bernardini ML, Filippucci E, Goteri G, Brandozzi G, Lemme G, Campanati A, Grassi W, Offidani A. Clinical, power Doppler sonography and histological assessment of the psoriatic plaque: short-term monitoring in patients treated with etanercept. Br J Dermatol. 2011;164(1):33–7.
55. Gutierrez M, Filippucci E, Salaffi F, Di Geso L, Grassi W. Differential diagnosis between rheumatoid arthritis and psoriatic arthritis: the value of ultrasound findings at metacarpophalangeal joints level. Ann Rheum Dis. 2011;70(6):1111–4.
56. Tehranzadeh J, Ashikyan O, Anavim A, Shin J. Detailed analysis of contrast-enhanced MRI of hands and wrists in patients with psoriatic arthritis. Skeletal Radiol. 2008;37(5):433–42.

57. De Agustín JJ, Moragues C, De Miguel E, Möller I, Acebes C, Naredo E, Uson J, Rejon E, Mayordomo L, Garrido J. A multicentre study on high-frequency ultrasound evaluation of the skin and joints in patients with psoriatic arthritis treated with infliximab. Clin Exp Rheumatol. 2012;30(6):879–85.
58. Naredo E, Möller I, de Miguel E, Batlle-Gualda E, Acebes C, Brito E, Mayordomo L, Moragues C, Uson J, de Agustín JJ, Martínez A, Rejón E, Rodriguez A, Daudén E, Ultrasound School of the Spanish Society of Rheumatology and Spanish ECO-APs Group. High prevalence of ultrasonographic synovitis and enthesopathy in patients with psoriasis without psoriatic arthritis: a prospective case-control study. Rheumatology (Oxford). 2011;50(10):1838–48.
59. Wortsman X, Holm EA, Gniadecka M, Wulf HC, Jemec GBE. Real time spatial compound imaging of skin lesions. Skin Res Technol. 2004;10:23–31.
60. Wortsman X, Sazunic I, Jemec GBE. Sonography of plantar warts. J Ultrasound Med. 2009;28:787–93.
61. Wortsman X, Jemec GBE, Sazunic I. Anatomical detection of inflammatory changes associated to plantar warts. Dermatology. 2010;220:213–7.
62. Young SR, Bolton PA, Downie J. Use of high-frequency ultrasound in the assessment of injectable dermal fillers. Skin Res Technol. 2008;14(3):320–3.
63. Schelke LW, Van Den Elzen HJ, Erkamp PP, Neumann HA. Use of ultrasound to provide overall information on facial fillers and surrounding tissue. Dermatol Surg. 2010;36 Suppl 3:1843–51.
64. Grippaudo FR, Mattei M. The utility of high-frequency ultrasound in dermal filler evaluation. Ann Plast Surg. 2011;67(5):469–73.
65. Wortsman X, Wortsman J, Orlandi C, Cardenas G, Sazunic I, Jemec GB. Ultrasound detection and identification of cosmetic fillers in the skin. J Eur Acad Dermatol Venereol. 2012; 26(3):292–301.
66. Wortsman X, Wortsman J. Polyacrylamide fillers on skin ultrasound. J Eur Acad Dermatol Venereol. 2012;26(5):660–1.
67. Wortsman X, Wortsman J. Sonographic outcomes of cosmetic procedures. Am J Roentgenol. 2011;197:W910–8. doi:10.2214/AJR.11.6719.

Chapter 5
Knobology

Victor V. Rao

Introduction

Ultrasound knobology can be intimidating for some users. A new laptop or cart-based ultrasound system may be difficult to operate initially because every ultrasound device manufacturer uses its own unique nomenclature and operating system. The systems vary so the same function may have a different name or use depending on the model.

Ultrasound systems work on the same basic principles. Most modern systems have preset functions which optimize the ultrasound system without much adjustment. These are factory presets and some systems may also allow you to make your own custom presets. The newer pocket ultrasound devices have very few buttons and knobs and may be easier to use. We will attempt to simplify the process of getting acquainted to an ultrasound system.

Common Knobs/Buttons

Power

Press the power button to activate the ultrasound system. Depending upon the manufacturer the system may have a specific boot time of few seconds up to 1 min or longer. There are some pocket ultrasound systems that turn on automatically when the cover of the system is opened. There may be a short boot time of up to 1 min (Fig. 5.1).

V.V. Rao, M.B.B.S., D.M.R.D., R.D.M.S. (✉)
Ultrasound Institute, University of South Carolina School of Medicine, Columbia, SC, USA
e-mail: Victor.Rao@uscmed.sc.edu

J.M. Daniels, R.A. Hoppmann (eds.), *Practical Point-of-Care Medical Ultrasound*, DOI 10.1007/978-3-319-22638-5_5

Fig. 5.1 Showing typical power button used on a laptop ultrasound device

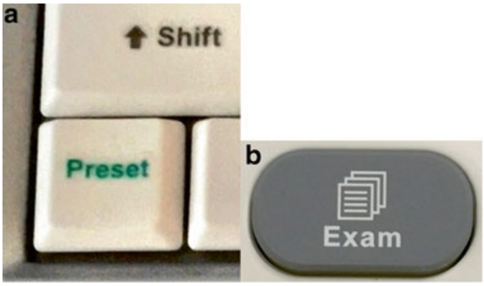

Fig. 5.2 Showing the preset button (**a**) also labeled as an exam button (**b**) on an ultrasound device

Preset

The preset button or the exam button is perhaps one of the most important buttons in an ultrasound system. Selecting the right present for that particular region of the body makes scanning much easier. Built-in software assists not only with labeling and measurement but will make the video image much clearer. For example, if you were scanning a pregnant patient in the second trimester and did not select the obstetrical preset for the second trimester, you will not be able to calculate the gestational age using the fetal parameters such as BPD, FL, or AC if you were scanning the patient using abdominal settings. Also note that the acoustic output of the probe may be higher than is recommended for fetal ultrasound (Fig. 5.2a, b).

Freeze

Most modern ultrasound systems are always recording and dumping data as they record new data. So, at any point in time when you press the freeze button, the user can scroll back through the previous few frames on the internal memory of the device. Once you unfreeze, the data from the previous scan is deleted unless specifically saved by the user. The amount of data that is stored while scanning can be adjusted by the user by logging into the system configuration or system settings. Small pocket ultrasound devices may not allow you to manipulate such settings (Fig. 5.3).

Fig. 5.3 Showing the freeze button on a laptop ultrasound device. Press to freeze an image and press again to unfreeze and start real-time scanning

Fig. 5.4 Showing the gain knob

Gain

The gain control knob allows the user to increase or decrease the overall brightness or darkness of an image. As a rule, try to represent clear fluids or blood with the black color (anechoic). Try to optimize the image to represent the true characteristics of the organ being scanned. Turn the knob clockwise to increase the overall image gain and counterclockwise to reduce the overall brightness of the image on the monitor. The auto button in the center can automatically optimize the gain setting. It works best during spectral Doppler mode.

Keep in mind that the gain control knob will increase or decrease the brightness only during B-mode imaging. If you are using color Doppler then it will increase or decrease the sensitivity of the color Doppler display and during spectral Doppler it will enhance or reduce the brightness of the spectral Doppler tracing (Fig. 5.4).

Depth

Depth control lets you adjust the maximum depth of the ultrasound region being scanned and displayed on the monitor. Try to adjust the depth to show the structure of interest completely without cropping it and also add 1–2 cm margin to make sure

Fig. 5.5 Showing depth control buttons

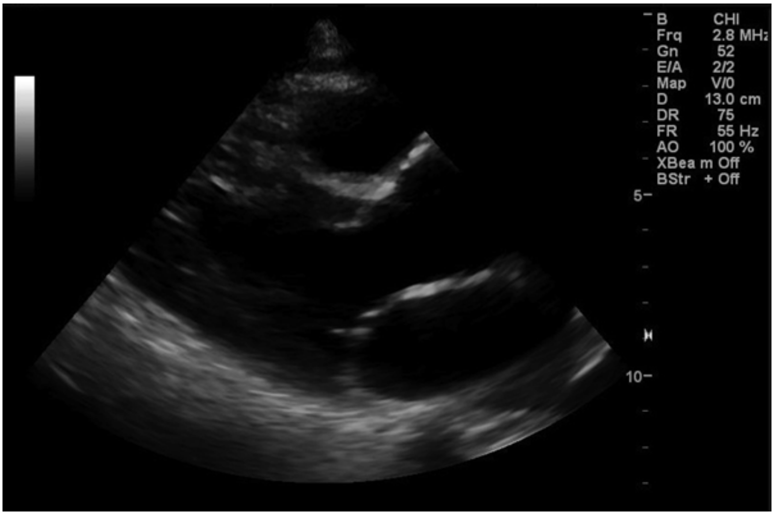

Fig. 5.6 Showing the left parasternal long axis (PLAX) view of the heart with proper depth settings. The depth setting in this example is set at 13 cm

there is no pathology around the structure. For example if you are scanning the abdominal aorta, then make sure that the posterior wall of the abdominal aorta is included as well as 1–2 cm beyond the posterior wall of the abdominal aorta (Figs. 5.5, 5.6, and 5.7).

Focus

The focus function allows the user to adjust the level of the focus of the ultrasound beam onto different structures during real time scanning. For example, if you were performing a scan of the abdominal aorta then make sure that the focus is at the

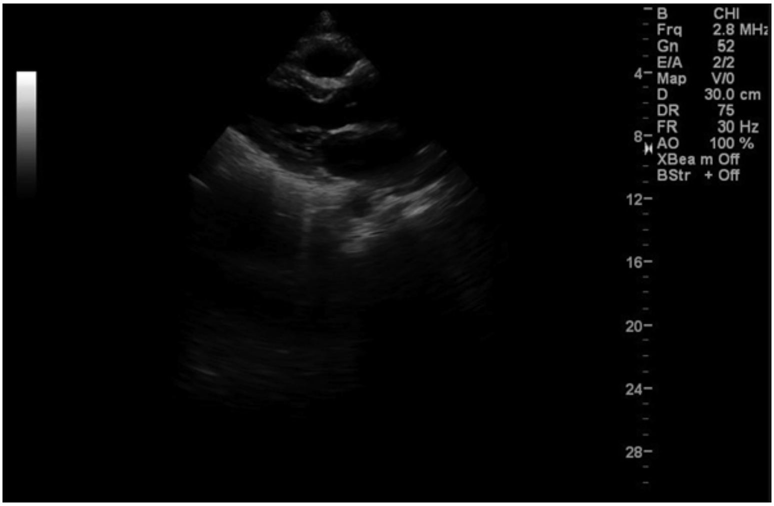

Fig. 5.7 Showing the left parasternal long axis (PLAX) view of the heart wrong depth settings. The depth is set too deep and thus the heart looks much smaller in size. Note that the depth setting in this example is set at 30 cm

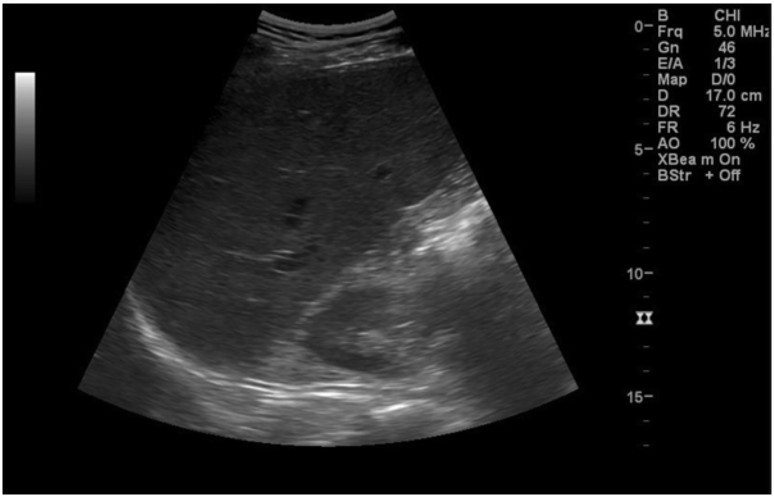

Fig. 5.8 Showing ultrasound image obtained with one focal point at the level of interest. See *white arrow* indicating focus level indicator

level of the aorta in the image. Image quality at the level of the focus is the sharpest. Beyond the focus the image quality begins to degrade. Some ultrasound systems only have presets and will not allow adjustment of the focus level. You can also increase or decrease the focus points. See images below. Increasing the focus points may at times cause the frame rate (FR) to decrease (Figs. 5.8 and 5.9).

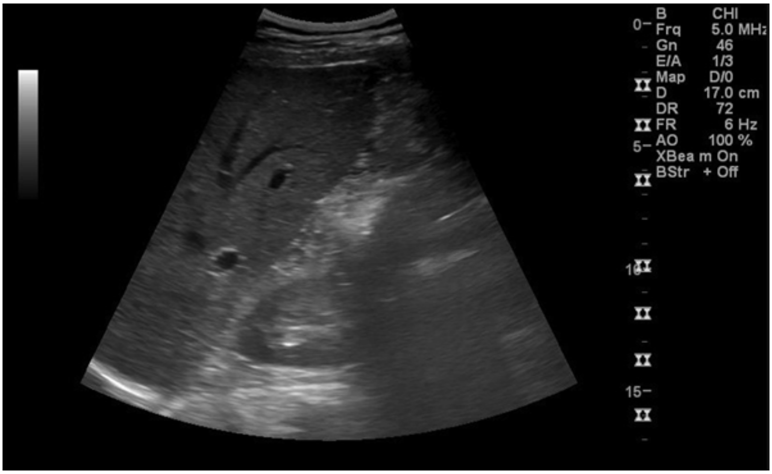

Fig. 5.9 Showing ultrasound image obtained with multiple focal points

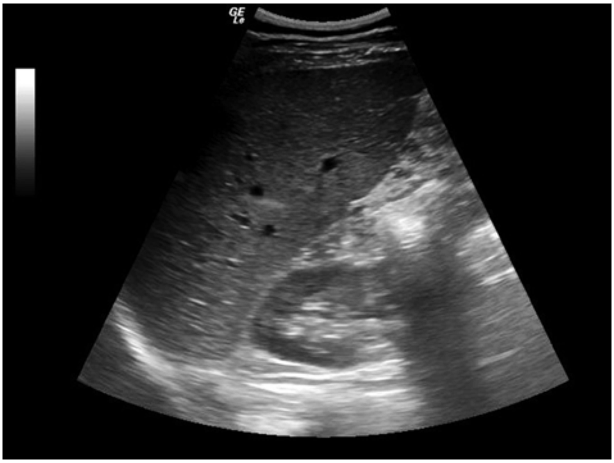

Fig. 5.10 Showing an oblique view through the right lobe of the liver with correct TGC settings

Time Gain Compensation (TGC)/Depth Gain Compensation (DGC)

The TGC is also designated as DGC by some manufacturers. The TGC control allows the user to select the brightness or darkness of an ultrasound image at different levels. The aim should be to have an ultrasound image that is evenly exposed or illuminated. Some individuals also use the liver as a reference to set the TGC settings. See images below (Figs. 5.10, 5.11, and 5.12).

Fig. 5.11 Showing TGC/DGC control on a typical laptop ultrasound device. This function may not be available on some smaller ultrasound devices and may be controlled automatically by the device

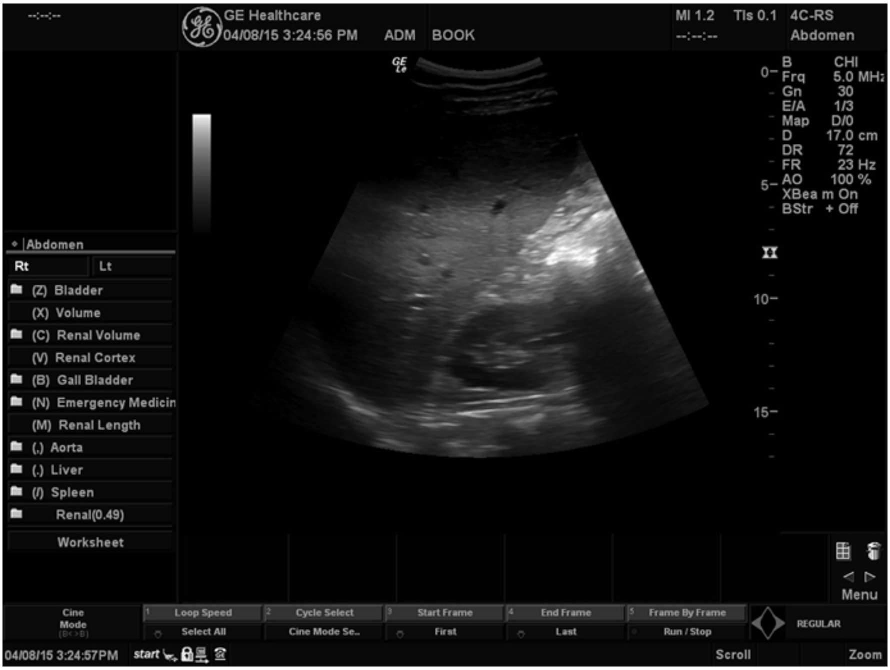

Fig. 5.12 Showing ultrasound image obtained by incorrect TGC setting in the near field

Measurement

As mentioned earlier, it would be critical to select the appropriate preset before attempting to scan the patient. You could scroll back from the last frozen image on the display and select the optimal image frame and proceed to perform standard

Fig. 5.13 Showing a measurement function activation button

Fig. 5.14 Showing the image and or video loop save buttons. In this example they are programmable and user defined. Some ultrasound systems may have fixed save functions allocated by default

ultrasound measurements. These details can be found in the user's manual of the device (Fig. 5.13).

Storing Images/Video Loops

The image storing capability will vary depending upon the ultrasound device and the manufacturer options. Since most modern ultrasound systems are digital so you have a variety of image storage options. You could store the image or a video loops lasting few seconds on the internal hard drive of the device or a USB flash drive or burn a CD or DVD or even transmit to a server to store the image on a PACS system. You still do have the ability to print on a thermal digital printer designed specifically for ultrasound image printing (Figs. 5.14 and 5.15).

Fig. 5.15 Showing a designated printer function button (this cannot be programmed to do other save function)

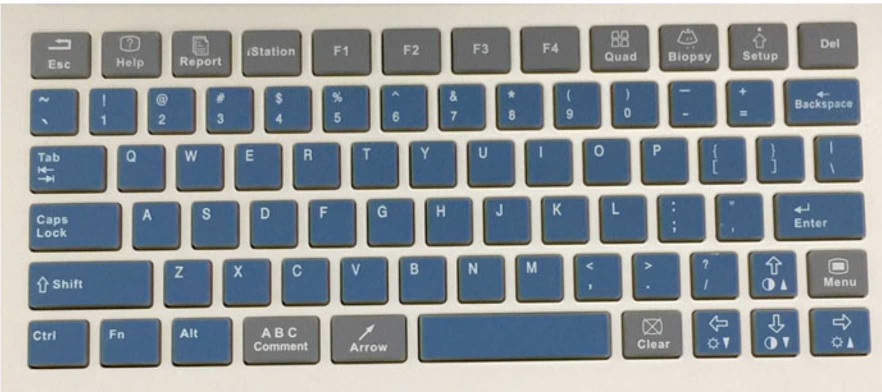

Fig. 5.16 Showing a typical alpha-numeric keyboard of a laptop size ultrasound device

Alpha-Numeric Keyboard

The keyboard is generally present in most ultrasound systems. But some pocket ultrasound devices have eliminated the keyboard and added an ability to add voice annotation. The idea of a keyboard is to annotate the ultrasound image so the user can label appropriately as to what organ or region of the body is being scanned and scan plane as well as a note on the pathology being documented. It is a good idea to annotate so you know what the image represents and the side of the body as well as pathology identifier. It would be very helpful for follow up at a later date. Try not to label on the image itself but on the space on the side of the image to give it a clean professional look (Fig. 5.16).

Fig. 5.17 Showing a B-mode button

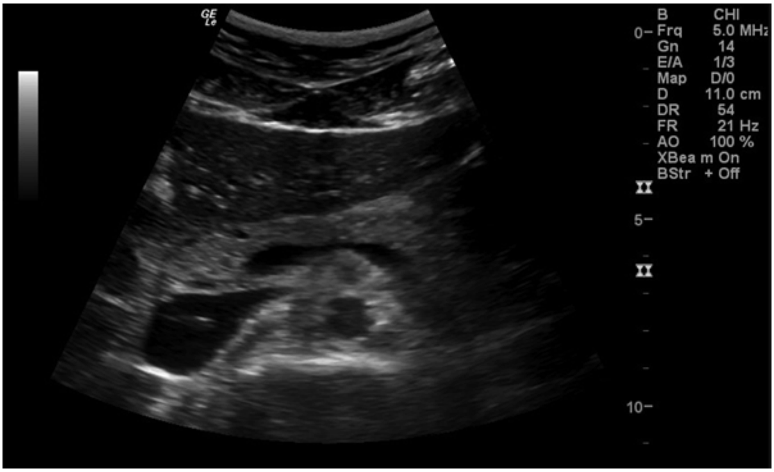

Fig. 5.18 Showing a typical B-mode or 2D ultrasound image

Modes

A-Mode

The A-mode is the amplitude mode. It is no longer available in most modern ultrasound systems. Some ophthalmology ultrasound systems may still have this available. While scanning in this mode, the information is displayed as spikes. The higher the spike, the more echogenic the reflecting surface.

B-Mode

B-mode is also known as "brightness" mode as the image is displayed as pixels along the *X*- and *Y*-axis. Some modern ultrasound systems may use a new terminology and call it 2D (two-dimensional) ultrasound. This mode of ultrasound is the most common form of diagnostic medical ultrasound imaging (Figs. 5.17 and 5.18).

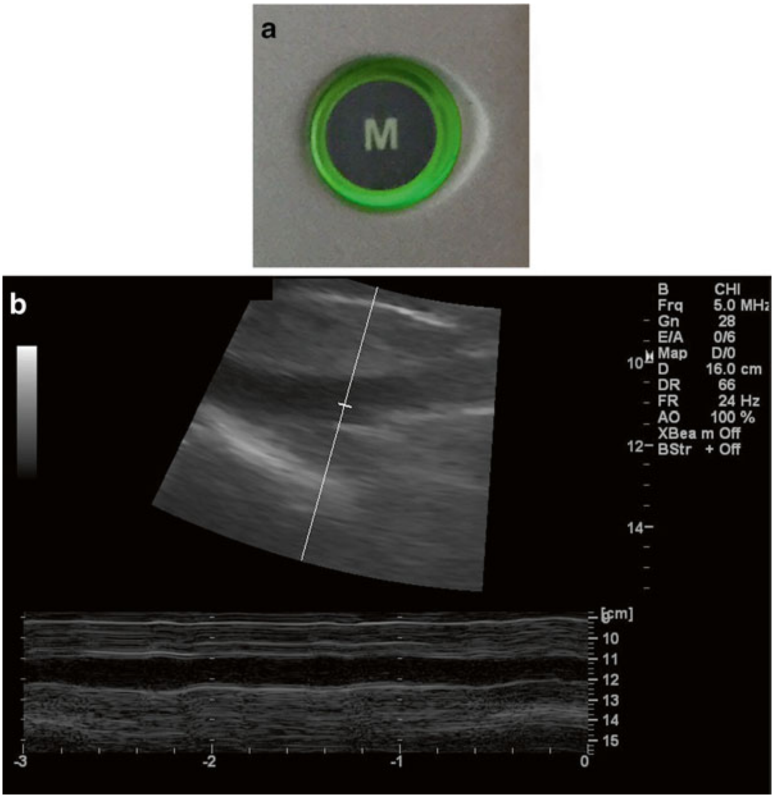

Fig. 5.19 (**a**) Showing the M-mode button. (**b**) Showing an M-mode image tracing obtained through the IVC

M-Mode

M-mode stands for motion-scape. It is used for imaging structures that can move under normal circumstances. Conventionally, it was designed for cardiac imaging, but additional uses include applications such as fetal heart rate determination and lately point-of-care applications such as lung ultrasound for pneumothorax and IVC ultrasound to determine approximate central venous pressure and volume status (Fig. 5.19a, b).

Color Doppler

This mode allows the user to determine qualitative information about blood flow such as direction of flow and differentiating between normal versus turbulent flow. During this mode the color Doppler box is superimposed upon the B-mode image

Fig. 5.20 Showing the color Doppler or color flow (CF) button

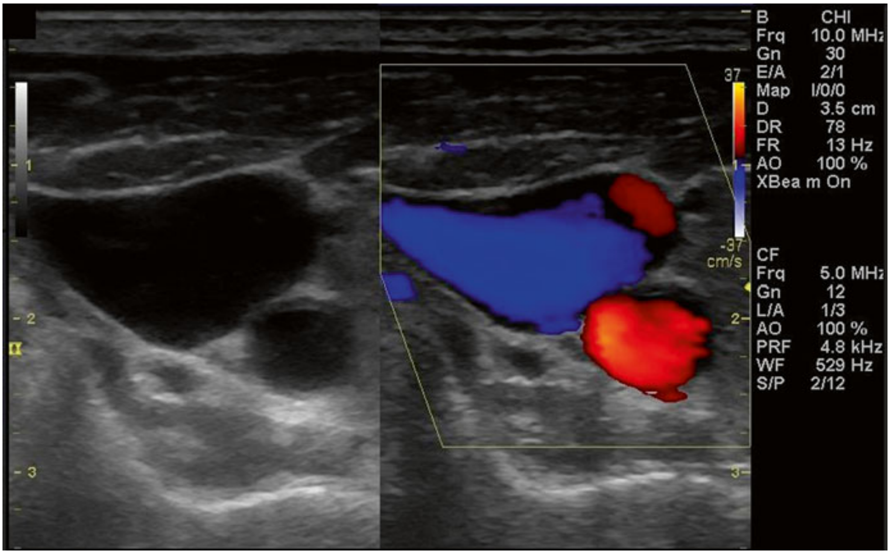

Fig. 5.21 Showing the transverse view of the right common carotid artery and the right internal jugular vein with B-mode display on the left side and the color Doppler mode on the *right*. Observe the legend on the *right* showing red above and *blue* below. Also, note the parameters of the B-mode and color Doppler (CF) mode. In this image the B-mode has a frequency of 10.0 MHz and the CF (Color Flow) Doppler mode has a frequency of 5.0 MHz

and color Doppler information is displayed only within that box. By default, the legend will show the red color representing flow towards the transducer and blue color will represent flow away from the transducer. But, some ultrasound systems may allow you to reverse the color (Figs. 5.20 and 5.21).

Power Doppler

This is a very sensitive mode. It overlays a color box over the B-mode ultrasound image. It can detect even small amount of blood flow as would be expected in inflammatory conditions such as tendinitis and cellulitis representing hyperemia in the tissue. It lacks directional information and cannot be utilized to determine turbulent flow (Figs. 5.22 and 5.23).

Fig. 5.22 Showing the power Doppler button

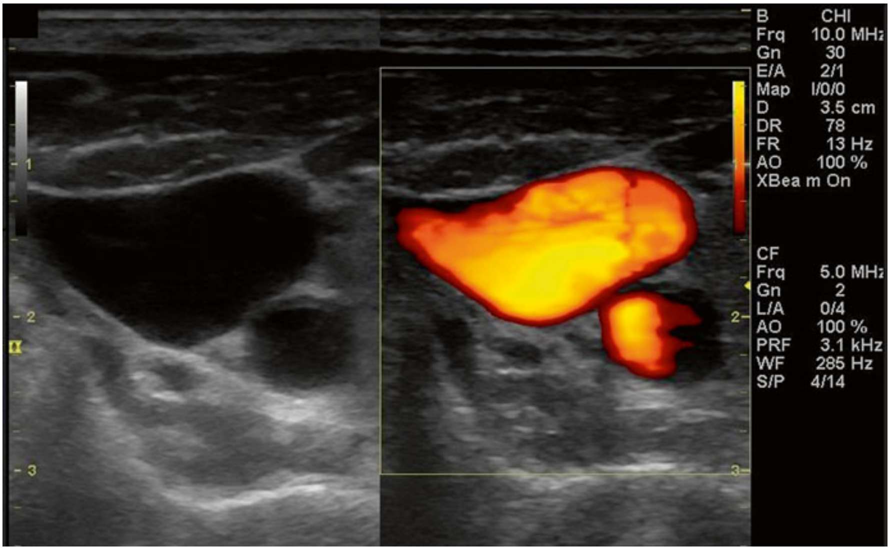

Fig. 5.23 Showing the monitor display during power Doppler mode. Observe that there is no *blue* color

Spectral Doppler/Pulse Wave Doppler

The pulse wave Doppler allows you to obtain a graphical tracing of the velocity range at a specific region in a blood vessel or heart chamber. You can determine the maximum or peak velocity at any point in a blood vessel as well as the end diastolic velocity and the nature of blood flow. For example, we can determine the peak systolic velocity beyond the region of stenosis in the internal carotid artery that in turn would help to grade the degree of stenosis (Figs. 5.24 and 5.25).

Fig. 5.24 Showing the spectral Doppler or pulse wave Doppler (PW) button

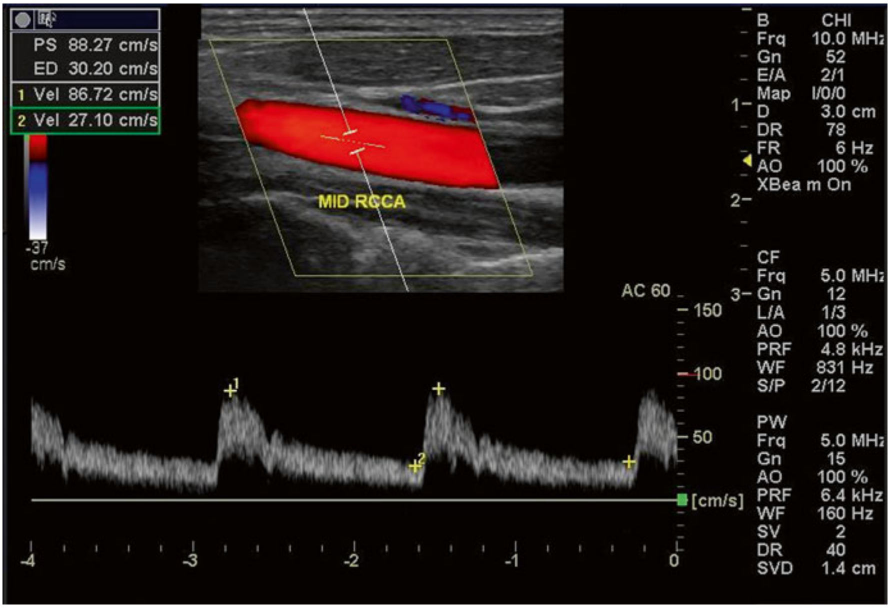

Fig. 5.25 Showing the monitor display during spectral Doppler mode

Common Probes/Transducers

There are multiple types of ultrasound probes available and they operate in pre-specified frequency ranges. You may have the ability to change the frequency within a specific range on some ultrasound systems. However, smaller pocket or hand-held ultrasound devices may automatically regulate the frequency depending upon the maximum depth settings.

There are basically three types of commonly used transducers or probes.

Fig. 5.26 Showing a typical convex low frequency transducer

*Low-frequency curvilinear or convextransducer***:** The frequency range of this transducer is generally in the 1.5–5.0 MHz range. Common applications would include abdominal ultrasound, trans-abdominal pelvic and Obstetrical/Gynecological scans and lung ultrasound. The probe provides a very wide field of view and has a maximum scan depth of up to 24–25 cm (Fig. 5.26).

High-frequency linear transducer: The frequency range of this transducer is generally in the 8.0–13.0 MHz range. Typical applications would include carotid ultrasound, small parts ultrasound such as thyroid and parathyroid imaging, soft-tissue and musculoskeletal ultrasound, DVT assessment, lung ultrasound. It is also used for ultrasound-guided procedures such as central venous access. The probe provides a rectangular field of view and has a maximum scan depth of up to 4–5 cm. The biggest limiting factor for this probe is that this transducer cannot be used to image structures that lie at a depth of greater than 5 cm from the skin surface. However, the probe does provide excellent image resolution (Fig. 5.27).

Low-frequency phased-array transducerfor cardiac imaging: This transducer is specifically designed to image the heart and has a very small footprint which allows the user to image the heart between the ribs, through intercostal spaces without the rib shadow artifact. Since it is a low-frequency transducer, it could potentially be used for imaging structures in the abdomen and pelvis region; however, the image quality is not as good as the convex transducer (Fig. 5.28).

*Endocavitary Transducers***:** Transvaginal probes fall into this category and would be ideal to scan for ectopic pregnancy or adnexal mass. This probe is a high frequency probe and therefore has better image quality. This probe should ideally be used as a supplement to trans-abdominal imaging. Another example is transrectal ultrasound transducers to scan the prostate. Before scanning, a probe sheath is rolled over the transducer to prevent contamination of the probe. Make sure to cover the transducer footprint with ultrasound coupling gel before putting on the transducer cover/sheath. You could also use a condom to cover the transducer.

Fig. 5.27 Showing a typical linear high frequency transducer

Fig. 5.28 Showing a phased array low frequency transducer specifically designed for cardiac imaging/ echocardiography

Ultrasound Coupling Gel: Ultrasound gel is commercially available. It should be applied on the transducer footprint prior to scanning. The gel allows 99 % transmission of the ultrasound beam into the patient's body. If no gel is applied, it will only allow 1 % transmission of the ultrasound beam into the patient's body and result in ultrasound images of very poor quality which would be of no use to make a diagnosis. Keep in mind that for performing ultrasound guided procedures, it is recommended to use the sterile ultrasound coupling gel available in small sachets. Also, use sterile ultrasound probe cover for ultrasound guided procedures.

Components of a Transducer

Transducer Housing

The transducer housing is electrically insulated and is made up of plastic. It houses the piezoelectric elements inside. The piezoelectric elements vary from probe to probe and also vary in number from one element to several hundreds or even thousands of elements. The piezoelectric elements are very thin generally and cannot be individually identified with the naked eye. Care must be taken not to drop the transducer as it could potentially damage the transducer elements or disrupt one or more electrical connections within the transducer.

Transducer Marker/Probe Orientation Marker

The marker could be a ridge or a dot on the housing of the transducer. In some transducers, it could be represented by a Light Emitting Diode (LED). It is recommended to position the transducer with the marker pointing in a specific direction while obtaining a standard ultrasound view. For example—while obtaining a transverse view of the abdominal aorta, the probe is oriented in a way with the probe marker pointing towards the patient's right side. Do note that it is the patient's right side, not the user's right side that is the reference side (Fig. 5.29).

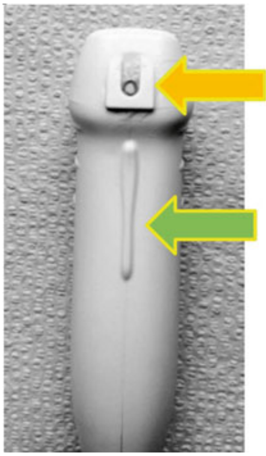

Fig. 5.29 Showing the transducer orientation marker. Note the ridge on the probe housing and the LED

Transducer Footprint

This is color-coded and this is the region from where the ultrasound beam comes out and goes into the patient's body. This also receives the echoes coming back from different tissues interfaces (Fig. 5.29).

Transducer wire

The transducer wire connects the transducer to the main console. In laptop based ultrasound systems, you have the ability to change probes. However, some small pocket ultrasound devices may be permanently attached to the main console. Take care not to twist the wire as that may lead to internal wire breakage after repeated abuse.

Image Views/Image Planes

Transverse View

To obtain a transverse view, scan with the probe marker pointing towards the patient's right side. On the ultrasound image, the left side of the patient will be displayed on the right side of the image display, while the left side will be displayed on the right side of the screen. This form of image orientation is similar to what is seen on CT scan images and some other forms of imaging modalities (Figs. 5.30 and 5.31).

Sagittal View

This can be obtained by scanning with the probe marker pointing towards the patient's head. The left side of the image corresponds to the cephalic end and the right side represents the caudal end as shown in Figs. 5.32, 5.33, and 5.34.

Coronal View

Orient the transducer with the marker pointing to the patient's head and the transducer aligned with the patient's coronal plane.

Fig. 5.30 Showing transducer footprint

Fig. 5.31 Showing probe position while obtaining a transverse view of the upper abdominal aorta

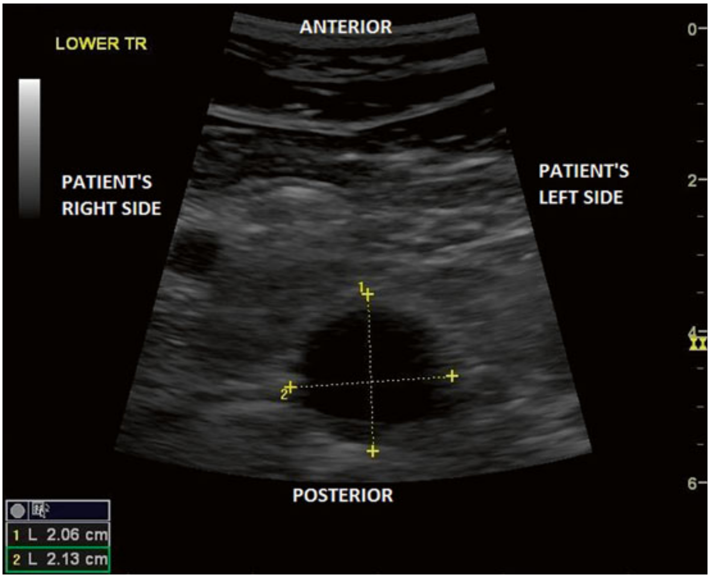

Fig. 5.32 Showing the transverse view of the abdominal aorta. The left side of the screen represents the right side of the patient and vice versa

Fig. 5.33 Showing probe position while obtaining sagittal view of the upper abdominal aorta

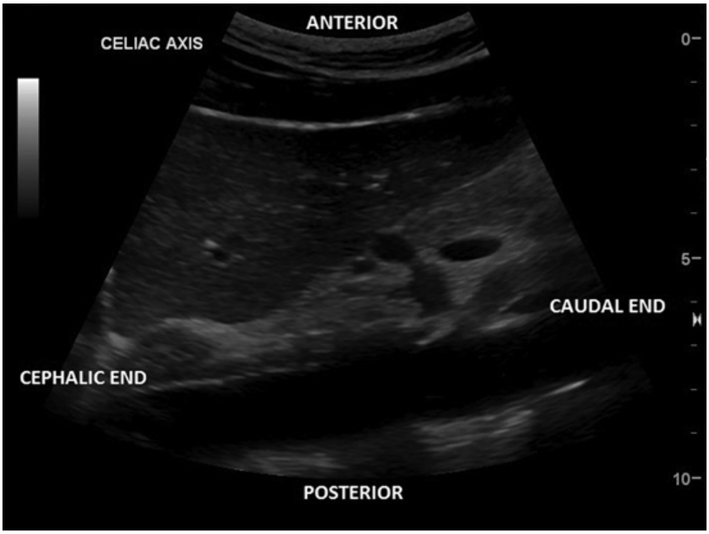

Fig. 5.34 Showing the mid sagittal view of the upper abdominal aorta. The *left* of the screen represents the cephalic end and the *right* represents the caudal end

Ultrasound System Selection

This could be a difficult task; however, you could have a systematic approach based upon the application. For example, if you were going to perform mainly cardiac imaging, then all you need is a system with a phased array transducer for echocardiography and this could also be utilized to image structures in the abdomen and pelvic region. However, if you want to perform mainly abdominal imaging, then a curvilinear low-frequency transducer would be the best option. If you do plan to perform musculoskeletal ultrasound, thyroid, joint imaging, soft tissue imaging, procedures such as central venous access, ultrasound guided joint injections, then a high-frequency linear transducer in the range of 6.0–13.0 MHz is recommended. You may also consider acquiring image storage capabilities such as a compatible DVD burner or ultrasound image printer or a mini-PACS system. However, if you want to just use the ultrasound device as a stethoscope for quick point-of-care use, then a pocket ultrasound device will be sufficient.

Pocket ultrasound devices vary in price from $5K–13K. A larger laptop ultrasound system may range from $20K–70K approximately. The price will vary based upon options selected such as image storage capability, software upgrades, number of transducers, and cart for mobility.

Before purchasing an ultrasound system make sure to look at all options and have an on-site demonstration by the vendor. Scan average and obese patients. Save images and compare with other systems. Select the system that provides the best image quality for the applications you are considering and the ease of use. Also, do consider a warranty option. Some manufacturers may provide an extended warranty.

Pros and Cons of Different POC Ultrasound Systems/Devices

Every system will have some pros and cons. In general, the pocket ultrasound devices do have limited capability. However, they do have the advantage of portability for point-of-care applications. They may also limit reimbursement. So before purchasing an ultrasound unit, especially if this is going to be used for exams and procedures to be billed, you must check with the insurance company regarding caveats on reimbursement.

The laptop systems will provide much more capability and are in reality a better choice. However, the biggest disadvantage is that it may not be very convenient to walk around the hospital with a laptop ultrasound system as compared to the pocket ultrasound device. It does yield better image quality, a larger image size and provide the ability to measure the full array of ultrasound based measurements and calculations.

Transducer Care

Ultrasound transducers require proper care. The ultrasound transducer should be cleaned effectively and disinfected and or sterilized strictly following the instructions of the manufacturer after every use on a patient.

Improper handling and not following recommended steps may cause damage to the transducer during transducer cleaning, disinfection, and sterilization, and could also void the manufacturer's warranty. Only use proper disinfectant recommended by the manufacturer. Different manufacturers may recommend different brands of transducer disinfectants. It is strongly recommended to follow the manufacturer's instructions to avoid damage to the transducer.

Most POC transducers are going to be in contact with the skin during scanning and require regular cleaning and low level disinfection after every use but some special transducers used for TEE, endocavity transducers and intraoperative transducers require very high level of disinfection.

During cleaning also take a moment to inspect the probe and the probe connector and wire for evidence of damage that can potentially jeopardizes the integrity of the transducer and make it unsafe for use on a patient. Contact your ultrasound vendor immediately to report any evidence of damage and immediately discontinue use of the transducer. Most systems will come with a user's manual which may be an online version or a USB flash drive or CD version for most ultrasound systems nowadays.

Chapter 6
Musculoskeletal

James M. Daniels and Alexei O. DeCastro

Approach to the Patient

When examining a patient's musculoskeletal (MSK) system, it is important that the examiner and the patient are comfortable. This means that the patient should be appropriately dressed in clothes such as a pair of shorts and short-sleeve shirt that would easily allow access to the extremities. The patient will be examined in a number of positions; therefore sitting on an examination table of appropriate height is very useful. Standard multipurpose examination tables sometimes pose ergonomic difficulties. A table about waist high in height allows the patient to comfortably sit or lie down while the examiner can access the limb that needs to be evaluated. A stool on wheels is optimum to allow the examiner to sit and move comfortably while scanning. Please see Fig. 6.1 for discussion on scanning of the musculoskeletal system without an assistant.

Selecting a Probe

Table 6.1 shows examples of the various probes and their use in MSK scanning. By far and away, the most used probe is a flat linear array probe. Its high frequency allows very high resolution scanning of tissue, but it limits the depth to only 2–3 cm. This is optimal for most structures. Deeper structures may require a low frequency

J.M. Daniels, MD, MPH, RMSK (✉)
Department of Family and Community Medicine and Orthopedic Surgery,
SIU Primary Care Sports Medicine Fellowship, Southern Illinois
University School of Medicine, Springfield, IL, USA
e-mail: jdaniels@siumed.edu

A.O. DeCastro, MD
Department of Family Medicine, Medical University of South Carolina, Charleston, SC, USA

J.M. Daniels, R.A. Hoppmann (eds.), *Practical Point-of-Care Medical Ultrasound*, DOI 10.1007/978-3-319-22638-5_6

Fig. 6.1 The patient sits on an exam table at a comfortable height for both patient and clinician. The ultrasound machine can be on the same side of the area on the body being scanned. The examiner sits comfortably on a stool that easily moves. The clinician holds the probe in the dominant hand, using the nondominant hand to make adjustments of the machine. Alternatively the machine can be on the opposite side being scanned and an assistant can operate the machine

Table 6.1 Types of probes and their use in MSK scanning

Type	Picture	mHz	Resolution	Depth	Use
Flat		8–12	High	2–3 cm	Most often used
Curved		3–5	Low	Over 5 cm	Hip Large patient Deep structure
Small footprint		8–12	Very high	Very superficial	Digits Wrist Ankle Foot Procedure

curvilinear probe to be used because it is capable of greater penetration, but does not provide the high resolution of the flat probe. Because of this capability, this probe may also be best utilized in large or obese patients. Some clinicians may use a small footprint, or hockey stick probe, that allows them to manipulate around small areas such as fingers, wrists and feet. While scanning, most use their dominant hand to

Fig. 6.2 Demonstrates proper technique to use when scanning. The probe is held with the thumb and index and ring fingers. The small and ring fingers are used to steady the probe against the skin

scan and their nondominant hand to make adjustments on the ultrasound machine. It is very important to keep the elbow to one side to prevent overuse injuries. Figure 6.2 views the proper anchoring and scanning technique that is recommended.

Scanning

Before starting to scan the patient, it is important that the proper patient identification is typed into the machine, and it is preferable that the machine is capable of recording a screenshot of the specific pathology that is noted. This screenshot must be saved especially if a procedure, such as injecting a joint or aspirating a cyst, is performed with ultrasound guidance. This may seem like a very straightforward process, but may vary from manufacturer to manufacturer. Clinicians should make themselves familiar with these features to be able to mark and copy scans. For the most part, ultrasound gel is used as the component between the probe and the skin. Some clinicians use a device called a standoff pad or immerse the digit being scanned in water to scan. These types of studies require more advanced skills and we recommend learning with the ultrasound gel. It is helpful to be generous with the gel in its application in order to facilitate better visualization.

Note that one side of the probe is usually marked with a notch or a small, raised hash mark which usually corresponds with an indicator on the left side of the ultrasound screen. Try to align the probe so that the left side of the probe correlates with the left side of the screen. This can be easily done by applying gel to the probe and simply running one's finger along the top of the probe starting at the side of the notch, which will then correlate with the left side of the screen. This also confirms that the proper probe is connected to the machine. The following sequence should then be followed:

1. The depth of the scan should be adjusted. The dial that controls depth should be clearly marked on the front of the scanner and the structure that is being scanned should be in the center of the screen. If the structure is on the top of the screen and there is a large amount of screen below, the depth needs to be increased. On the other hand, if the structure being scanned is on the bottom of the screen, the depth should be decreased to put the structure in the middle of the screen.
2. The focal zone should be adjusted. These most often can be seen as cross hashes on the side of the screen and they should be adjusted to correlate with the target. They should not be spaced throughout the whole screen, but focused on the area that needs to be scanned. Some machines have preset adjustments for each probe, so one can simply choose from various structures being scanned such as tendon or the area of the body such as the wrist.
3. The next thing that needs to be adjusted is the brightness or the gain on the machine. Many times the first scan shows the structures that are fairly close in contrast. The gain should be adjusted to easily depict the various structures that are being scanned. When attempting to look at a structure that is usually bright or hyperechoic such as a bone, that area can be compared to a structure that is relatively hypoechoic or darker such as the muscle. The gain should then be adjusted so that the best picture and contrast can be obtained.
4. The last thing to adjust is the doppler. There are two types of Doppler on most machines. The first is the power Doppler, which is important for evaluation of many rheumatological conditions. The power Doppler usually assesses the "power" of the blood flow to that area and roughly corresponds with microvasculature. The color Doppler, on the other hand, evaluates the direction of the blood flow, and is not as important as the power Doppler when scanning the musculoskeletal system. Table 6.2 describes the purpose and use of the various types of doppler that is superimposed on the musculoskeletal scan. This scan is often referred to as "gray scale" that we use to identify various anatomical structures. The Doppler is a box that is superimposed upon the gray scale. It is also important to note that there are many artifacts when using Doppler in MSK scanning. Random Doppler signals not correlating with anatomical structure should be ignored. To get the Doppler to the proper setting, one can scan over a bone and adjust the Doppler gain until the random artifacts cease.

Table 6.2 Doppler scan on MSK greyscale

	Purpose	Use
Color	Direction of flow	ID blood vessels
Power	Intensity of flow	ID inflammation, i.e., microflow or structures

Table 6.3 Point of care ultrasound terms describing scanned structures appearance compared to surrounding structures

Term	Reflectivity	Brightness	Example
Hyperechoic	High	White	Bone
Isoechoic	Equal	Same	Tendon
Hypoechoic	Low	Darker	Muscle
Anechoic	Absent	Black	Fluid-filled cyst cross-section blood vessel

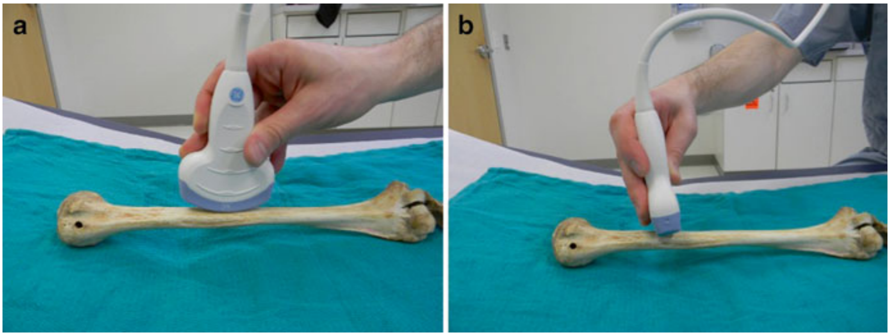

Fig. 6.3 Demonstrates anatomical planes on the body (**a**) long axis and (**b**) short axis

The color doppler is sometimes used to help differentiate between a vein and an artery but a much more helpful way to do this is by the use of sonopalpation, which will be described later. We discussed the gain previously, with reference to contrast or comparing one tissue to another. This is often used interchangeably with the echogenicity of the structure and it correlates to how bright something shows up on the screen. In general, a dense structure like a bone is hyperechoic; where a non-dense structure such as a collection of fluid is anechoic or black. Table 6.3.

It is important to be aware of the different anatomical planes in the body, and the difference between the terms long or short axis view of the structure. Figure 6.3 describes this. There are a number of maneuvers which make it much easier to identify structures using the probe. Figure 6.4 describes these and gives a number of examples.

Because an ultrasound scan is just an interpretation of sound waves bouncing off various objects, there can be a number of artifacts that can sometimes be confusing. A simple review of these can be found in Table 6.4. The most important artifact is anisotropy (pronounced annie sotropy). When scanning certain dense tissues like tendons and ligaments, the sound wave can bounce off at an odd angle. If the angle is less than 85°, a scan can give an appearance as if there is a dark, or anechoic, spot in the center of the tendon or ligament. This can lead the clinician to think that there is a tear when there is one not present. It is important to slide, sweep, toggle, or use the heel toe maneuvers to see if this anechoic, or black area, in the center of the tendon or ligament disappears. Probably the most important maneuver necessary

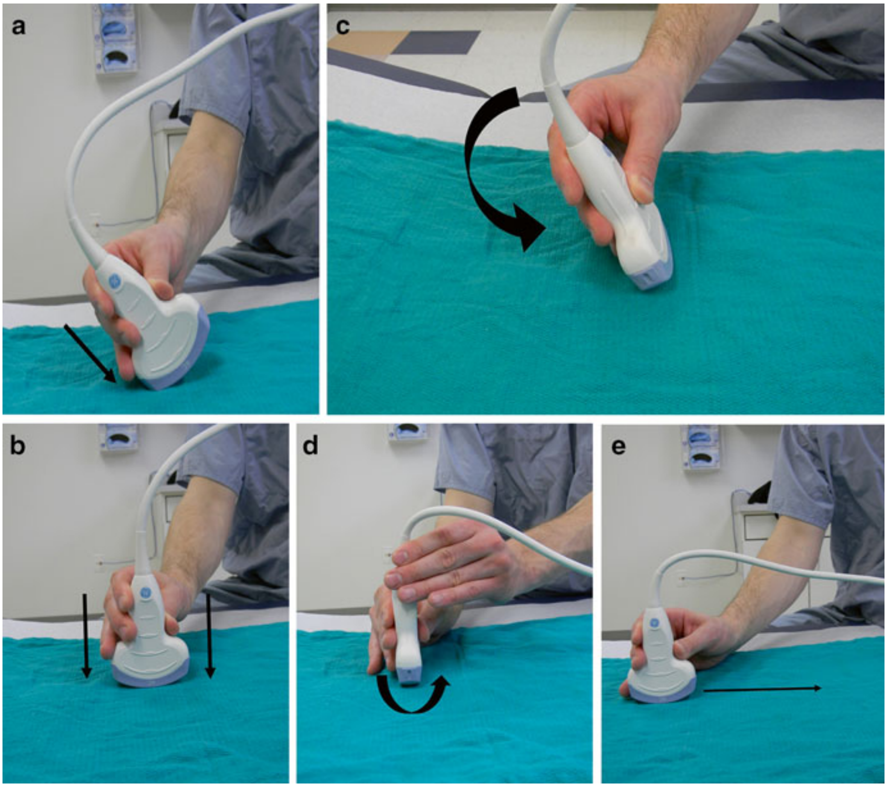

Fig. 6.4 Demonstrates probe movements (**a**) Rocking; (**b**) Compression; (**c**) Tilt; (**d**) Rotating; (**e**) Slide

to do this, is to be able to change the axis of the probe. To do this, the probe is left on the skin and the center of the probe is not moved at a specific point. The probe is then rotated clockwise or counter-clockwise around that point, to give a 90° opposite view of the structure being scanned. (This is demonstrated in Fig. 6.3.) To diagnose a torn tendon, it is important that the tear is evaluated in both the short and long axis to prevent a false positive test from anisotropy.

Normal Anatomy of the MSK System

Table 6.5 provides detailed description and picture of musculoskeletal tendon, ligament, peripheral nerve, bone, and cartilage. When evaluating various tissues, not only is the anatomy important, but also the appearance of these structures on the scan is. It is important that the starry night appearance of musculoskeletal muscle is visualized when it is scanned in the short axis and the sometimes feather or pennate

Table 6.4 Terms to describe various artifacts

	Reason	What you see	Example
Anisotropy	Angle of ultrasound wave won't reflect back at an angle less than 85°	A normally appearing bright (hyperechoic) structure appears black	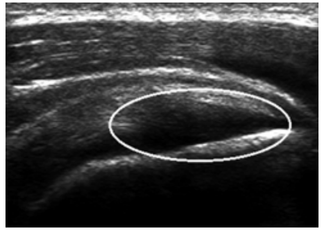
Acoustic shadowing	A dense tissue (bone) reflects most sound waves up so blocks evaluation of deeper structures	Area beneath structure may appear anechoic (black) or may not be able to ID structure beneath	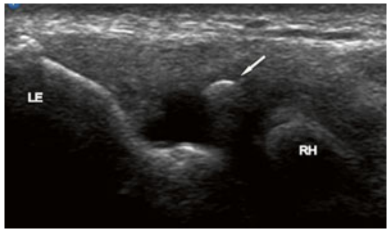

(continued)

Table 6.4 (continued)

	Reason	What you see	Example
Acoustic enhancement	A low density tissue (fluid) allows more sound waves to penetrate so deep structure may be more echogenic (bright)	Deeper structure may appear brighter than adjacent tissue	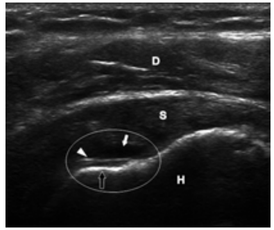
Reverberation artifact	Sound waves reflect back and forth between the transducer and a highly echogenic structure	• "Comet tail" appearance of crystals or foreign body • "Double line" of needle in long axis	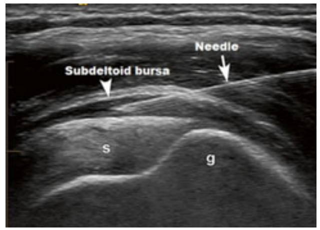

Table 6.5 Examples of normal tissue in MSK point of care ultrasound

Tissue	Short axis	Long axis
Skeletal muscle	Hyperechoic, wavy connective tissue mixed with hypoechoic muscle fibers	
	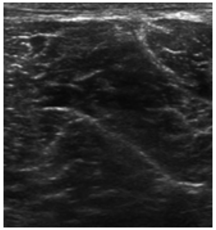 "Starry Night" appearance	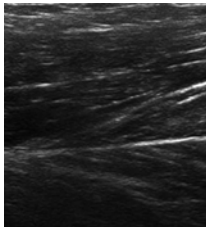 Pennate or "Feather" appearance
Tendon	Linear fibular pattern of a mixture of bright, echogenic tendon fibers with hypoechoic connective tissue	
	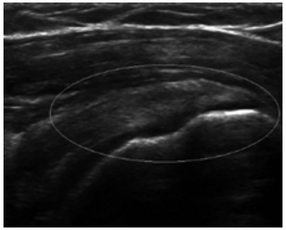 Connects muscle to bone	
Ligament	Tend to look like tendon, but collagen fibers are more aligned and densely packed	
	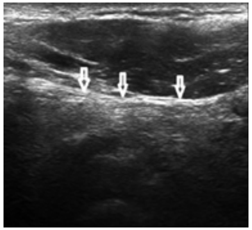 Connects bone to bone	

(continued)

Table 6.5 (continued)

<table>
<tr><th>Tissue</th><th>Short axis</th><th>Long axis</th></tr>
<tr><td rowspan="2">Peripheral nerve</td><td colspan="2">Hypoechoic nerve fibers embedded in hyperechoic epineurium material</td></tr>
<tr><td>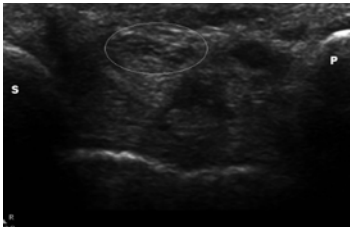

“Honeycomb”</td><td>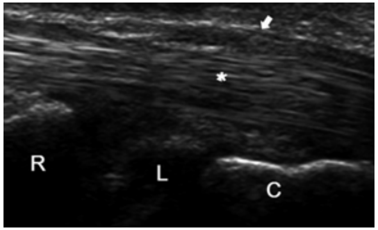

“Train Tracks”</td></tr>
<tr><td rowspan="2">Bone</td><td colspan="2">Hyperechoic bright linear line with inferior acoustic shadowing</td></tr>
<tr><td colspan="2">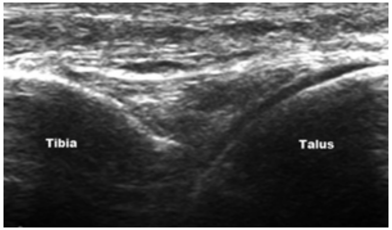
</td></tr>
<tr><td rowspan="2">Cartilage</td><td colspan="2">Anechoic (black) layer overlying bone</td></tr>
<tr><td colspan="2">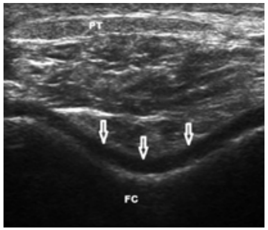
</td></tr>
</table>

appearance of certain muscles in the long axis. Ligaments and tendons have tightly packed collagen fibers which are highly echogenic (bright). This tissue almost always guarantees that there is going to be some type of anisotropy. The view of these structures in both long and short axis is imperative. Peripheral nerves are fairly easy to identify by their hypoechoic nerve fibers embedded in a hyperechoic epineurium material. On the short axis, they have a typical “honeycomb” appearance, where on long axis they look like “train tracks.” The bone is very hyperechoic or bright, and it is usually seen as a linear structure with acoustic shadowing. Articulate cartilage is seen at bone, and it is easily identified by a black or anechoic layer that overrides the bone.

How to Use POCUS as It Pertains to the MSK System: What Does the Evidence Show?

From the ongoing “Rational Clinical Examination” series published in JAMA with evidence based diagnoses, a number of comments were made about the MSK system.

1. There is not a reliably accurate test when checking for labral tears in the shoulder.
2. There are not very many single useful tests when evaluating ligamentous or meniscal injuries of the knee, although a global examination of the knee with the history and mechanism of injury is very useful. (i.e., Lachman Maneuver to check for ACL tear and McMurray’s Test to check for meniscal tear, which were both not found to be very accurate when used in a primary care setting.)
3. Point-specific muscles of the rotator cuff when tested do correlate with MRI findings. Figure 6.5 demonstrates on how to test various muscles of the rotator cuff.
4. Diagnose and nerve entrapment, specifically to carpal tunnel. Tests, such as Tinels, Phalans Test, are not as useful as once believed. The pattern of symptoms seem to be more useful and this can be seen using the CAT scan diagram (Fig. 6.6).
5. Evaluation of MSK system common area that is overlooked or under taught in the training of primary care clinicians. Fortunately, the use of POCUS allows us to evaluate not only the anatomy, but the physiology of the musculoskeletal system.

Common POCUS MSK Findings

Bicep Tendon

Figure 6.7 demonstrates the patient positioning and clinician when evaluating the shoulder. The biceps tendon can be evaluated with the arm at the side and the elbow flexed 90° with the palm up. The linear array probe is used on the anterior aspect of

Fig. 6.5 Test of cuff muscles (**a**) subscapularis; (**b**) infraspinatus; (**c**) supraspinatus; (**d**) teres minor

the shoulder and it is swept side-to-side until the bicipital groove is seen. At this point, the bicipital tendon can be evaluated and followed either caudal or cephalad. If a "halo" or fluid collection is near the bicipital tendon, this can oftentimes be used by clinician as evidence of an effusion in the shoulder. This can help differentiate whether the patient has a serious problem or more rotator cuff issues. Absence of the bicipital tendon and bicipital groove indicates a torn bicep muscle or tendon. The patient can be placed in the "Betty Boop" position shown in Fig. 6.7 and these rotator intervals can be evaluated. This has a high correlation with rotator cuff pathology. Other tendons of the body can also be evaluated. This could include the Achilles tendon. The linear array probe is placed in the short axis position on the posterior aspect of the leg with the patient lying supine. The probe can be placed at the calcaneus and moved superiorly so the Achilles tendon can be easily evaluated. The patient can then be asked to plantar flex against resistance and this places stress on the Achilles tendon which can open up tears that may not otherwise be easily seen. Figure 6.8 demonstrates the scanning technique used for Achilles tendon tears.

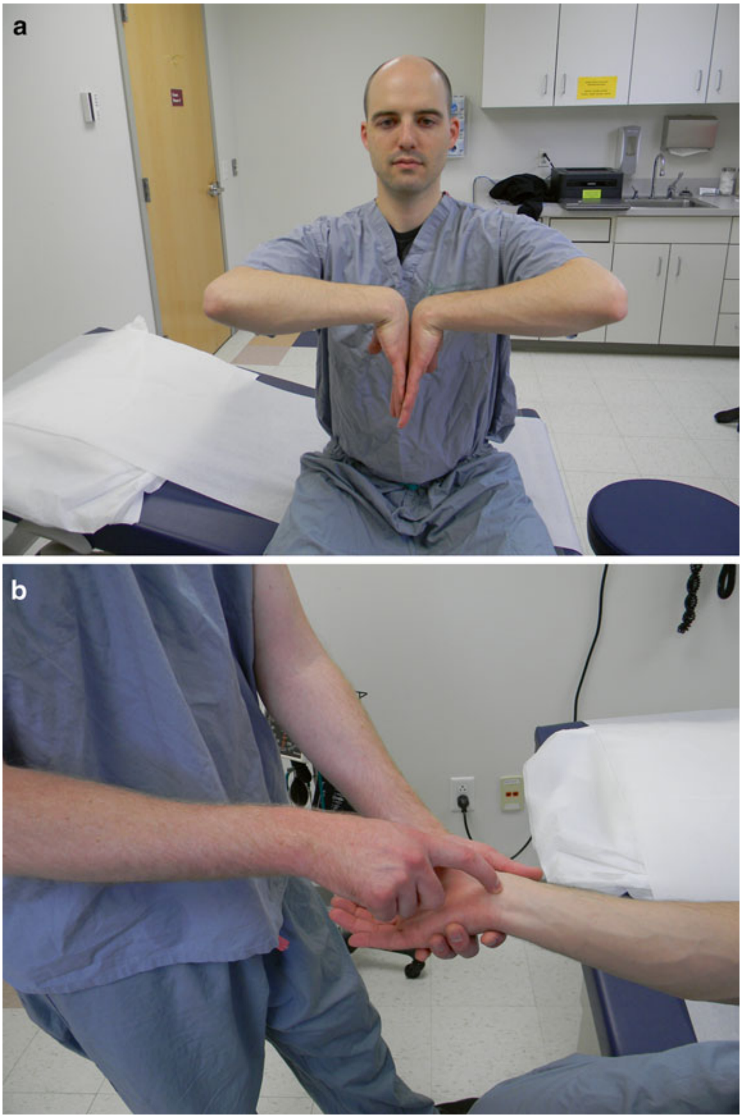

Fig. 6.6 Testing of (**a**) Phalens and (**b**) Tinels for carpal tunnel syndrome

Other tendons can easily be used by using these techniques described here.

Tendon Sheaths/Tenosynovitis

The first dorsal compartment of the wrist is located at the base of the thumb, right where the linear array probe can be placed in short axis and proximally until it crosses the wrist crease. At this point in time two tendons can easily be seen. If they

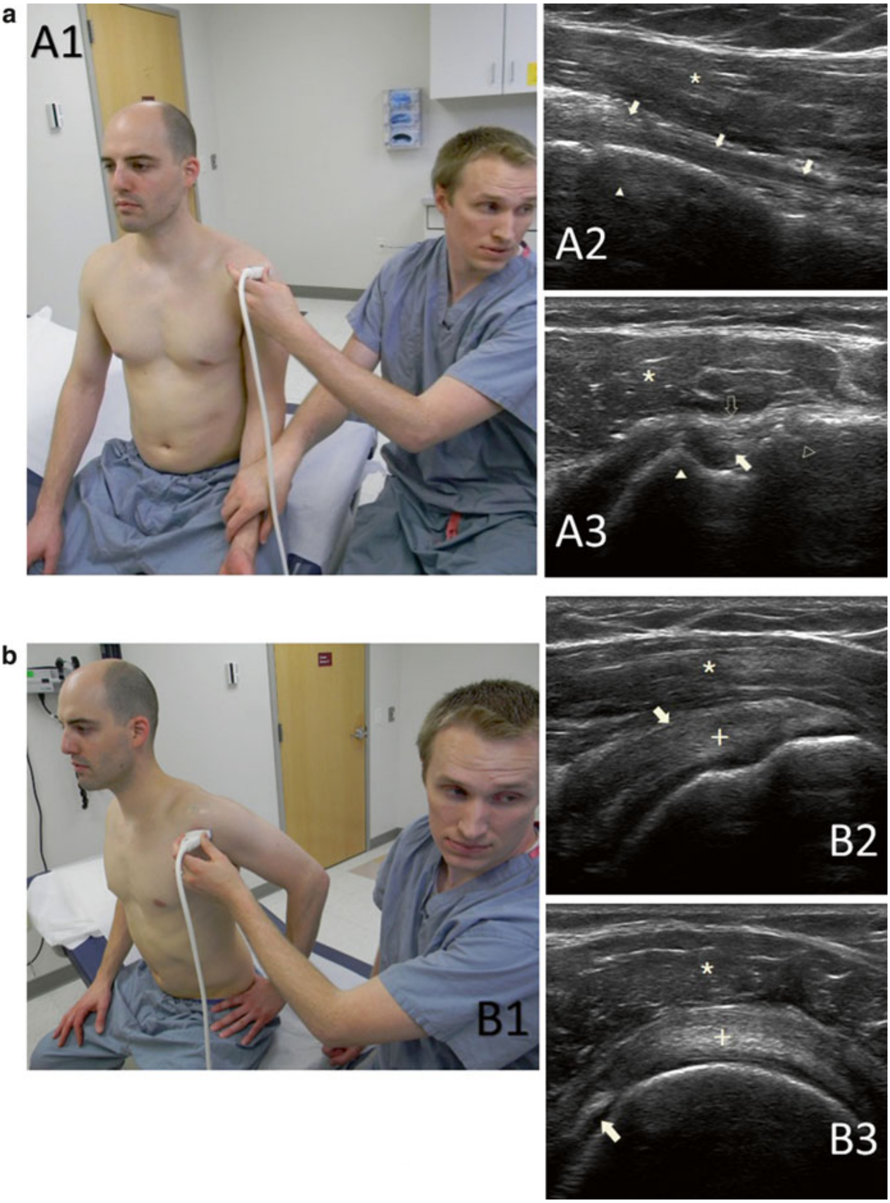

Fig. 6.7 (**a**) (*A1*) Demonstration of patient positioning and clinician when evaluating the shoulder. (*A2*) Biceps long axis (*white arrow* = biceps tendon; *Arrowhead* = humerus; *Asterisk* = deltoid) and (*A3*) Biceps short axis (*white arrow* = biceps tendon; *black arrow* = transverse ligament; *white arrowhead* = lesser tuberosity; *black arrowhead* = greater tuberosity). (**b**) (*B1*) Demonstration of patient in the "Betty Boop" position. (*B2*) Betty Boop long axis view demonstrates supraspinatus (*white arrow* = subdeltoid bursa; target = supraspinatus tendon; *Asterisk* = deltoid). (*B3*) Betty Boop short axis view demonstrates rotator cuff interval (*white arrow* = biceps tendon; target = supraspinatus tendon; *asterisk* = deltoid)

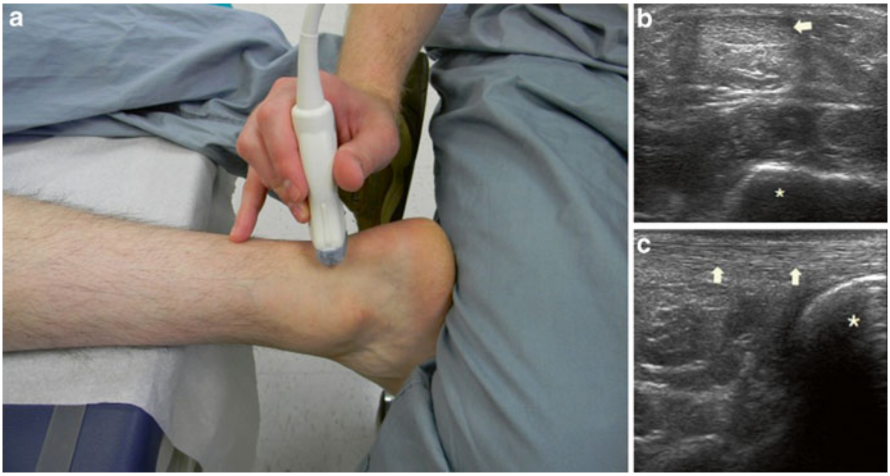

Fig. 6.8 (**a**) Scanning technique for Achilles tendon. (**b**) Short axis (**c**) Long axis (*white arrow* = Achilles tendon; *Asterisk* = Calcaneus)

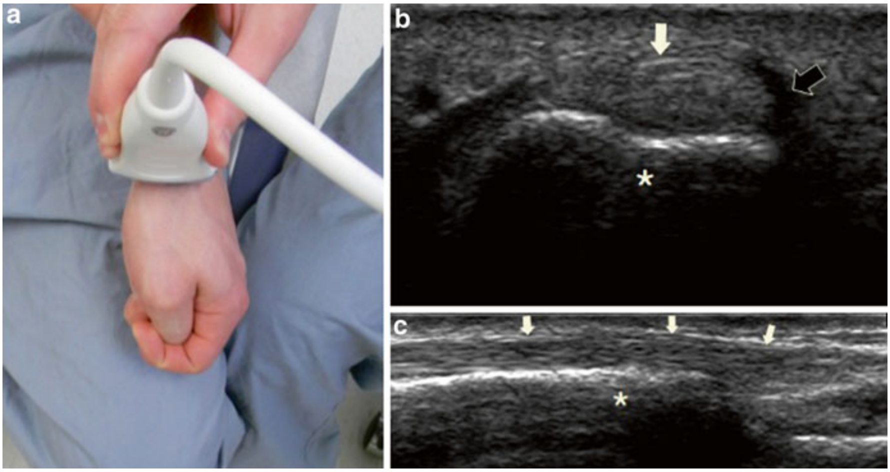

Fig. 6.9 (**a**) Scanning technique for DeQuervain Tenosynovitis. (**b**) Long axis (*white arrow* = first dorsal compartment; *black arrow* = CMC joint) (**c**) Short axis (*white arrow* = first dorsal compartment; *black arrow* = hypoechoic fluid collection around tendon within tendon sheath; *asterisk* = radius)

have "halo" around them, then this correlates with deQuervain's tenosynovitis of the first dorsal compartment. After this is identified, the tendon sheath can be injected with 1 % Lidocaine under ultrasound guidance (Fig. 6.9).

Joints can easily be evaluated using the linear array probe. (Structures that are close to the hip may need to be evaluated with a curvilinear probe.) The linear probe can easily be scanned across one of the joints of the digits, such as the thumb or great toe. Some clinicians prefer to use a small footprint probe to manipulate around

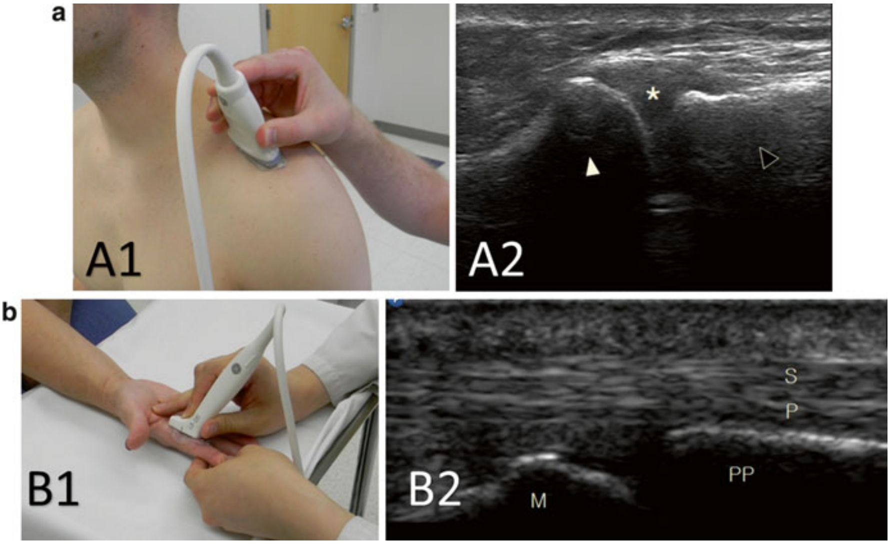

Fig. 6.10 (**a**) (*A1*) AC Joint scanning technique. (*A2*) AC joint within the synovial membrane (*Asterisk* = AC joint; *white arrowhead* = acromium; *black arrowhead* = clavicle). (**b**) (*B1*) Scanning technique for digit. (*B2*) Finger, ventral, longitudinal. (S = flexor digitorum superficialis; P = flexor digitorum profundus; M = Metacarpal; PP = proximal phalanx)

these tight areas. Figure 6.10a shows the AC joint of a patient and Fig. 6.10b shows that of a joint of one of the digits.

Gout Versus Pseudogout

Gout and Pseudogout can be evaluated in this circumstance. The power doppler can be turned on which can reveal whether there is increased inflammation or blood flow in the joint. Then, on the gray scale, one can evaluate small crystals that can be deposited in that joint. If the crystals are right underneath the articular process, these are uric acid crystals. Ones that are more randomly spread throughout the joint, are associated with pseudogout. Use of ultrasound also allows for identification of tophi, which can be formed with longstanding gout. These tophi are oftentimes not seen on radiographs, but easily visualized using ultrasound. The use of the ultrasound allows for a whole new dimension in the diagnosis of gout and pseudogout.

Nerves

A number of peripheral nerves can be easily evaluated using the point of care ultrasound. They are oftentimes associated with local peripheral nerve and artery. These can be differentiated from each other by the use of sonopalpation. In other words,

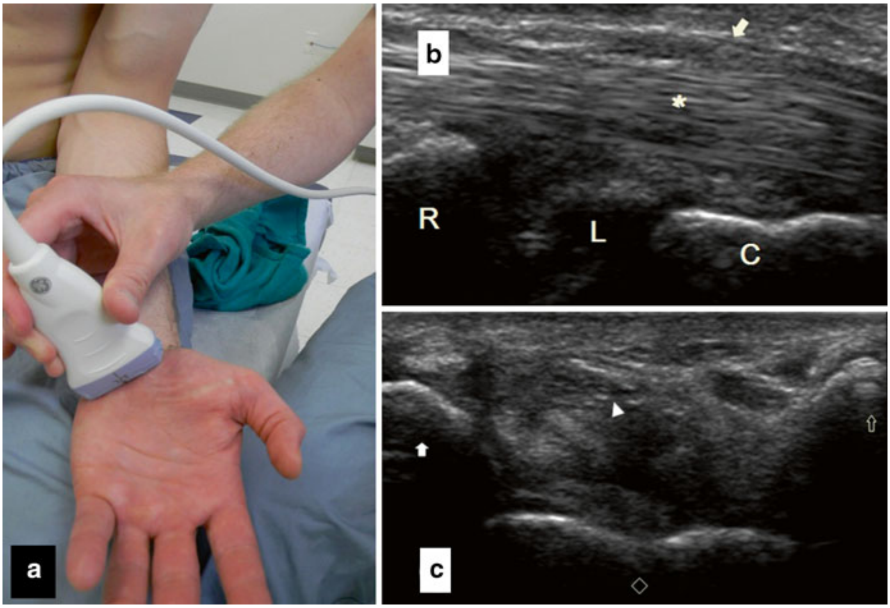

Fig. 6.11 (**a**) Scanning technique for median nerve. (**b**) Long axis (*white arrow* = median nerve; *asterisk* = flexor digitorum; R = radius; L = Lunate; C = Capitate) (**c**) Short axis (*white arrowhead* = median nerve transverse; *white arrow* = scaphoid; *black arrow* = pisiform, Square = Lunate)

increased pressure to sonographic probe is applied to the area being scanned. The structures that are easily compressible such as veins and soft tissues are compared to those that cannot be compressed, such as a tendon sheath or arteries. By using the point of care ultrasound, superficial nerves such as the median nerve can be evaluated easily for nerve entrapment and other pathology. See Fig. 6.11.

E. Muscles

Muscles can be easily evaluated. As described above, when the shoulder is scanned, the patient can be placed in the "Betty Boop" position and the rotator interval can be evaluated.

Chapter 7
Obstetrics/Gynecology

John Rocco MacMillan Rodney

Introduction

Point-of-care pelvic ultrasound is the basis for obstetrical and nonobstetrical risk stratification [1]. The most common indications for POC sonography are vaginal bleeding, irregular menses, amenorrhea, pelvic pain, palpable pelvic mass, ovarian cyst, lost IUD. Common indications related to pregnancy are uncertain dates, pregnancy of unknown location, decreased fetal movement, threatened abortion, suspected preterm labor, suspected malpresentation. Ultrasound is not a substitute for a pelvic exam, although there has been questioning of the utility of the traditional pelvic exam during the management of a threatened abortion in the emergency department [2, 3].

Products of conception and embryonic tissue are frequently discovered in the vaginal vault during a speculum exam. Examination of the vaginal vault and cervix is integral to the evaluation of vaginal bleeding for both pregnant and nonpregnant patients. Suspicious cervical lesions, vulvar masses, as well as signs of trauma related to sexual abuse, are frequently detected only through direct visualization [4].

J.R.M. Rodney, M.D., RDMS (✉)
Department of Family Medicine Obstetrics, Christian Brothers University, Memphis, TN, USA
e-mail: roccorodney@gmail.com

J.M. Daniels, R.A. Hoppmann (eds.), *Practical Point-of-Care Medical Ultrasound*, DOI 10.1007/978-3-319-22638-5_7

Initial Approach

Before performing bedside sonography, the physician should understand how the equipment works. Fumbling with the controls disrupts the examination, generates unnecessary patient anxiety, and can be interpreted as incompetence. The physician should be familiar with the published guidelines for the indications, performance, and the documentation of ultrasound examinations [5–8].

For obstetrical cases, anticipate a mother's questions regarding the general health, estimated gestational age, and gender assignment of the pregnancy [9]. In cases of suspected anomalies or threatened fetal viability, prepare for questions regarding the prognosis of the pregnancy, particularly if the patient is experiencing vaginal bleeding. Above all, be gentle and honest. A 2004 study of women with fetal anomalies demonstrated that women preferred accurate rather than immediate information regarding fetal prognosis [10].

The initial image orientation is determined by the positional relationship between the patient and probe (Figs. 7.1 and 7.2). The patient's position may be modified throughout the examination. Elevating the hips, for example, can help evaluate deeper structures.

During ultrasound examinations, the gravid uterus may compress the maternal inferior vena cava, causing maternal flushing, nausea, anxiety, and discomfort. These manifestations of maternal vascular obstruction are part of the supine hypotensive syndrome. Placing the patient in the upright or left lateral decubitus position usually provides immediate relief [11].

Probe Selection and Scanning Techniques

Sonographic evaluation of the pelvis can be performed either transabdominally using the curvilinear array or transvaginally using the endocavitary transducer.

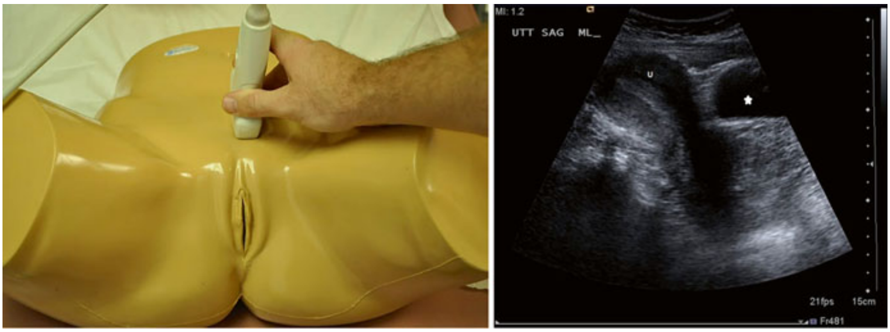

Fig. 7.1 *Left*—Curvilinear probe with orientation marker out of field of view. *Right*—Curvilinear probe with the orientation marker on the lateral side

Fig. 7.2 *Left*—For the transverse plane, the marker is pointed toward the mannequin's right side. *Right*—Transabdominal image of the uterus (U) in the transverse (*axial*) plane. The bladder (*star*) creates an anterior acoustic window

Fig. 7.3 *Left*—The Curvilinear probe positioned for the axial view. *Right*—The probe is rotated to produce the sagittal view

Transabdominal Sonography Using the Curvilinear Probe

The transabdominal approach allows evaluation of various pelvic and intra-abdominal structures, including the hepatorenal space (*Morison pouch*) and gallbladder [12]. The transabdominal view has two planes: sagittal and axial (Fig. 7.3). Often the sagittal view is described as longitudinal. The axial plane may be described as transverse. To begin, hold the probe in the right hand with the thumb touching the probe's orientation marker (often a ridge). The marker should correspond to a dot on the upper left portion of the screen. Images at the top of the screen are closer to the probe. Images at the bottom of the screen are farther away from the probe.

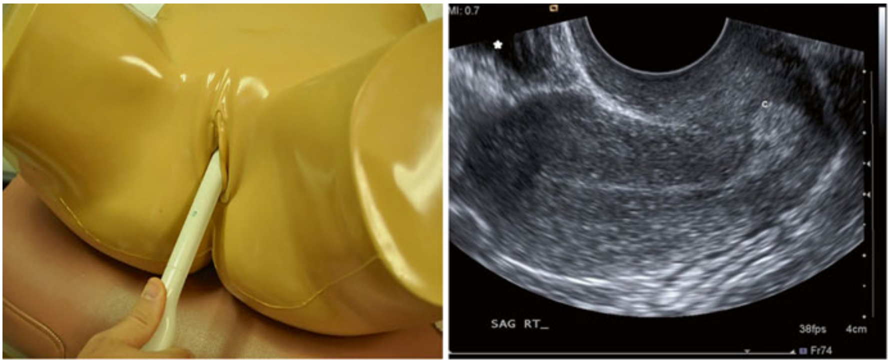

Fig. 7.4 *Left*—An endocavitary transducer introduced into a mannequin. Note the probe's marker pointing toward the 12 o'clock position, generating a sagittal image. *Right*—Contrast the semicircular representation of the endocavitary probe to the arch of the curvilinear probe. The bladder (*star*) and cervix (C) are represented on the screen

Fig. 7.5 *Left*—While inside the mannequin, the probe is rotated 90° counterclockwise to generate the coronal view. Note the marker pointing toward the 9 o'clock position. *Right*—The resultant coronal image of the uterus, gestational sac, fallopian tubes, and ovaries

Transvaginal Sonography with the Endocavitary Probe

During a transvaginal ultrasound, the endocavitary probe (EC) operates at depths between 5 and 10 cm. The anatomy is visualized in two planes: the longitudinal (sagittal) (Fig. 7.4) and the coronal (transverse or axial) (Fig. 7.5). Before starting the examination, ask the patient to empty their bladder to make the exam more comfortable for the patient and to improve visualization. The operator places conductance gel on the probe tip and covers the transducer with a sheath or condom. The sonographer then places lubricant on the outside of the cover. After informing the patient, the EC probe is inserted and the exam begins with the marker at the 12 o'clock position.

Fig. 7.6 A retroverted uterus with calipers measuring the endometrial stripe. The cervix is located on the screen's right, and the fundus is on the left. Note the more balanced gain setting in this view

The Longitudinal Plane

By convention, the longitudinal view is the first plane obtained when performing TVS. When the probe marker points toward the ceiling, the sagittal plane is displayed on the screen with clear visualization of the long axis of the uterine body and endometrial stripe. The cervix is on the screen's right side, and the bladder is on the screen's upper left portion (Fig. 7.6). Difficulty obtaining this standard view can signify anatomical variation or erroneous machine settings.

The Coronal Plane

To obtain a coronal view of the uterus, rotate the EC probe counterclockwise 90° moving the marker from the 12 o'clock to the 9 o'clock position (Fig. 7.7). The image plane is now perpendicular to the uterine body and divides the patient into cephalic and caudal regions.

The screen's left and right sides should represent the patient's right and left, respectively. The transvaginal probe is moved vertically or horizontally or may also be rotated. These maneuvers can be disorienting but gather essential information for diagnosis. The sonographer maintains orientation by limiting the probe's rotation to the 90° between 9 and 12 o'clock.

To systematize the description and performance of bedside TVS, we divide the pelvis into nine sectors to be evaluated in both the longitudinal and coronal planes (Fig. 7.8).

Fig. 7.7 Coronal probe position obtained after rotating the probe counterclockwise by 90°. The probe's marker is no longer visible and points toward the patient's right thigh

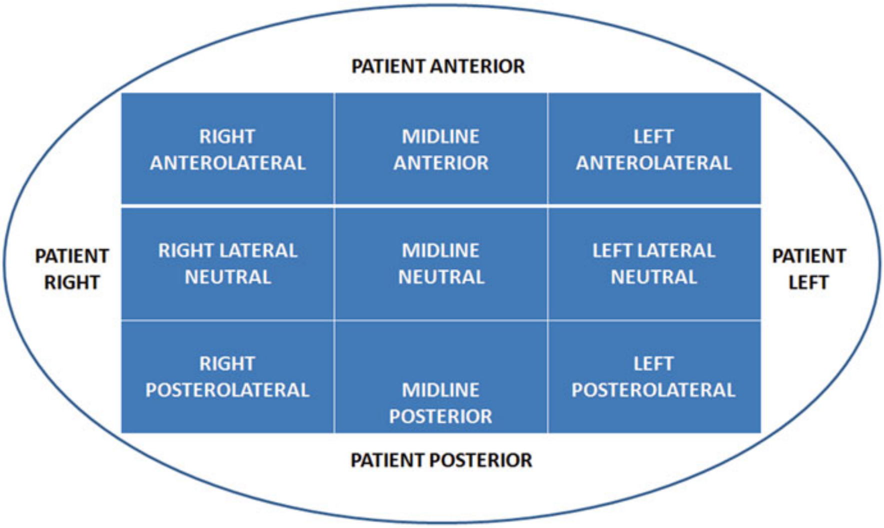

Fig. 7.8 Descriptive map of the endocavitary probe position. Rotate the probe counterclockwise by 90° to obtain a coronal view

The Nonobstetrical Sonographic Examination

The Cervix

The cervix is the lower portion of the uterus that communicates with the vagina through the endocervical canal. Like the uterus, the cervix is a vascular, hormonally responsive tissue with glandular components. These endocervical glands can become obstructed (Nabothian Cysts) (Fig. 7.9), especially during ovulation.

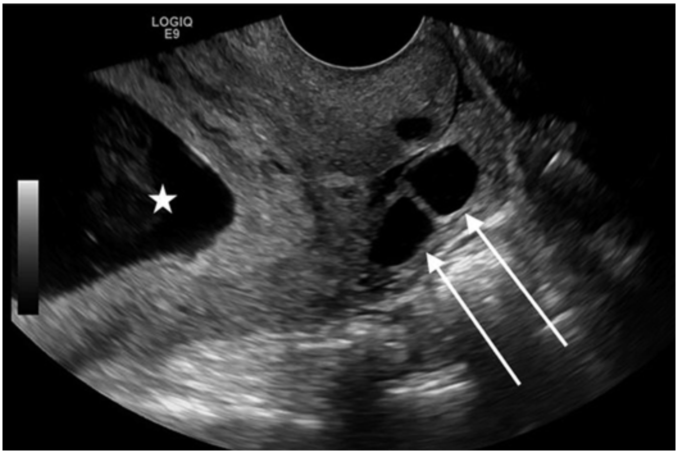

Fig. 7.9 Nabothian cysts (*arrows*) are obstructed endocervical glands. The cystic fluid is a vascular and anechoic with a surrounding thin, hyperechoic wall. Note the adjacent gestational sac (*star*) with the placenta covering the internal cervical os

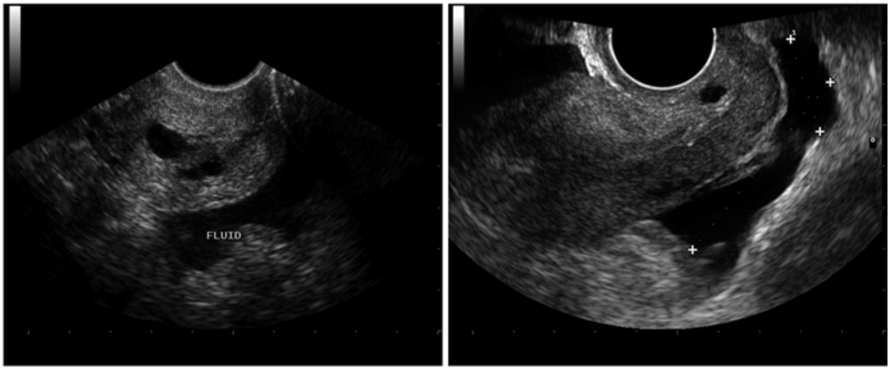

Fig. 7.10 *Left*—complex fluid with clots and debris in the Pouch of Douglas. A hemorrhagic corpus luteal cyst ruptured during the first trimester. *Right*—Transvaginal sagittal image with simple, gravity dependent free fluid in Pouch of Douglas

The cervical length (CL) should be measured transvaginally in the sagittal plane using a straight line to connect the internal and external os, the [13]. The CL reliably predicts the likelihood of preterm birth [14, 15]. It is usually greater than 30 mm. When it measures less than 25 mm prior to 24 weeks gestation, the cervix is considered shortened [14, 16, 17].

- Describe the length and morphology of the cervix.
- Evaluate the posterior cul-de-sac (Pouch of Douglas) for free fluid (Fig. 7.10).

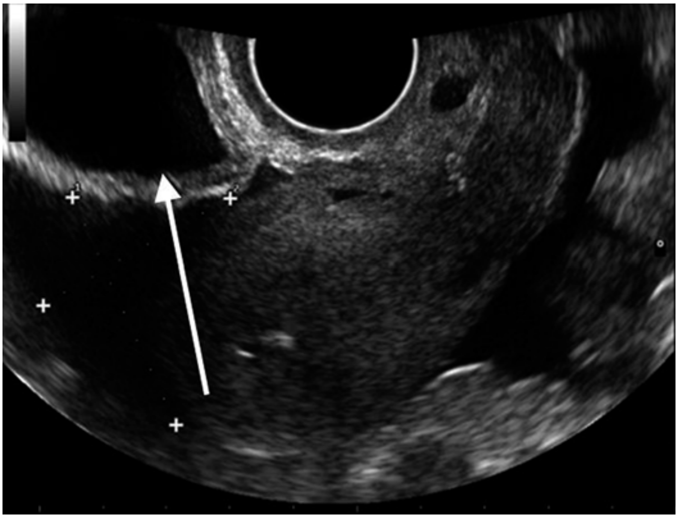

Fig. 7.11 Sagittal view of free fluid surrounding the uterus. Note the Pouch of Douglas, the triangular bladder (*arrow*), and solitary nabothian cyst

The Uterus

The average nongravid uterus measures 7 cm long and 3–4 cm in width and height [18]. The uterine volume increases after each pregnancy. Roughly the size and shape of a pear, the nulliparous uterus is composed of three layers: the covering serosa, the muscular hypoechoic myometrium, and the dynamic hyperechoic endometrium that lines the intrauterine cavity [19].

The relationship between the uterine body and cervix determines uterine position. To describe this relationship, the sonographer relates the long axis of the uterus to the vaginal canal (version) and cervix (flexion).

- Note if the uterine position is anteverted or retroverted.
  - With anteversion, the fundus points anteriorly toward the bladder (Fig. 7.11).
  - With retroversion, the fundus points posteriorly away from the bladder (Fig. 7.12).
  - With anteflexion, the anterior aspect of the bladder is concave (Fig. 7.13).
  - With retroflexion, the bladder wall is convex (Fig. 7.14).
- Measure the uterine length from the fundus to the cervix in the sagittal plane.
- Measure the uterine height (depth) perpendicularly to the length using an antero-posterior measurement in the same longitudinal plane.
- The uterine width is the largest measurement obtainable in the coronal view.
- Measure the endometrial thickness or stripe.

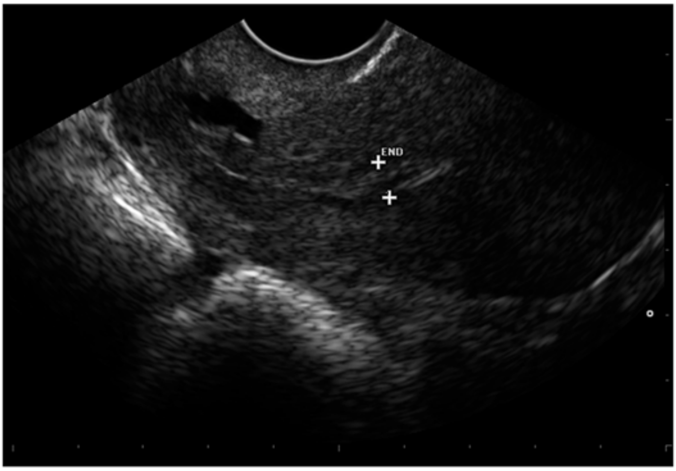

Fig. 7.12 Sagittal image of retroverted, retroflexed uterus with endometrial stripe measurement (calipers). The fundus opposes the bladder and nabothian cysts are noted

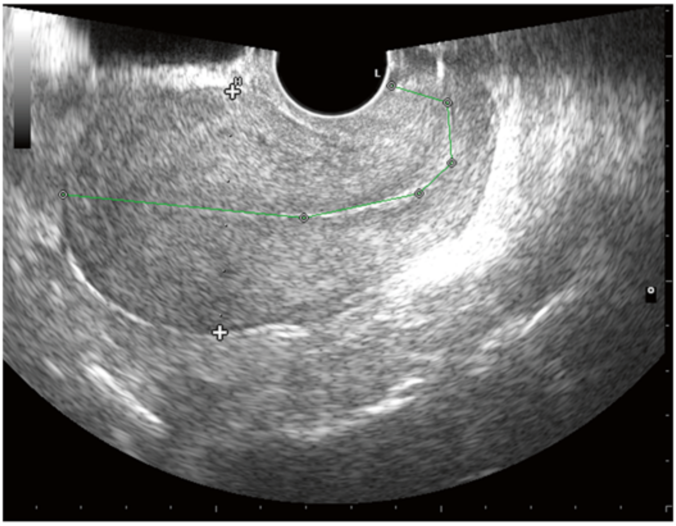

Fig. 7.13 Transvaginal image demonstrating an anteverted, anteflexed uterus in the sagittal plane. Notice the high gain function counfounding interpretation by decreasing the contrast resolution

The Fallopian Tube (Salpinx)

The fallopian tubes cannot be visualized in the absence of pathology or iatrogenesis. Near the patient's midline, the uterus surrounds the interstitial portion of the salpinx. The extrauterine isthmus widens into the infundibulum and fimbria, which opens directly into the peritoneum. A visible, fluid-filled hydrosalpinx suggests

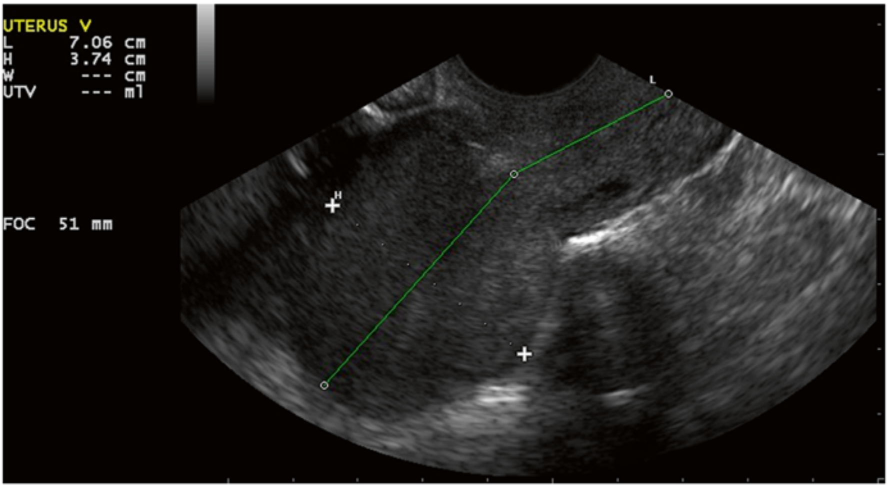

Fig. 7.14 Sagittal image of an anteverted and retroflexed uterus. Calipers are measuring the length of the uterus. Note the convex appearance of uterus

previous tubal surgery or pelvic inflammatory disease (PID). A hydrosalpinx may appear cystic with incomplete septations and endosalpingeal folds that look like "beads on a string." The dilated fallopian tube should be differentiated from the adjacent ovary to ensure a correct diagnosis [20].

The Ovaries

Like the uterus, the ovary is a hormonally responsive organ that changes appearance with the menstrual cycle. The ovaries are measured in three perpendicular orthogonal planes. The transvaginal longitudinal plane best measures the length and height (anterior–posterior diameter); the transvaginal coronal view best measures the width. Premenopausal, nondominant ovaries measure approximately 2 cm × 2 cm × 2 cm [21]. A normal, nondominant ovarian volume measures less than 10 cc.

Ovarian volume decreases with age and oral contraceptive use [21]. Initially, each ovary contains several follicles that measure less than 1 cm in diameter. After 7 days, a single ovarian follicle emerges and will grow to a diameter slightly greater than 2 cm. This dominant follicle will then rupture and become the vascular corpus luteum, which on sonography has a crenulated appearance and thickened wall [22].

- Locate the cornua and attempt to visualize the salpinx.
- Normal fallopian tubes are difficult to identify.
- Sweep out from the axial plane of the uterine fundus and locate the iliac vessels and identify the ovaries (Fig. 7.15).
- Measure the ovarian height, width, and length using two orthogonal planes.
- Describe the ovarian morphology.

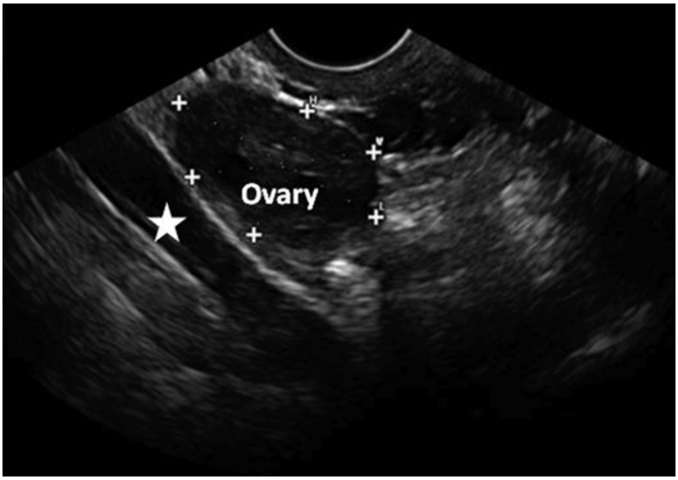

Fig. 7.15 Right (intraperitoneal) ovary with adjacent, (retroperitoneal) iliac vasculature (*star*). The ovarian fossa abuts the hypgastric artery and vein

Common Nonobstetrical POCUS Findings

Simple Ovarian Cysts

On transvaginal ultrasound, 2 % of pregnant women and 10 % of all women will have a functional ovarian cyst or cysts [23, 24]. Follicles generally have a diameter less than 2–2.5 cm, and a cyst's diameter usually exceeds 2.5 cm. For simple cysts in premenopausal women, repeat ultrasound at 6-week intervals so the images will correspond with a new cycle at a different phase than the previous examination. If a cyst is unilocular and has a diameter less than 10 cm, the malignant potential is less than 0.1 % [20, 25].

Corpus Luteum Cysts

The corpus luteum forms in the potential space left by a ruptured, dominant follicle. Corpus luteum cysts are the most common ovarian masses during early pregnancy. These cysts can hemorrhage, torse, or rupture. Under these circumstances, patients present with acute abdominal pain. In pregnancy, corpus luteum cysts (Fig. 7.16) may persist for 16 weeks and exceed 10 cm in diameter [26–28].

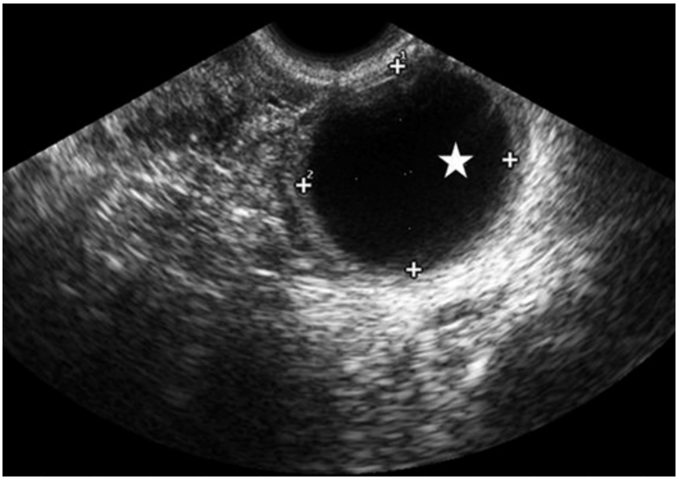

Fig. 7.16 Beta-hCG stimulated the corpus luteum (*star*) to produce progesterone. A corpus luteum cyst is an example of a functional cyst and has a thickened wall. It is not uncommon to see echogenic hemorrhagic material within the cysts

Hemorrhagic Cysts

With a rich vascular supply, the cystic morphology of the hemorrhagic corpus luteum has a varied appearance that is related to the formation and absorption of blood clots. On ultrasound, hemorrhage can have a reticular, cobweb appearance within a complex cyst. In general, cystic hemorrhage should resolve within 2 months [20].

For premenopausal women:

- Hemorrhagic cysts measuring less than 3 cm do not require description or repeat testing.
- Hemorrhagic cysts between 3 and 5 cm merit description but not repeat testing.
- Hemorrhagic cysts greater than 5 cm in diameter merit description and repeat testing in 6–12 weeks, at the beginning of a subsequent menstrual cycle.

A hemorrhagic cyst in a postmenopausal woman is considered malignant until proven otherwise.

Pelvic Pain

Pelvic pain can be classified as either acute or chronic and is related to menses and pregnancy. The investigation of pelvic pain drives almost half of gynecological diagnostic laparoscopies [29]. In general, non-cyclic chronic pelvic pain must persist for at least 3 months irrespective of menses. Cyclic chronic pelvic pain changes with relation to the menstrual cycle and persists for at least 6 months [26]. Common causes of both cyclic and non-cyclic chronic pelvic pain include endometriosis, adenomyosis, postoperative adhesions, and fibroids. For this chapter, our focus is on acute pelvic pain related to the adnexa and uterus in the nonpregnant patient [30].

Adnexal Torsion

Adnexal torsion is a sudden disruption of adnexal arterial blood flow. Patients with ovarian torsion experience acute abdominal pain. Risk factors include preexisting adnexal enlargement, often secondary to an occult teratoma or ovarian cyst. Use the following facts to aid rapid diagnosis and intervention: [26, 29, 31].

- The torsed ovary appears grossly enlarged, often five times larger than average.
- The presence of arterial or venous blood flow does not reliably exclude torsion.
- 20 % of cases present during pregnancy.
- Teratomas and ovarian cysts are frequent causes of acute torsion.

Pelvic Inflammatory Disease (PID)

PID includes endometritis, salpingitis, tubo-ovarian abscesses, and pelvic peritonitis. The Centers for Disease Control (CDC), specify in their diagnostic criteria for PID that the patient must have uterine, adnexal, or cervical motion tenderness [30, 32]. In the USA, PID is diagnosed over one million times annually. The incidence of chlamydia has quadrupled over the last 25 years, with particularly high rates in urban environments. In some neighborhoods, more than 25 % of young women test positive for chlamydia [33].

Without treatment, many women with PID will partially resolve the initial painful symptoms but will become infertile secondary to chronic inflammation. For diagnosing PID, pelvic ultrasound has a high sensitivity and specificity and may simultaneously exclude other obstetrical and gynecological causes. A dilated, fluid-filled hydrosalpinx is present in most cases of PID. Cine-looping can help differentiate a folded, dilated tube from a septated cyst. Color Doppler can distinguish an iliac vein or anomalous varix from a dilated fallopian tube.

Acute Salpingitis and Tubo-ovarian Abscess (TOA)

Salpingitis is inflammation of the fallopian tube that can progress to an abscess (Fig. 7.17). Tubal inflammation and its sequelae fall within the broader categories of acute or chronic PID. Sonography has improved the clinician's ability to accurately diagnose pelvic infectious disease: [3, 26, 34]

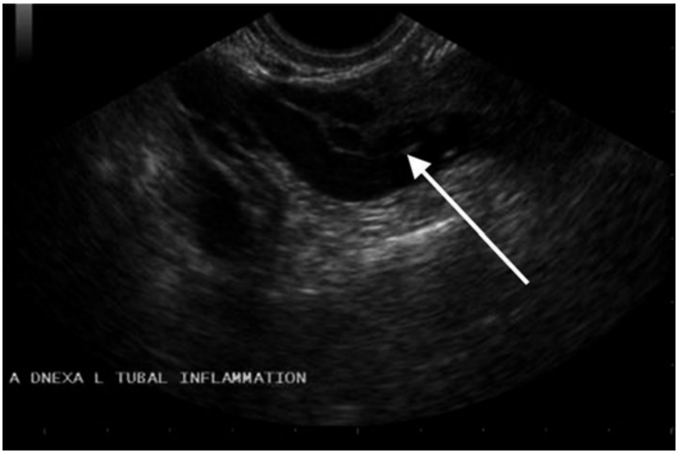

Fig. 7.17 Left ovary with adjacent hydrosalpinx. Note the tortuous, serpiginous appearance of the affected tube (*arrow*). The incomplete septations of a hydrosalpinx can be mistaken for a complex ovarian cyst

- A hypervascular fallopian tube can be described sonographically as hyperemic.
- Endovaginal ultrasound is better than a bimanual examination for diagnosing PID.
- The sonographer can use the free hand to supplement the ultrasound investigation performed with the other hand.
- The sliding organ sign will be positive since adhesed or inflamed organs do not slide easily and have blurred margins as opposed to healthy structures that may be compressed and move freely.

Polycystic Ovarian Syndrome

Affecting more than 6 % of the population, polycystic ovarian syndrome (PCOS) is a disorder of androgen metabolism that can cause infertility and pregnancy complications, such as gestational diabetes, preeclampsia, and preterm birth [35, 36]. The diagnosis can be established with two of the three following Rotterdam Criteria:

1. Menstrual disturbance.
2. Hyperandrogenism (defined clinically or by serum testing).
3. Polycsystic ovaries.

Polycystic Ovaries

The sonographic diagnosis of PCOS has evolved with advances in ultrasound imaging and has also become more controversial. With more sophisticated equipment, the sonographic component of the diagnosis can require one polycystic ovary with

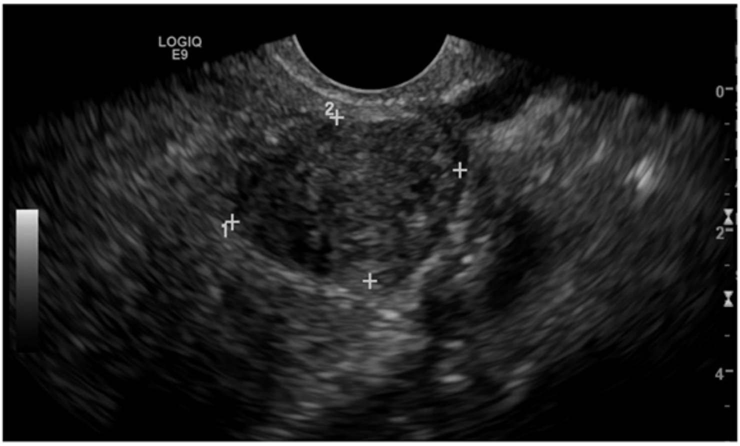

Fig. 7.18 Smooth contoured mass within the uterine myometrium representing a fibroid

at least 12 follicles. The ovarian volume should measure greater than 10 cc. The measured ovary should not have a dominant follicle, and the patient should not be taking oral contraceptive pills [35].

The diagnosis of PCOS should never be based on an isolated sonographic finding. At most, an ovary can suggest but not diagnose PCOS in the absence of other criteria. Hirsutism affects approximately 60 % of patients with PCOS and with confirmed hyperandrogenism [36, 37].

Uterine Fibroids (Leiomyomata)

Uterine fibroids (Fig. 7.18) are benign muscular tumors that can be found throughout the myometrium. Fibroids affect over one-third of women and grow under the influence of estrogen. A fibroid may outgrow its blood supply and can necrose and cause pain and bleeding [38].

On ultrasound, fibroids are often hyperechoic, spherical structures that can be described as submucosal, subserosal, or intramural. At times, they are pedunculated, meaning connected to the uterus via a vascular stalk.

Abnormal Uterine Bleeding

A diagnosis of exclusion, abnormal uterine bleeding describes hemorrhage deviant from a previously normal menstrual cycle. This diagnosis compels the performance of a thorough anatomical, obstetrical, hormonal, infectious, and oncologic evaluation. Normal menses are bleeding episodes that last between 2 and 7 days and occur every 24–35 days.

Patients should relate the frequency, pattern, amount, and duration of their cycles. Patient age stratifies risk but does not narrow the differential diagnosis. Over 80 % of endometrial cancers initially present with postmenopausal bleeding [19, 39].

Common Obstetrical POCUS Findings

Developmental Milestones and Dating

During early development, the gestational sac diameter of an *intrauterine pregnancy* (IUP) increases by 1 mm a day and should be visible at 3–4 mm in size [40]. The presence of a *yolk sac* denotes an intrauterine pregnancy [41] (Figs. 7.19 and 7.20).

Fig. 7.19 Intrauterine pregnancy with yolk sac and embryo

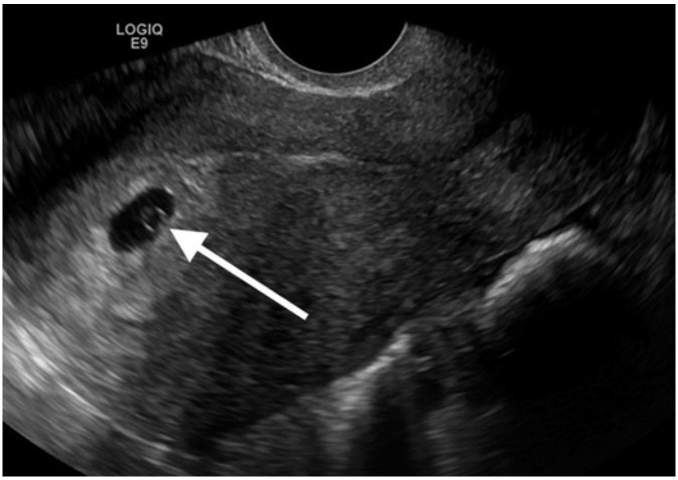

Fig. 7.20 A yolk sac (*arrow*) confirms an intrauterine pregnancy

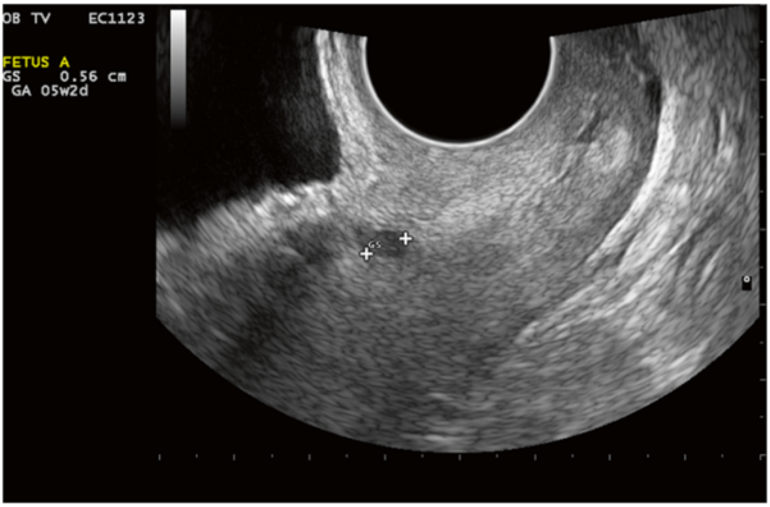

Fig. 7.21 Gestational sac measuring 5.6 mm corresponding to an EGA of 5 weeks and 2 days

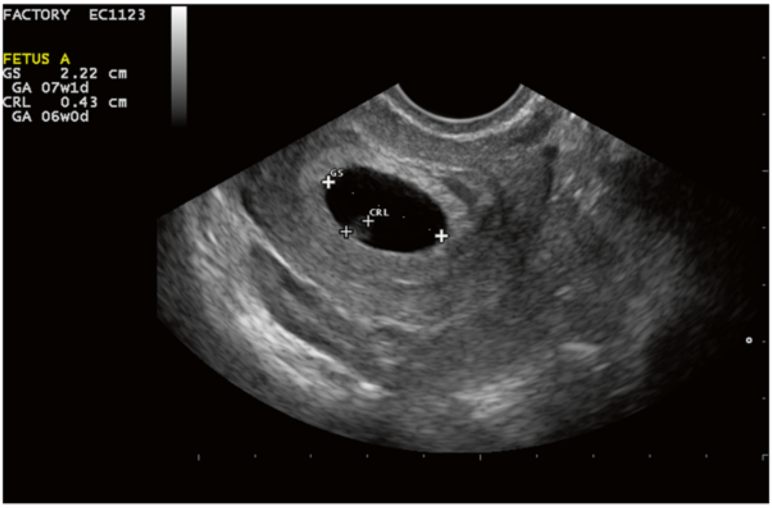

Fig. 7.22 Crown rump length (CRL) of 4.3 mm at 6 weeks gestation

- *Week 5*: The gestational sac diameter is generally greater than 3 mm, and the serum hCG level exceeds 1000 mIU/mL (Fig. 7.21). To calculate the gestational age, add 30 to the mean sac diameter (MSD) in mm to estimate the gestational age [40].
- *Week 6*: At 6 weeks, the yolk sac is the first structure seen within the gestational sac and should be seen once the MSD exceeds 13 mm (Fig. 7.22). The serum hCG is greater than 2500 mIU/mL. The fetal heart flickers on the screen [40, 42].

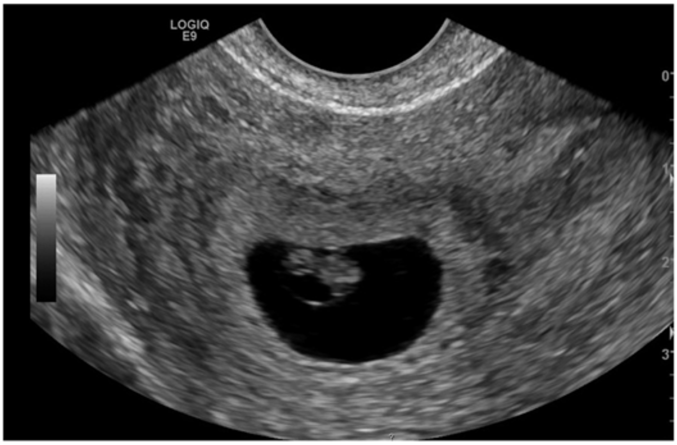

Fig. 7.23 Yolk sac and 7 week intrauterine embryo

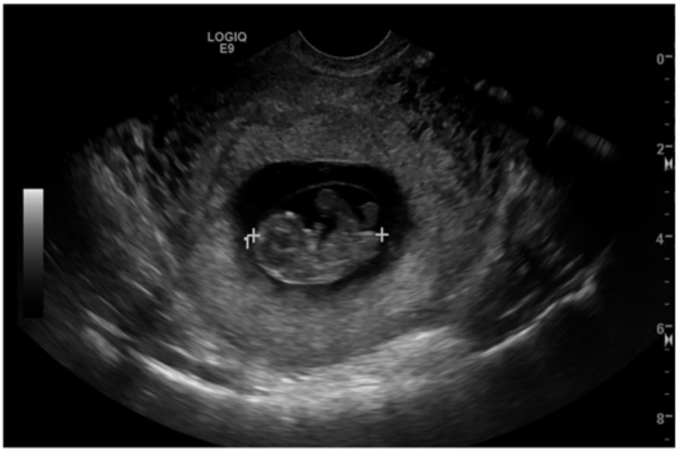

Fig. 7.24 Embryo with physiological midgut herniation. The amnion does not fuse with the chorion until the early second trimester. The space between the amnion and chorion is not a subchorionic hemorrhage

- *Week 7*: The CRL is between 9 and 14 mm; the heart rate measures 130–160 beats per minute. The fetal pole should be visualized, and the serum B-hCG is greater than 5000 mIU/mL (Fig. 7.23). To estimate gestational age in days, add 42 to the crown rump length [40, 43].
- *Week 8*: The umbilical cord and amnion can be visualized. The brain cavity and choroid plexus can be seen [44, 45] (Fig. 7.24).
- *Week 9*: The embryonic heart rate peaks at 170–180 beats per minute (Fig. 7.25).
- *Week 10:* embryo has developed into a fetus and completed organogenesis (Fig. 7.26).

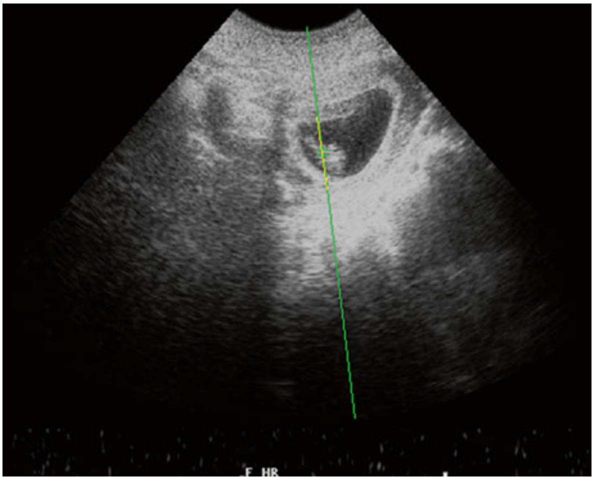

Fig. 7.25 Fetal heart rate at the upper limit of normal

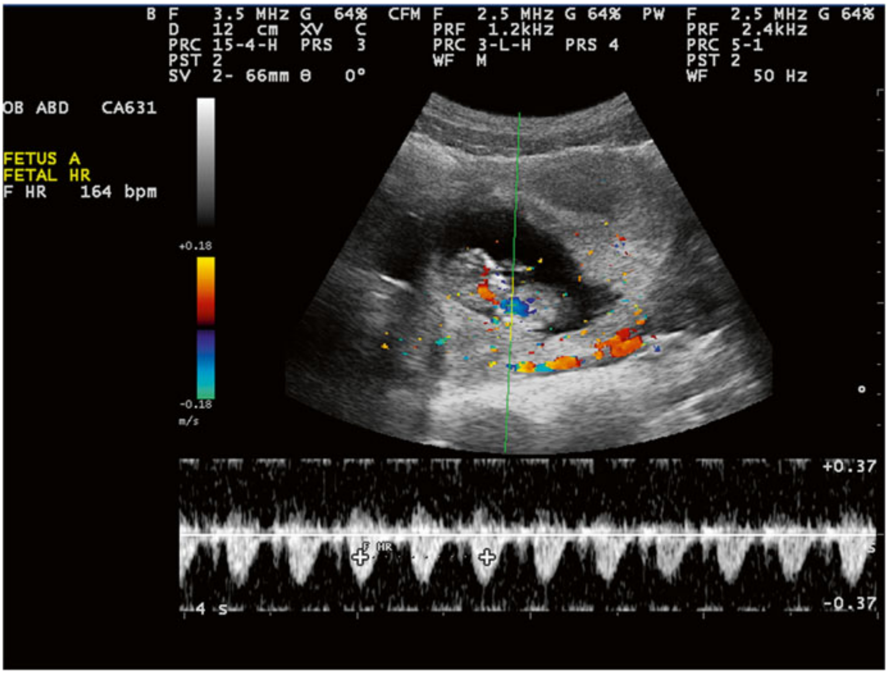

Fig. 7.26 Fetus at 10 weeks gestation with completed organogenesis and humanoid appearance. The fetal heart rate should be measured using M-Mode to minimize exposure as defined by the ALARA principle

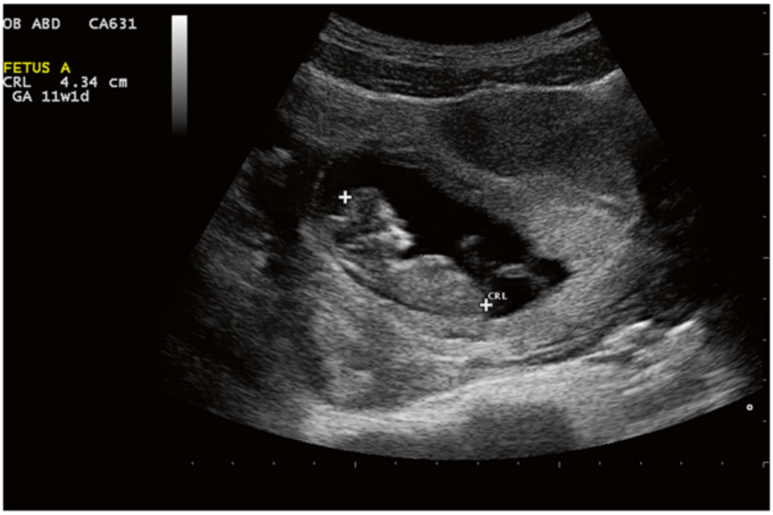

Fig. 7.27 CRL of 11 week 1 day gestation with posterior cranial ossification. Midgut herniation appears to have resolved but can persist to 12 weeks

- *Week 11*: Visualization of the occiput marks the beginning of ossification (Fig. 7.27).
- *Week 12*: Midgut herniation should have resolved at this point.

Key Points

The crown rump length (CRL) at 10 weeks is the best method for calculating the estimated gestational age (EGA) [46]. In general, the CRL is within 5 days of the expected delivery date (EDD) [46]. The biparietal diameter (BPD) is accurate before 20 weeks gestation [46].

The adjusted ultrasound age (AUA) is a better predictor of the EDD than the last menstrual period (LMP) before 20 weeks gestation [46].

Vaginal bleeding in early pregnancy can represent an ectopic pregnancy, a potential miscarriage, normal physiology, or developing pathology. When a premenopausal woman presents with painful vaginal bleeding, immediately perform a urine pregnancy test, an ultrasound, and a pelvic exam. The initial scan should assess for free fluid in Morison pouch and the pouch of Douglas [47]. Both transabdominal and transvaginal ultrasound should be rapidly performed while labs are processed and medications are administered.

The differential diagnoses are based on the gestational age of the pregnancy, the amount and character of the blood, and the presence and character of pain. These data determine clinical decisions and management [48].

- A positive urine pregnancy test correlates with a serum *beta human chorionic gonadotropin* (β-hCG) level greater than 50 mIU/mL.

- A blood type and *Rhesus (Rh) D antigen* screen should be drawn, along with a quantitative β-hCG.
- Pregnancy can be visualized at the "discriminatory zone," which corresponds to a β-hCG of 1500 mIU/mL for an endovaginal sonogram [49].
- At a β hCG level between 6000 and 8000 mIU/mL, the embryo should be visualized transabdominallly.

Ectopic Pregnancy

Ectopic pregnancy is the leading cause of death in the first trimester. Risk factors for ectopic pregnancy include previous ectopic pregnancy, prior tubal surgery, pelvic inflammatory disease, and fertility treatment. For patients with a previous ectopic pregnancy, the recurrence rate approaches 20 %. An overwhelming majority (97 %) implant into the fallopian tube. For visual detection, the detection of an adnexal mass with ultrasound has a sensitivity of 84 %, a specificity of 99 %, and a positive predictive value of 96 % [40, 42, 43, 50].

Many other visual and laboratory factors can confound a definitive diagnosis. For example, a pseudogestational sac can be seen within the uterus in 20 % of cases. Patients undergoing fertility are at particular risk for heterotopic pregnancies. Finally, many cases have no sonographic evidence of pregnancy inside or outside the uterus.

Pregnancy of Unknown Location

Over two-thirds of ectopic pregnancies initially present with a B-hCG less than 1000 mIU/mL. Approximately 15 % of these sonographically indeterminate cases will have an ectopic pregnancy. The management is largely determined by the hemodynamic status of the patient.

Traditionally, patients with suspected ectopic pregnancy have been followed using serial serum beta HCG testing, sometimes using a level of 2000 mIU/mL as the threshold for intervention. In 2011, Doubilet et al. performed a retrospective study analyzing outcomes in indeterminate cases and found the following:

- A viable term birth occurred after an initial indeterminate scan with a β-hCG level above 4000 mIU/mL.
- If a woman with an initially indeterminate ultrasound was found to have a live intrauterine pregnancy, fetal viability through the first trimester and the probability of a live term birth had no relation to the initial serum β-hCG.

The authors suggested that hemodynamically normal patients should be assessed with serial sonography and questioned the value of repeated measurements of the serum β-hCG [49]. The following statements should aid decisions:

- Use serial B-hCG's to follow a suspected ectopic [51].
- Use serial sonography to assess the health of a documented intrauterine pregnancy.

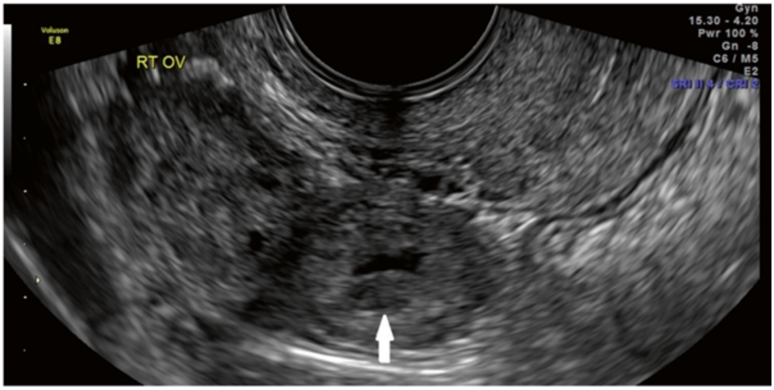

Fig. 7.28 Tubal ectopic pregnancy (*arrow*). The salpinx surrounds the embryo demonstrating the "tubal ring" sign

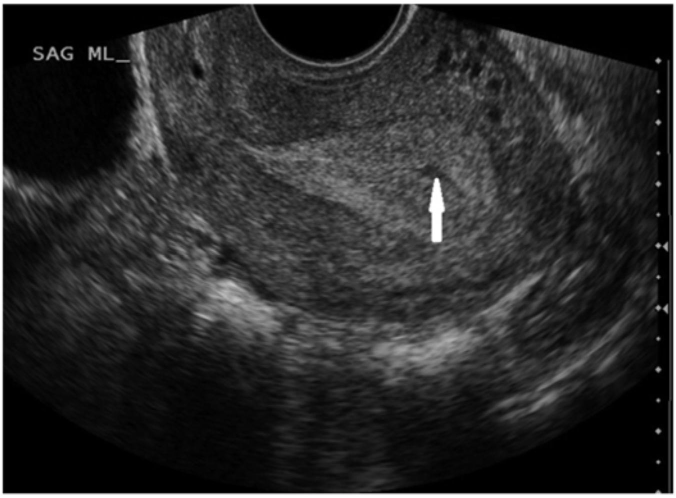

Fig. 7.29 Tear-drop shaped hypechoic focus within the endometrial cavity suggests a pseudogestational sac (*arrow*)

In emergency situations, the presence of free-fluid in *Morison pouch* has a strong association with ruptured ectopic or other acute intraabdominal pathology, which forms the basis for both transabdominal and transvaginal sonography in acute cases [52]. Regardless of pregnancy location, the endometrium thickens as part of the hormonally driven decidual reaction from pregnancy implantation. A thickened endometrium with free-fluid in the cul-de-sac is suspicious but not pathognomonic for ectopic pregnancy.

Ultrasound may demonstrate a "tubal ring" (Fig. 7.28) created by the trophoblast of pregnancy within a hyperechoic, symmetrically walled tube [53].

A *pseudogestational sac* (Fig. 7.29) s a central, intrauterine fluid collection that is surrounded by a reactive decidua. During the exam, a pseudosac may have irregular borders and a complex, mercurial architecture [52]. A gestational sac is eccentric within the endometrium, while a pseudosac is within the endometrial stripe.

Threatened Abortion

Spontaneous vaginal bleeding during the first trimester is a common clinical presentation is termed *a threatened abortion,* and increases the risk of miscarriage, and causes significant maternal concern [51]. The fastest way to reassure a mother is to measure the fetal heart rate using a portable Doppler. Doppler alone, however, cannot reliably detect the fetal heart tones during the first trimester. Physician sonographer must prepare for situations where the fetal heart beat will be absent or slower than expected.

Sonographic Evaluation of Fetal Cardiac Activity

The embryonic heart beat should be visible when the CRL exceeds 4 mm (Fig. 7.30). As the pregnancy develops, specific rate thresholds predict demise and viability:

- After 6 weeks gestation, the heart rate should exceed 100 beats per minute.
- A rate less than 80 beats per minute has been associated with a 100 % risk of embryonic demise.

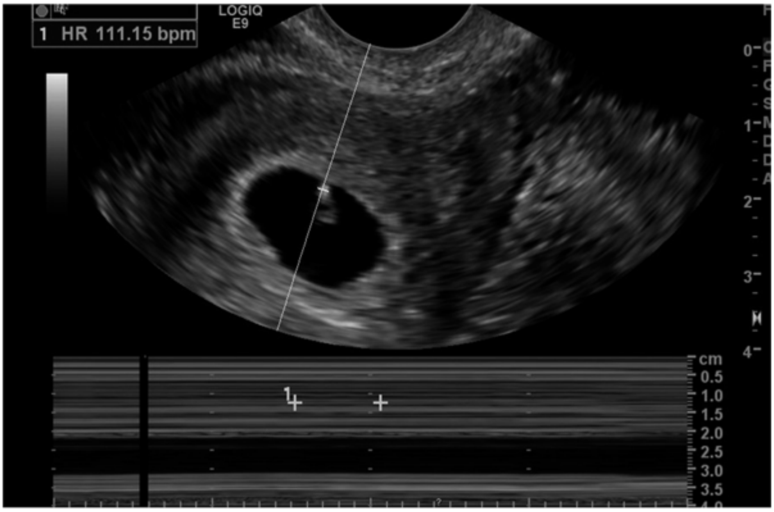

Fig. 7.30 The embryonic heart beat is detectable at 5 weeks gestation. At 9 weeks, the heart rate peaks around 170 beats per minute

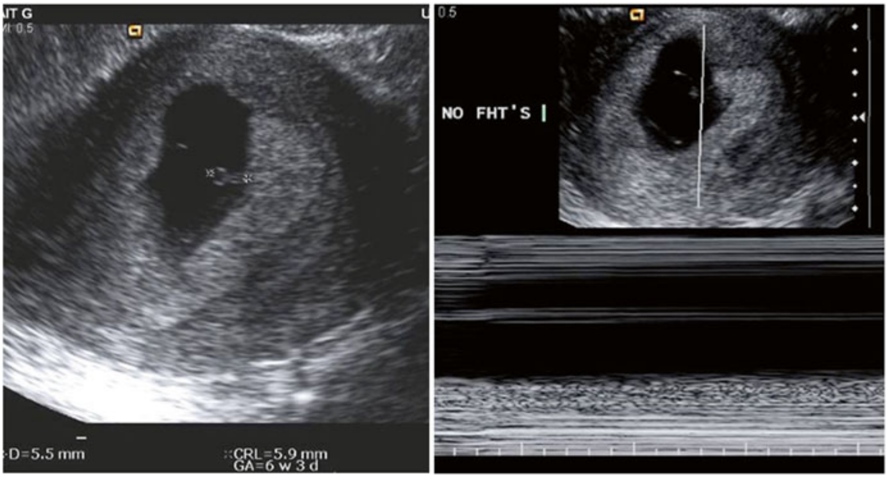

Fig. 7.31 *Left*—a 5.9 mm crown rump in a 6 week 3 day embryo. *Right*—an embryonic demise with absent heart motions

- After 7 weeks, a heart rate less than 120 beats per minute is associated with pregnancy loss [54, 55].

Unless associated with threatened maternal health, a suspicious rate should be followed sonographically until cardiac activity is not detected. Many institutions have protocols that confirm the absence of cardiac activity and embryonic demise that require two physicians documenting 3 min of absent cardiac activity.

Embryonic Demise

Confirmed by the absence of cardiac activity, a nonviable intrauterine embryo measuring greater than 5 mm defines an embryonic demise (Fig. 7.31). The morphology of and relationship between specific structures, such as the gestational and yolk sacs, increase the suspicion of demise:

- An embryonic pole (<5 mm in length) with no interval growth over the course of a week suggests demise [40].
- A difference of less than 5 mm between the mean sac diameter and the embryonic length is associated with greater than a 90 % risk of spontaneous abortion [40, 51, 54].

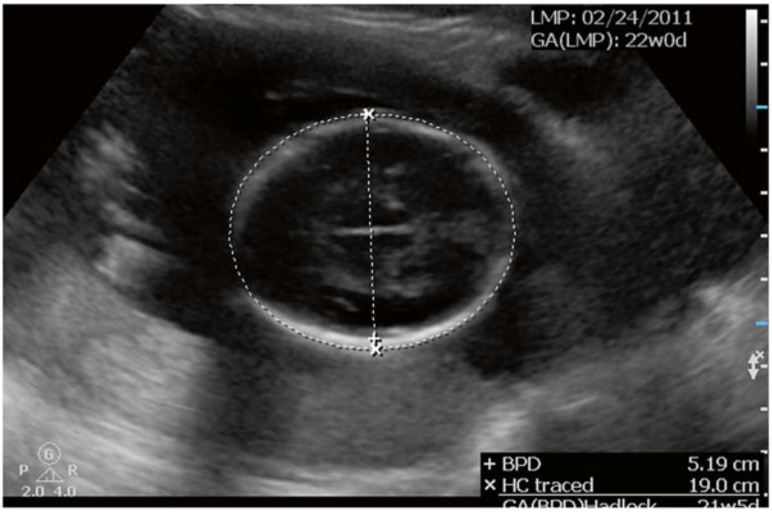

Fig. 7.32 Biparietal diameter using the "leading-edge to leading edge" technique

Composite Gestational Age

Using more than one parameter to calculate the gestational age significantly increases the accuracy of the adjusted ultrasound age (AUA). The most commonly used composite gestational age calculation is the Hadlock formula, which include the biparietal diameter (BPD), the head circumference (HC), the femur length (FL), and the abdominal circumference (AC) to calculate the adjusted ultrasound age (AUA) and the estimated fetal weight (EFW).

Of note there are regional and ethnic variations that should determine the formula used to calculate the estimated gestational age and weight. High altitude, for example, is associated with smaller fetuses. Therefore, babies in Denver are dated using different composite ultrasound formulas than babies scanned in Houston. The Biparietal Diameter (BPD) should include the thalamus, CSP, and falx (Fig. 7.32).

The Abdominal Circumference (*AC*) (Fig. 7.33) is measured at the level of the stomach and the confluence of the left portal and umbilical vein. When measuring, avoid the distorting effects of excessive mechanical pressure. The AC has the greatest interobserver and intraobserver variation of the biometric fields. In general, the AC is a poor solitary measure of the gestational age, but it is the most important determinant of the estimated fetal weight [56].

The Femur Length (*FL*) (Fig. 7.34) can be measured at 12 weeks, once ossification is underway. The FL is measured from the greater trochanter to the lateral condyle.

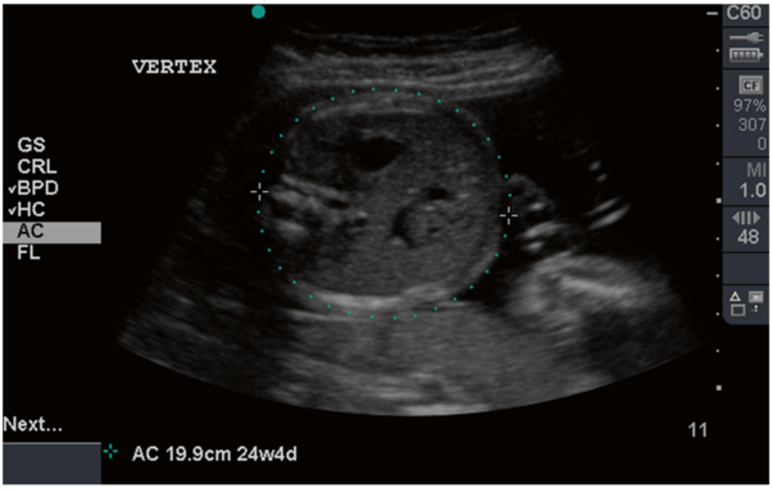

Fig. 7.33 The abdominal circumference (AC) measured at the plane of the stomach and "hockey stick" shaped confluence of the umbilical and left portal veins. Only one anterior and one posterior rib are visualized. This axial plane prevents the distorting effects of an inappropriate angle of incidence

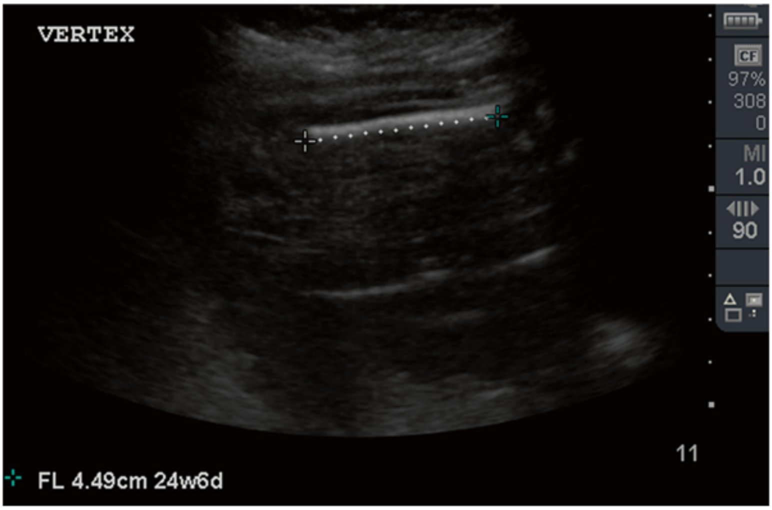

Fig. 7.34 The femoral length (FL) should not be used as an independent dating variable after 22 weeks gestation. The measurement is taken from the greater trochanter to the lateral condyle

References

1. Moore CL, Copel JA. Point-of-care ultrasonography. N Engl J Med [Internet]. 2011 Feb 24 [cited 2011 Oct 4];364(8):749–57. http://www.ncbi.nlm.nih.gov/pubmed/21345104.
2. Seymour A, Abebe H, Pavlik D, Sacchetti A. Pelvic examination is unnecessary in pregnant patients with a normal bedside ultrasound. Am J Emerg Med [Internet]. 2010 Feb [cited 2012 Jan 9];28(2):213–6. http://www.ncbi.nlm.nih.gov/pubmed/20159393.
3. Close RJ, Sachs CJ, Dyne PL. Reliability of bimanual pelvic examinations performed in emergency departments. West J Med [Internet]. 2001 Oct [cited 2011 Oct 15];175(4):240–4; discussion 244–5. http://www.pubmedcentral.nih.gov/articlerender.fcgi?artid=1071590&tool=pmcentrez&rendertype=abstract.
4. Cook RL, Hutchison SL, Østergaard L, Braithwaite RS, Ness RB. Systematic review: noninvasive testing for Chlamydia trachomatis and Neisseria gonorrhoeae. Ann Intern Med [Internet]. 2005 Jun 7 [cited 2012 Jan 9];142(11):914–25. http://www.ncbi.nlm.nih.gov/pubmed/15941699.
5. ACOG Practice Bulletin No. 101: Ultrasonography in pregnancy. Obstet Gynecol [Internet]. 2009 Feb [cited 2011 Aug 17];113(2 Pt 1):451–61. http://www.ncbi.nlm.nih.gov/pubmed/19155920.
6. AIUM practice guideline for the performance of obstetric ultrasound examinations. J Ultrasound Med [Internet]. 2010 Jan [cited 2012 Jan 8];29(1):157–66. http://www.ncbi.nlm.nih.gov/pubmed/20040792 29.
7. AIUM practice guideline for the performance of pelvic ultrasound examinations. J Ultrasound Med [Internet]. 2010 Jan [cited 2012 Jan 8];29(1):166–72. http://www.ncbi.nlm.nih.gov/pubmed/20040793.
8. AIUM practice guideline for documentation of an ultrasound examination. J Ultrasound Med [Internet]. 2009 Jan [cited 2012 Jan 8];28(1):110–3. http://www.ncbi.nlm.nih.gov/pubmed/19106369.
9. Georgsson Ohman S, Grunewald C, Waldenström U. Perception of risk in relation to ultrasound screening for Down's syndrome during pregnancy. Midwifery [Internet]. 2009 Jun [cited 2011 Dec 13];25(3):264–76. http://www.ncbi.nlm.nih.gov/pubmed/17920172.
10. Alkazaleh F, Thomas M, Grebenyuk J, Glaude L, Savage D, Johannesen J et al. What women want: women's preferences of caregiver behavior when prenatal sonography findings are abnormal. Ultrasound Obstet Gynecol [Internet]. 2004 Jan [cited 2012 Jan 7];23(1):56–62. http://www.ncbi.nlm.nih.gov/pubmed/14971001.
11. Oxford CM, Ludmir J. Trauma in pregnancy. Clin Obstet Gynecol [Internet]. 2009 Dec [cited 2012 Jan 13];52(4):611–29. http://www.ncbi.nlm.nih.gov/pubmed/20393413.
12. Hangiandreou NJ. AAPM/RSNA physics tutorial for residents. Topics in US: B-mode US: basic concepts and new technology. Radiographics [Internet]. [cited 2011 Dec 10];23(4):1019–33. http://www.ncbi.nlm.nih.gov/pubmed/12853678.
13. Berghella V, Kuhlman K, Weiner S, Texeira L, Wapner RJ. Cervical funneling: sonographic criteria predictive of .preterm delivery. Ultrasound Obstet Gynecol [Internet]. 1997 Sep [cited 2012 Jan 12];10(3):161–6. http://www.ncbi.nlm.nih.gov/pubmed/9339522.
14. Iams JD, Goldenberg RL, Meis PJ, Mercer BM, Moawad A, Das A et al. The length of the cervix and the risk of spontaneous premature delivery. National Institute of Child Health and Human Development Maternal Fetal Medicine Unit Network. N Engl J Med [Internet]. 1996 Feb 29 [cited 2011 Aug 19];334(9):567–72. http://www.ncbi.nlm.nih.gov/pubmed/8569824.
15. Bartha JL, Romero-Carmona R, Martínez-Del-Fresno P, Comino-Delgado R. Bishop score and transvaginal ultrasound for preinduction cervical assessment: a randomized clinical trial. Ultrasound Obstet Gynecol [Internet]. 2005 Feb [cited 2012 Jan 1];25(2):155–9. http://www.ncbi.nlm.nih.gov/pubmed/15660437.
16. Berghella V, Ness A, Bega G, Berghella M. Cervical sonography in women with symptoms of preterm labor. Obstet Gynecol Clin North Am [Internet]. 2005 Sep [cited 2012 Jan 1];32(3):383–96. http://www.ncbi.nlm.nih.gov/pubmed/16125039.

17. Berghella V, Owen J, MacPherson C, Yost N, Swain M, Dildy GA et al. Natural history of cervical funneling in women at high risk for spontaneous preterm birth. Obstet Gynecol [Internet]. 2007 Apr [cited 2011 Aug 17];109(4):863–9. http://www.ncbi.nlm.nih.gov/pubmed/17400847.
18. Merz E, Miric-Tesanic D, Bahlmann F, Weber G, Wellek S. Sonographic size of uterus and ovaries in pre- and postmenopausal women. Ultrasound Obstet Gynecol [Internet]. 1996 Jan [cited 2012 Jan 6];7(1):38–42. 31 http://www.ncbi.nlm.nih.gov/pubmed/8932630.
19. Sweet MG, Schmidt-Dalton TA, Weiss PM, Madsen KP. Evaluation and management of abnormal uterine bleeding in premenopausal women. Am Fam Physician [Internet]. 2012 Jan 1 [cited 2012 Jan 13];85(1):35–43. http://www.ncbi.nlm.nih.gov/pubmed/22230306.
20. Levine D, Brown DL, Andreotti RF, Benacerraf B, Benson CB, Brewster WR et al. Management of asymptomatic ovarian and other adnexal cysts imaged at US Society of Radiologists in Ultrasound consensus conference statement. Ultrasound Q [Internet]. 2010 Sep [cited 2011 Oct 16];256(3):943–54. http://www.ncbi.nlm.nih.gov/pubmed/20823748.
21. Van Voorhis BJ. Ultrasound assessment of the uterus and fallopian tube in infertile women. Semin Reprod Med [Internet]. 2008 May [cited 2012 Jan 6];26(3):232–40. http://www.ncbi.nlm.nih.gov/pubmed/18504698.
22. Macklon NS, Fauser BC. Impact of ovarian hyperstimulation on the luteal phase. J Reprod Fertil Suppl [Internet]. 2000 Jan [cited 2012 Jan 1];55:101–8. http://www.ncbi.nlm.nih.gov/pubmed/10889839.
23. Leiserowitz GS. Managing ovarian masses during pregnancy. Obstet Gynecol Surv [Internet]. 2006 Jul [cited 2012 Jan 1];61(7):463–70. http://www.ncbi.nlm.nih.gov/pubmed/16787549.
24. Leiserowitz GS, Xing G, Cress R, Brahmbhatt B, Dalrymple JL, Smith LH. Adnexal masses in pregnancy: how often are they malignant? Gynecol Oncol [Internet]. 2006 May [cited 32 2011 Aug 23];101(2):315–21. http://www.ncbi.nlm.nih.gov/pubmed/16310839.
25. Givens V, Mitchell GE, Harraway-Smith C, Reddy A, Maness DL. Diagnosis and management of adnexal masses. Am Fam Physician [Internet]. 2009 Oct 15 [cited 2012 Jan 6];80(8):815–20. http://www.ncbi.nlm.nih.gov/pubmed/19835343.
26. Cicchiello LA, Hamper UM, Scoutt LM. Ultrasound evaluation of gynecologic causes of pelvic pain. Obstet Gynecol Clin North Am [Internet]. 2011 Mar [cited 2012 Jan 6];38(1):85–114, viii. http://www.ncbi.nlm.nih.gov/pubmed/21419329.
27. Eyvazzadeh AD, Levine D. Imaging of pelvic pain in the first trimester of pregnancy. Radiol Clin North Am [Internet]. 2006 Nov [cited 2011 Oct 22];44(6):863–77. http://www.ncbi.nlm.nih.gov/pubmed/17147990.
28. McRae A, Murray H, Edmonds M. Diagnostic accuracy and clinical utility of emergency department targeted ultrasonography in the evaluation of first-trimester pelvic pain and bleeding: a systematic review. CJEM Can J Emerg Med care = JCMU J Can soins médicaux d'urgence [Internet]. 2009 Jul [cited 2011 Aug 23];11(4):355–64. http://www.ncbi.nlm.nih.gov/pubmed/19594975.
29. Shwayder JM. Pelvic pain, adnexal masses, and ultrasound. Semin Reprod Med [Internet]. 2008 May [cited 2012 Jan 7];26(3):252–65. http://www.ncbi.nlm.nih.gov/pubmed/18504700.
30. Kruszka PS, Kruszka SJ. Evaluation of acute pelvic pain in women. Am Fam Physician [Internet]. 2010 Jul 15 [cited 33 2012 Jan 1];82(2):141–7. http://www.ncbi.nlm.nih.gov/pubmed/20642266.
31. Price J, Farmer G, Harris J, Hope T, Kennedy S, Mayou R. Attitudes of women with chronic pelvic pain to the gynaecological consultation: a qualitative study. BJOG [Internet]. 2006 Apr [cited 2011 Oct 2];113(4):446–52. http://www.ncbi.nlm.nih.gov/pubmed/16489938.
32. Workowski KA, Berman SM. Sexually transmitted diseases treatment guidelines, 2006. MMWR Recomm Rep [Internet]. 2006 Aug 4 [cited 2012 Jan 11];55(RR-11):1–94. http://www.ncbi.nlm.nih.gov/pubmed/16888612.
33. Burstein GR, Gaydos CA, Diener-West M, Howell MR, Zenilman JM, Quinn TC. Incident Chlamydia trachomatis infections among inner-city adolescent females. JAMA [Internet]. 1998 Aug 12 [cited 2012 Jan 1];280(6):521–6. http://www.ncbi.nlm.nih.gov/pubmed/9707141.

34. Brown T, Herbert ME. Medical myth: bimanual pelvic examination is a reliable decision aid in the investigation of acute abdominal pain or vaginal bleeding. CJEM [Internet]. 2003 Mar [cited 2011 Oct 17];5(2):120–2. http://www.ncbi.nlm.nih.gov/pubmed/17475104.
35. Porter MB. Polycystic ovary syndrome: the controversy of diagnosis by ultrasound. Semin Reprod Med [Internet]. 2008 May [cited 2012 Jan 11];26(3):241–51. http://www.ncbi.nlm.nih.gov/pubmed/18504699.
36. Radosh L. Drug treatments for polycystic ovary syndrome. Am Fam Physician [Internet]. 2009 Apr 15 [cited 2012 Jan 34 8];79(8):671–6. http://www.ncbi.nlm.nih.gov/pubmed/19405411.
37. Lujan ME, Chizen DR, Pierson RA. Diagnostic criteria for polycystic ovary syndrome: pitfalls and controversies. J Obstet Gynaecol Can [Internet]. 2008 Aug [cited 2012 Jan 1];30(8):671–9. http://www.pubmedcentral.nih.gov/articlerender.fcgi?artid=2893212&tool=pmcentrez&rendertype=abstract.
38. Evans P, Brunsell S. Uterine fibroid tumors: diagnosis and treatment. Am Fam Physician [Internet]. 2007 May 15 [cited 2011 Sep 27];75(10):1503–8. http://www.ncbi.nlm.nih.gov/pubmed/17555142.
39. Apgar BS, Kaufman AH, George-Nwogu U, Kittendorf A. Treatment of menorrhagia. Am Fam Physician [Internet]. 2007 Jun 15 [cited 2012 Jan 8];75(12):1813–9. http://www.ncbi.nlm.nih.gov/pubmed/17619523.
40. Goldstein SR. Early pregnancy: normal and abnormal. Semin Reprod Med [Internet]. 2008 May [cited 2012 Jan 7];26(3):277–83. http://www.ncbi.nlm.nih.gov/pubmed/18504702.
41. Tan S, Pektas MK, Arslan H. Sonographic evaluation of the yolk sac. J Ultrasound Med [Internet]. 2012 Jan [cited 2012 Jan 13];31(1):87–95. http://www.ncbi.nlm.nih.gov/pubmed/22215774.
42. Paspulati RM, Turgut AT, Bhatt S, Ergun E, Dogra VS. Ultrasound assessment of premenopausal bleeding. Obstet Gynecol Clin North Am [Internet]. 2011 Mar [cited 2012 Jan 6];38(1):115–47, viii. http://www.ncbi.nlm.nih.gov/pubmed/21419330 35.
43. Perriera L, Reeves MF. Ultrasound criteria for diagnosis of early pregnancy failure and ectopic pregnancy. Semin Reprod Med [Internet]. 2008 Sep [cited 2012 Jan 11];26(5):373–82. http://www.ncbi.nlm.nih.gov/pubmed/18825605.
44. Bethune M. Management options for echogenic intracardiac focus and choroid plexus cysts: a review including Australian Association of Obstetrical and Gynaecological Ultrasonologists consensus statement. Australas Radiol [Internet]. 2007 Aug [cited 2012 Jan 10];51(4):324–9. http://www.ncbi.nlm.nih.gov/pubmed/17635467.
45. Sepulveda W. Velamentous insertion of the umbilical cord: a first-trimester sonographic screening study. J Ultrasound Med [Internet]. 2006 Aug [cited 2012 Jan 10];25(8):963–8; quiz 970. http://www.ncbi.nlm.nih.gov/pubmed/16870889.
46. Degani S. Fetal biometry: clinical, pathological, and technical considerations. Obstet Gynecol Surv [Internet]. 2001 Mar [cited 2012 Jan 10];56(3):159–67. http://www.ncbi.nlm.nih.gov/pubmed/11254152.
47. Chen PC, Sickler GK, Dubinsky TJ, Maklad N, Jacobi RL, Weaver JE. Sonographic detection of echogenic fluid and correlation with culdocentesis in the evaluation of ectopic pregnancy. AJR Am J Roentgenol [Internet]. 1998 May [cited 2011 Aug 17];170(5):1299–302. http://www.ncbi.nlm.nih.gov/pubmed/9574606.
48. Poulose T, Richardson R, Ewings P, Fox R. Probability of early pregnancy loss in women with vaginal bleeding and a singleton live fetus at ultrasound scan. J Obstet Gynaecol [Internet]. 2006 Nov [cited 2011 Aug 23];26(8):782–4. 36 http://www.ncbi.nlm.nih.gov/pubmed/17130030.
49. Doubilet PM, Benson CB. Further evidence against the reliability of the human chorionic gonadotropin discriminatory level. J Ultrasound Med [Internet]. 2011 Dec [cited 2012 Jan 6];30(12):1637–42. http://www.ncbi.nlm.nih.gov/pubmed/22123998.
50. Mehta TS, Levine D, Beckwith B. Treatment of ectopic pregnancy: is a human chorionic gonadotropin level of 2,000 mIU/mL a reasonable threshold? Radiology [Internet]. 1997 Nov [cited 2011 Aug 17];205(2):569–73. http://www.ncbi.nlm.nih.gov/pubmed/9356647.

51. Prine LW, MacNaughton H. Office management of early pregnancy loss. Am Fam Physician [Internet]. 2011 Jul 1 [cited 2012 Jan 13];84(1):75–82. http://www.ncbi.nlm.nih.gov/pubmed/21766758.
52. Braffman BH, Coleman BG, Ramchandani P, Arger PH, Nodine CF, Dinsmore BJ et al. Emergency department screening for ectopic pregnancy: a prospective US study. Radiology [Internet]. 1994 Mar [cited 2011 Aug 17];190(3):797–802. http://www.ncbi.nlm.nih.gov/pubmed/7509494.
53. Hajenius PJ, Mol F, Mol BWJ, Bossuyt PMM, Ankum WM, van der Veen F. Interventions for tubal ectopic pregnancy. Cochrane Database Syst Rev [Internet]. 2007 Jan [cited 2011 Aug 23];(1):CD000324. http://www.ncbi.nlm.nih.gov/pubmed/17253448.
54. Doubilet PM, Benson CB. Outcome of first-trimester pregnancies with slow embryonic heart rate at 6–7 weeks gestation and normal heart rate by 8 weeks at US. Radiology [Internet]. 2005 Aug [cited 2011 Aug 17];236(2):643–6. http://www.ncbi.nlm.nih.gov/pubmed/15994999.
55. Falco P, Milano V, Pilu G, David C, Grisolia G, Rizzo N et al. Sonography of pregnancies with first-trimester bleeding and a viable embryo: a study of prognostic indicators by logistic regression analysis. Ultrasound Obstet Gynecol [Internet]. 1996 Mar [cited 2011 Aug 17];7(3):165–9. http://www.ncbi.nlm.nih.gov/pubmed/8705406.
56. Kiserud T, Johnsen SL. Biometric assessment. Best Pract Res Clin Obstet Gynaecol [Internet]. 2009 Dec [cited 2012 Jan 12];23(6):819–31. http://www.ncbi.nlm.nih.gov/pubmed/19632901.

Chapter 8
Eye (Ocular)

Dae Hyoun Jeong and Satyakant Chitturi

Key Points

- The point-of-care ocular ultrasound is a rapid, noninvasive bedside procedure that will be valuable for the evaluation of a wide range of ocular pathologies in real-time and will be a very useful tool for enhancing physical examination of the eye.
- Ocular ultrasound technique can be easily performed with appropriate training.
- The indication of the ocular ultrasound is not only for ocular trauma and to evaluate foreign bodies but also to assess visual changes, ocular pain, head injuries, and structural abnormalities.
- Dynamic ultrasound may help to detect subtle abnormalities, such as a small retinal tear or vitreous hemorrhage.

Introduction

Eye complaints are common in primary care, composing approximately 2 % of all visits. The eye is superficially located fluid filled structure which is ideal for point-of-care ultrasound evaluation. Ultrasonography (US) is a preferred first imaging modality used in eye and orbit assessment because it gives quick and reliable information in a simple, real-time, and noninvasive manner. It can provide clinical information that may not be readily obtainable through physical or slit-lamp exams when hyphema, cataract, or orbital swelling makes direct visualization of posterior chamber difficult. Training time needed to obtain skills to perform point-of care

D.H. Jeong, M.D. (✉) • S. Chitturi, M.D., M.B.B.S.
SIU Primary Care Sports Medicine Fellowship,
Southern Illinois University School of Medicine, Quincy, IL, USA
e-mail: djeong@siumed.edu; drcsatya@gmail.com

J.M. Daniels, R.A. Hoppmann (eds.), *Practical Point-of-Care Medical Ultrasound*, DOI 10.1007/978-3-319-22638-5_8

ultrasound examinations of the eye is not extensive. Even though CT and MRI are still very important for comprehensive evaluation of many orbital and ocular pathologies, they may not be immediately available and cannot provide real-time or dynamic image as ultrasound.

Indication for Ocular Ultrasound

Point-of-care ultrasound can be used to detect many ophthalmic conditions, which includes:

- Suspected foreign body.
- Ocular trauma.
- Ocular pain.
- Decreased vision or loss of vision.
- Head injury, or suspected increased intracranial pressure (ICP).

Ocular Ultrasound Examination Technique

Patient Positioning. Ideally, when possible, the patient should be placed in a supine position with the head slightly rotated to the side contralateral to the eye being studied. This prevents spilling of the ultrasound gel. The ultrasound machine and the examiner are to be on the patient's right side so that the examiner can scan with the right hand (Fig. 8.1).

Fig. 8.1 Ultrasound machine and examiner should be on the patient's right side to allow for scanning with the right hand

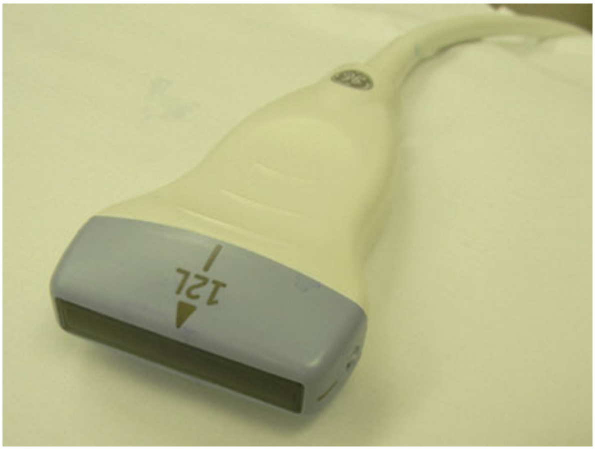

Fig. 8.2 Linear array transducer

Ultrasoundmachine and setting. The eye is particularly vulnerable to thermal hazard since the lens and the aqueous and vitreous humors have no cooling blood supply. The ultrasound model and probe used for eye exam should be appropriate to the ophthalmic purpose and ophthalmic preset should be chosen for safety. The depth should be set to visualize all the structures of globe including the optic nerve. Use ophthalmic setting or preset, if available. The gain should be set appropriately to create a hypoechoic posterior chamber. Otherwise, use the “small parts” or digit preset for the best image quality for the eye exam. If gain is set too high, it can cause small artifacts which can confuse the examiner to overcall pathology. In contrast, if gain is set too low, it can cause examiner to miss subtle pathology.

Transducer. The eye is superficial structure which is best visualized with high frequency probe. For point-of-care ocular ultrasonography, High-frequency (7.5–10 MHz or higher frequency range) linear array transducer with small footprint is used to match with the eye socket size (Fig. 8.2).

Gel application. Water-soluble ultrasound gel will function as an acoustic coupling medium between the transducer and skin. After the eyes are closed, a copious amount of ultrasound gel should be used to cover the entire eye lid. It will make layer for transducer to float over and will prevent it from direct pressure to the globe. Any pressure to the globe could make discomfort or potentially cause damage to the eye. The gel for an ocular ultrasound exam does not need to be sterile but it is recommended to use sterile gel which is less irritating to the eye or to place a piece of Tegaderm (transparent film dressing) to the closed eyelid before applying the gel (Fig. 8.3). When Tegaderm is applied to the closed eyelid, make sure to get rid of all air bubbles to avoidproduction of the artifact (Fig. 8.4).

Fig. 8.3 Application of Tegaderm ensuring air bubbles are removed

Fig. 8.4 Application of copious amount of gel on the Tegaderm patch

Transducer Placement and Scanning Technique

The transducer should be well stabilized by resting the hand holding the probe on the patient. The examiner's arm will be less fatigued when it is held like a pen while fingers and palm can be rested on the maxilla and nasal bridge. There are two views of ocular ultrasound exam; transverse view (the pointer toward patient's right) (Fig. 8.5) and longitudinal view (the pointer toward patient's head) (Fig. 8.6). When scanning in both planes, it is very important to sweep the transducer from up and down in transverse plane, side to side in longitudinal plane, tilt and fan the transducer for complete and thorough evaluation. Dynamic scan can be performed by

Fig. 8.5 Transverse view

Fig. 8.6 Longitudinal view

asking the patient to move his or her eyes slowly up and down and side to side and in all four directions while maintaining a closed eyelid. While color flow and pulsed-wave Doppler can aid in evaluating the central retinal artery and vein, their use greatly increases the amount of energy (and heat) in the eye. We do not recommend the use of any eye Doppler setting to evaluate the eye at the present time.

Anatomy of the Normal Eye

The normal eye appears as a circular and hypoechoic structure on the ultrasound (Figs. 8.7 and 8.8). It is approximately 24–25 mm in diameter, with minimal individual variation. The eyeball lies on the orbit surrounded fat. The eyeball contains two compartment; anterior chamber and the posterior chamber.

The anterior chamber is filled with anechoic fluid (aqueous humor) and is bordered by the cornea anteriorly, iris and anterior reflection of the lens capsule posteriorly. The cornea appears as a thin convex hyperechoic layer which overlies the entire anterior chamber, parallel to the eyelid. It is contiguous with the sclera. The iris and ciliary body are seen as hyperechoic linear structures extending from the peripheral globe towards lens. The lens is biconvex structure which appears anechoic in the center with hyperechoic anterior and posterior margins.

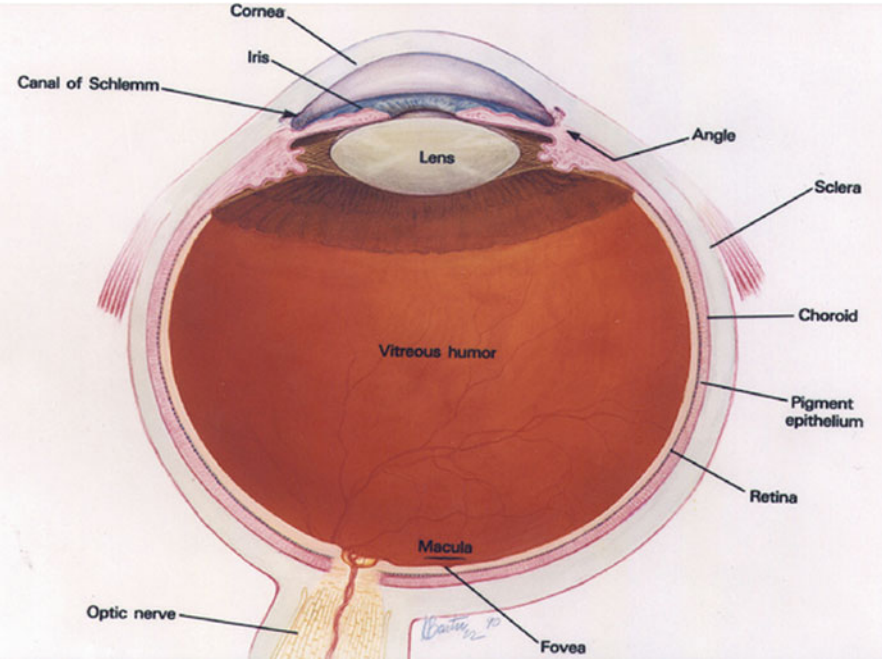

Fig. 8.7 Normal eye anatomy

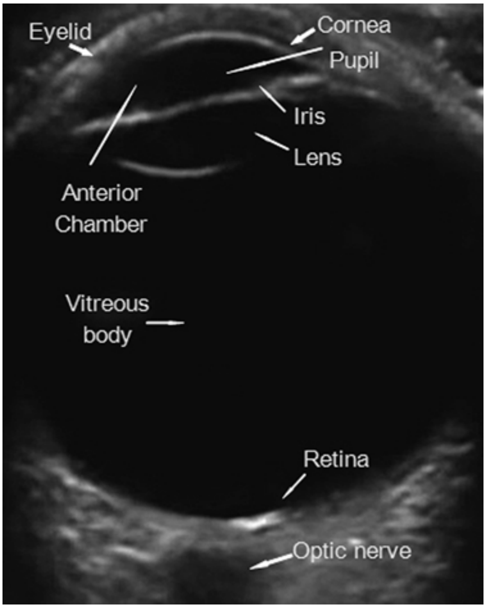

Fig. 8.8 Ultrasound image of a normal eye

The posterior chamber is filled with anechoic vitreous fluid, posterior to the lens. Vitreous is largely anechoic in a young healthy eye but opacities can commonly be seen in older patients. The posterior border of the globe consists of the retina, choroid and sclera. The normal retina cannot be differentiated from the other choroidal layers on the ultrasound. The choroid attaches firm to the retina on the optic nerve head and the ora serrata which can be observed on the ultrasound scan.

The evaluation of the retrobulbar area includes optic nerve, extraocular muscles and bony orbit. The optic nerve is visible posteriorly and centrally as a hypoechoic linear region extending posteriorly. The surrounding optic nerve sheath appears hyperechoic.

The central retinal artery (CRA) and vein and the ophthalmic artery (OA) and vein adjacent to the optic nerve can be easily distinguished. The ophthalmic artery is the larger vascular structure.

Common Ocular Pathology

Globe Rupture

Globe rupture typically results from traumatic injury and is an ophthalmologic surgical emergency. A ruptured globe (Fig. 8.9) is considered as a relative contraindication for ocular ultrasound exam because the vitreous extrusion can be made even worse if the intraocular pressure is increased by the pressure of the transducer.

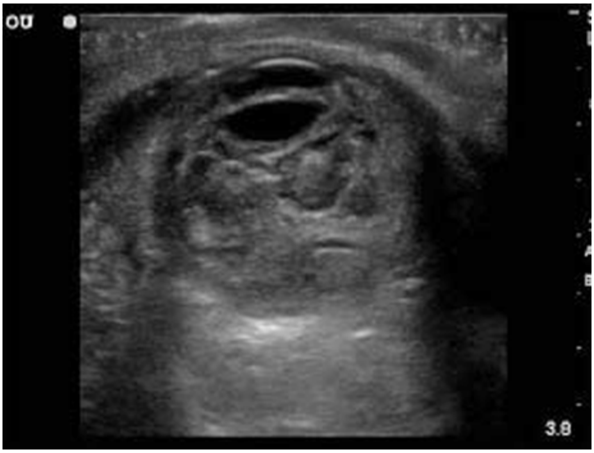

Fig. 8.9 Globe rupture

Small perforations of the globe with little loss of vitreous may not be easy to detect. The examiner should be very careful to minimized pressure by applying a thick bed of ultrasound gel during the exam if the patient has experienced trauma and there is any possibility that may have damaged the globe. In that case, thorough slit-lamp examination with fluorescein should be done as well as Seidel test.

Intraocular Foreign Body

An intraocular foreign body (IOFB) often can be challenging to identify clinically (Fig. 8.10). Orbital CT scan is still considered as the gold standard for this injury. It may not be readily available and ultrasound can be used. Regardless of the radio-opacity of the object, the ocular ultrasound can play an important role to detect IOFB with high sensitivity (87–86 %) and specificity (92–96 %). Intraocular foreign bodies are identified by hyperechoic acoustic profile with comet-tail artifacts.

Retinal Detachment and Posterior Vitreous Detachment

Retinal detachment (RD) is an ophthalmic emergency so the early diagnosis is critical to prevent vision loss. Typically, patients with RD present with a sudden, painless, monocular visual impairment and the sensation of looking through a curtain, accompanied by flashes and floaters (Fig. 8.11).

A posterior vitreous detachment (PVD) may have a similar presentation with complaints of floaters or brief flashes. Both PD and PVD may be difficult to be detected on physical examination by ophthalmoscopy, especially when the detachment is small. The point-of-care ultrasound allows quick and accurate diagnosis and differentiation between RD and PVD (Fig. 8.12).

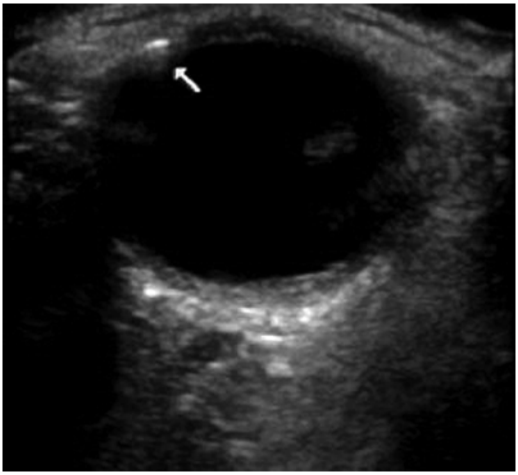

Fig. 8.10 Metallic foreign body embedded in the eye (*arrow*)

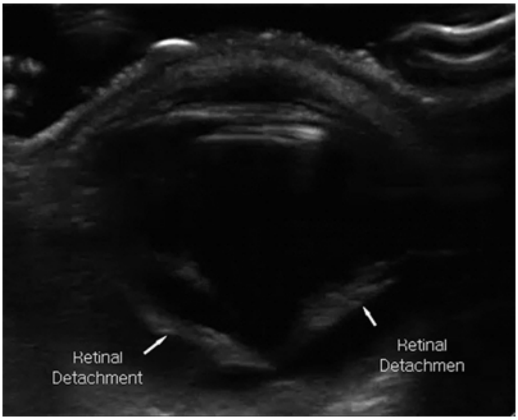

Fig. 8.11 Well-defined V-shape appearance of retinal detachment (RD) anchored at Ora-Serrata and Optic disk. Note that the RD does not cross the midline, optic disk (photo courtesy of Jonathan dela Cruz, MD)

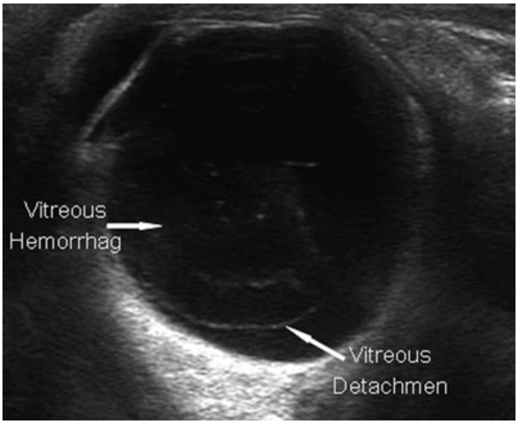

Fig. 8.12 Thinner and smoother appearance of posterior vitreous detachment (PVD). The PVD crosses midline

RD appears as a thick, highly reflective undulating membrane floating in the substance of the vitreous body. A detached retina can be seen floating and moving within the vitreous body with eye movements. The retina is firmly tethered to ora serrata and the optic nerve head, so even complete RD will not cross the midline of the posterior chamber. It will remain attached to the optic nerve head posteriorly and the oral serrata in the ciliary body anteriorly, producing a classic "V-shape." The apex of the V is tethered to the optic disk. A new RD may be freely mobile compared to older RD which may appear stiff with eye movements.

In contrast, a PVD will cross the midline. A PVD may also appear as a V-shaped linear structure lifted off the posterior surface of the globe but it is thinner, smoother, and more mobile than retinal detachments.

Occasionally RD and PVD may occur together. In this case, the more anterior structure will be the PVD with RD being more posterior.

A choroid detachment can be distinguished by its smooth, thick, bulging convex shape that remains fixed with eye movements.

Vitreous Hemorrhage

A vitreous hemorrhage (VH) (Fig. 8.13) often presents clinically with floaters, brief flashes (photopsia) and even blindness if it is large. It can result from trauma but may occur spontaneously with proliferative diabetic retinopathy, PVD or RD. The sonographic appearance of vitreous hemorrhage demonstrates heterogeneous, echogenic layers in the posterior chamber in anterior-posterior orientation due to gravitational forces. Small vitreous hemorrhages can be detected by increasing the gain of the ultrasound machine. This may provide wave-like, semi-mobile images when the eye moves gently in all four quadrants. This mimics "clothes in a washing

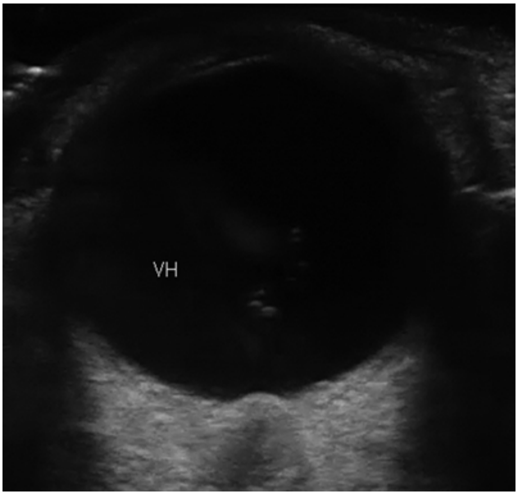

Fig. 8.13 Vitreous hemorrhage (photo courtesy of Jonathan dela Cruz, MD)

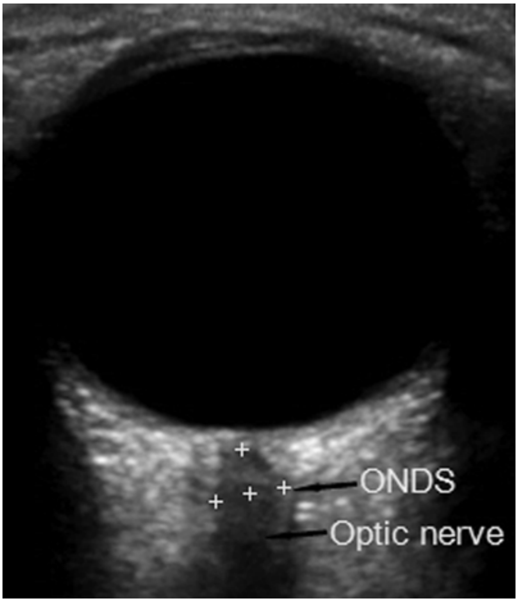

Fig. 8.14 Measure optic nerve sheath diameter (ONSD) 3 mm posterior to the retina. The diameter <5 mm is normal in an adult

machine" or "swaying seaweed." New mild hemorrhages appear as small dots or linear areas of low reflective mobile vitreous opacities, whereas blood organizes and forms membranes in more severe and older hemorrhages.

Optic Nerve Sheath Diameter

The ultrasound measurement of the optic nerve sheath diameter (ONSD) is a simple, rapid, reliable, and noninvasive procedure, which makes it as a useful tool in the assessment of elevated intracranial pressure (ICP) (Fig. 8.14). The optic nerve is a direct extension of the subarachnoid space of the central nervous system and the correlation between the optic nerve sheath diameter (ONSD) and ICP has been well established. ONSD will be increased due to transmission of elevated ICP to the subarachnoid space surrounding optic nerve.

The measurement of ONSD by point-of-care ultrasound can be used to assess for elevated ICP in patients with trauma, intracranial hemorrhage, hypertensive, cerebral edema, or cerebral infection, which will lead to prompt management and better outcome.

The ONSD is measured 3 mm posterior to the optic nerve sheath–retina junction. The ONSD of both eyes are measured in both transverse and sagittal planes. The average of the two measurements can then be calculated. According to the literature, the normal ONSD is defined as 5 mm or less in adult, 4.5 mm or less in children (1–15 years), and 4 mm or less in children less than 1 year of age. In adults,

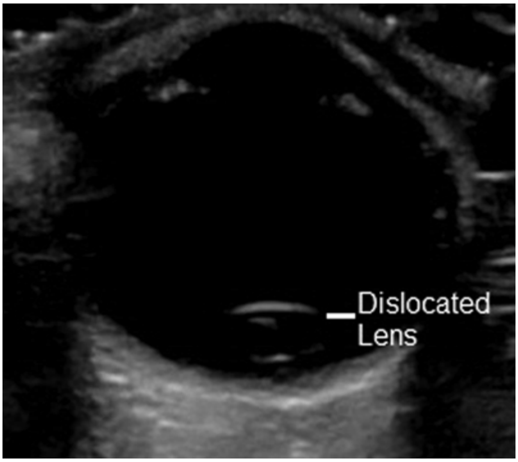

Fig. 8.15 Lens dislocation

ONSD above 6 mm is considered as significant increase in ICP. The cutoff value for increased ONSD has been debated and is the subject of ongoing research. Papilledema may be noted in patients with elevated ICP on ultrasound evaluation.

Lens Dislocation or Subluxation

Lens dislocation (Fig. 8.15) leads to acute vision loss. Blunt trauma is the most common cause of lens dislocation. It can be either complete dislocation or subluxation. When the lens is completely dislocated, it is usually found free-floating in the vitreous body. Another possible location of the dislocated lens includes the anterior chamber. Diagnosing a lens subluxation is more subtle. In a subluxation, the lens will slip out of position with ocular movement.

Pupillary Light Reflex

Pupillary light reflex is essential for assessing neurologic and ophthalmologic conditions. The Point-of-care ultrasonography is a feasible adjunct to the conventional eye examination when the evaluation of the pupillary reflex becomes challenging with surrounding edema or hyphema.

To check the pupillary reflex with the ultrasound, the patient should be placed in a dark room and instructed to look at his or her feet with eyes closed. The examiner places the probe on the superior part of the eye orienting the beam caudad to transect the front of the eye. Next, a light is shone in the normal contralateral eye while the other eye is scanned. Movement of the iris confirms that the reflex is present (Fig. 8.16a, b).

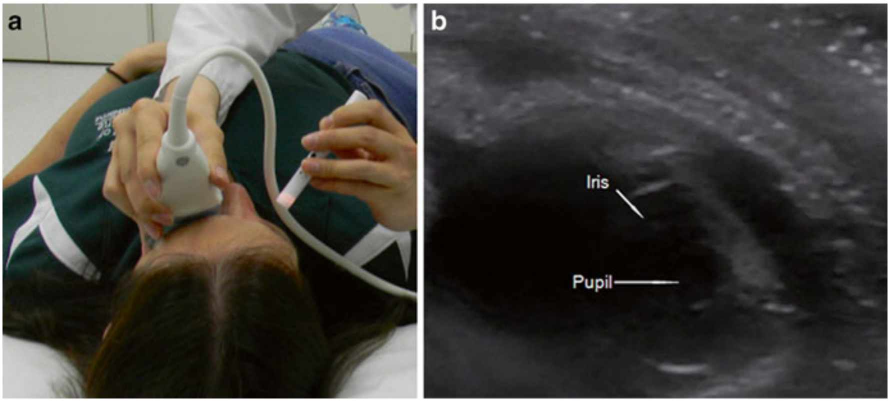

Fig. 8.16 (**a**) Patient positioning when doing a pupillary light reflex exam. (**b**) The pupil is well visualized in this image through the superior eyelid

Pearls and Pitfalls

- If there is any suspicion for globe rupture, copious amounts of sterile gel should be applied to the closed eyelid so that the transducer does not actually have to make contact with the eyelid.
- Any pressure on the traumatic eye could be detrimental.
- The eye is particularly vulnerable to thermal hazard so the model used should be appropriate to the ophthalmic purpose, or ophthalmic preset should be selected for eye exam for safety.
- At the present time, we do not advocate the use of Doppler of any kind to the eye.

Suggested Readings

1. Soni et al. Point-of care ultrasound. Elsevier; 2015.
2. Levitov et al. Bedside ultrasonography in clinical medicine. McGraw-Hill; 2011.
3. Dudea. Ultrasonography of the eye and orbit. Med Ultrason. 2011.
4. Roque et al. Bedside ocular ultrasound. Crit Care Clin. 2014;30:227–41.
5. Kelker et al. Bedside ocular ultrasound in the emergency department. Eur J Emerg Med. 2014;21:246–53.
6. Hightower et al. Detection of increased intracranial pressure by ultrasound. J Spec Oper Med. 2012;12.
7. Hassen et al. Accuracy of optic nerve sheath diameter measurement by emergency physicians using bedside ultrasound. J Em Med. 2014.
8. Frasure et al. Bedside ultrasound diagnosis of vitreous hemorrhage and traumatic lens dislocation. Am J Em Med. 2013;31.
9. Vrablik et al. The diagnostic accuracy of bedside ocular ultrasonography for the diagnosis of retinal detachment: a systematic review and meta-analysis. Ann Emerg Med. 2015.

10. Schott et al. Pitfalls in the use of ocular ultrasound for evaluation of acute vision loss. J Emerg Med. 2013.
11. Shinar et al. Use of ocular ultrasound for the evaluation of retinal detachment. J Emerg Med. 2011.
12. Wiswell, Bellamkonda-Athmaram. Sonographic consensual pupillary reflex. West J Emerg Med. 2012;13(6).

Chapter 9
Pediatrics

Antonio Riera

Approach to the Patient

When examining a pediatric patient with ultrasound, it is vital for the examiner to consider the child's age and developmental stage. Scans should be obtained with parents in the room and next to their child. It is appropriate to engage the child and their parents before performing your scan. You should explain, in simple terms, to the patient and parent the general steps you will undertake. Some children can be sensitive to the texture and temperature of the ultrasound gel. When the gel is placed on the probe, you should allow a child to touch the gel with their fingers before applying on their body. This is reasonable to perform for any child over 2 years of age. Have a soft wipe handy so that you may clean off the gel when done (keep in mind that some toddlers may instinctively want to eat or taste the gel). Children and adolescents should be kept comfortably dressed throughout the procedure. You can offer a blanket or sheet to keep them covered. It is only necessary to expose those body parts that you are planning to scan, so having the patient dress in a full gown may not be necessary. If the child or adolescent is lying on a stretcher or examination bed, it is advisable to either sit on the stretcher, examination bed or a chair so that you are at eye level or lower with respect to patient. This is far less intimidating than standing and hovering over a child with an ultrasound probe in hand. Remember to reassure both child and their parents that the scan itself will not hurt. This is true even in the setting of pediatric fractures as studies have shown that when the scans are properly performed, they do not increase a child's level of pain [1, 2]. Explain that they will feel the probe pushed against the skin and that the gel is used so that only gentle pressure, if any at all, needs to be exerted. Most mothers

A. Riera, M.D. (✉)
Department of Pediatric Emergency Medicine, Yale-New Haven Children's Hospital, New Haven, CT, USA
e-mail: antonio.riera@yale.edu

J.M. Daniels, R.A. Hoppmann (eds.), *Practical Point-of-Care Medical Ultrasound*, DOI 10.1007/978-3-319-22638-5_9

will understand the safety and low risk nature of ultrasounds since they would have personal experience during their routine prenatal care. If a child seems frightened before starting, you may perform a practice scan on yourself or their parent. Whenever appropriate, you should try to make it fun and suggest that you are going to take a picture of "how things look on the inside" and that you can all look together on the "computer screen." Providing a general timeline and a simple task for the child to perform during the scan will often help with cooperation. For example, you may say "This picture will last as long as it takes to brush your teeth. Your job is to relax and keep your body still while you watch the screen or pick something else to do with mom." For some children, distraction with books, videos, music or games using any available item can be a helpful adjunct. For infants, positioning and comfort can be enhanced by allowing them to lay supine on a parent's lap. Figure 9.1 is a good example of how to position yourself, the caregiver, and the portable ultrasound machine during a pediatric scan.

Selecting a Probe

There is no "ideal" probe to be selected during the examination of a pediatric patient. The choice of probe will be dictated by the patient's age, body habitus, and most importantly—the actual indication for your ultrasound scan. Low frequency probes

Fig. 9.1 Approach to ultrasound examination of a young child. The examiner is positioned sitting on the stretcher on the same side as the ultrasound machine, so that the probe wire and examiner do not have to cross over the child's body. The parent is positioned next to child on the opposite side of the machine, so she is visible at all times and able to provide comfort and distraction by engaging the child in a book activity

are typically designed with curvilinear footprints which provide more tissue penetration while sacrificing some detail and overall resolution. Higher frequency probes are generally designed with linear footprints which offer tremendous resolution of superficial structures but a limited capacity for depth and tissue penetration. Phased-array probes, which can range in frequency from 8 to 1 MHz are usually employed for cardiac imaging, although curvilinear probes may be used as well. In certain situations, children that are obese may require scanning with curvilinear probes in order to visualize their relatively superficial structures of interest. Smaller footprint probes are available. These allow clinicians to work with smaller body parts. During ultrasound scans, most clinicians hold the probe in their dominant hand while making adjustments to the machine with their non-dominant hand. Holding the probe at the very end with the ulnar side of one's hand in direct contact with the patient's skin will allow for greater stability and maneuverability of the probe.

Scanning

Ultrasound is considered to be an operator dependent diagnostic test. This means that unlike a typical radiograph, where images are obtained and interpreted based on standard views (e.g., chest PA and lateral), the acquisition of good ultrasound images is dependent on the skill and technique of the sonographer (the individual performing the ultrasound). For pediatrics, performance characteristics of ultrasound scans do not necessarily mimic those expected of adult patients. A classic example is the differential sensitivity when performing a focused abdominal assessment in trauma (FAST) exam. The diagnostic accuracy for "ruling out" hemoperitoneum after blunt abdominal trauma is less reliable in children (60–70 %) when compared to adults (90–95 %) [3, 4]. Another example is the evaluation of appendicitis. Ultrasound visualization rates of the appendix in the pediatric population have been shown to exhibit wide ranges of detection and accuracy [5, 6]. Inaccurate examinations are possible when the sonographer is inexperienced, the child has an obese body habitus, or there is a low clinical pretest probability for appendicitis before the ultrasound is performed [7]. For these reasons, ultrasound results should be interpreted in conjunction with clinical findings to properly assess for appendicitis risk in the pediatric population.

The procedure for performing ultrasound scans in children should be similar to steps taken during other ultrasound examinations.

1. Obtain verbal agreement from the child and parent that the ultrasound will be performed.
2. Review the reasoning behind your ultrasound scan. It is always a good idea to describe what you will be looking for during the study. This often will take on the form of a "yes or no" question. For example, if you are interested in diagnosing the presence or absence of a drainable soft tissue fluid collection, it is

reasonable to lay out what the next steps will be if a collection is found. You should discuss any potential limitations before the scan is performed and always interpret the ultrasound findings in context to the clinical exam.

3. Proper name and ID information should be inputted on the machine.
4. Familiarize yourself with the ultrasound machine that will be used. This is a vital step because the knobs, functions, and displays on ultrasound machines do vary by manufacturer. Basic equipment knowledge will help save time during your scan and lead to a smoother interaction between you, the patient, and their family.
5. Select the desired probe and liberally apply ultrasound gel. The gel may be cold depending on storage conditions and the room temperature. Review this with any child and allow them to touch the gel so they may feel its texture.
6. When the probe and overlying gel come in contact with skin, please mind your orientation. The convention is for the "notch" or indicator to point towards the patient's head when long-axis or longitudinal scans are performed and towards the patient's right side when short-axis or transverse scans are performed.
7. The scanning depth may need to be adjusted during the ultrasound. You want to focus your structure of interest so that it is clearly visible in the center of the monitor. Peripheral structures and thin children generally require low depth settings while deeper structures and obese children will require greater depth adjustments.
8. The gain function may need to be adjusted during the ultrasound. This essential function can be considered to serve as a volume amplifier. If the images on the screen appear too dark (hypoechoic), then you should increase the gain. Conversely, if the images on the screen appear too bright (hyperechoic), the gain should be decreased. Some machines allow you to increase the gain in either the top half or bottom half of the screen, and others offer an optimize button which automatically sets a gain level for you.
9. The Doppler function may need to be used during the ultrasound. Color Doppler provides information related to the intensity and direction of movement of any given structure. Red color indicates flow towards your probe and blue color indicates flow away from the probe. This is useful when visualizing and differentiating vascular structures. Power Doppler provides non-directional motion information with a greater sensitivity over areas that have lower flow rates.
10. A complete scan of your structure or area of interest is achieved by rocking back and forth, or "fanning" the probe while it remains in contact with the same area of the skin in one location. This will allow you to fully evaluate that particular area and find the "best" angle for image storage. This should be repeated after repositioning the probe by 90° so that you have fanned images in one location using both the long-axis view and a short-axis view.
11. Ensure to record a short video clip (preferable) or still image of your examination. These are typically stored in a HIPAA protected database which allow for subsequent review and enhance quality assurance.

Normal Anatomy of Pediatrics

The other chapters have reviewed normal ultrasound findings as they relate to different body systems in adults. In general, the same principles described in these chapters will also apply for most pediatric scans. In this section, we review some important ultrasound indications that are specific to a pediatric population.

1. Hydrocephalus.

   (a) Cranial ultrasound is an excellent and noninvasive tool for brain imaging during the neonatal period and is the study of choice for the initial assessment of neonatal hydrocephalus [8, 9]. Hydrocephalus is the accumulation of fluid within the ventricular system of the brain. The unique presence of open fontanels easily allows one to evaluate for the presence of hydrocephalus using cranial ultrasound. Selection of a probe that fits over the anterior fontanel is recommended. A phased-array probe is commonly selected given its relatively small footprint size. The examination should consist of coronal and sagittal views. For coronal views, the probe is placed directly over the open fontanel with the indicator pointing to the infant's right. For sagittal views, the probe is rotated so that the indicator now points to the front of the infant's forehead. The probe should be slowly fanned back and forth in each of these orientations to assess for ventricular enlargement over different sections of the brain. The depth setting is adjusted so that the base of the skull can be seen on the bottom portion of the monitor, a distance of 7–9 cm is a typical starting point. Special precautions should be exercised for this patient population. Given the immature immune systems of neonatal patients, careful attention should be paid to proper hand washing and probe cleansing before and after the ultrasound examination. Given the susceptibility to rapid heat loss, patients should be scanned in a warm environment (or well wrapped with blankets to maintain normal body temperature) and efforts should be made to warm the ultrasound gel before it is applied on the newborn's head. Figures 9.2 and 9.3 depict changes observed with increasing hydrocephalus in coronal and parasagittal planes.

2. Intussusception.

   (a) Intussusception is a common pediatric abdominal emergency, with the highest incidence in children <2 years of age. Clinical presentations can vary and include nonspecific symptoms such as crying episodes, abdominal pain, vomiting, and lethargy. "Currant jelly" stools are a late finding which are suggestive of ongoing bowel ischemia. A high index of suspicion for pediatric intussusception is imperative to minimize associated morbidities when operative management is necessitated. Ultrasound is an accurate and preferred method for the diagnosis of pediatric intussusception [10, 11]. Furthermore, it is an ultrasound application that can be readily learned by novice physician sonographers [12]. A high frequency, linear probe is used

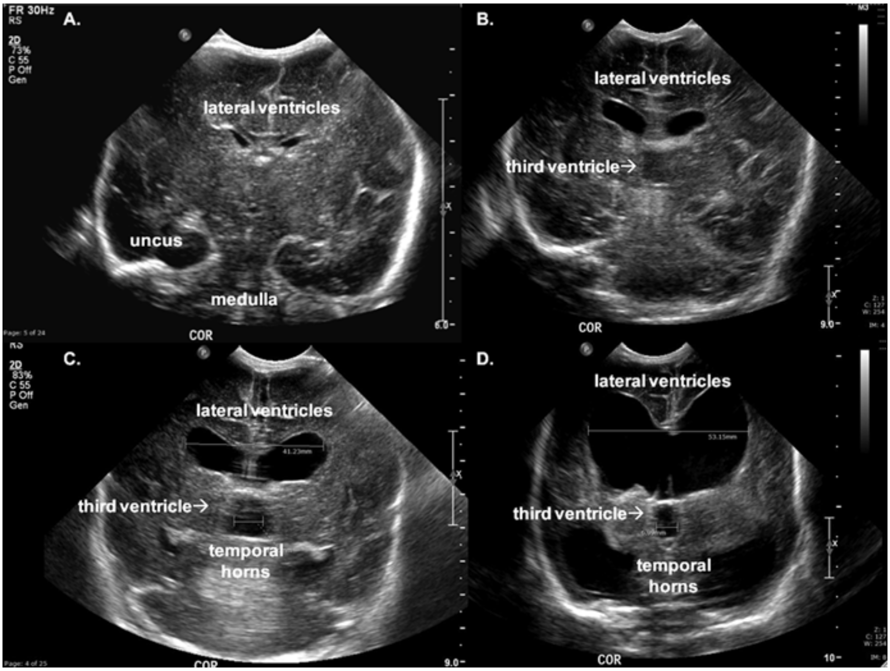

Fig. 9.2 Coronal view near the foramen of Monro depicting normal anatomy in image (**a**) and worsening hydrocephalus as seen in the frontal and temporal horns of the lateral ventricles in images (**b–d**)

to obtain views of all four abdominal quadrants. The scan should begin in the right lower quadrant. With the indicator pointing towards the patient's right, a transverse view of the psoas muscle should be obtained, as this is a helpful anatomical landmark found in close proximity to the spine (Fig. 9.4). While the patient lays supine, the probe is slowly brought cephalad towards the liver. Upon reaching the right upper quadrant, the probe is rotated 90° with the indicator now pointing towards the child's head. The probe is now brought across the abdomen in a longitudinal orientation until reaching the left upper quadrant. At this point the probe is again rotated 90° and a transverse scan of the left side of the abdomen down to the left lower quadrant is obtained. Ileo-colic intussusception is most commonly identified by the appearance of a "target sign" in the transverse orientation. In this view the intussusceptum is the part of bowel that is entrapped by the intussuscipiens, which forms the circular outer wall of the intussusception. Normal bowel can have a spectrum of different appearances depending on the amount of air, fluid, fecal material, and ingested matter that is present. Figure 9.5 contrasts the appearance of an ileo-colic intussusception with otherwise normal appearing bowel.

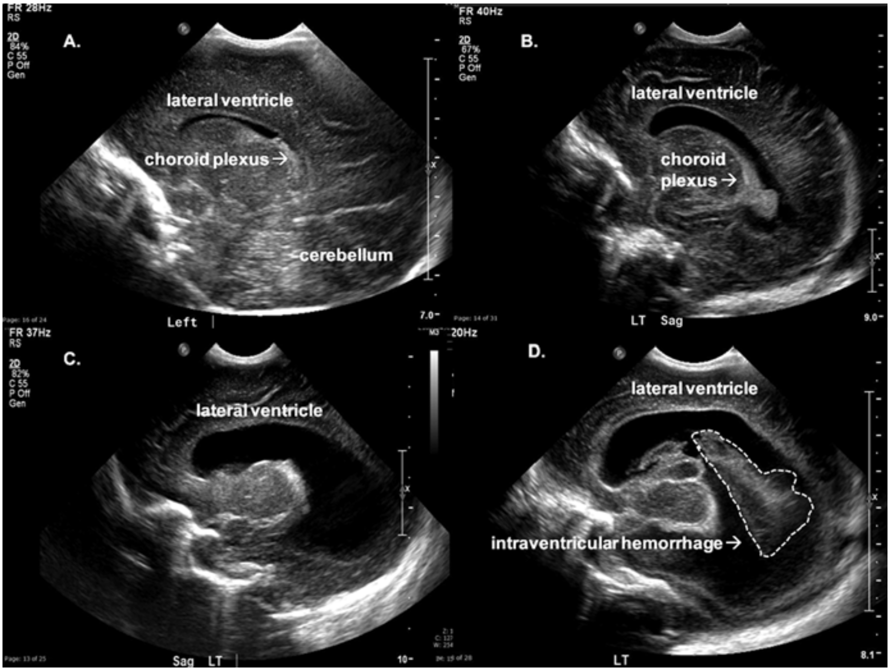

Fig. 9.3 Left parasagittal view directly over the lateral ventricle depicting normal anatomy in image (**a**) and worsening hydrocephalus as seen through the body of the lateral ventricle in images (**b**–**d**)

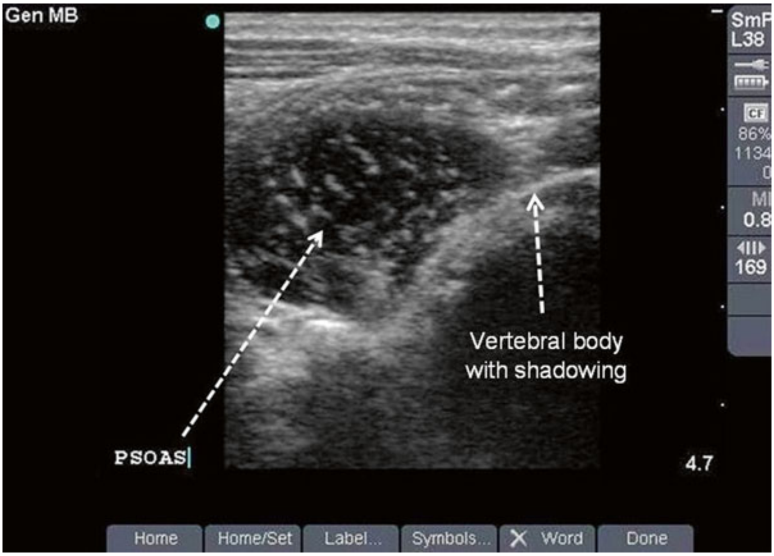

Fig. 9.4 Transverse view of the psoas muscle in the right lower quadrant. The muscle is well defined and is found lateral to the iliac vessels and vertebral column. The "speckled pattern" caused by muscle striations as seen in cross section helps to distinguish this landmark from other structures

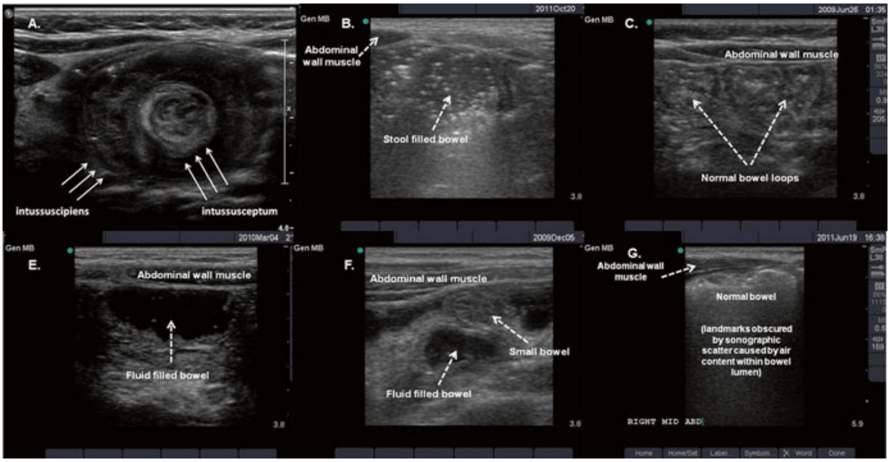

Fig. 9.5 Image (**a**) depicts the classic "target sign" appearance in transverse orientation of an ileocolic intussusception. Images (**b**–**g**) represent examples of normal bowel as seen by high frequency ultrasound

3. Pyloric stenosis.

   (a) Infantile hypertrophic pyloric stenosis (PS) causes gastric outlet obstruction and presents as persistent, forceful, non-bilious vomiting during the newborn period (usually around 3–12 weeks of age). Palpation of an "olive" during examination of the right upper quadrant may be appreciated, but this finding lacks sufficient sensitivity to reliably rule out the condition. Ultrasound by an experienced operator is the gold standard diagnostic test for PS. A linear probe can be used to obtain longitudinal and transverse views of the pylorus beside the gastric antrum. With the indicator pointing to the infant's right, a transverse midline view distal to the xiphoid process is a common starting point. Crying infants can be given oral sucrose, a pacifier or be held by their parents to allow for a better study. Administration of Pedialyte or other clear liquid before the ultrasound scan (which displaces air as fluid fills the antrum) and slight rotation of the infant into a right lateral decubitus position will improve one's ability to visualize the pylorus. The liver acts as an acoustic window and in most cases, a longitudinal view of the pylorus can be found below and adjacent to the liver edge. On longitudinal view, the presence of a "hamburger" may suggest the diagnosis. Ultimately, three measurements are commonly performed: the pyloric muscle thickness (normal measurement is ≤ 3 mm), the pyloric muscle length (normal measurement is ≤ 15 mm), and the pyloric diameter (normal measurement is ≤ 11 mm) [13]. Measurements at or above these cut off values in full term infants support the diagnosis of PS, especially if gastric contents are not visualized to pass the pylorus during sonographic evaluation. A false positive interpretation is possible if the pyloric muscle and channel are imaged at

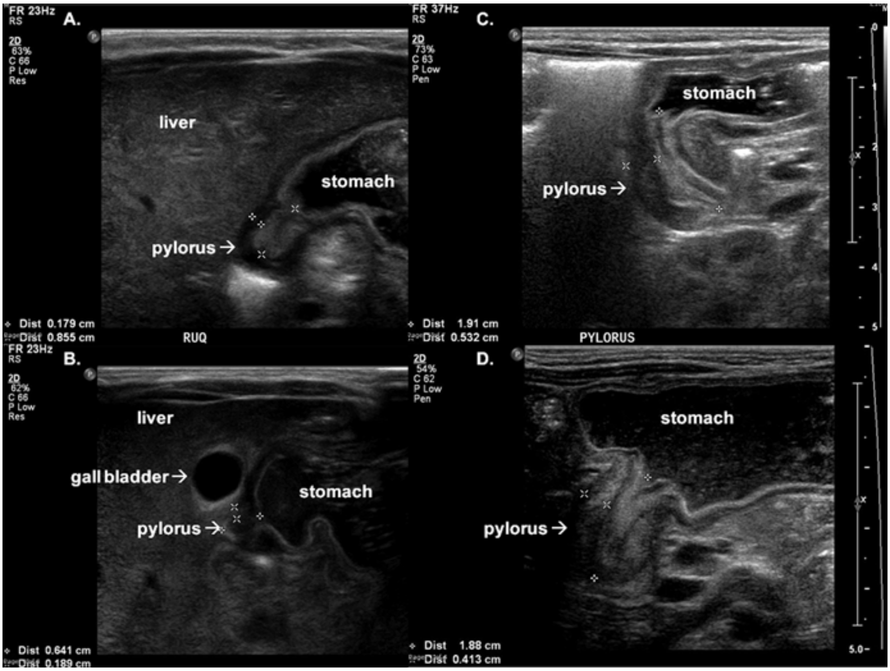

Fig. 9.6 Images (**a**, **b**) depict normal pylorus measurements in longitudinal view with muscle wall thicknesses of 1.8 and 1.9 mm, and channel lengths of 8.6 and 6.4 mm, respectively. Images (**c**, **d**) depict findings consistent with pyloric stenosis with single muscle wall thickness of 5.3 and 4.1 mm, and channel lengths of 19 mm

an oblique angle, pylorospasm is present or there is a fluid-filled duodenal bulb. A false negative interpretation is possible if overlying bowel gas creates poor visualization of the pylorus. Figure 9.6 depicts a comparison between the normal anatomy and a hypertrophied pyloric muscle. Note the "hamburger" appearance on longitudinal view.

4. Supracondylar fractures.

   (a) Supracondylar fractures are the most common type of pediatric elbow fracture and typically present after falls on out-stretched hands (FOOSH) by school age children. The gold standard diagnostic test is a lateral elbow radiograph. This X-ray is taken with the elbow at 90° flexion and needs to be positioned so that a "true lateral" film is available for accurate interpretation. Pain with elbow manipulation can impede the proper positioning of "true lateral" elbow X-rays. A spectrum of supracondylar fractures exist. Type-I fractures are suggested by the presence of an abnormal posterior fat pad as the only finding on initial elbow X-rays. Ultrasound can be a helpful tool during the evaluation of elbow injuries and can be used to detect supracondylar fractures with high sensitivity [14]. A high frequency linear probe is used to

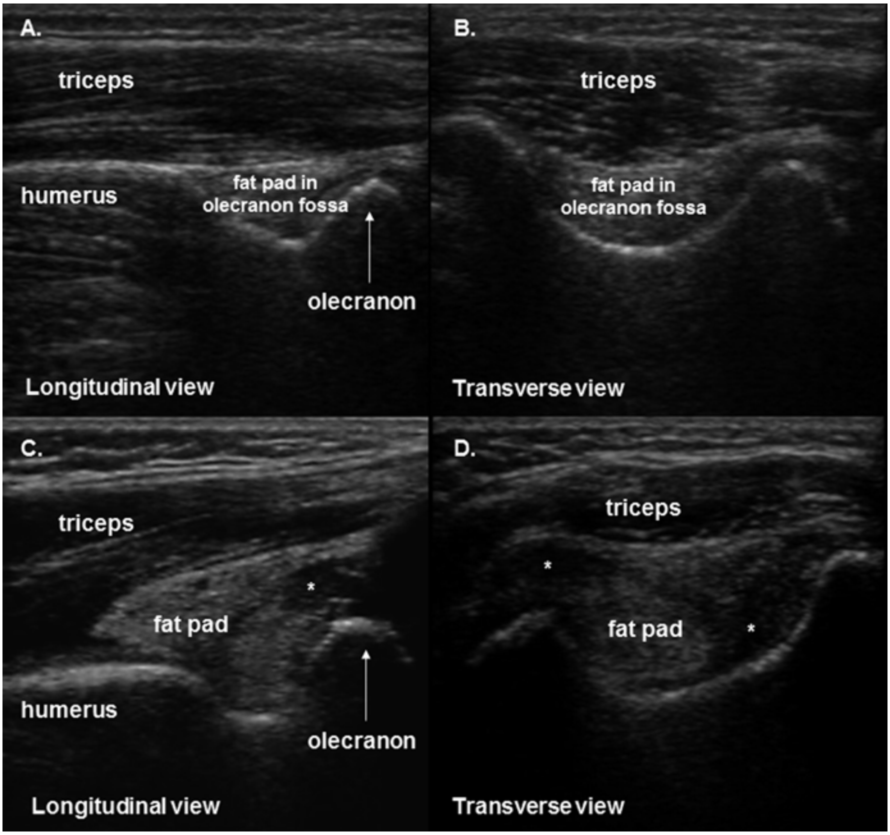

Fig. 9.7 Images (**a**, **b**) depict normal elbow anatomy. Note that the fat pad is well positioned over the olecranon fossa and lays flat relative to the hyperechoic bony cortex. Images (**c**, **d**) were taken from a child with a Type-I supracondylar fracture. Note the elevated fat pad relative to the bony cortex in both views. The *asterisks* mark a hypoechoic fluid collection which, in the setting of trauma, is consistent with a hemarthrosis

obtain both longitudinal and transverse views of the elbow joint. The classic finding on ultrasound is elevation of the posterior fat by a hypoechoic fluid collection in the presence of a hemarthrosis. Elbow effusions seen on ultrasound after a traumatic injury should raise suspicion for the presence of a coexisting or occult pediatric elbow fracture. Figure 9.7 depicts a comparison between the normal anatomy of the pediatric elbow joint and the presence of an elbow effusion in both longitudinal and transverse views.

5. Transient synovitis.

   (a) Transient synovitis is a common pediatric cause of hip pain, and typically presents with a limp after a preceding viral infection in a school age child. It is a benign condition which does have history and exam features that can overlap with more serious conditions. A bedside ultrasound evaluation can help narrow the differential diagnosis for the child with a limp if a hip effusion is found. In the setting of trauma or a fall, a hip effusion should raise concern for the presence of a coexisting or occult fracture. Furthermore, a hip effusion alone cannot distinguish between transient synovitis, bacterial arthritis, or lyme arthritis (in lyme endemic areas). A combination of clinical factors (fever and ability to bear weight) and inflammatory markers (elevated leukocyte counts, erythrocyte sedimentation rates, and c-reactive protein) must be evaluated together to properly risk stratify the need to perform hip arthrocentesis in a pediatric patient [15, 16]. To diagnosis a hip effusion, a linear probe is used to obtain a longitudinal view of the hip joint. With the patient's leg slightly abducted and externally rotated, the probe is placed along the long axis of the femoral neck with the indicator pointing cephalad towards the acetabulum. The classic finding on ultrasound is a hypoechoic fluid collection greater than 5 mm which courses along the anterior surface of the femoral neck. Figure 9.8 depicts a comparison between the normal anatomy of the pediatric hip joint and the presence of a hip effusion in the longitudinal orientation.

How to Use POCUS as It Pertains to Pediatrics: What Does the Evidence Show?

From the ongoing "rationale clinical examination" series published in JAMA of evidence based diagnoses, several comments were made related to pediatrics.

1. From the Chapter "Does This Infant Have Pneumonia?"

   Auscultation is relatively unreliable for examination of infants. Chest radiographic findings may be negative in infants with early bacterial pneumonia.

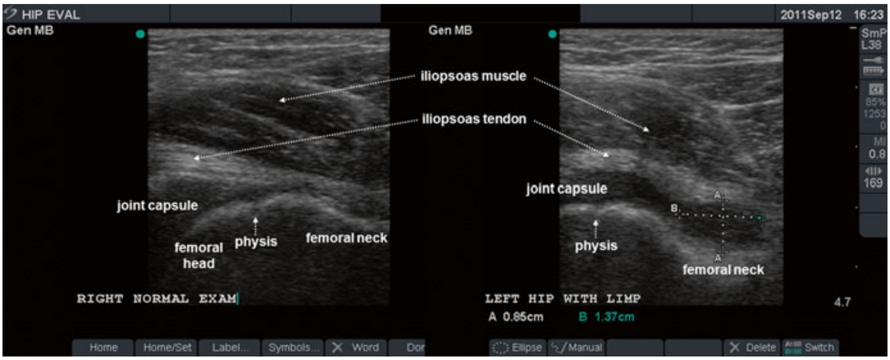

Fig. 9.8 Comparison view of a normal pediatric hip and a left hip effusion. Note the abnormal fluid collection has a convex appearance and courses anterior to the femoral neck. The hyperechoic tendon can create a false impression that fluid is present in the joint capsule at the level of the femoral head. Thus, it is important to look directly above the femoral neck to assess for the presence of a hip effusion, which typically measures >5 mm from anterior to posterior

The most important physical exam finding is initial observation of the respiratory rate while the child is at rest, which should occur during two 30-s intervals or during a full minute. Findings on exam that suggest pneumonia include tachypnea, chest retractions, grunting, nasal flaring and abnormal sounds on auscultation. The presence of multiple findings increases diagnostic certainty while absence of all findings (abnormal respiratory rest, signs related to work of breathing, abnormal breath sounds) makes the diagnosis doubtful.

2. From the Chapter "Is This Child Dehydrated?"

   Dehydration is an important cause of morbidity and mortality. However, the literature shows that clinical findings of dehydration are imprecise, with only fair to moderate agreement among examiners. Common laboratory tests such as BUN and bicarbonate levels help if they are markedly abnormal and should not be used alone to rule in or rule out dehydration. Given the imperfect nature of predicting the exact degree of dehydration, the physical exam should be used to quantify dehydration as "none," "some," or "severe."

3. From the Chapter "Does This Patient Have Strep Throat?"

   No single element of the medical history or physical exam is sufficient to accurately diagnose streptococcal pharyngitis. Streptococcal pharyngitis is most common in children (compared to infants and adults). In the presence of any of the following: tonsillar exudates, enlargement/tenderness of cervical lymph nodes, absence of cough, and fever greater than 38 °C; appropriate testing should be performed to help guide antibiotic management. Untreated streptococcal pharyngitis can last up to 10 days. Antibiotic treatment decreases severity and duration of symptoms, transmission rates and the risk of developing suppurative complications, which among others, include peritonsillar abscess (PTA) formation.

POCUS Pediatric Findings During When Challenges in Clinical Assessments Exist

Assessment for Pneumonia in an Infant with Difficulty Breathing

POCUS can serve as a helpful adjunct towards the evaluation of tachypneic infants. There is growing evidence that suggests ultrasound can detect pediatric pneumonias with greater sensitivity than traditional chest radiographs [17, 18]. The relative poorly calcified bone and appearance of consolidations that extend to the visceral pleura help to explain ultrasound's ability to find pathology in an anatomic region dominated by bone and air, which theoretically should act as deterrents to good ultrasound transmission. A potential limitation, however, is that a comprehensive lung scan should include multiple views of all regions of the thorax. With the patient either supine or upright, a high-frequency linear probe with the indicator pointing towards the child's head can be used to interrogate the superior and inferior portions of the anterior and lateral chest walls. Normal lung appearance will have visible sliding between visceral and parietal pleura, and the pleural line will appear as a hyperechoic line below the level of the ribs. Findings which suggest focal areas of subpleural consolidation can have variable appearances, shapes, and sizes. Advanced consolidations can produce a hyperechoic branching or lenticular pattern caused by the presence of air bronchograms and lung tissue "hepatization" above the diaphragm. Early pneumonias should be suspected in the presence of focal "B-lines." These lines are a produced when abnormal fluid/inflammation is present within alveoli and the interstitial space. B-lines extend from the pleural line, move horizontally with lung sliding, and dive deep vertically towards the bottom of the monitor. Figure 9.9 shows POCUS findings in a toddler with a left sided pneumonia. Furthermore, POCUS is an excellent tool for evaluating pleural effusions. The child is positioned upright and a low-frequency, curvilinear probe with the indicator pointing cephalad is used. The longitudinal view of the right upper quadrant should include both the hyperechoic diaphragm (middle of screen) and liver (right side of screen). The longitudinal view of the left upper quadrant should include both the hyperechoic diaphragm (middle of screen) and spleen (right side of screen). Normal assessment of the lung zone involves the presence of an artificial reflection, known as a "mirror image," of the respective solid organ behind the diaphragm (left side of screen). When a pleural effusion is present instead, a hypoechoic fluid collection of varying size can be seen adjacent to and above the level of the diaphragm (Fig. 9.10).

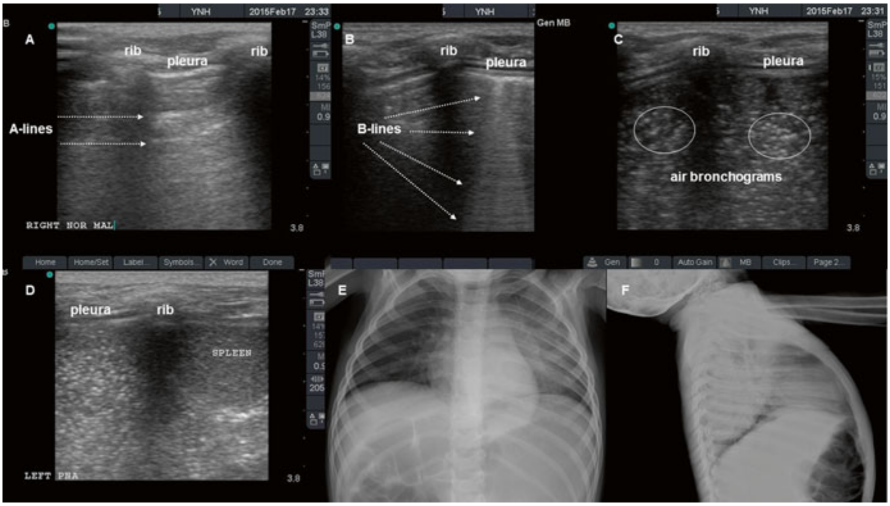

Fig. 9.9 Ultrasound findings in a toddler with a left lung consolidation. Image (**a**) shows the normal appearance of the right lung with the presence of horizontal a-lines (reverberation artifacts). Images (**b–d**) are left sided mid-axillary views moving from a more cephalad to caudal position. Image (**b**) depicts pathologic deep vertical B-lines or "comet tails" that dive all the way down to the bottom of the screen. Image (**c**) shows air bronchograms seen in transverse orientation represented by prominent punctate hyperechoic spots. Image (**d**) shows the "hepatization" of lung created by consolidation directly above the spleen. Images (**e**, **f**) are the corresponding AP and Lateral chest radiographs (note that the left lung consolidation is best seen on the lateral view)

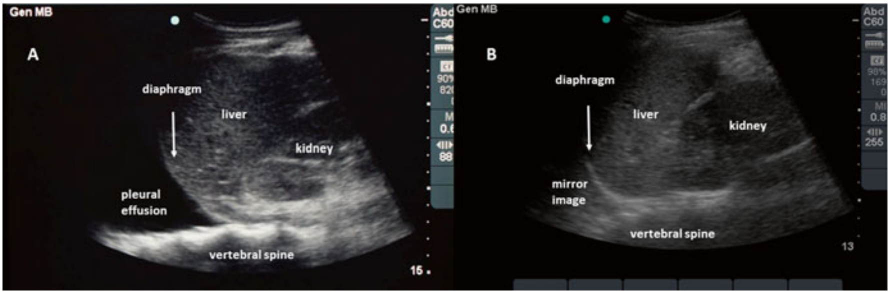

Fig. 9.10 The following images are longitudinal views of the right upper quadrant at the level of the diaphragm. The diaphragm is a hyperechoic, curved structure. In image (**a**), a pleural effusion (hypoechoic appearance) is present behind the diaphragm. In image (**b**), the normal lung tissues are not visible. Instead, the liver appears to be "flipped" behind the diaphragm (which appears on the left side of the screen with the indicator pointing towards the head) because of an expected mirror imaging artifact

Assessment of Hydration Status in a Child with Diarrhea

POCUS can serve as a helpful adjunct towards the evaluation of dehydrated children. Hydration status can be measured through volume assessment of the inferior vena cava (IVC). Two primary views should be obtained. The first is a transverse view of the relationship between the IVC and aorta just below the xiphoid process. Using a low-frequency curvilinear probe with the indicator directed towards the right of the patient, the intra-abdominal structures are viewed in cross-section. The horseshoe shaped vertebral body with posterior shadowing in the far-center part of the screen is an important landmark to identify. The aorta (Ao) is a pulsatile, hypoechoic structure coursing anterior to the vertebral body. The IVC is a non-pulsatile hypoechoic structure that is found to the left of the aorta on the screen. Anterior-posterior (AP) measurements are obtained for each vessel; the Ao during systole and the IVC during expiration at its maximal diameter. Inspiration leads to increased venous return and an expected collapsibility of the IVC during a state of euvolemia. In order to do this you will likely need to save a still image and toggle with the machine's cursor feature (in essence measuring both the Ao and IVC at their greatest AP diameters). Figure 9.11 depicts the typical anatomy on an abdominal transverse view. An "ideal" IVC/Ao ratio approaches 1.0. As this ratio falls below 0.8, the presence of 5 % dehydration or greater is likely to be present [19, 20]. Lower ratio cutoffs will exhibit greater specificity for significant dehydration but at the expense of lower sensitivity, as some cases will likely be missed if the ratio cutoff is set too low. The second view commonly used to interrogate the IVC is a longitudinal view as it is seen entering the right atrium below the xiphoid process. A phased-array probe with the indicator direct towards the patient's head is typically used. For optimal viewing, reorientation by angling the probe towards the patient's right side may be necessary. The AP diameter of the IVC can be measured

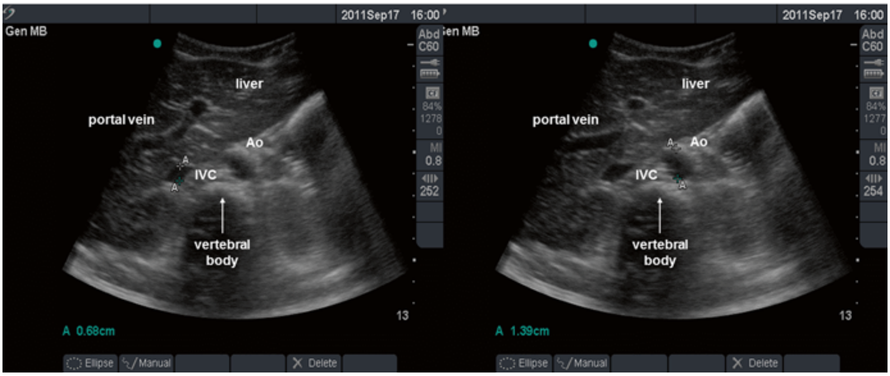

Fig. 9.11 In this transverse abdominal view, the maximal IVC diameter measures 0.68 cm and the maximal Ao diameter measures 1.39 cm. This IVC/Ao ratio of 49 % suggests intravascular volume depletion

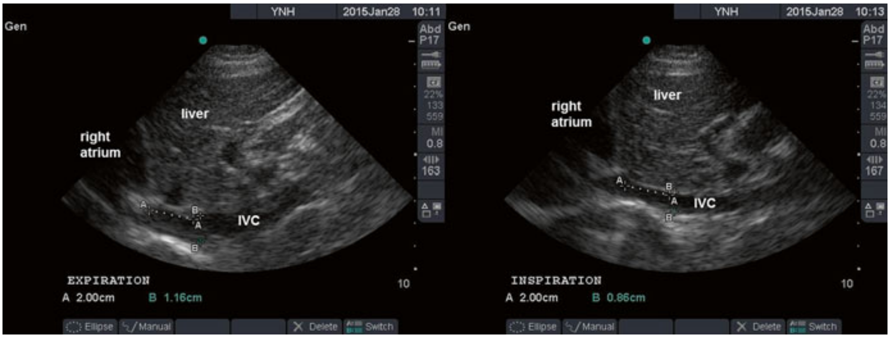

Fig. 9.12 IVC seen in its longitudinal orientation as it enters the right atrium using a subxiphoid view with a phased array probe. Note the normal collapsibility of the IVC during inspiration as venous return is augmented. The measured caval index is $[(1.16 - 0.86) \div 1.16] \times 100 = 26\%$.

in both expiration (most plump) and inspiration (most collapsed) at a point roughly 2 cm proximal to its insertion into the right atrium. During inspiration, IVC collapsibility >50 % is indicative of volume depletion and poor preload. Similarly, the caval index $[(\text{IVCmax} - \text{IVCmin}) \div \text{IVCmax}] \times 100$ is another measurement method that has been shown to correlate with central venous pressures. A caval index close to 100 % suggests complete collapse during a state of volume depletion, while a caval index close to 0 % suggests no collapse during a state of volume overload [21]. Figure 9.12 depicts the normal variation in the pattern of IVC collapsibility with a corresponding caval index of 26 % during a normal respiratory cycle in a child that is clinically euvolemic.

Assessment of Peritonsillar Abscess in an Adolescent with Sore Throat

POCUS can serve as a helpful adjunct towards the evaluation of tonsillar infections. A PTA is a common deep neck infection in the pediatric population. It most often occurs in the adolescent age group. The predominant causative bacteria are group A streptococcus, but Staphylococcus aureus and polymicrobial anaerobes are other important pathogens to consider. The infection is usually caused by direct extension of acute tonsillitis. Patients tend to have sore throat, drooling, fever, and a “hot potato” or muffled voice. Exam findings that suggest the presence of a PTA include asymmetric swelling and erythema of the soft palate, deviation of the uvula to the contralateral side, and trismus. The clinical exam alone, however, may not reliably differentiate a peritonsillar cellulitis from a more advanced PTA. Ultrasound has been shown to reliably diagnose the presence of a PTA and increase success rates of aspiration procedures [22, 23]. A high frequency endocavitary probe can be used to evaluate the peritonsillar region. Patients should be evaluated while sitting in an upright position. Topical benzocaine spray or nebulized lidocaine can be used as a local anesthetic and premedication with an anti-inflammatory agent is often helpful. A sterile cover is placed directly on to the endocavitary probe. Care should be taken to remove all air so there is direct contact between the probe and its cover. The moist nature of the oropharynx precludes the need for applying gel to the cover’s surface (the gel may cause patient discomfort as there is no easy way to wipe or remove afterwards). The endocavitary probe is advanced towards the affected tonsillar space with the indicator pointing towards the patient’s right. The tonsil on the affected side should be identified first and used as a starting landmark. At that point, redirecting the probe laterally will allow visualization of the peritonsillar tissues. A PTA will appear as a hypoechoic, isoechoic, or heterogenous mass with margins that contrast it from the surrounding tissue. Posterior acoustic enhancement is a prominent finding [24]. A practical approach is to first identify the tonsil on the affected side. If an adjacent fluid collection is present, regardless of echogenic appearance, it is likely to represent a PTA [25]. Ultrasound also allows for localization of the internal carotid artery which is found posterior to the abscess cavity using color Doppler. In patients with significant trismus or who are otherwise unable to cooperate with intraoral ultrasound, a transcutaneous approach is an alternative method that can be used to interrogate for abscess collections [26]. The technique for this approach requires placement of a linear high frequency probe under the angle of the mandible with the patient’s head rotated to the opposite direction. In comparison to the intraoral approach, the PTA will appear deeper on the screen. It may be helpful to adjust the monitor’s depth settings and increase the gain function when performing a transcutaneous approach. Figure 9.13 compares the sonographic findings using these two techniques.

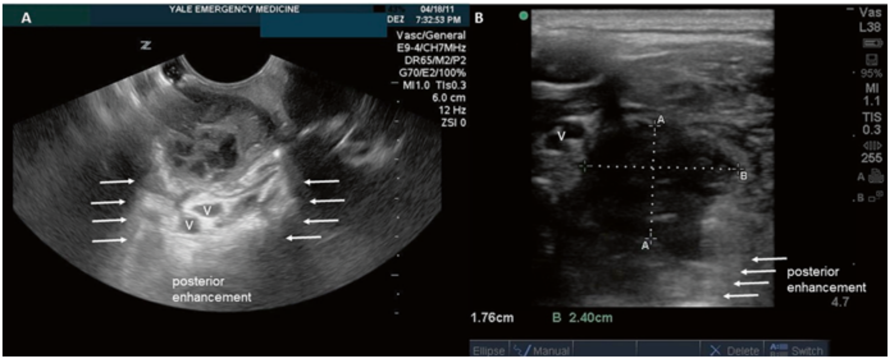

Fig. 9.13 The following images are consistent with peritonsillar abscess. Image (**a**) identifies a PTA using an endocavitary probe. Note the heterogeneous appearance with central hypoechoic pockets, nearby vascular structures (v) behind the abscess, and posterior enhancement (image courtesy of Rachel Liu, MD). Image (**b**) shows a PTA using a linear probe. The wall is well defined with a hypoechoic collection measuring 1.8 × 2.4 cm and posterior enhancement is present (image courtesy of Lorraine Ng, MD)

References

1. Chaar-Alvarez FM, Warkentine F, Cross K, Herr S, Paul RI. Bedside ultrasound diagnosis of nonangulated distal forearm fractures in the pediatric emergency department. Pediatr Emerg Care. 2011;27(11):1027–32.
2. Cross KP, Warkentine FH, Kim IK, Gracely E, Paul RI. Bedside ultrasound diagnosis of clavicle fractures in the pediatric emergency department. Acad Emerg Med. 2010;17(7):687–93.
3. Holmes JF, Gladman A, Chang CH. Performance of abdominal ultrasonography in pediatric blunt trauma patients: a meta-analysis. J Pediatr Surg. 2007;42(9):1588–94.
4. Ma OJ, Mateer JR, Ogata M, Kefer MP, Wittmann D, Aprahamian C. Prospective analysis of a rapid trauma ultrasound examination performed by emergency physicians. J Trauma. 1995;38(6):879–85.
5. Garcia Pena BM, Mandl KD, Kraus SJ, Fischer AC, Fleisher GR, Lund DP, et al. Ultrasonography and limited computed tomography in the diagnosis and management of appendicitis in children. JAMA. 1999;282(11):1041–6.
6. Doria AS, Moineddin R, Kellenberger CJ, Epelman M, Beyene J, Schuh S, et al. US or CT for diagnosis of appendicitis in children and adults? A meta-analysis. Radiology. 2006;241(1):83–94.
7. Schuh S, Man C, Cheng A, Murphy A, Mohanta A, Moineddin R, et al. Predictors of non-diagnostic ultrasound scanning in children with suspected appendicitis. J Pediatr. 2011;158(1):112–8.
8. Brouwer MJ, de Vries LS, Pistorius L, Rademaker KJ, Groenendaal F, Benders MJ. Ultrasound measurements of the lateral ventricles in neonates: why, how and when? A systematic review. Acta Paediatr. 2010;99(9):1298–306.
9. Steggerda SJ, Leijser LM, Walther FJ, van Wezel-Meijler G. Neonatal cranial ultrasonography: how to optimize its performance. Early Hum Dev. 2009;85(2):93–9.
10. Hryhorczuk AL, Strouse PJ. Validation of US as a first-line diagnostic test for assessment of pediatric ileocolic intussusception. Pediatr Radiol. 2009;39(10):1075–9.

11. Verschelden P, Filiatrault D, Garel L, Grignon A, Perreault G, Boisvert J, et al. Intussusception in children: reliability of US in diagnosis – a prospective study. Radiology. 1992;184(3): 741–4.
12. Riera A, Hsiao AL, Langhan ML, Goodman TR, Chen L. Diagnosis of intussusception by physician novice sonographers in the emergency department. Ann Emerg Med. 2012;60(3): 264–8.
13. Rohrschneider WK, Mittnacht H, Darge K, Troger J. Pyloric muscle in asymptomatic infants: sonographic evaluation and discrimination from idiopathic hypertrophic pyloric stenosis. Pediatr Radiol. 1998;28(6):429–34.
14. Rabiner JE, Khine H, Avner JR, Friedman LM, Tsung JW. Accuracy of point-of-care ultrasonography for diagnosis of elbow fractures in children. Ann Emerg Med. 2013;61(1):9–17.
15. Cook PC. Transient synovitis, septic hip, and Legg-Calve-Perthes disease: an approach to the correct diagnosis. Pediatr Clin North Am. 2014;61(6):1109–18.
16. Perry DC, Bruce C. Evaluating the child who presents with an acute limp. BMJ. 2010;341:c4250.
17. Ho MC, Ker CR, Hsu JH, Wu JR, Dai ZK, Chen IC. Usefulness of lung ultrasound in the diagnosis of community-acquired pneumonia in children. Pediatr Neonatol. 2015;56(1):40–5.
18. Shah VP, Tunik MG, Tsung JW. Prospective evaluation of point-of-care ultrasonography for the diagnosis of pneumonia in children and young adults. JAMA Pediatr. 2013;167(2): 119–25.
19. Chen L, Hsiao A, Langhan M, Riera A, Santucci KA. Use of bedside ultrasound to assess degree of dehydration in children with gastroenteritis. Acad Emerg Med. 2010;17(10): 1042–7.
20. Jauregui J, Nelson D, Choo E, Stearns B, Levine AC, Liebmann O, et al. The BUDDY (Bedside Ultrasound to Detect Dehydration in Youth) study. Crit Ultrasound J. 2014;6(1):15.
21. Nagdev AD, Merchant RC, Tirado-Gonzalez A, Sisson CA, Murphy MC. Emergency department bedside ultrasonographic measurement of the caval index for noninvasive determination of low central venous pressure. Ann Emerg Med. 2010;55(3):290–5.
22. Costantino TG, Satz WA, Dehnkamp W, Goett H. Randomized trial comparing intraoral ultrasound to landmark-based needle aspiration in patients with suspected peritonsillar abscess. Acad Emerg Med. 2012;19(6):626–31.
23. Loock JW. A randomised trial comparing intraoral ultrasound to landmark-based needle aspiration in patients with suspected peritonsillar abscess. Clin Otolaryngol. 2013;38(3):245–7.
24. O'Brien E, Valley VT, Summers RL. Intraoral sonography of peritonsillar abscesses: feasibility and sonographic appearance. Ann Emerg Med. 1999;34(4):S26.
25. Kew J, Ahuja A, Loftus WK, Scott PM, Metreweli C. Peritonsillar abscess appearance on intra-oral ultrasonography. Clin Radiol. 1998;53(2):143–6.
26. Araujo Filho BC, Sakae FA, Sennes LU, Imamura R, de Menezes MR. Intraoral and transcutaneous cervical ultrasound in the differential diagnosis of peritonsillar cellulitis and abscesses. Braz J Otorhinolaryngol. 2006;72(3):377–81.

Chapter 10
The Thorax

Jonathan dela Cruz, Brad Cowley, Chinmay Patel, and Sevan Yeghiazarian

Approach to the Patient

Evaluation of the thorax through POCUS requires an understanding of a few basic concepts. When approaching the patient it is important that they are gowned in a way to allow easy access to the posterior and anterior chest while providing modest coverage of sensitive areas. Pulmonary assessments are the most commonly performed thoracic scans and are the exams that will be focused on in this chapter. They are usually performed with the patient in either the supine or sitting position. When considering the best patient positioning method it is important to note the lungs are large organs that can be filled with material of varying density, namely air and fluid. Air rises while fluid will be gravity dependent. In the supine position air will rise to the anterior chest and fluid to the posterior chest. In a sitting position, air will rise towards the apices of the lungs while fluid will gravitate towards the diaphragm. When deciding the best position to exam a patient the most important determining factor is patient condition. When examining an acutely dyspneic patient a supine position may cause them increased discomfort to require more respiratory effort. In these situations keeping in mind the gravity dependency of air and fluid will allow appropriate interpretation of most exams that will be covered in this section.

J. dela Cruz, M.D., R.D.M.S. (✉) • B. Cowley, D.O. • C. Patel, D.O. • S. Yeghiazarian, M.D.
Division of Emergency Medicine, Southern Illinois University School of Medicine, Springfield, IL, USA
e-mail: jdelacruz@siumed.edu; drheyo@gmail.com; cpatel@siumed.edu; sevan.yeghiazarian@gmail.com

J.M. Daniels, R.A. Hoppmann (eds.), *Practical Point-of-Care Medical Ultrasound*, DOI 10.1007/978-3-319-22638-5_10

Selecting a Probe

Bedside assessments using ultrasound requires the use of a moderate to high frequency linear probe types. Assessments of the lungs usually do not require a large window or depth of visualization. The periphery of the lungs tends to shed light into any pathology that might be occurring centrally. A high frequency linear probe lends itself well to evaluating superficial structures. High resolution of structures is also needed given the artifact or echoes air produces. Air can be thought as the “enemy” of ultrasound and a barrier to transmission of ultrasound waves. The production of ultrasound images is dependent on the information an ultrasound machine receives regarding the change in exam medium densities. Anatomic structures are differentiated by boundaries created by varying densities of tissues (fat vs. muscle vs. fascia, etc.). When the difference of densities between two adjacent structures are large a very large echo is produced that cannot be interpreted well by an ultrasound machine. Air and bone have densities measuring 100–1000 times the difference when compared to other tissues in the body. Using a high frequency probe helps to combat some of these shortcomings. Moderate frequency linear probes can be used when needing to assess deeper structures of the lungs and thorax. The most common probe used is a curvilinear probe. Examples of uses for this probe type including assessing large areas of consolidation or effusion.

Scanning

The first step with all POCUS exams is ensuring the exam is being done on the correct patient and that the proper identifying information has been inputted into the ultrasound machines archiving system. The method for this varies manufacturer to manufacturer so consulting your vendor on the specific archiving system you are using may be needed. The following sequence should then be performed in preparation before performing and of the exams discussed in this section.

1. Moderate to high frequency linear probe selection—A high frequency linear probe lends itself well for examining the lungs. On some occasions a curvilinear probe can be used which has a lower frequency. Although this lower frequency results in lower resolution, deeper assessments can be performed when needed.
2. B-mode imaging selection—There are many different types of imaging modes an ultrasound can be placed in. B-mode (brightness mode) is the most commonly used and the one most are familiar with. In this mode the ultrasound machine depicts a grey-scale image of the exam medium. There should be a B-mode button that sets the machine to this imaging modality. Some manufacturers may call this “2D” mode or some other nomenclature. Please consult your vendor on the proper mode.
3. Orientate yourself to the screen and probe—A basic B-mode screen during a high frequency linear probe and curvilinear probe exam is depicted in Fig. 10.1.

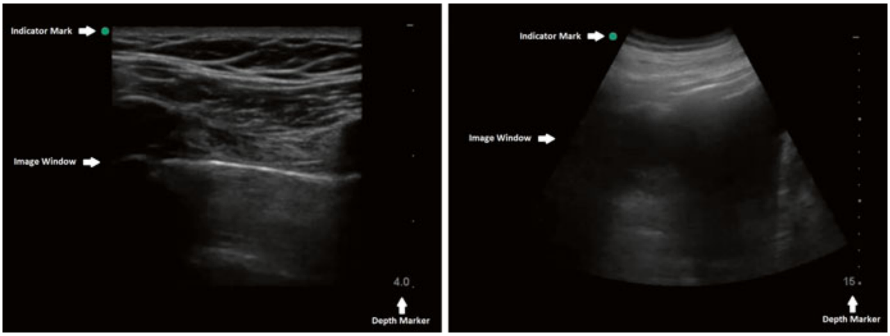

Fig. 10.1 Depiction of basic B-mode screens of a high frequency linear probe (*left*) and a curvilinear probe (*right*)

Fig. 10.2 Examples of curvilinear (*left*) and high frequency linear (*right*) probes with corresponding indicator marks

An indicator dot should be located on the left upper corner of the image window. If the indicator is not located there, change the settings per the vendors instructions. All discussions and examples in this chapter will require this orientation. This indicator will correlate to a groove or stripe on the ultrasound probe (Fig. 10.2). To test this, applying gel on the probe surface closest to the groove or stripe should correlate with gel media being displayed on the left side of the image window.

4. Adjust the depth—Most lung ultrasound exams can be done with a visual depth of 3–4 cm. Each ultrasound screen will have a depth caliper to the side of the image window. Usually this caliper is on the right side of the screen. Adjust the depth using the proper depth button or dial to achieve a maximum depth of 3–4 cm.
5. Position your patient and begin scanning—It is best for most POCUS pulmonary exams to be done with the patient in the supine position. If clinical condition makes this unavailable, place the patient in their most comfortable position taking note again that air will rise and fluid will fall.

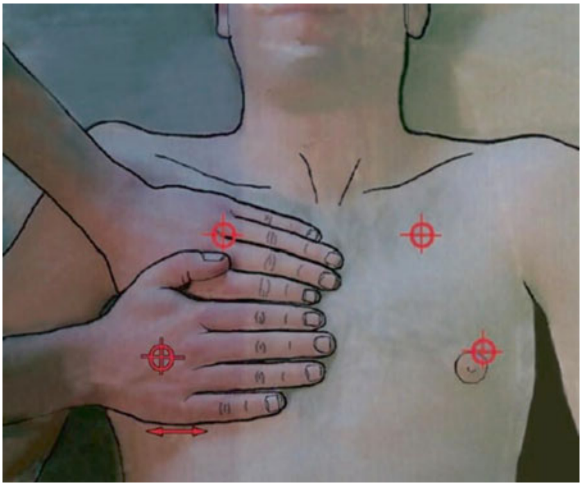

Fig. 10.3 The BLUE points. The upper hand is applied with the little finger against the lower border of the clavicula (in its long axis). The finger tips touch the midline. The lower hand is applied below the first hand. The thumbs do not count. The upper BLUE point is at the base of the middle and ring fingers of the upper hand (upper cross). The lower BLUE point is in the middle of the palm of the lower hand (lower cross). In this subject, the lower BLUE point is near the nipple. This definition makes a symmetric analysis, usually avoiding the heart. The lower edge of the lower hand roughly indicates the phrenic line (*arrow*), i.e., the end of the lung. Note that the shape of the hands has been studied in order to correct the obliquity of the clavicula, yielding a roughly transversal phrenic line (from *Whole Body Ultrasonography in the Critically Ill*, Springer)

There are three main lung windows (areas commonly scanned) used for POCUS assessment of the pulmonary system. They are known as the upper and lower BLUE-points (Fig. 10.3) and posterior and/or lateral alveolar and/or pleural syndrome (PLAPS) point (Fig. 10.4).

These areas allow evaluation of lungs free of obstructive anatomy (such as the heart) and have been found to be accurate for evaluating for consolidation and effusions [1]. When scanning these areas, the indicator marking on the probe should be pointed toward the patient's head, achieving a long axis view of the pulmonary system. The probe should be oriented perpendicular to the coronal plane of the body except during the PLAPS point view where the probe should be oriented pointing towards the central axis of the body along the posterior axillary line.

Normal Anatomy of the Pulmonary System

When examining the pulmonary system in any of the three lung windows the anatomy is similar except for one small difference that may occur in the PLAPS point view. The basic images obtained in a normal patient will appear as in Fig. 10.5. The landmarks that first help to orientate one to an image of a lung are the rib shadows.

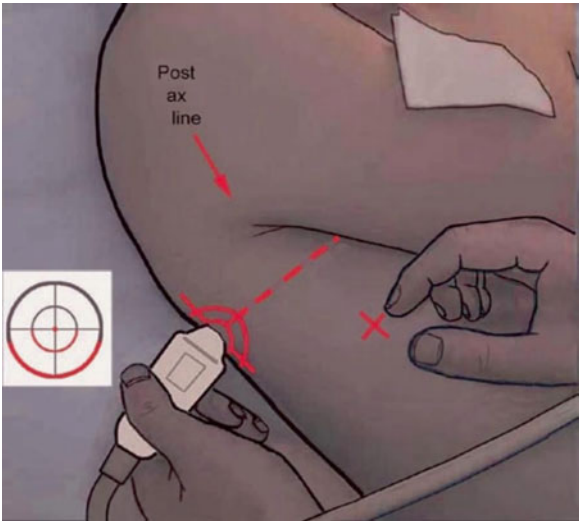

Fig. 10.4 The PLAPS point (PLAPS: posterolateral alveolar and/or pleural syndrome). The probe is applied at the PLAPS point, i.e., the intersection between the transversal line continuing the lower BLUE point (*dotted line*), and the longitudinal posterior axillary line (*arrow*), or, as seen here, as far as possible behind. This will immediately detect small and large pleural effusions (and 90 % of cases of alveolar consolidations in the critically ill patient) (from *Whole Body Ultrasonography in the Critically Ill*, Springer)

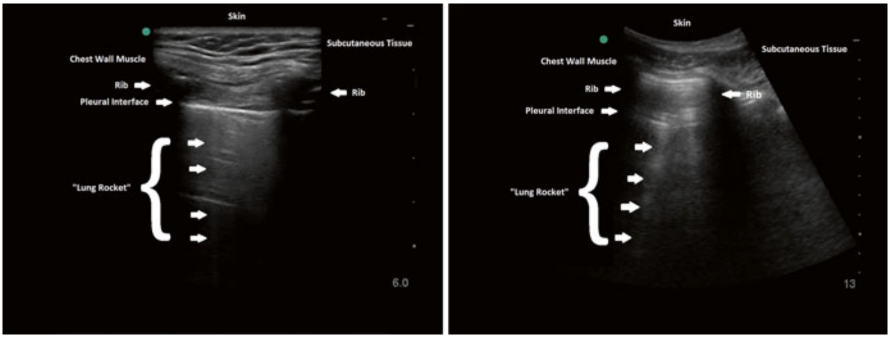

Fig. 10.5 Basic images obtained in a normal patient

These can best be described as bright hyperechoic arcs with posterior shadowing. It is customary to include two rib shadows and an intercostal space in a viewing window. Above the rib shadows is a layer of chest wall muscle that should appear as striated linear fibers that run across the top of the ribs. Above the muscle layer usually sits a more hypoechoic layer of subcutaneous fat and then skin. These layers also appear linear. Below the level of the ribs and in the intercostal space lies the window the lungs. The first image seen is the pleural interface with the chest wall.

This is depicted as a hyperechoic line traversing the intercostal space. In real time imaging, the line can be observed to be sliding back and forth as the patient breaths. Below this line lies the lung parenchyma. This area is displayed as a grainy hypoechoic region below the pleural line. Given the amount of air present, not a lot of lung tissue can be visualized. Therefore the ultrasound is grainy in appearance. It is important to note that a normal lung will have fluid filled alveoli near the pleura. These fluid filled alveoli produce a "reverberation" artifact consisting of hyperechoic arcs that move down to the bottom of the screen. This results in an appearance of moving white lines that move with the slide of the pleura. These are commonly referred to "flashlights," "comet tails," or "lung rockets." Seeing 2–4 of these in an intercostal space is normal.

How to Use POCUS as It Pertains to the Pulmonary System: What Does the Evidence Show?

From the ongoing *Rational Clinical Examination* series published in JAMA of evidence-based clinical diagnoses [2], many disappointing findings were elucidated and discussed concerning the clinical exam and physician gestalt in regard to the pulmonary system.

1. There is no individual finding or combination of physical exam findings that will accurately rule out airflow limitation.
2. A clinician's overall impression showed wide variability in their ability to diagnoses all levels of severity of airflow limitation (15–95 % sensitivity).
3. There are no combinations of a patient's medical history or physical examination findings that are sufficient to confirm the diagnosis of pneumonia.
4. The predictive rules for pneumonia only yield a maximum positive probability of disease of 50 % in the absence of chest radiography.
5. There was considerable interobserver variability in the recording of a patient's symptoms and a clinician's physical examination findings when the diagnosis of pneumonia was considered.
6. There are no individual items in the patient's medical history, either the presence of or absence of, to reduce the odds of disease enough to exclude pneumonia as a diagnosis or to increase the odds enough to confirm the diagnosis without a chest radiograph.
7. Neither the presence nor the absence of crackle on thoracic auscultation was sufficient enough to rule in or rule out the diagnosis of pneumonia.
8. Clinical examination alone is inaccurate in either the diagnosis of or exclusion of pulmonary emboli. (The physician's clinical gestalt is not particularly discriminating).
9. Clinical prediction rules (Wells, Simplified Wells, Geneva, PIOPED, and PISA-PED) are all equally sufficient to stratify patients into low, moderate and high probability categories.

The use of POCUS gives the clinician another route of diagnostic imaging to help rule in or rule out multiple pulmonary disease processes and anatomical discrepancies without the harm of radiation exposure from chest radiography and computed tomography. It also allows this assessment to be done at the bedside.

Given the potential critical nature of pneumothoraces, rapid detection can lead to earlier intervention and stabilization of the patient. The ability to rapidly exclude this diagnosis also can allow attention to focus on other critical issues that occur in an ill patient. The use of bedside ultrasound has been shown to significantly decrease the time to a diagnosis of a pneumothorax [3], with an average time to diagnosis around 3 min. This favorably compares to 20 min required by use of conventional plain films in the referenced study. Given the importance of accurate and reliable diagnosis, there have been many studies over the last 10 years attempting to determine the sensitivity and specificity of POCUS for bedside ultrasound. A pooled meta-analysis shows that POCUS had a pooled sensitivity of 78.6 % and a pooled specificity of 98.4 %, which is significantly improved over plain films which had a pooled sensitivity of 39.8 % and pooled specificity of 99.3 % [4]. While subgroup analysis shows variation related to operator skill level, the data supports the use of POCUS for the initial evaluation for patients with suspected pneumothoraces.

POCUS has also been shown to be a reliable is in diagnosis of pneumonia. In fact multiple studies have shown lung ultrasound to be more sensitive than chest radiography for the diagnosis of pneumonia [5–8]. A systematic review and meta-analysis was done using ten studies with a combined sample size of 1172 participants. It showed a pooled sensitivity of 94 % and specificity of 96 %. It was concluded that lung ultrasound performs well for the diagnosis of pneumonia when conducted by experienced sonographers—although more studies are needed to establish its reliability when used by less experienced physicians [9].

The BLUE-protocol, published in 2008, is an algorithm for lung ultrasound designed for immediate diagnosis of acute respiratory failure. The diagnoses of interest included pulmonary edema, pneumonia, asthma/COPD, pulmonary embolism, and pneumothorax. Thoracic ultrasound was used to assess the presence or absence of three items: artifacts (horizontal A lines or vertical B lines), lung sliding, and alveolar consolidation and/or pleural effusion. When this information was applied to a decision tree, the accurate diagnosis was made in >90 % of cases [10].

Common POCUS Pulmonary Findings

Pneumothorax

The evaluation for pneumothorax using POCUS is based on the physiologic principle that when a patient has a pneumothorax, the lung parenchyma is no longer sliding against the chest wall. This is due to the fact a layer of air lies between the lung parenchyma and chest wall cavity. During this exam the patient should be in the supine position, then both the upper and lower BLUE-points are evaluated as

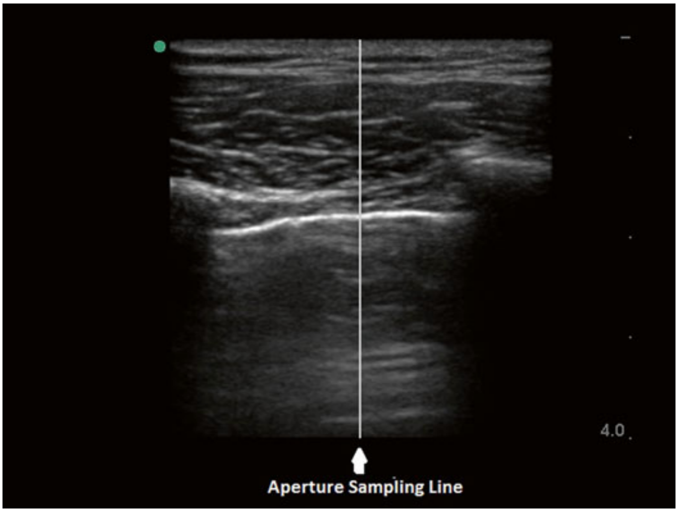

Fig. 10.6 M-mode depiction placing sampling aperture in the intercostal space

described earlier. Normally the pleural line should be identified just below the chest wall muscles and normal lung physiology will demonstrate "sliding" as the visceral and parietal pleural move against each other during respiration. The absence of sliding suggests air between these two pleural, and is highly suggestive of pneumothorax. In cases where lung sliding is difficult to determine, an ultrasound mode called M-Mode (motion mode) can be used. In this mode a specific ultrasound aperture is graphed over time. M-mode can be selected by pressing the appropriate M-mode button on the ultrasound. A line the will appear on the screen (Fig. 10.6) representing the aperture to be graphed. This line should be placed down the intercostal space and then graphed usually by pressing the m-mode button again. The resultant graph will depict straight horizontal lines where no movement is occurring and grainy areas where movement is occurring. In this view, the typical view of normal lung physiology and pleural sliding is described as a "seashore" while findings of a "stratosphere" or loss of pleural sliding are suggestive of pneumothorax (Fig. 10.7).

In addition to evaluation for lung sliding, the presence of "lung rockets" should be searched for. The absence of these lines again suggests a disrupted pleural interface. The absence of pleural sliding and "lung rockets" strongly suggest pneumothorax.

Interstitial Consolidation (Pneumonia)

Consolidated lung has increased fluid content and decreased aeration. This pathology allows for ultrasound visualization of pneumonia. Assessments for pneumonia using POCUS are best performed with the patient in the sitting position with the

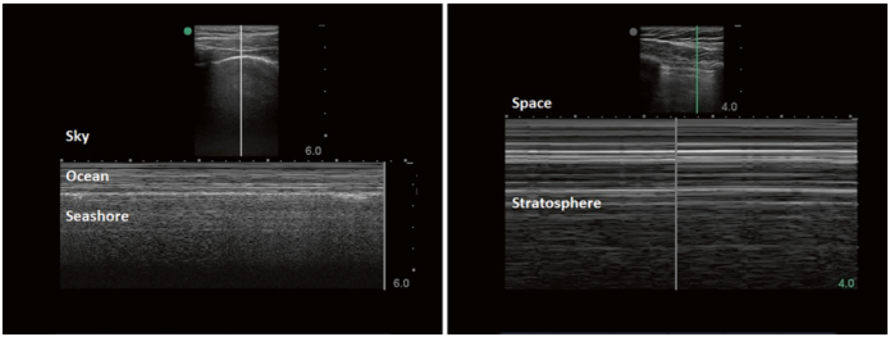

Fig. 10.7 Comparison of normal M-mode "Seashore Sign" (*left*) and pneumothorax "Stratosphere Sign" (*right*)

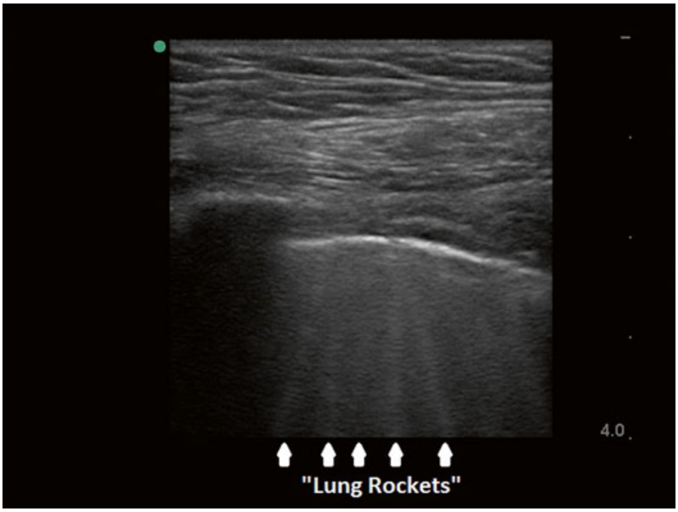

Fig. 10.8 Example of interstitial consolidation findings of numerous "lung rockets"

probe placed at the PLAPS point as described earlier. Given increased fluid content in the lungs one of the first findings one will notice is the presence of more than the usual 2–4 "lung rockets" as the increased fluid causes more reverberation artifact (Fig. 10.8) With decreased aeration the echoing effect air has in disrupting the visualization of lung tissue is loss the consolidated lung takes on the appearance of denser, more hyperechoic organs like liver and spleen. With disease progression, certain areas develop increased echogenicity, causing a more heterogeneous appearance of the lung on ultrasound. Within the consolidation, multiple bright dots and branching linear structures may be seen which represent sonographic air bronchograms (Fig. 10.9). If instead fluid has filled the bronchial tree, then fluid bronchograms will appear and the branching pattern will appear dark or hypoechoic.

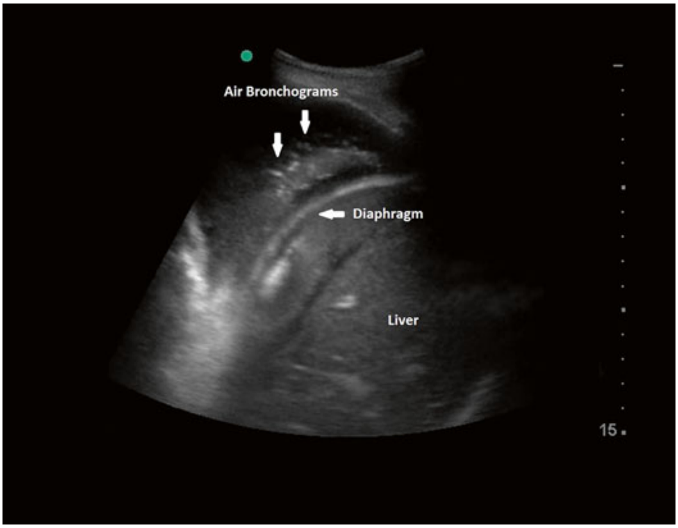

Fig. 10.9 Curvilinear probe assessment of lower right lung. Just above the diaphragm is the consolidation exhibiting multiple bright hyperechoic dots or air bronchograms

Pleural Effusion

Pleural effusions are easily identifiable using POCUS. Large amounts of fluid in the chest wall cavity result in decreased aeration and increased echogenicity of lung structures making them more identifiable. Assessments for effusion using POCUS are best performed with the patient in the sitting position with the probe placed at the PLAPS point as described earlier. With the patient in the sitting position this allows for gravity dependent fluid to settle in the lower sections of the lung of which the PLAPS point visualizes well. One of the first findings suggesting an effusion is present a market increase in the number of "lung rockets" visualized in an intercostal space. As discussed earlier 2–4 "lung rockets" per intercostal space is normal. When more are present interstitial consolidation is a consideration. When the number of "lung rockets" increases to the point where they start coalescing, creating "broad-looking lung rockets," large amounts of fluid in the alveoli and interstitial spaces is suspected (Fig. 10.10). In many cases, enough fluid is present to where the fluid can displace the lung parenchyma away from the chest wall much like air does in a pneumothorax. However, given fluid is a fantastic anechoic medium, instead of the disruptive echoing seen below the chest wall in a pneumothorax, a large effusion will present itself as a dark black area in between the chest wall and pleural line (Fig. 10.11). The lung will appear as if it is floating in the black anechoic fluid in real time. POCUS for pleural effusion is not only helpful for discerning dyspneic patients with cancer, ascites, or heart failure, but also can help direct optimal placement of thoracentesis needle for treatment.

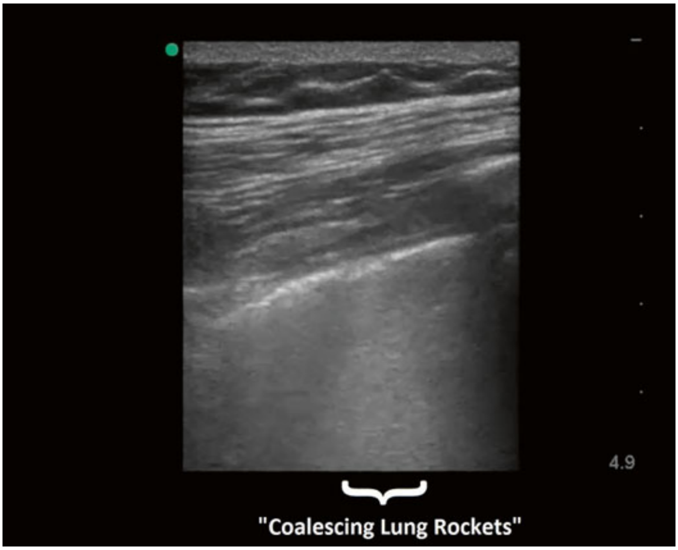

Fig. 10.10 Examination of severe alveolar fluid showing coalescing “lung rockets” forming a broad based single “lung rocket”

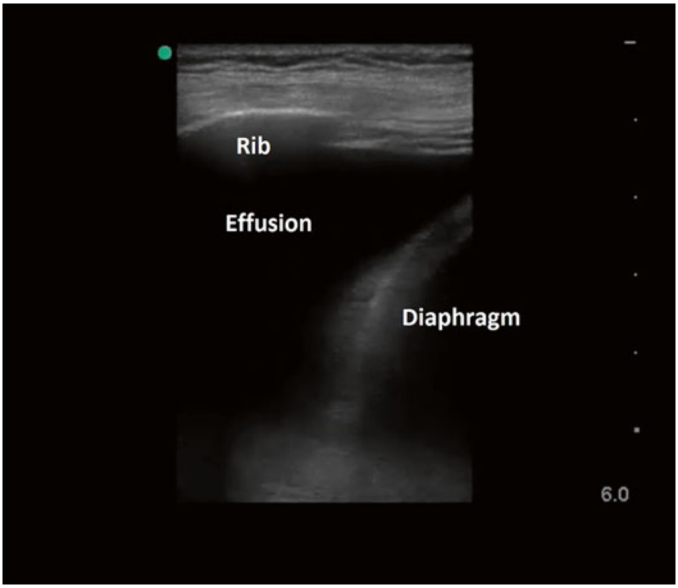

Fig. 10.11 Examination performed in the lower lung field of an effusion. Notice the curved edge of the diaphragm with an anechoic area of fluid above it

References

1. Lichtenstein DA, Mezière GA. The BLUE-points: three standardized points used in the BLUE-protocol for ultrasound assessment of the lung in acute respiratory failure. Crit Ultrasound J. 2011;3(2):109–10.
2. Simel D, et al. The Rational Clinical Examination: Evidence-Based Clinical Diagnosis. New York: McGraw-Hill Professional, 2009.
3. Mao Z, et al. Rapid detection of pneumothorax by ultrasonography in patients with multiple trauma. Crit Care. 2006;10(4):R112.
4. Alrajab S, et al. Pleural ultrasonography versus chest radiography for the diagnosis of pneumothorax: review of the literature and meta-analysis. Critical Care. 2013;17(5):R208.
5. Reissig A, et al. Lung ultrasound in the diagnosis and follow-up of community-acquired pneumonia: a prospective, multicenter, diagnostic accuracy study. Chest J. 2012;142(4):965–72.
6. Alkhayat F, Alam-Edeen H. Value of chest ultrasound in diagnosis of community acquired pneumonia. Egypt J Chest Dis Tubercul. 2014;64:1047–51.
7. Cortellaro F, Colombo S, Coen D, Duca PG. Lung ultrasound is an accurate diagnostic tool for the diagnosis of pneumonia in the emergency department. Emerg Med J. 2012;29:19–23.
8. Bourcier JE, Paquet J, Seinger M, et al. Performance comparison of lung ultrasound and chest x-ray for the diagnosis of pneumonia in the ED. Am J Emerg Med. 2014;32(2):115–8.
9. Chavez MA, Shams N, Ellington LE, Naithani N, Gilman RH, Steinhoff MC, Santosham M, Black RE, Price C, Gross M, Checkley W. Lung ultrasound for the diagnosis of pneumonia in adults: a systematic review and meta-analysis. Respir Res. 2014;15(1):50.
10. Lichtenstein D, Mezière G. Relevance of lung ultrasound in the diagnosis of acute respiratory failure. The BLUE-protocol. Chest. 2008;134:117–25.

Index

J.M. Daniels, R.A. Hoppmann (eds.), *Practical Point-of-Care Medical Ultrasound*, DOI 10.1007/978-3-319-22638-5